REACTOR ENGINEERING

TU ELECTRIC
Generating Division

RXE-91-005

METHODOLOGY FOR REACTOR CORE RESPONSE TO STEAMLINE BREAK EVENTS

MAY 1991

Mark A. Grace
Richard M. Rubin

Reviewed: Stephen M. Maier Date: 5/30/91
Stephen M. Maier
Supervisor, Transient Analysis

Reviewed: Mickey R. Killgore Date: 5/30/91
Mickey R. Killgore
Supervisor, Reactor Physics

Approved: Date: 5-30-91
Randall L. Janne
Manager, Nuclear Fuel

Approved: Ausaf Husain Date: 5/30/91
Ausaf Husain
Director, Reactor Engineering

ACKNOWLEDGEMENTS

This report is the result of a significant development effort in which numerous individuals participated. The Reactor Engineering Department expresses special thanks to Messrs. F. X. Statuti, D. W. Hiltbrand, H. B. Giap, W. J. Boatwright, and J. L. Westacott, for their contributions to the development of the analysis methodology presented in this report.

DISCLAIMER

The information contained in this report was prepared for the specific requirements of Texas Utilities Electric Company (TUEC), and may not be appropriate for use in situations other than those for which it was specifically prepared. TUEC PROVIDES NO WARRANTY HEREUNDER, EXPRESSED OR IMPLIED, OR STATUTORY, OF ANY KIND OR NATURE WHATSOEVER, REGARDING THIS REPORT OR ITS USE, INCLUDING BUT NOT LIMITED TO ANY WARRANTIES ON MERCHANTABILITY OR FITNESS FOR A PARTICULAR PURPOSE.

By making this report available, TUEC does not authorize its use by others, and any such use is forbidden except with the prior written approval of TUEC. Any such written approval shall itself be deemed to incorporate the disclaimers of liability and disclaimers of warranties provided herein. In no event shall TUEC have any liability for any incidental or consequential damages of any type in connection with the use, authorized or unauthorized, of this report or the information in it.

ABSTRACT

This report describes the TU Electric methodology for the analysis of the core response to steamline break events. A complete description of the regulatory bases, computer codes and models, and analytical techniques for the analysis of these events is provided for both at power and zero power steamline breaks. Representative analyses are presented to demonstrate the application of the TU Electric methods. Sensitivity studies are presented to identify key analysis parameters, justify analysis assumptions and techniques, and determine the limiting cases. It is concluded that the TU Electric methodology for steamline break analysis is acceptable for licensing applications.

TABLE OF CONTENTS

LIST OF TABLES

LIST OF FIGURES

CHAPTER 1

INTRODUCTION

1.1 Purpose

The purpose of this report is to describe and demonstrate the methodology intended to be used by TU Electric for analyzing the steamline break events (FSAR Sections 15.1.4 and 15.1.5). The steamline break events include transients initiated by either a failure of a steam dump, safety, or relief valve or by an actual rupture in the steam system. The methodology described in this report is applicable to the Comanche Peak Steam Electric Station (CPSES) and expands on transient analysis and core thermal hydraulic methodologies described previously [1,2]. Parametric studies are presented to demonstrate the sensitivity of the consequences of steamline break events to a variety of assumptions. The results of the sensitivity studies formulate the bases for the limiting case(s) which will be included in licensing submittals.

1.2 Description of the Event

The steam releases arising from either a failure of a steam dump, safety or relief valve or by an actual rupture in the secondary steam system would result in an initial increase in steam flow which decreases during the event as the steam pressure decreases. The increase in steam flow from the steam generators causes an increase in the energy removal rate from the Reactor Coolant System (RCS) and results in a reduction of coolant temperature and pressure. In the presence of a negative moderator temperature coefficient, the cooldown causes an increase in the core reactivity. The rate at which the core power increases to match the increased steam load demand is greatest when the reactivity coefficients are the

most negative (typically at the end of life in the fuel cycle).

If steamline break occurs while the reactor is at power, the core power increases from its initial level due to positive reactivity insertion from the RCS cooldown. The reactor will asymptotically approach a power level equal to the steam energy release rate unless terminated by a reactor trip and/or safeguards actuation. A low steamline pressure signal provides steamline isolation and safety injection actuation. The main steamline isolation valves (MSIVs) are closed on the steamline isolation signal. If a safety injection actuation occurs, the safety injection system pumps are started and the feedwater isolation valves are closed. For postulated breaks downstream of the MSIVs, the break flow would be stopped completely, terminating the transient. If the break is upstream of a MSIV, the break flow is terminated from all but one of the steam generators.

If the cooldown rate is large relative to the negative reactivity insertion from the safety injection system, the reactor may return to power, especially if a rod cluster control assembly (RCCA) is assumed to be stuck in its fully withdrawn position after reactor trip. The reactor power will ultimately decrease to the decay heat level as the steam blowdown decreases with the decreasing steam pressure and as the boron concentration in the RCS increases. The cooldown will terminate when the affected steam generator is dry. Normal plant cooldown will continue with auxiliary feedwater being supplied to the intact steam generators.

Should the reactor be subcritical at the time the steamline break occurs, the event would be similar to the at-power steamline break scenario following the reactor trip. However, the amount of stored energy with the RCS initially at hot

shutdown conditions is less than the amount of stored energy following a reactor trip from at-power conditions. Therefore, the RCS cooldown and resultant approach to criticality following a reactor trip from at-power conditions is less severe than a steamline break postulated to occur at initial hot shutdown conditions. A return to power following a steamline break is a potential problem mainly because of the high radial power peaking which may exist assuming the most reactive RCCA to be stuck in its fully withdrawn position.

1.3 Plant Description

CPSES is a two unit pressurized water reactor (PWR) site. Both units are Westinghouse designed four-loop plants with a rated core thermal power of 3411 MW_{th}. The Reactor Coolant System for each unit consists of four heat transfer loops connected in parallel to the reactor vessel. Each loop contains a Reactor Coolant Pump (RCP) and a steam generator. In addition, a pressurizer is connected to one of the four reactor coolant loops.

The steam generator design includes an integral steam outlet nozzle flow restrictor with an equivalent flow area of 1.4 [illegible]. The four main steamlines are interconnected through a pressure-equalizing header located downstream of the MSIVs. Each steamline is provided with one power-operated atmospheric relief valve (ARV) and five spring-loaded safety valves located upstream of the MSIVs.

A Reactor Protection System (RPS) is provided to monitor safety related parameters and to initiate appropriate actions necessary to bring the reactor to a safe condition if abnormal plant conditions occur. Signals from the RPS can actuate a reactor trip, safety injection, steamline isolation, and

feedwater isolation. Each of these provide a mitigative function for the steamline break event.

1.4 Summary

The information provided in this report demonstrates that TU Electric has developed an acceptable methodology for the analysis of steamline break events for licensing applications. The report is organized as follows:

Chapter 2 contains a discussion of the regulatory bases for the analysis of the steamline break events, including the identification of event acceptance criteria.

Chapter 3 provides a complete description of the TU Electric methodology, including computer codes and models, choice of analysis assumptions, and analytical techniques. Representative analyses are presented in this chapter to demonstrate the application of the methodology for both the at-power and zero power steamline break events. In addition, sensitivity studies are performed to justify the selection of various modeling techniques and input assumptions, to identify the parameters important to the steamline break event, and to determine the limiting analysis case(s).

The overall conclusions of the report are stated in Chapter 4. References are listed in Chapter 5.

A comparison of the representative TU Electric analysis to the current CPSES FSAR Analysis is presented in Appendix A.

CHAPTER 2

REGULATORY REQUIREMENTS

2.1 General Design Criteria

Title 10 of the Code of Federal Regulations [3], Part 50 (10CFR50), requires that a Final Safety Analysis Report (FSAR) be prepared which includes information that describes the facility, presents the design bases and limits of operation, and presents a safety analysis of the facility as a whole. The purpose of the safety analyses is to demonstrate that the reactor facility can be operated without undue risk to the public health and safety. Appendix A of 10CFR50 establishes the minimum requirements for the General Design Criteria (GDC) for nuclear power plants. The American National Standard "Nuclear Safety Criteria for the Design of Stationary Pressurized Water Reactor Plants," (ANSI N18.2-1973) [4], was developed to amplify the guidance provided by the GDC. Additional requirements beyond those contained in the GDC have been established by the Nuclear Regulatory Commission (NRC) and have been committed to in establishing the safety analyses for CPSES. These requirements (industry standards, regulatory guides, NUREGs, etc.) are documented in the FSAR [5] and the Safety Evaluation Report (SER) [6] issued by the NRC and form the licensing basis for CPSES.

An objective of 10CFR is to establish the requirements for the protection of the public health and safety from the uncontrolled release of radioactivity. The FSAR Chapter 15 safety analyses are performed to demonstrate that the consequences of the postulated transients and accidents do not exceed the established dose acceptance limits defined in the CFR. The NRC regulates the compliance with these dose limits under the provisions of 10CFR20 and 10CFR100, depending on the

expected frequency of occurrence of the event. 10CFR20 provides the requirements for determining maximum acceptable levels of radioactivity in restricted and unrestricted areas, while 10CFR100 provides Reactor Site Criteria in determining the maximum acceptable offsite doses.

A defense-in-depth design philosophy is employed to safely terminate and mitigate the consequences of transients and accidents. Section II of the GDC provides the criteria for protection by use of multiple fission product barriers. The three physical barriers that constitute the defense-in-depth philosophy are the fuel/clad, reactor coolant system, and containment. The FSAR Chapter 15 events are analyzed in terms of their effect on these physical barriers since there is a relationship between barrier integrity and dose. The specific effects of transients and accidents on the physical barriers are documented in Chapter 15 of the FSAR. Other sections of the GDC establish extensive requirements on the reactor protection and reactivity control systems, fluid systems, reactor containment, and fuel and radioactivity control. The GDC also requires that consideration be given to the single failure criterion and redundancy and diversity of mitigation and protection systems.

2.2 Event Classification

ANSI Standard N18.2-197[illegible] is used to classify plant conditions or incidents in accordance with their anticipated frequency of occurrence and consequences. The standard also provides general design requirements for each event category. The general principle applied in relating the general design requirements to the plant condition is that the most frequent occurrences should yield little or no adverse consequences to the public, and the improbable extreme situations, having the potential for the greatest adverse consequence to the public,

shall have a low probability of occurrence. The standard divides the spectra of plant conditions into four categories. These categories are:

1. Condition I: Normal Operation;
2. Condition II: Incidents of Moderate Frequency;
3. Condition III: Infrequent Faults; and,
4. Condition IV: Limiting Faults.

Condition I: Normal Operation

Condition I occurrences are operations that are expected frequently or regularly in the course of power operation, refueling, maintenance, or plant maneuvering. These occurrences shall be accommodated with margin between any plant parameter and the value of that parameter which would require either automatic or manual protective action.

Condition II: Incidents of Moderate Frequency

Condition II occurrences (or Anticipated Operational Occurrences) include incidents, any one of which may occur during a calendar year. There are several design requirements specified for Condition II events. These requirements are:

1. Condition II incidents shall be accommodated with, at most, a shutdown of the reactor with the plant capable of returning to operation after corrective action;

2. A Condition II event, by itself, cannot generate a more serious incident of the Condition III or IV type without other incidents occurring independently;

3. A Condition II event shall not cause consequential loss of function of any barrier to the escape of radioactive products;

4. Any release of radioactive materials in effluents to unrestricted areas shall be in conformance with 10CFR20.

Condition III: Infrequent Faults

Condition III occurrences include incidents, any one of which may occur during the lifetime of the plant. The following design requirements are associated with Condition III occurrences:

1. Condition III incidents shall not cause more than a small fraction of the fuel elements in the reactor to be damaged, although sufficient fuel element damage might occur to preclude resumption of operation for a considerable outage time;

2. The release of radioactive material resulting from a Condition III incident may exceed the dose guidelines of 10CFR20, but shall not be sufficient to interrupt or restrict public use of those areas beyond the exclusion radius; and,

3. A Condition III event shall not, by itself, generate a Condition IV fault or result in a consequential loss of function of the reactor coolant system or reactor containment barriers.

Condition IV: Limiting Faults

Condition IV occurrences are faults that are not expected to occur, but are postulated because their consequences would

include the potential for the release of significant amounts of radioactive material. Condition IV faults are the most limiting design cases (i.e., "Design Basis Accident"). Two design requirements are associated with Condition IV occurrences. These requirements are:

1. Condition IV faults shall not cause a release of radioactive material that results in an undue risk to public health and safety exceeding the guidelines of 10CFR100; and,

2. A single Condition IV fault shall not cause a consequential loss of required functions of systems needed to cope with the fault including those of the reactor coolant system and the reactor containment system.

2.3 Acceptance Criteria

The safety analysis approach used to define the acceptance criteria is to determine the limits on plant physical parameters which, if exceeded, could lead to a fission product barrier failure. The acceptance criteria provide a tangible means of evaluating the barrier performance with respect to the more generic criteria of the GDC. The FSAR Chapter 15 events are analyzed in terms of their effect on the physical barriers since there is a relationship between barrier integrity and dose.

While the value of the physical parameters (i.e., RCS pressure, temperature, etc.) for which barrier failure occurs may not be accurately known, the value does provide a reference point against which the margin to probable barrier failure can be measured. The acceptance limit is the value of a physical parameter which, if exceeded, would decrease the

confidence level in the integrity of the barrier. The amount of margin to the point of potential barrier failure is dependent upon the desired confidence level. The margin between the acceptance limit of a physical parameter and the point of probable (or assumed) barrier failure is defined as the "margin of safety." Thus, the GDC requirement to design with margin is satisfied by meeting the appropriate acceptance limit(s).

For example, GDC 20 requires that the protection system automatically initiate appropriate systems to assure that specified acceptable fuel design limits are not exceeded as a result of anticipated operational occurrences. This criterion can be satisfied by demonstrating that a reactor trip occurs in sufficient time to maintain the fuel/clad barrier integrity.

There are several aspects of the steamline break events which must be considered. If a Main Steam System depressurization occurs as a result of an inadvertent opening of a valve, the constraints imposed on Condition II events must be met. If an actual pipe rupture occurs in the Main Steam System, possible concerns regarding core integrity, dose releases, containment response, pipe whip, etc., must be considered. This report addresses only the issue of core integrity. The steamline break events presented within this report are categorized below with acceptance criteria specified for each classification.

Condition II: Incidents of Moderate Frequency

The accidental depressurization of the Main Steam System (FSAR Chapter 15.1.4) can be caused by the inadvertent opening, with failure to close, of either the steam dump, relief, or safety valve. The acceptance criteria for these ANS Condition II

events are established to preclude any fission product barrier degradation thus satisfying the limits of 10CFR20 and the GDC [7]. The specific acceptance criteria are as follows [8]:

1. There is at least a 95% probability that departure from nucleate boiling (DNB) will not occur on the limiting fuel rods at the 95% confidence level (95/95). DNB is evaluated in terms of the departure from nucleate boiling ratio, DNBR, which is the ratio of the predicted DNB heat flux calculated by an empirical correlation to the actual local heat flux. The criterion on DNBR is that the calculated minimum DNBR must not be less than the design limit value;

2. Pressures in the Reactor Coolant System and Main Steam System are maintained less than 110% [9] of their design limits. The CPSES Reactor Coolant System and Main Steam System design pressures are 2500 psia and 1200 psia, respectively; and,

3. There is at least a 95% probability that the peak kW/ft fuel rods will not exceed the UO_2 melting temperature at the 95% confidence level. By precluding UO_2 melting, the fuel geometry is preserved and possible adverse effects of molten UO_2 on the cladding are eliminated.

Condition III and IV: Infrequent and Limiting Faults

For an actual rupture of a pipe in the Main Steam System, the general criteria are that short-term and long-term core coolability are achieved [10], and that the offsite dose consequences must be within the guidelines of 10CFR100. A Main Steam System pipe rupture with an equivalent area of less than six inches in diameter is classified as an ANS Condition III event, while larger breaks are classified as ANS Condition

IV events. The specific acceptance criteria are as follows:

1. Although DNB and possible clad perforation are not necessarily unacceptable for the Condition III and IV steamline break events, the more restrictive acceptance criteria of satisfying the 95/95 DNB design basis is applied in evaluating the potential for core damage;

2. For the Condition III event, the offsite dose consequences must be a small fraction (interpreted as less than 10%) of the 10CFR100 guidelines of 25 REM whole body and 300 REM to the thyroid;

3. For the Condition IV event, the offsite dose consequences must be well within (interpreted as less than 25%) the 10CFR100 guidelines stated above; and,

4. The Reactor Coolant System and Main Steam System pressures must be maintained below acceptable design limits, considering potential brittle as well as ductile failures.

The acceptance criteria regarding the Reactor Coolant System and Main Steam System overpressurization are not challenged by the steamline break events since the characteristics of the transient result in a depressurization of both systems.

CHAPTER 3

METHOD OF ANALYSIS

Consistent with Regulatory Guide 1.70 [11] and NUREG-0800 [8, 12], the steamline break analysis methodology is developed considering various assumed initial conditions that are relevant to the event to ensure that the condition(s) leading to the most severe consequences have been identified. Generally, the parameters and assumptions which are important to the steamline break events are those which affect the cooldown rate, reactivity feedback, core power distribution, and operational characteristics of the Reactor Protection System (RPS) including the Engineered Safety Features Actuation System (ESFAS). The TU Electric analysis methodology for the steamline break events is described in this chapter. Representative analyses, and the sensitivity to various assumed initial conditions and modeling assumptions as well as break sizes and potential single failures are presented within this section.

3.1 Overview of Techniques

3.1.1 Steamline Break at Power

For the at power steamline break event, a spectrum of power levels and break sizes are considered to ensure that the condition(s) leading to the most severe consequences have been identified. An analytical approach consistent with that described in the transient analysis methods and the core thermal hydraulic methods topical reports [1, 2] is used to evaluate the steamline break event occurring while the reactor is at power. This transient is analyzed using two different computer codes. First, the RETRAN-02 computer code [13] is used to generate the system transient response. Then, the

VIPRE-01 computer code [14] is used to perform the DNBR analyses based on the system transient response from RETRAN-02.

3.1.2 Steamline Break at Hot Shutdown

The steamline break at hot shutdown transient is analyzed with three different computer codes. RETRAN-02 is used to model the system thermal hydraulic response to a steamline break. Statepoints of core power, reactivity, inlet temperature, flow, pressure, and boron concentration are generated for the transient. Since the system transient analysis is performed with a point kinetics model, reactivity checks are made incorporating spatial effects to ensure that the RETRAN-02 point kinetics model overpredicts the total change in reactivity, thus producing a conservative transient. The reactivity checks and core power distributions are calculated using the SIMULATE-3 three-dimensional full core neutronics code, based on the statepoints generated with RETRAN-02. The DNBR calculations are then performed with the VIPRE-01 code using the statepoints from the RETRAN-02 system thermal hydraulic analysis and the axial and radial power distributions from SIMULATE-3.

3.2 Computer Codes

RETRAN-02

The RETRAN-02 computer code is the principal analytical tool used by TU Electric to perform the system transient analysis portion of the steamline break events. RETRAN-02 was developed under the sponsorship of the Electric Power Research Institute (EPRI) to perform simulations of reactor system transients. RETRAN-02 has the flexibility to model many different accident scenarios and plant conditions. As such,

the NRC has stipulated in the Safety Evaluation Report (SER) for RETRAN-02 [15, 16] that each user describe their application of the code. TU Electric has previously described the application of RETRAN-02 to various accident analyses in reference 2. Further, TU Electric has used RETRAN-02 to perform the analysis of the Steam Generator Tube Rupture event [17] currently presented in the CPSES FSAR. This report describes the application of RETRAN-02 to the steamline break event.

VIPRE-01

The VIPRE-01 computer code [14] is the principal analytical tool used to perform the reactor core thermal hydraulic analyses. VIPRE-01 was developed under the sponsorship of EPRI to perform reactor core thermal hydraulic analyses involving the calculations of heat flux, fluid conditions, and DNBR. With the VIPRE-01 code, the reactor core can be modeled as a number of quasi-one-dimensional flow paths or channels that communicate laterally by diversion crossflow and turbulent mixing. Equations for conservation of mass, momentum (axial and lateral), and energy are solved to predict the liquid enthalpy, axial flow rate, lateral flow rate per unit length, and momentum pressure drop for each core region. The VIPRE-01 code can perform both steady-state and transient analyses using time dependent boundary conditions for core inlet flow and enthalpy, system pressure, and core power as input.

SIMULATE-3

All neutronics calculations use the SIMULATE-3 three dimensional, two group core simulator computer code. The CASMO-3/TABLES-3 computer codes provide cross sections for input to SIMULATE-3. These codes and their use in TU Electric

methodology are discussed in reference 18. The particular features of SIMULATE-3 which are important to the steamline break analysis include pin power reconstruction and non-uniform core inlet temperature and flow distribution.

3.3 Steamline Break at Power

The steamline break transient occurring while the reactor is at power results in an increase in the core power from its initial level due to the positive reactivity insertion from the RCS cooldown. The reactor will asymptotically approach a power level equal to the steam energy release rate unless terminated by a reactor trip and/or safeguards actuation. The initial power level, turbine load demand, reactivity feedback, and break size are the primary parameters which influence the course of the steamline break transient.

The purpose of the evaluation of the steamline break event occurring while the reactor is at power is to demonstrate that the plant protection systems perform their intended function to protect the core against overpower conditions prior to reactor trip. Following the reactor trip and steamline isolation, a single steam generator may continue to blow down if the break is located upstream of the MSIV. Although the reactor may return to power as a result of the continued cooldown, this phase of the transient is bounded by the steamline break initiated at hot shutdown conditions. This is due to the greater amount of stored energy in the RCS following a reactor trip from power compared to the initial hot shutdown condition stored energy.

3.3.1 Calculational Models

3.3.1.1 System Thermal Hydraulic Analysis

For steamline breaks occurring while the reactor is at power, the turbine load controller maintains a constant steam flow to the turbine by opening the turbine control valve as the steam pressure decreases. The steam flow to the turbine will continue until a turbine trip or steamline isolation occurs. Steamline breaks occurring while the reactor is at power will thus result in a near uniform blowdown of all four steam generators prior to closure of the main steam isolation valves. Therefore, a single-loop version of the RETRAN-02 model [2] is used for the at-power steamline break analyses.

The CPSES RETRAN-02 system model includes representations of both the primary and the secondary coolant systems. The primary system models include representations for all of the RCS piping and the reactor coolant pumps, a non-equilibrium pressurizer model (including a separate surge line) with relief and safety valves, and a detailed reactor vessel model. The secondary system components modeled include the steam generators, the steam piping to the turbine, main and auxiliary feedwater, and various isolation and relief valves. All protection and control systems important to the plant transient response have been modeled (including the turbine load controller). A point kinetics model is used to simulate the core power response to reactivity changes resulting from variations in boron concentration, control rod position, fuel temperature, and coolant density. A DNBR evaluation model is incorporated into the RETRAN-02 system model to monitor the DNBR trend during the event. However, compliance with the DNB acceptance criterion is demonstrated using the detailed TU Electric core thermal hydraulic methodology [1].

A modification to the RETRAN-02 model described in Reference 2 was made for the steamline break at power analyses. To allow for a constant steam exit quality of 100% throughout the transient, the steam generator secondary side model is represented by a single saturated volume. This model maximizes the effluent enthalpy and thus maximizes the energy removal. In addition, a dry steam blowdown removes less mass from the steam generator, keeping the overall primary-to-secondary heat transfer coefficient constant near the nominal value for an extended period of time. A noding diagram of the RETRAN-02 system model used for the at-power steamline break analyses is shown in Figure 3.3-1.

3.3.1.2 Core Thermal Hydraulic Analysis

The CPSES VIPRE-01 core thermal hydraulic model used to perform the DNBR analyses for the at-power steamline break events is based on the model described in Reference 1. The CPSES VIPRE-01 model was developed in accordance with the modeling guidelines in the VIPRE-01 code manuals [14] and the modeling requirements specified in the VIPRE SER [19]. A summary of the CPSES VIPRE-01 model is provided in Table 3.3-1.

3.3.2 Analytical Methods

This transient is analyzed using the RETRAN-02 and VIPRE-01 computer codes. First, the RETRAN-02 computer code is used to generate the system transient response using the 1-loop system model described in Section 3.3.1.1. This portion of the analysis determines the steam flow, RCS cooldown, reactivity, core power, and pressure transient, in addition to the time of reactor trip. Then, the VIPRE-01 computer code is used to perform the DNB analyses based on the system transient response from RETRAN-02.

From the RETRAN-02 calculated system response, statepoints are generated. The statepoints are a tabulation of core average heat flux, core inlet temperature, and pressure at a given instant in the transient. A conservative steady state core thermal hydraulic analysis is performed using the statepoints provided by the RETRAN-02 system transient analysis as boundary conditions. The DNB analysis uses the statepoint boundary condition(s) which correspond to the most limiting set of conditions, with respect to DNB, at a given point in the transient (e.g., the conditions at the time of peak heat flux). The DNBR evaluation model incorporated within the RETRAN-02 system model provides the DNBR trend during the event to assist in the selection of the limiting statepoint condition(s).

As discussed in Section 2.3, the following acceptance criteria are applied to this event:

1. The minimum DNBR remains greater than the 95/95 design limit;
2. Fuel centerline temperatures do not exceed the melting point.

Three cases at initial power levels of 102%, 70%, and 30% are analyzed. The initial conditions, reactivity parameters, and system performance characteristics are selected to be conservative relative to the event acceptance criteria.

A spectrum of break sizes ranging from approximately 0.025 ft^2 per loop to 1.4 ft^2 per loop is considered for each power level analyzed. The upper limit on the break size corresponds to the effective area of the integral steam outlet nozzle flow restrictor for the steam generators. The lower limit is chosen to encompass the FSAR Chapter 15.1.3 Excessive Increase

in Secondary Steam Flow event (10% step load increase) which does not result in or require an automatic reactor trip.

3.3.2.1 Transient Simulation

The steam flow from the steam generator or steamline is calculated using the Moody [20] correlation incorporated in the RETRAN-02 code with an additional assumption of a contraction coefficient equal to 1.0. The break is simulated by adding a junction with a valve, to the first main steam volume downstream of the steam generator, that discharges to the atmosphere (14.7 psia). Steam flow to the turbine is assumed to continue at its initial rate to simulate the turbine load controller. The turbine load controller maintains a constant steam flow to the turbine by opening the turbine control valve as the steam pressure decreases. The steam flow to the turbine will continue until a turbine trip or steamline isolation occurs.

3.3.2.2 Analysis Assumptions

The initial operating conditions assumed in these analyses are the most adverse with respect to the margin to DNB consistent with steady state operation. The conditions include allowances for calibration and instrument errors, i.e., minimum pressure, maximum coolant average temperature, and minimum RCS flow rate. The greatest reactivity insertion and resultant power increase as a result of a steamline break occurs when the reactivity coefficients are the most negative (typical of end of life conditions). Therefore, maximum moderator and doppler reactivity feedback is used in the analysis. Consistent with the current licensing basis [5] and the philosophy described in Reference 1, control system operations are assumed only when action normally taken by the control system results in a more severe event consequence.

The control systems of interest for the steamline break event are discussed below:

1. Pressurizer Pressure Control System - A steamline break results in a cooldown and depressurization of the RCS. A greater RCS depressurization and a conservative prediction of the minimum DNBR would result without pressurizer heater operation. Therefore, no credit is taken for their operation. The pressurizer PORVs will not be actuated during the event since the pressure decreases from event initiation.

2. Pressurizer Level Control System - The operation of the Chemical and Volume Control System (CVCS) would increase the RCS mass and thereby maintain pressurizer level and pressure. Therefore, no credit is taken for the operation of the CVCS.

3. Turbine Control System - The turbine load controller is simulated to maintain a constant steam flow rate to the turbine as the steam pressure decreases.

4. Steam Generator Water Level Control System - The steam generator water level control system is modeled by matching the feedwater flow rate to the increased steam flow rate, thus producing an increased amount of heat extraction in the steam generator. This assumption also ensures that a conservative overall heat transfer coefficient is predicted throughout the event by preventing any tube bundle uncovery.

5. Reactor Control System - Operation of the Reactor Control (or Rod Control) system, due to a mismatch in the turbine and reactor power, would lessen the severity of the event. The reactor power increases due to the reactivity

feedback, while the turbine power remains constant at the initial value or decreases as the load controller reaches its limit. These effects would result in an insertion of the control rods and thereby lessen the event consequences. However, the limiting break size (the one which produced the lowest DNBR) is analyzed with automatic rod control to study the effects.

The Reactor Protection System functions to mitigate the consequences of the steamline break event. The specific reactor trip function which provides the protection depends on the initial power level and the break size. The reactor trips which provide the primary protection for a steamline break are:

1. Safety Injection Signal on low steamline pressure,
2. Overpower N-16,
3. Overtemperature N-16,
4. Low pressurizer pressure and,
5. High neutron flux.

The various setpoints and time delays for the RPS are selected to provide sufficient operating margin to prevent spurious actuations, yet still provide adequate reactor protection. The difference between the limiting trip setpoint assumed for the analysis and the nominal Technical Specification setpoint represents an allowance for instrumentation channel error and setpoint error.

Various instrumentation delays are associated with each trip function, including delays in signal actuation, in opening the trip breakers, and in the release of the rods by the control rod drive mechanisms. The total delay to trip is defined as the time delay from the time that trip conditions are reached to the time the rods are released and begin to fall.

No single active failure in any system or component required for mitigation will adversely affect the consequences of this event.

The rate of negative reactivity insertion following a reactor trip is a function of the acceleration of the rod cluster control assemblies and the variation in rod worth as a function of rod position. The trip insertion characteristics are based on the assumption that the highest worth control rod is stuck in its fully withdrawn position, and a conservative differential rod worth based on a highly bottom skewed axial power shape.

The detailed VIPRE-01 core thermal hydraulic analysis uses the statepoint condition(s) generated by RETRAN-02 as boundary conditions in addition to design values for the core axial and radial power distributions (typically, 1.55 chopped cosine and 1.55 $F_{\Delta H}$). The core axial power distribution used in the analysis is consistent with the calculational bases for the Overtemperature and Overpower N-16 trip setpoints [21]. For the cases initiated at the lower power levels, the design value of $F_{\Delta H}$ is adjusted to allow for control rod insertion causing a more peaked radial power profile.

3.3.3. Results

The at-power steamline break events have been analyzed using the TU Electric analysis methodology described in the previous sections. The input assumptions used in the analyses are typical of those used in FSAR type analyses and reflect the current CPSES design bases. Table 3.3-2 summarizes the input assumptions used in the analyses. The limiting trip setpoints and time delays assumed for the RPS functions for the steamline break analysis are given in Table 3.3-3.

To demonstrate compliance with the DNBR acceptance criterion, the TUE-1 critical heat flux correlation was used. The TUE-1 correlation has a 95/95 DNBR limit of 1.16 [22, 23]. As described in the core thermal hydraulic methods topical [3], a TUE-1 DNBR design limit value will be specified which is higher than the correlation limit to provide for sufficient margin to offset anticipated DNBR penalties. The selection of the TUE-1 DNBR design limit value is beyond the scope of this report. However, a TUE-1 DNBR design limit of 1.35 is selected for illustrative purposes.

Compliance with the fuel centerline melt acceptance criterion is demonstrated by comparing the linear heat generation rate (LHGR) at the core hot spot to the maximum limiting LHGR which does not result in fuel centerline melt. A core thermal overpower limit of 118% has been demonstrated to preclude fuel centerline melting independent of the core axial power distribution effects [21].

The effects of various break sizes and power levels have been analyzed. The results show that any at-power steamline break event falls into one of three categories, depending upon the initial power level and break size. The first category of steamline break events has the ESFAS as the primary source of reactor protection. The second category has the Overpower or Overtemperature reactor trips actuated for primary protection. And, the third category does not require any automatic reactor protection system actuation to mitigate the event.

Following any steamline break, the steam generators depressurize due to the increased steam flow and resultant increase in feedwater flow in response to a steam/feedwater flow mismatch. The increased heat transfer rate in the steam generators causes a cooldown of the RCS. With a negative

moderator temperature coefficient, the core power increases from its initial value due to the positive reactivity caused by the RCS cooldown. During this period, the margin to the RPS and ESFAS setpoints decrease.

The results for the 102% initial power cases show that for break sizes of 0.29 ft^2 per loop or larger, the primary source of protection is the ESFAS. Figures 3.3-2 and 3.3-3 show the plant transient response to a steamline break representative of this category (a 0.50 ft^2 per loop break), and Table 3.3-4 provides the sequence of events. For cases that fall within this category, the rapid steam generator depressurization generates an ESFAS low steamline pressure signal which actuates safety injection, thus providing a reactor trip. For the 0.29 ft^2 per loop break case (the smallest break size in this category) the low steamline pressure signal is generated within 8.0 seconds. The rather quick generation of the low steamline pressure signal does not allow a significant RCS cooldown prior to the reactor trip. Therefore, the reactor power increases only a small amount prior to the trip. The minimum DNBR during the event occurs at the time of the rod motion from reactor trip and remains well above the 1.35 acceptance limit. The peak thermal power also remains well below 118% of nominal power, thus precluding any fuel centerline melting.

For the second category of steamline break cases, a reactor trip is generated by the Overpower N-16 trip function prior to reaching a low steamline pressure signal. Figures 3.3-4 and 3.3-5 show the plant transient response to a steamline break representative of this category (0.285 ft^2 per loop break), and Table 3.3-5 provides the sequence of events. The cases within this second category are characterized by a slower steam generator depressurization than those cases within the first category. Thus, the RCS can experience a greater

cooldown, resulting in a more substantial reactor power increase compared to those cases within the first category. As shown in the figures, the Overpower N-16 reactor trip occurs in time to prevent the core thermal power from exceeding 118% of nominal power, and the minimum DNBR remains above the 1.35 acceptance limit.

The steamline break cases within the third category do not result in (or require) any automatic RPS actuation. Figures 3.3-6 and 3.3-7 show the plant transient response to the largest steamline break which falls within this category (0.0625 ft^2 per loop), and Table 3.3-6 provides the sequence of events. The cases within this category are very similar to the Excessive Increase in Secondary Steam Flow transient (FSAR Chapter 15.1.3) analyzed in Reference 1. The transient response shows that the reactor power asymptotically approaches a power level equal to the steam energy release rate. The DNBR decreases from its initial value reflecting the higher equilibrium power, but remains well above the 1.35 acceptance limit. The core thermal power does not reach 118% of nominal power during the event.

The results of the 102% initial power cases are summarized in Figure 3.3-8 for the spectrum of break sizes analyzed. The maximum steam flow rate, peak core thermal power, and minimum DNBR are shown as a function of the break area per loop. The summary results show that none of the cases violate the DNBR acceptance limit of 1.35 and the thermal overpower limit of 118% of nominal. The limiting break size which yields the lowest DNBR for the 102% initial power cases corresponds to that which provides essentially a simultaneous low steamline pressure and Overpower N-16 protective function.

The results of the 70% and 30% initial power cases exhibit similar trends as those in the 102% initial power cases over

the spectrum of break sizes considered. The 70% initial power cases fall into one of the three categories previously described, but the 30% initial power cases do not have the second category of cases (those which trip on Overpower N-16). The break size spectrum for each category is different for the partial power cases than the 102% power cases due to the additional margin to the RPS trip functions at the lower power levels.

Figures 3.3-9 through 3.3-14 illustrate the transient response for the 70% initial power cases for a representative break size within each category, and Tables 3.3-7 through 3.3-9 provide the sequence of events. Figures 3.3-15 through 3.3-18 show the transient response for the 30% initial power level cases for a representative break size within the first and third categories, and Tables 3.3-10 and 3.3-11 provide the sequence of events.

A summary of the maximum steam flow, peak heat flux, and minimum DNBR results for the 70% and 30% initial power cases is provided in Figure 3.3-19, along with the summary of the results for the 102% initial power cases for comparative purposes. As can be seen from this summary figure, the 102% initial power level represents the limiting initial power level for evaluating the steamline break at power events.

The limiting 102% initial power case was also analyzed with automatic rod control, and the results are shown in Figures 3.3-20 and 3.3-21. The reactor power increase, due to the moderator reactivity feedback, causes a mismatch between the turbine and reactor power resulting in the stepping in of the control rods. The automatic rod control operation thus limits the power increase resulting in a higher DNBR and a less severe transient.

3.3.4 Summary

The at-power steamline break events have been analyzed using the analytical techniques described in Section 3.3.2, and input assumptions typical of FSAR analyses. Sensitivity studies were performed on the initial power level and break size to ensure that the limiting at-power steamline break event was considered. For all of the cases analyzed, the calculated minimum DNBR remained above the design limit value and the peak thermal power did not exceed the 118% limit value. The results of this study show that the limiting power level, with respect to the event acceptance criteria, is 102% power. It was also shown that the primary reactor protection function for event mitigation is dependent upon the break size. Generally, the larger breaks (greater than approximately 0.3 ft^2 per loop) are not limiting due to the quick generation of a low steamline pressure safety injection signal. Intermediate break sizes (between about 0.1 ft^2 and 0.3 ft^2 per loop) are typically the limiting cases since they result in the highest overpower situation relying on the Overpower N-16 reactor trip function. The breaks within this category provide enough of a steam release to result in a relatively high core power increases, but not a low steamline pressure signal. The smaller steamline breaks (less than about 0.1 ft^2 per loop) generally do not result in or require a reactor trip, and therefore are not limiting.

3.4 Steamline Break at Hot Shutdown

With the reactor subcritical, either initially or due to a reactor trip from power, a steamline break could potentially cause the reactor to approach or return to critical due to an excessive cooldown and loss of shutdown margin. However, the amount of stored energy with the RCS initially at hot shutdown conditions is less than the amount of stored energy following

a reactor trip from at power conditions. Therefore, the RCS cooldown and resultant approach to criticality following a reactor trip from at power conditions is less severe than a steamline break postulated to occur at initial hot shutdown conditions. A return to power following a steamline break is a potential problem mainly because of the high radial power peaking which may exist assuming the most reactive RCCA to be stuck in its fully withdrawn position. Protection for the steamline break from initial hot shutdown conditions is provided by the safety injection and steamline isolation functions.

3.4.1 Calculational Models

3.4.1.1 System Thermal Hydraulic Analysis

The RETRAN-02 computer code is used to perform the system transient analysis portion of the steamline break analysis. If a steamline break is postulated to occur upstream of a MSIV or should a single MSIV fail to close, the break flow would be terminated in all but one of the steam generators. Due to this asymmetry, a multi-loop version of the CPSES RETRAN-02 system model is used to analyze the effects of the potential loss of shutdown margin and resultant criticality.

A two-, three-, or four-loop version of the CPSES RETRAN-02 system model as described in Reference 1 can be used to model the asymmetric aspects of the steamline break event occurring from initial hot shutdown conditions. To model the various main and auxiliary feedwater flow conditions, a four-loop system model is used (shown in Figure 3.4-1).

The following modifications to the multi-loop RETRAN-02 model described in reference 1 were made for the analysis of the steamline break at hot shutdown:

Steam Generator/Main Steam System

The steam generator heat transfer model couples the excessive steam release to the RCS transient. The heat transfer in the steam generator depends on the overall primary-to-secondary heat transfer coefficient (UA). To obtain a conservative UA throughout the transient, several steam generator modeling changes are made to the CPSES RETRAN-02 model in Reference 1. First, as in the at-power steamline break analyses, the steam generator secondary side model was modified to be represented by a single saturated volume to allow for a constant steam exit quality of 100%. A second modification was made to reduce the effective steam generator tube bundle height to delay any possible tube bundle uncovery during the event. The combination of a one-node secondary side steam generator model with a dry steam blowdown and reduced tube bundle height results in a conservatively high energy removal rate which maximizes the severity of the core transient. For simplicity, the steamlines are not modeled. Each steam generator has junctions to model the feedwater, auxiliary feedwater, steam flow (at initialization), safety valves, and the break flow.

Reactor Vessel

The eight volume reactor vessel model in Reference 1 is modified to a fifteen volume model to account for the effects of the coolant asymmetries during the steamline break event. The downcomer, lower plenum, core, and upper plenum are each divided into two volumes. The volume associated with the faulted loop represent 25% of the total volume, and the volume associated with the intact loops represent 75% of the total volume. The core heat conductors are also divided in accordance with the 75%/25% split used for the volume representation.

The core region is split into two channels to allow for a weighting of the reactivity feedback effects. The lower and upper plenum volumes are divided to provide for coolant mixing among the loops. Separate downcomer volumes are provided for the intact loop and faulted loops to provide complete separation of the fluid conditions (i.e., no mixing is assumed in the downcomer annulus). The reactor vessel upper head dead volume is split horizontally to provide a better representation of the relatively stagnant flow in this region. Flow exists from the dead volume to the upper plenum volume through a zero resistance junction. This assumption conservatively delays the refill of the upper head following the rapid depressurization and flashing of the fluid in this region.

Reactor Vessel Mixing

The coolant from the various reactor coolant loops begins to mix upon entry into the reactor vessel. The interloop mixing occurs in the downcomer, lower plenum, core region, and upper plenum as the coolant travels through the vessel. In the steamline break event in which a single steam generator continues to blow down following steamline isolation, potentially large temperature differences can occur between the affected and unaffected loops. Without complete interloop mixing, the colder water associated with the affected loop flows primarily through the core sector closest to that reactor vessel inlet.

The reactor vessel mixing model developed for use in the steamline break analysis can simulate any degree of mixing within the lower and upper plena through the use of user specified mixing fractions. Independent inputs for the lower and upper plena are used in the model to vary the degree of mixing from "no mixing" to "perfect mixing". "Perfect mixing"

for the core inlet refers to the instantaneous complete thermal mixing of the coolant entering the reactor vessel from the affected and unaffected reactor coolant loops. "No mixing" for the core inlet signifies that the coolant in the affected reactor coolant loop flows through its associated core sector without any thermal mixing with the fluid from the unaffected loops. Similar definitions apply to the outlet plenum mixing with the exception that the coolant flow is from the core region and into the hot-leg piping.

The modeling of the mixing in the plena is controlled by transferring heat between the two lower (or two upper) plenum volumes through a nonconducting heat exchanger to achieve the desired core inlet fluid conditions. This mixing model thus provides the capability to simulate unique core inlet conditions for the sectors of the core associated with the affected and unaffected reactor coolant loops.

Reactor Kinetics

The RETRAN-02 code utilizes a point kinetics model to simulate the core power response to reactivity changes resulting from variations in coolant density, fuel temperature, and boron concentration. The values of the physics parameters used in the point kinetics model are calculated using the three-dimensional, two-group core simulator code SIMULATE-3 (see Section 3.4.1.2).

The reactor vessel mixing model provides unique core inlet conditions for the core sectors associated with the affected and unaffected loops. Further, it is assumed that the core power distribution is uniform (consistent with the 75%/25% volume split) which causes an underprediction of the reactivity feedback in the high power region near the stuck rod. The core channel average coolant properties are

calculated in the system model for each sector and are combined to provide the core average coolant properties for use in the point kinetics model. The combining of the affected and unaffected core channel properties include weighting factors which place greater importance on the affected channel. Thus, the RETRAN-02 point kinetics model is conservative with respect to the three-dimensional neutronics calculations.

Engineered Safety Features Actuation System

During the course of a steamline break, the ESFAS is actuated to mitigate the consequences of the event. The ESFAS functions include steamline isolation, feedwater isolation, and safety injection, all of which are simulated in the RETRAN-02 system model. The setpoints and time delays for the ESFAS are selected to provide sufficient operating margin to prevent spurious actuations, yet still provide adequate reactor protection.

There are several delays inherent to the operation of the safety injection system, which must be accounted for in the analysis, before the borated water from the Refueling Water Storage Tank (RWST) reaches the core. Time delays for signal processing, pump startup, valve positioning, and emergency diesel startup (if offsite power is lost) are considered in the analysis. In addition, the low concentration boric acid solution must be purged from the safety injection lines before the borated water from the RWST reaches the core.

The safety injection into the RCS cold legs is modelled with fill junctions where the injection flow rate is dependent upon the cold leg pressure (see Figure 3.4-2). Included in the system model is a calculation of the integrated safety injection flow to determine the time to purge the unborated

water from the safety injection system lines. This purge time calculation requires that a complete volume replacement of the fluid in the safety injection lines occur before any boron is injected into the reactor coolant system.

3.4.1.2 Nuclear Analysis

The core neutronic analysis provides the reactor physics input (Doppler and moderator density reactivity defects, and boron worth) for the system transient analysis, and the core axial and radial power distributions for the DNB analysis. Further, this analysis quantitatively confirms the conservatism of the net reactivity change predicted by the RETRAN-02 point kinetics model for the transient.

The reactor response to the steamline break transient is relatively slow, permitting SIMULATE-3 steady state calculations at selected statepoints. The SIMULATE-3 calculation models the full core in three dimensions. All calculations supporting the steamline break analysis assume end of life (EOL) core conditions (when the moderator temperature coefficient is the most negative). All control rods are assumed to be fully inserted, with the exception that the most reactive control rod is stuck in the fully withdrawn position. In addition, the coldest core inlet temperature associated with the affected reactor coolant loop is assumed to occur in the sector with the stuck rod.

The Doppler and moderator density defects and boron worth, provided for use in the systems transient analysis, have added conservatism which accounts for the minimum uncertainty in neutronics parameters as identified in Reference 18. The Doppler defect is determined as a function of the core average fuel temperature, and the moderator density defect is calculated as a function of the core average moderator

density. Typical curves of the Doppler and moderator density defects for use in the system transient analysis are shown in Figures 3.4-3 and 3.4-4, respectively.

Statepoint calculations are performed with SIMULATE-3 to confirm the conservatism of the net reactivity change predicted by the RETRAN-02 point kinetics model during the transient. The statepoints generated by the RETRAN-02 analysis are a tabulation of the nuclear power, core average heat flux, affected and unaffected core sector inlet conditions (temperature and mass flow rate), boron concentration, and system pressure during the transient. The effects of non-uniform core inlet conditions are included in the model. The calculations assume the reactor is initially at hot zero power conditions with all rods except the most reactive fully inserted, and boron and xenon free. The boron and xenon free assumption results in an initial shutdown margin approximating that assumed in the system transient analysis. The change in reactivity from the start of the transient to the statepoint condition generated from the RETRAN-02 analysis is determined. The net change in reactivity predicted with the SIMULATE-3 model is verified to be less than that predicted by the RETRAN-02 point kinetics model, thus ensuring conservatism in the analysis.

The DNB analysis for this event requires radial and axial power distributions. The core calculations which confirm the conservatism of the net reactivity prediction also provide the necessary power distributions for the DNB analysis. The distributions computed include the assembly average radial power distribution for the whole core, and the pin power distributions within the hot assembly for the hot typical, hot thimble, and surrounding channels. The axial power distributions provided are for the core average, hot assembly, and peak pin within the hot assembly. Illustrations of the

power distributions are shown in the discussion of the results of the analysis (Section 3.4.2.3).

When radial power peaking is expected to be more severe than normal operating conditions, an augmentation factor is applied to $F_{\Delta H}$. The augmentation factor is defined as the ratio of the design $F_{\Delta H}$ limit to the maximum calculated $F_{\Delta H}$ at normal full power conditions. For the steamline break transient, the augmentation factor is calculated at end of life. This augmentation factor is applied to the calculated relative integral power of each of the hot fuel pins.

3.4.1.3 Core Thermal Hydraulic Analysis

The VIPRE-01 computer code [14] is used to perform the reactor core thermal hydraulic analyses. The VIPRE-01 code uses the RETRAN-02 statepoint boundary conditions for core inlet temperature and flow, system pressure, and core thermal power as input. In addition, core axial and radial power distributions from SIMULATE-3 are input to VIPRE-01.

The CPSES VIPRE-01 core thermal hydraulic model used to perform the DNB analyses for the steamline break at hot shutdown is a modified version of the base model described in Reference 2. The modifications are made to account for the non-uniform core inlet conditions and highly peaked radial power distribution typical of the steamline break at hot shutdown. The modifications to the base model are discussed below, and a summary is provided in Table 3.4-1.

As in the base model, a single-stage analysis is performed where subchannels and fuel assemblies are modeled in one simulation. Since it is not necessary to model individual assemblies far removed from the high power region of the core, lumped channels representing these assemblies are simulated.

A thirty-one channel model, which consists of eighteen subchannels and thirteen lumped channels, is used to represent the reactor core as shown in Figure 3.4-5 and 3.4-6. The eighteen subchannels include a hot standard channel (Channel 12), a hot thimble channel (Channel 7), and sixteen subchannels bordering the hot channels (Channels 1-6, 8-11 and 13-18). The standard channels contain four fuel rods, and the thimble channels contain three fuel rods and a thimble guide tube. The hot channels contain the peak power rod(s) in the hot assembly. Two lumped channels (19 and 20) border the sixteen subchannels and the remaining channels in the hot assembly are lumped into one channel (Channel 21). The eight assemblies surrounding the hot assembly are each individually modeled with a single lumped channel (Channels 22 - 29). The remaining assemblies in the core quadrant, and in the rest of the core, are lumped into single channels (Channels 30 and 31, respectively).

As described in Reference 2, a dummy rod model is used to represent the fuel rods for steady state DNB analysis. The rod surface heat flux is specified as an input parameter based on the RETRAN-02 statepoint boundary conditions. A uniform six-inch axial nodal length is specified along the fuel rods for consistency with the SIMULATE-3 calculation of the axial power distribution. SIMULATE-3 provides separate axial power distributions for the hot fuel rod, hot assembly, and core average, all of which can be directly used in the VIPRE-01 model. Each fuel rod is also assigned a radial power factor that determines the rod power relative to the average core power. The SIMULATE-3 calculations provide the radial power distribution used in the VIPRE-01 analysis for each assembly in the core in addition to the individual rod power distribution within the hot assembly. Other than the modifications described, the CPSES VIPRE-01 model remains unchanged.

3.4.2 Analytical Methods

The methodology for the analysis of the steamline break event at hot shutdown conditions is outlined in the calculational flow diagram shown by Figure 3.4-7. This transient is analyzed using three different computer codes. First, the RETRAN-02 computer code is used to generate the system transient response using the multi-loop system model described in Section 3.4.1.1. This portion of the analysis is performed to generate the statepoint conditions for use in the nuclear analysis and core thermal hydraulic analysis. The SIMULATE-3 code is then used to calculate the axial and radial power distributions based on the statepoint conditions from RETRAN-02. The RETRAN-02 statepoint conditions and the SIMULATE-3 core power distributions are then used in the VIPRE-01 code to perform the DNB analyses. The SIMULATE-3 calculations also confirm that the net change in reactivity from the event initiation to the statepoint condition is less than that predicted by the RETRAN-02 point kinetics model.

3.4.2.1 Transient Simulation

The break is simulated by using a junction and valve added to each of the steam generator secondary volumes (steamlines are not modeled). The break junctions on each steam generator are opened at event initiation allowing critical flow from the steam generators discharging to the atmosphere (14.7 psia). The steam flow from the steam generator is calculated using the Moody correlation [20] incorporated in the RETRAN-02 code with an additional assumption of a contraction coefficient equal to 1.0. For a hypothetical double-ended rupture simulation, the break valves on three of the intact loops close upon receipt of a steamline isolation signal, while the blowdown continues through the break valve on the affected

loop. Further discussion on break sizes, types, and location is included in Section 3.4.2.3.

3.4.2.2 Analysis Assumptions

The analysis is performed using initial conditions, reactivity parameters, and system performance characteristics which are conservative relative to the event acceptance criteria. These assumptions are consistent with those used in the FSAR Chapter 15.1.4 and 15.1.5 steamline break analyses. The reactor is assumed to be initially at hot shutdown conditions since this represents the most pessimistic initial condition. Should the reactor be just critical or operating at-power at the time of the steamline break, the reactor will be tripped by the RPS as demonstrated earlier in Section 3.3. Following the trip from at-power, the RCS contains more stored energy than at no-load conditions, the coolant average temperature is higher than at no-load, and there is appreciable energy stored in the fuel. Thus, the additional stored energy must be removed via the cooldown caused by the steamline break before the no-load conditions of RCS temperature and shutdown margin are reached. After the additional stored energy has been removed, the cooldown and reactivity insertions proceed in the same manner as in the analysis which assumes no-load condition at time zero.

As discussed in Section 2.3, the more restrictive acceptance criterion of satisfying the 95/95 DNB design basis is applied in evaluating the potential for core damage. The TUE-1 correlation [22, 23] is used to evaluate the DNBR for those cases where the pressure remains greater than or equal to 1500 psia (the lower limit of the TUE-1 correlation), and the W-3 correlation [24, 25] is used for those cases where the pressure is less than 1500 psia. Consistent with the at-power steamline break DNB analyses, the TUE-1 DNBR design limit of

1.35 is selected for illustrative purposes. The W-3 correlation has been approved by the NRC [26] for analysis with system pressures as low as 500 psia, with a 95/95 design limit of 1.45. An independent confirmation of the 95/95 design limit was performed using the VIPRE-01 code and low pressure test data [27]. The results indicate that the VIPRE-01 code adequately predicts the DNBR with a 95/95 design limit of 1.45.

The following conditions are assumed for the steamline break analysis:

1. The reactor is at hot shutdown conditions with no decay heat. Any decay or residual heat would retard the cooldown;

2. A minimum EOL shutdown margin at no-load conditions with the most reactive control rod stuck in its fully withdrawn position is assumed. The shutdown margin used in the analysis is consistent with the plant Technical Specifications;

3. The moderator density and Doppler defects correspond to an EOL rodded core with the most reactive rod in the fully withdrawn position;

4. The core properties associated with the affected and unaffected sectors of the core are conservatively combined to obtain average core properties for use in the point kinetics model (50% of the reactivity feedback is weighted to the affected quadrant of the ccre);

5. A conservatively small amount of interloop mixing is assumed. The affected core inlet sector is assumed to receive 80% of its flow from the faulted loop and 20%

from the intact loops. The affected core outlet sector flow to the faulted loop is assumed to remain 73% unmixed and 27% mixed;

6. Minimum capability for injection of concentrated boric acid solution corresponding to the most restrictive single failure in the Safety Injection System is assumed. Of the ECCS systems, only the Safety Injection System is modeled. The safety injection flow corresponds to that delivered by one centrifugal charging pump delivering full flow to the RCS via the cold leg header;

7. No credit is taken for the low concentration borated water, which must be swept from the lines downstream of the RWST (complete volume replacement) prior to the delivery of concentrated boric acid to the reactor coolant loops;

8. After a Safety Injection signal is generated (including instrumentation delays), the high head charging pump is started and appropriate valves begin to operate. Appropriate time delays are included to account for the startup of the safety injection charging pump and the sequential valve realignment to the RWST (i.e., the borated water source is only assumed available after the full repositioning of the valves). The delay of sweeping the volume downstream of the RWST prior to the delivery of the borated water is included in the model. For the case without offsite power, an additional delay is assumed to start the diesels and to load the necessary safety injection equipment onto them;

9. Full power nominal feedwater flow is assumed from event initiation until feedwater isolation occurs;

10. Maximum auxiliary feedwater flow (all three AFW pumps) is assumed throughout the event with a conservative flow split between the affected steam generator and the intact steam generators;

11. Conservative steam generator heat transfer characteristics are maintained during the course of the transient;

12. In computing the steam flow during the steamline break, the Moody Curve for $fL/D = 0$ is used;

13. Power peaking factors corresponding to the most reactive rod stuck in the fully withdrawn position and non-uniform core inlet coolant conditions are determined. The coldest core inlet temperature is assumed to occur in the sector with the stuck rod;

14. A double-ended rupture (DER) of a pipe in the Main Steam System is assumed. The effective throat area of the steam generator outlet nozzles are 1.4 ft^2, which is considerably less than the main steam pipe area. Thus, the nozzles serve to limit the maximum steam flow for a DER to 1.4 ft^2 per loop.

To demonstrate the conservatism of the TU Electric methodology, parametric studies are performed on those parameters and assumptions important to the steamline break event and the results are discussed in the following section. Parameters considered include various modeling assumptions, system initial conditions, break sizes, reactivity feedback, and RPS setpoints and time delays. An assessment is performed to identify the limiting single active failure with respect to the event acceptance criteria. This single failure is assumed in the analysis of the steamline break event.

3.4.3 Results

3.4.3.1 Reference Case

A representative analysis (Reference Case) has been performed using assumptions typical of those used in the FSAR analysis. Table 3.4-2 provides a summary of the initial conditions used for this analysis. The results of the Reference Case are shown in Figures 3.4-10 and 3.4-11 and Table 3.4-3 provides the sequence of events.

The transient is initialized at critical zero power conditions and is immediately brought to the subcritical condition prior to initiating the event. This is accomplished by inserting enough negative reactivity to bring the reactor subcritical by an amount equivalent to the minimum Technical Specification shutdown margin requirement (1600 pcm). At that time (0.1 seconds), the steamline break is initiated coincident with full main and auxiliary feedwater flow. The rapid steam generator depressurization causes the low steamline pressure setpoint to be reached at 0.96 seconds, which generates the steamline isolation and safety injection signals. The safety injection signal starts the charging pump and also provides feedwater line isolation. Prior to closure of the steamline and feedwater line isolation valves, all four steam generators depressurize and blow down through the break. The uncontrolled steam release rate also decreases as the steam generators depressurize. Following the steamline and feedwater line isolation at 7.96 seconds, only one steam generator continues to blow down.

The excessive steam release causes the heat extraction rate in the steam generators to increase, resulting in a reduction in the reactor coolant system temperature and pressure (see Figures 3.4-10 and 3.4-11). The pressurizer level is also

decreasing in response to the large cooldown of the RCS. Once the pressurizer empties, the RCS pressure decreases at a slightly faster rate until the saturation pressure is reached in the reactor vessel upper head. The bubble formed in the upper head of the reactor vessel acts like a pressurizer. The pressure then stabilizes as the safety injection flow begins to increase the RCS inventory.

The initial decrease in the coolant temperature results in the cooling of the fuel rods as evident from the initial increase in the heat flux. The increasing heat flux in the first 10 seconds is due to the increasing delta-T between the fuel rods and the coolant since the coolant temperature initially decreases faster than the fuel rod temperature. As the fuel cools down, the heat flux decreases prior to the large increase attributable to the power generation. The large reactivity insertion from the moderator density and Doppler feedback overcomes the shutdown margin at approximately 13.9 seconds. The reactor returns to critical and then begins generating power. A rapid increase in the reactor power occurs until the fuel heats up enough to cause the total reactivity to begin to decrease through the Doppler reactivity feedback. The reactor power continues to increase, but at a significantly reduced rate, until the boron reaches the core (at approximately 203 seconds) causing the reactivity to become negative.

The nuclear analysis provided a check of the reactivity change from the start of the transient to the statepoint conditions and calculations of radial and axial power distributions for use in the core thermal hydraulic analysis. Figure 3.4-12 shows that the change in reactivity predicted by RETRAN-02 is greater than that predicted by the three dimensional neutronics model, thus verifying the conservatism in the

RETRAN-02 analysis. Figures 3.4-13 and 3.4-14 show the calculated radial and axial power distributions.

The core thermal hydraulic analysis was performed using the statepoint boundary conditions from the RETRAN-02 transient results and the core radial and axial power distributions from the nuclear analysis. Since the RCS pressure is less than the 1500 psia limit of the TUE-1 correlation, the W-3 correlation is used. The minimum DNBR predicted by the W-3 correlation for this Reference Case is greater than the 1.45 limit.

3.4.3.2 Parametric Studies

For the steamline breaks occurring while the reactor is initially at hot shutdown conditions, the effects of various assumptions are determined separately and are compared to a Reference Case analysis. Generally, the parameters and assumptions which are important to the steamline break event are those which affect the cooldown rate, reactivity feedback, core power distribution, and operational characteristics of the RPS and ESFAS. The parametric studies are performed by varying an individual parameter and comparing the results to the Reference Case. The results of the parametric studies demonstrate that the Reference Case represents a conservative analysis.

The parametric study is grouped into eight categories:

1. Reactivity parameters;
2. Reactor vessel mixing;
3. Modeling assumptions;
4. Initial conditions;
5. Break size and type;
6. RPS/ESFAS performance characteristics;
7. Single failure considerations;
8. Loss of offsite power.

The results of the Reference Case are plotted on the same figure as the results of the parametric studies to illustrate the parameter's effect.

Category 1: Reactivity Parameters

The total reactivity feedback is determined by the moderator density and Doppler defects, and boron worth. Other reactivity parameters which may affect the steamline break transient include the shutdown margin, delayed neutron fraction, and prompt neutron lifetime.

Moderator Density Defect. Figures 3.4-15 and 3.4-16 provide the transient results assuming a ± 10% variation in the moderator density defect. The moderator density feedback is one of the more important parameters which affect the steamline break event. As can be seen from the figures, a 10% increase in the moderator density defect results in a higher and faster return to power and conversely, a 10% decrease results in a lower return to power when compared to the Reference Case. The minimum DNBR decreases 1.0% for a 10% increase in the moderator defect and, a 10% decrease in moderator density defect results in a 10.2% increase in the minimum DNBR.

Doppler Defect. The results of the ± 10% variation in the Doppler defect are shown in Figures 3.4-17 and 3.4-18. The effect of the 10% increase in the Doppler defect is a slightly higher initial peak in the total reactivity due to the cooldown of the moderator and fuel. However as the power increases, the increased Doppler defect results in a slightly lower peak return to power and a 2.5% higher minimum DNBR. The 10% decrease in the Doppler defect has the opposite affect of the 10% increase case. The minimum DNBR is 2.6% lower than

the Reference Case value for a 10% decrease in the Doppler defect.

Boron Worth. The steamline break event is insensitive to the value of the boron worth as illustrated in Figures 3.4-19 and 3.4-20. This is due to the fact that the event reaches a near equilibrium condition prior to any boron reaching the core. Shortly after the boron reaches the core, the reactivity becomes negative causing the power to begin decreasing. The minimum DNBR during the event occurs at the time of peak power just prior to the entry of the boron to the core, therefore a ± 10% change in the boron worth has no affect on the minimum DNBR.

Shutdown Margin. A decrease in the shutdown margin to 1300 pcm was analyzed, and the results are shown in Figure 3.4-21. The effect of the lower shutdown margin is to cause a faster return to power and to a higher value. The resultant minimum DNBR is 6.3% lower than the Reference Case value. An increase in the shutdown margin to 2400 pcm results in a noticeable decrease in the peak power as shown on Figure 3.4-22. The minimum DNBR for the 2400 pcm shutdown margin case is 31.4% higher than the Reference Case value.

Reactivity Weighting. The total reactivity insertion, predicted by RETRAN, from the beginning of the event to the statepoint condition is verified to be conservative by the nuclear analysis (Section 3.4.1.2). The nuclear analysis takes into account the spatial effects of the high fuel temperature near the stuck rod location and the non-uniform core inlet temperature conditions. The Reference Case resulted in an overprediction of the total reactivity insertion when a reactivity weighting of 50% to the affected quadrant of the core was used (see Figure 3.4-12). Therefore, a case was investigated with a reactivity weighting of 25% to

the affected quadrant (or no preferential weighting). Figure 3.4-23 shows the transient results for a reactivity weighting of 25% to the affected quadrant. The return to power is lower by approximately 2% when compared to the Reference Case, and the resultant minimum DNBR is 10.0% higher. It should be noted that for the case without any preferential reactivity weighting, the total reactivity predicted by RETRAN remains conservative with respect to the nuclear analysis. This overprediction of the reactivity insertion by RETRAN is due to the many other conservatisms in the analysis; primarily the high moderator density defect, and the uniform core power distribution in the RETRAN model (i.e. the affected quadrant represents only 25% of the total core power generation when the actual power in this quadrant would be significantly higher). The combination of these two assumptions leads to a very conservative prediction in the reactivity feedback.

Stuck Rod Assumption. A case was analyzed assuming no stuck control rod to determine the importance of the stuck rod assumption. The assumption is that the shutdown margin increases to 2400 pcm, therefore the system transient results remain the same as those depicted in Figure 3.4-22 described earlier. The nuclear analysis calculates peaking factors which are based on all rods inserted. The resultant minimum DNBR for this case is 89.1% higher than the Reference Case. It should be noted that even though the RETRAN analysis predicted a return to power for this case, the nuclear analysis shows that the core will remain subcritical.

Category 2: Reactor Vessel Mixing

Reactor Vessel Inlet Mixing. The Reference Case assumed that the flow from the reactor coolant loop associated with the affected steam generator flows through the quadrant with the stuck rod 80% unmixed and 20% mixed with the other loops. The

upper plenum mixing assumption was that the flow from the affected core sector entered the faulted loop 73% unmixed and 27% mixed. These are typical FSAR assumptions. Several cases were examined where the inlet plenum mixing was varied from no mixing to perfect mixing while holding the upper plenum mixing constant at the Reference Case value. The results are shown in Figures 3.4-24 through 3.4-26 for no mixing, 50% mixing, and perfect 100% mixing, respectively. The results show that for more inlet mixing than the Reference Case, there is very little change in the peak return to power (although the rate at which the power increases is slower for the cases with more mixing). However for no mixing, the return to power is a little faster with a peak power 1.5% higher than the Reference Case. The minimum DNBR for these three cases and the Reference Case are plotted versus the level of inlet mixing on Figure 3.4-27. As can be seen from this figure, assuming less inlet mixing than that in the Reference Case results in only a small (3.0%) decrease in the minimum DNBR, and assuming additional inlet mixing provides a relatively large (16% - 18%) increase in the minimum DNBR.

Reactor Vessel Outlet Mixing. To study the effects of the outlet mixing assumption, the inlet mixing was held constant at the Reference Case value and the outlet mixing was varied from no mixing to perfect mixing. The results are shown in Figures 3.4-28 through 3.4-30 for no mixing, 50% mixing, and perfect 100% mixing, respectively. For the case with no outlet mixing, colder water flows to the affected loop resulting in a faster steam generator depressurization, thus causing a lower vessel inlet temperature for that loop. However, with the warmer water flowing to the three intact loops, the steam generator pressures increase to a higher equilibrium pressure after the steamline isolation causing the vessel inlet temperature to increase for those loops. The net effect is an initially quicker rise in power compared to the

Reference Case, but an eventual decrease in power as the intact steam generators pressurize and cause a higher overall reactor vessel inlet temperature. A very small reduction (1.9%) in the minimum DNBR is calculated for the case without any vessel outlet mixing.

The case with more outlet mixing (50%) than the Reference Case results in warmer water flowing to the faulted steam generator. This causes the faulted steam generator to depressurize a little slower than in the Reference Case and thus results in a higher faulted loop vessel inlet temperature. However, the three intact loops have cooler water flowing to the steam generators causing them to reach a lower equilibrium pressure condition following the steamline isolation. This effect causes the vessel inlet temperature for the three intact loops to be lower. The lower overall reactor vessel inlet temperature and slightly higher peak power (less than 1%) results in a higher calculated minimum DNBR value (6.3% higher than in the Reference Case).

The perfect outlet mixing case has the same trends as the 50% mixing case only slightly more pronounced. The three intact steam generators reach a lower equilibrium pressure, and the faulted steam generator depressurizes slower than in the Reference Case. The overall reactor vessel inlet temperatures are thus lower, causing a higher (1.7%) peak return to power than in the Reference Case. The calculated minimum DNBR is 12.4% higher than the Reference Case value.

The minimum DNBRs for the three mixing cases and the Reference Case are plotted in Figure 3.4-31. As can be seen from this figure, the minimum DNBR is fairly insensitive (1.9% change) to a decrease in the amount of outlet mixing from the Reference Case value, but an increase in the outlet mixing

from the Reference Case value results in a more substantial increase (6.0% - 12%) in the minimum DNBR..

It should be noted that the core heat conductor modeling assumption does not credit the fact that the affected quadrant of the core will produce more power than the unaffected portion of the core. This assumption leads to a lower moderator temperature rise through the affected sector which has two effects. The first is a very conservative reactivity feedback prediction since the actual moderator and fuel temperatures would be higher in that quadrant (the three dimensional neutronics analysis verifies the conservatism of the reactivity prediction). The other effect is that the coolant temperature at the outlet of the affected quadrant of the core is lower than would be expected. The already conservative outlet mixing assumption (73% unmixed) is further enhanced by this effect.

Category 3: Modeling Assumptions

Four different modeling assumptions were investigated to determine their relative importance and affect on the steamline break. Various main and auxiliary feedwater flow rates and distributions, the location of the pressurizer (faulted loop), steam generator tube height, and the break flow correlation, were examined.

Main and Auxiliary Feedwater Assumptions. The Reference Case assumed that the full nominal feedwater flow was distributed evenly to all of the steam generators and that the maximum auxiliary feedwater flow was preferentially flowing to the faulted steam generator (75% to faulted, 25% split between two intact, and 0% to the third intact steam generator). These assumptions are very conservative and are typical of what is assumed in the FSAR analyses.

Three cases were examined without any main feedwater and with various auxiliary feedwater configurations. The first cass assumed the Reference Case auxiliary feedwater distribution, and the results are shown on Figure 3.4-32. The return to power is slightly slower than the Reference Case, but eventually reaches nearly the same peak power level and minimum DNBR valuo. The second case assumed an equal distribution of auxiliary feedwater and the results are shown on Figure 3.4-33. Again, the return to power is slower than the Reference Case and reaches nearly the same peak power level with a slightly higher minimum DNBR value. This case however, turns around a little sooner due to the degraded heat transfer in the faulted steam generator as the level begins to drop below the top of the tube bundle. A third case was examined without any auxiliary feedwater, and the results are shown on Figure 3.4-34. As expected, the rate and peak return to power are less than the Reference Case and the minimum DNBR is approximately 3.3% higher.

A case was examined with the Reference Case main feedwater distribution and an equal auxiliary feedwater distribution to all of the steam generators. The results for this case, shown in Figure 3.4-35, indicate that the additional cooling in the three intact steam generators provide a slightly higher return to power (less than 0.5%). Ho ever, the level in the faulted steam generator falls below the top of the tube bundle due to the lower auxiliary feedwater flow in that loop, thus causing some degradation in the heat transfer. The minimum DNBR for this case is not significantly different (1.1% higher) than the Reference Case.

Another series of cases were examined with the Reference Case distribution for the auxiliary feedwater and various main feedwater configurations. All three case assumed that the

main feedwater was being delivered to the faulted steam generator only. The results are shown on Figures 3.4-36 through 3.4-38 for 100%, 220%, and 250% of nominal feedwater flow, respectively. All of the cases experience a slightly slower return to power since there is less cooling available from the intact steam generators. In all cases, the peak return to power is within 0.2% of the Reference Case value, and the minimum DNBR values are higher by 1.7%.

Location of the Pressurizer. A case was examined with the pressurizer located on the loop associated with the faulted steam generator, and the results are shown on Figure 3.4-39. Initially the affected loop does not cool as fast since the hotter pressurizer fluid is mixing with the flow to the faulted steam generator, thus causing a slower power increase relative to the Reference Case. However, once the pressurizer empties, the peak return to power is essentially identical to the Reference Case value (within 0.1%) and the minimum DNBR is 2.4% higher.

Steam Generator Tube Height Reduction. The steam generator model used for the Reference Case had the built-in assumption of a reduction in the effective height of the steam generator tube bundle to delay any degraded heat transfer as the liquid level decreases. A case was examined without the reduction in the effective tube bundle height and the results are shown in Figure 3.4-40. As can be seen from the figure, the results are nearly identical except that a small amount of heat transfer degradation is predicted prior to the power turnaround due to the boron injection. The peak return to power is within 0.1% of the Reference Case with no distinguishable difference in the minimum DNBR values.

Break Flow Modeling. The Reference Case used the Moody curve with fL/D = 0 for calculating the break flow during the event. Another case was examined using an isoenthalpic expansion model [28] to predict the break flow, and the results are shown on Figure 3.4-41. The isoenthalpic expansion model predicted a slightly lower break flow rate which results in a return to power rate which is a little less than the Reference Case. However, the power level approaches the Reference Case value (within 0.1%) when a quasi equilibrium condition is reached prior to the turnaround. The minimum DNBR is essentially the same as the Reference Case value.

Category 4: Initial Conditions

Four different initial conditions were investigated to determine their relative importance and effect on the steamline break. The initial pressurizer pressure and level, steam generator mass, and reactor coolant system flow rate were examined.

Initial Pressurizer Pressure. The Reference Case assumed an initial pressurizer pressure of 2250 psia consistent with that assumed in the FSAR analysis. Two other cases were analyzed with initial values of 2280 and 2208 psia, and the results are shown on Figures 3.4-42 and 3.4-43, respectively. As can be seen from the figures, a change in either direction on the initial pressurizer pressure has a very little effect on the pressurizer pressure transient early in the event, but the equilibrium conditions (and calculated minimum DNBR) reached during the event are nearly identical to the Reference Case.

Initial Pressurizer Level. The Reference Case assumed an initial pressurizer level of 75% of span consistent with the nominal programmed level at hot zero power conditions and with the FSAR analysis. Initial values of 20% and 30% were

analyzed, and the results are shown on Figures 3.4-44 and 3.4-45, respectively. The effect on the rate and peak return to power values compared to the Reference Case is minimal for either of the cases. The 20% initial level case results in a 0.2% lower peak power, and the 30% initial level case results in a 0.2% higher peak power. However, the lower initial level case results in approximately a 100 psia lower pressurizer pressure and the higher initial level case results in nearly a 250 psia higher pressure. The net effect on the minimum DNBR is small, with the slightly higher power being offset by the higher pressure, and the lower power being offset by the lower pressure.

Initial Steam Generator Water Mass. The Reference Case assumed a very conservative initial steam generator water mass corresponding to 110% of the nominal value at hot zero power to delay the possible tube bundle uncovery. Initial steam generator masses corresponding to 100% of nominal and 90% of nominal were analyzed and the results are shown on Figures 3.4-46 and 3.4-47, respectively. The effect of a lower initial mass is to cause the steam generators to depressurize a little faster resulting in a slightly lower reactor vessel inlet temperature and a quicker return to power. However, both cases eventually reach the same peak power as the Reference Case. The 90% of nominal mass case also results in a tube bundle uncovery prior to the power turnaround from the boron (the 100% case did not result in tube bundle uncovery). The minimum DNBR for each case is slightly greater than the Reference Case value.

Initial Reactor Coolant System Flow Rate. The Reference Case assumed an initial RCS flow rate corresponding to the thermal design flow rate (lowest possible) for both the system transient response and the core thermal hydraulic response. An RCS flow rate corresponding to 10% higher than the thermal

design flow rate was analyzed and the results are shown on Figure 3.4-48. The higher flow rate in the system analysis provides for a better coupling of the steam generator to the RCS resulting in a slightly greater cooldown and a 0.3% higher peak return to power. However, the core thermal hydraulics analysis calculated a 1.4% higher minimum DNBR due to the higher mass flow rate through the core.

Category 5: Break Size and Type

There are three types of steamline breaks which have been analyzed. The first is termed a "Double Ended Rupture," DER, which corresponds to a circumferential break in a pipe with both ends displacing each other such that an equal area is exposed from each end of the broken pipe. For example, a 1.0 ft^2 DER on the steamline associated with steam generator-1 would result in steam generator-1 blowing down through a 1.0 ft^2 area while steam generators-2, -3, and -4 would equally share a 1.0 ft^2 area.

The second type of steamline break is the "Split" break. A split break is a rupture in the steamline which does not result in the complete severance of the pipe. An example would be a 1.0 ft^2 longitudinal crack in the steamline which results in all four steam generators equally sharing the 1.0 ft^2 break area until steamline isolation occurs. Following steamline isolation, 1 steam generator may continue to blow down through the 1.0 ft^2 area if the break is upstream of the MSIV or if the MSIV fails to close.

The third type of steamline break is the inadvertent opening of a steam dump, safety, or relief valve (or sometimes referred to as the "credible" steamline break). Two different credible steamline breaks have been considered. The first is a "uniform credible" break which is essentially identical to

the split break except that the maximum possible break area is limited to the area of the steam safety valve. The second type is the "non-uniform credible" break which is the blowdown of a single steam generator through one of the mentioned valves (the other loops are isolated).

Double Ended Rupture. A spectrum of DERs has been considered ranging from a 5.6 ft^2 break area down to a 0.1 ft^2 area, and the results are shown on Figures 3.4-49 through 3.4-54 for representative cases spanning the break area range. As expected, the largest DER results in the maximum and fastest return to power. The minimum DNBR for each case is plotted versus the break area, and the results are shown on Figure 3.4-55.

Split Breaks. A spectrum of split break areas ranging from 1.4 ft^2 down to 0.1 ft^2 has been considered, and the results are shown on Figures 3.4-56 through 3.4-59 for selected cases. The overall system response to split breaks is very similar to the DER cases. The upper value on the split break area considered is based on the maximum area through which a single steam generator can blow down (limited by the integral flow restrictors) following steamline isolation. Any split break area larger than this would be very similar in nature to one of the larger DER cases. For example, a 4.0 ft^2 split break would be seen as a uniform depressurization of all the steam generators with each one having an effective break area of 1.0 ft^2 prior to steamline isolation. Following steamline isolation, the steam flow from three of the steam generators is terminated, and one steam generator continues to blow down but does not share the break area. Therefore, the single steam generator blows down through a 1.4 ft^2 area following the steamline isolation. Any DER of 1.4 ft^2 or larger would bound the large split break since following the steamline isolation for either type of break, a single steam generator

blow down is limited by the integral flow restrictor area (1.4 ft^2). The minimum DNBRs for the split breaks are plotted versus the break area and are shown on Figure 3.4-60. Similar to the DER cases, the larger the break area, the lower the minimum DNBR.

Opening of a Steam Dump, Relief or Safety Valve. As discussed earlier, the uniform credible steamline break is identical to the split breaks, but limited to a maximum area corresponding to that of a steam safety valve. Therefore, those cases were not repeated. The non-uniform credible steamline breaks were analyzed for a spectrum of areas ranging from 0.08 ft^2 to 0.15 ft^2, and the results for the case corresponding to a steam generator safety valve area are shown on Figure 3.4-61. The peak return to power is approximately 6% and thus the minimum DNBR is meaninglessly high.

Category 6: RPS/ESFAS performance characteristics

The next category of parametric studies involves the operational characteristics of the RPS or ESFAS. Four cases were analyzed to demonstrate the sensitivity to the system performance requirements. The Reference Case assumes that the MSIV and feedwater isolation valves are fully closed within 7.0 seconds after reaching the actuating setpoint.

A case was analyzed with a 10.0 second steamline isolation response time, and the results are shown on Figure 3.4-62. As expected, the extended blowdown of the three unaffected steam generators results in a faster RCS temperature decrease and thus a 1.8% higher return to power. The minimum DNBR is not significantly different from the Reference Case value due to the lower overall reactor vessel inlet temperatures and less temperature difference between the coolant loops (which provides lower power peaking).

A second case was analyzed with just the feedwater isolation time increased to 10.0 seconds, and the results are shown on Figure 3.4-63. The additional feedwater had little effect on the results, with a peak power which is 0.3% higher. Again, the minimum DNBR is not significantly different from the Reference Case value. The results are consistent with the sensitivity study on the feedwater distributions (Category 3).

A combination of the above two cases was analyzed with both the steamline and feedwater line isolation response time increased to 10.0 seconds. The results, shown on Figure 3.4-64, show that the peak power is approximately 2.3% higher. The additional main feedwater and the extended blowdown of the intact steam generators provide a lower overall reactor vessel inlet temperature and less of a non-uniform inlet temperature distribution resulting in lower peaking factors. The net effect on the minimum DNBR is a 5.9% increase (primarily due to the colder inlet temperature and lower power peaking - both of which provide a DNB benefit which offset the higher core power).

A sensitivity case was performed to determine the effect of not providing a safety injection actuation on the low steamline pressure signal. All remaining functions were assumed to occur (i.e., steamline and feedwater line isolation). The results for this case are shown on Figure 3.4-65 and are nearly identical to the Reference Case, with the exception that the safety injection actuation occurs slightly later and the signal is provided by the low pressurizer pressure safety injection trip function. With the power essentially at a plateau prior to the boron reaching the core, the effect of the slight delay in the boron reaching the core is unnoticeable.

Category 7: Single Failure Consideration

The steamline break event has been evaluated considering each single active failure in the safety-related protection systems required for mitigation of the event. The single failures which could make the steamline break event more severe are those which cause a more rapid cooldown of the RCS or those which affect the capability to mitigate the reactor power increase.

The single failure considered in the Reference Case analysis was the failure of one safeguards train to deliver full safety injection flow (only one centrifugal charging pump is credited). The effect of this failure is a delay in the mitigation of the reactor power increase due to the longer delay in the time to sweep the unborated water from the safety injection system lines. However, this effect is not very significant since the core power rises quickly during the first one and a half minutes to a plateau dictated by the steam energy release prior to any boron reaching the core. With full safety injection available, the borated water reaches the core sooner thus mitigating the transient earlier, but the core power at that time is not significantly less than the case with only one train of safety injection. The main cause of this effect is the modeling assumption which requires the complete volume replacement of the fluid in the safety injection lines prior to any boron entering the reactor coolant system (i.e., no "forward flow mixing" is allowed). The time it takes to purge the safety injection lines is greater than the time to reach a near equilibrium core power with either one or two trains of safety injection available.

A single failure which either increases the steam releases or provides additional feedwater (main or auxiliary) to the steam generators could result in an increased cooldown of the RCS.

Each steamline is equipped with a MSIV so that a break at any location in the main steam system can not result in more than one steam generator blowing down following steamline isolation even with a postulated failure of a single MSIV. Steam generator flow restrictors are an integral part of the steam nozzle with an effective throat area of 1.4 ft^2, which is considerably less than the main steam pipe area. Therefore, the nozzles serve to limit the maximum steam flow for a break at any location.

Sustained high feedwater flow could cause an additional cooldown of the RCS. Therefore, in addition to the normal control action which will close the main feedwater valves, a safety injection signal will rapidly close all feedwater control valves and feedwater isolation valves, trip the main feedwater pumps, and close the feedwater pump discharge valves. The redundancy in the feedwater isolation capability prevents a postulated single failure from resulting in additional main feedwater flow. The auxiliary feedwater system is also designed with passive flow restrictor devices which limit the maximum amount of auxiliary feedwater which can be delivered to a depressurizing steam generator. A very conservative assumption in the Reference Case analyses was made however, which assumed that 75% of the total auxiliary feedwater flow capability was delivered to the faulted steam generator.

Category 8: Loss of Offsite Power

The assumptions regarding the loss of offsite power were evaluated to determine its effect on the consequences of the steamline break event. The loss of offsite power affects the transient in two ways. First, the delay to start the safety injection is increased by the time required to start the

diesel generators. Second, the loss of power to the reactor coolant pumps reduces the flow in the RCS.

A case was analyzed with a loss of offsite power assumed to occur coincident with the generation of the Safety Injection signal. The timing of the loss of offsite power is conservative since the diesel generators will start upon receipt of a Safety Injection signal or on an undervoltage condition on the emergency buses (indicative of a loss of offsite power). The transient results for this case are shown on Figure 3.4-66. As can be seen from the figure, the loss of the forced circulation makes the transient less severe than the case with forced circulation (Reference Case). This is due to the decoupling of the RCS from the secondary system since the lower RCS flow rate causes a decrease in the heat transfer rate in the steam generator. The reduced cooldown rate results in a slower approach to criticality and a lower peak power. The calculated minimum DNBR for this case was extremely high compared to the Reference Case.

3.4.4 Summary

The steamline break at hot shutdown event has been analyzed using the analytical techniques described in Section 3.4.2 and input assumptions typical of FSAR analyses. The results of the analysis show that the DNBR acceptance criterion is met for the limiting Reference Case.

The results of the parametric studies demonstrate that the Reference Case analysis performed with the TU Electric methodology represents a conservative analysis. The following summarizes the results of the parametric studies:

Category 1: Reactivity Parameters

The results for the moderator density and Doppler defects, shutdown margin, and reactivity weighting studies show that for a pessimistic change in a parameter value, the resultant decrease in the minimum DNBR was not as large as the increase in the minimum DNBR for an equally optimistic change in the parameter value (e.g., the +10% increase in the moderator density defect resulted in a 1.0% decrease in the minimum DNBR, and the -10% change resulted in a 10.2% increase in the minimum DNBR). The transient has also been shown to be insensitive to the boron worth, and very non-limiting without the assumption of a stuck control rod. Therefore, the combined set of reactivity parameters and assumptions used in the Reference Case analysis are conservative with respect to actual or expected values.

Category 2: Reactor Vessel Mixing

The degree of mixing assumed in the Reference Case is typical of what is commonly used in FSAR analyses and is conservative with respect to the expected mixing which would normally occur. The results showed that the change in the minimum DNBR for a further decrease in the amount of inlet mixing is very small compared to the large DNB benefit achieved with more inlet mixing. The outlet mixing study had similar results with even a lesser sensitivity to a pessimistic change. The effect of the conservative plena mixing assumptions used in the Reference Case analysis combined with the uniform core power distribution model in RETRAN, and the preferential reactivity weighting to the affected core sector, provide an overall conservative representation of the reactivity feedback as demonstrated by the SIMULATE-3 calculated reactivity results.

Category 3: Modeling Assumptions

The reactor core response was not significantly affected by variations in the four different modeling assumptions (main and auxiliary feedwater flow rates and distributions, location of the pressurizer, steam generator tube height, and the break flow choking correlation).

Category 4: Initial Conditions

The four different initial condition assumptions investigated (pressurizer pressure and level, steam generator water mass, and RCS flow rate) had very little effect on the reactor core response.

Category 5: Break Size and Type

The results of the sensitivity study showed that the reactor core response is sensitive to the break size and type with the limiting case being the largest DER as assumed in the Reference Case analysis.

Category 6: RPS/ESFAS Performance Characteristics

The increased delay on the main steamline and feedwater line isolation functions had very little affect on the core response analysis. The impact of not providing a safety injection actuation on a low steamline pressure signal was also insignificant.

Category 7: Single Failure Consideration

Since each steamline is equipped with a MSIV, no more than one steam generator can blow down following steamline isolation even with a failure of a MSIV to close. Further, redundant

feedwater isolation capability exists to prevent the uncontrolled addition of main feedwater to the steam generators. The single failure which affects the capability to mitigate the event is the failure of one safety injection train. However, a safety injection train failure does not significantly affect the core response results.

Category 8: Loss of Offsite Power

The loss of offsite power affects the steamline break transient by causing an increased delay in the delivery of safety injection and by reducing the RCS flow due to the loss of power to the reactor coolant pumps. The results showed that the case without offsite power is much less severe than the Reference Case analysis which assumed offsite power was maintained.

CHAPTER 4

CONCLUSION

The TU Electric methodology for the analysis of the core response to steamline break events has been presented. A complete description of the regulatory bases, computer codes and models, and analytical techniques for the analysis of these events is included in this report. Representative analyses have been presented to demonstrate the application of the TU Electric methods. Sensitivity studies were performed to identify key analysis parameters, justify analysis assumptions and techniques, and determine the limiting cases. It can be concluded that the TU Electric methodology for steamline break analysis is acceptable for licensing applications.

CHAPTER 5

REFERENCES

1. Lo, S. S., DeVore, C. V., Boatwright, W. J., "Transient Analysis Methods For Comanche Peak Steam Electric Station Licensing Applications," RXE-91-001, TU Electric, February, 1991.

2. Sung, Y. X. and Giap, H. B., "VIPRE-01 Core Thermal Hydraulic Analysis Methods For Comanche Peak Steam Electric Station Licensing Applications," RXE-89-002, TU Electric, June 1989.

3. Code of Federal Regulations, Title 10 - Energy, Revised as of January 1, 1990.

4. ANSI N18.2-1973, "Nuclear Safety Criteria for the Design of Stationary Pressurized Water Reactor Plants."

5. Comanche Peak Steam Electric Station Final Safety Analysis Report, Amendment 80, November 1990.

6. "Safety Evaluation Report related to the operation of Comanche Peak Steam Electric Station, Units 1 and 2," NUREG-0797, Supplement No. 24, USNRC, April 1990.

7. 10 CFR Part 50, Appendix A, General Design Criteria 10, 15, 20, 25, and 26, Revised as of January 1, 1990.

8. Standard Review Plan, NUREG-0800, Section 15.1.4, "Inadvertent Opening of a Steam Generator Safety or Relief Valve," Revision 1 - July 1981, U.S. Nuclear Regulatory Commission.

9. ASME Boiler and Pressure Vessel Code, Section III, "Nuclear Power Plant Components," American Society of Mechanical Engineers, 1971.

10. 10 CFR Part 50, Appendix A, General Design Criteria 27, 28, 35, Revised as of January 1, 1990.

11. Regulatory Guide 1.70, Revision 2, "Standard Format and Content of Safety Analysis Reports for Nuclear Power Plants," U.S. Nuclear Regulatory Commission.

12. Standard Review Plan, NUREG-0800, Section 15.1.5, "Steam System Piping Failures Inside and Outside of Containment (PWR)," Revision 2 - July 1981, U.S. Nuclear Regulatory Commission.

13. McFadden, J. H., et al., "RETRAN-02, A Program for Transient Thermal Hydraulic Analysis of Complex Fluid Flow Systems," NP-1850-CCM-A, Revision 4, Electric Power Research Institute, November 1988.

14. Stewart, C. W., et al., "VIPRE-01: A Thermal Hydraulic Code for Reactor Cores," Vol. 1-3 (Rev. 2), Vol. 4, and 5, NP-2511-CCM, Revision 2, Electric Power Research Institute, July 1985.

15. Thomas, C. O., "Acceptance for Referencing of Licensing Topical Reports EPRI CCM-5, 'RETRAN - A Program for One Dimensional Transient Thermal Hydraulic Analysis of Complex Fluid Flow Systems,' and EPRI NP-1850-CCM, 'RETRAN-02 - A Program for Transient Thermal Hydraulic Analysis of Complex Fluid Flow Systems,' NRC Letter to T. W. Schnatz, UGRA Chairman, Attachment: "Safety Evaluation Report on RETRAN - A Program for Transient Thermal Hydraulic Analysis of Complex Fluid Flow Systems," September 4, 1984.

16. Thadani, A. C., "Acceptance for Referencing Topical Report EPRI NP-1850-CCM-A, Revisions 2 and 3 Regarding RETRAN02/MOD003 and MOD004," NRC Letter to R. Furia, GPU Nuclear Corporation, Enclosure: "Safety Evaluation by the Office of Nuclear Reactor Regulation Relating to RETRAN-02, Versions MOD003 and MOD004," October 19, 1988.

17. Boatwright, W. J., Maier, S. M., and Lo, S. S., "Design Basis Analysis of a Postulated Steam Generator Tube Rupture Event for Comanche Peak Steam Electric Station, Unit 1," RXE-88-101-P, TU Electric, March 1988.

18. Edwards, D. J., et al., "Steady State Reactor Physics Methodology," RXE-89-003-P, TU Electric, July 1989.

19. Rossi, C. E., "Acceptance for Referencing of Licensing Topical Report, EPRI NP-2511-CCM, 'VIPRE-01: A Thermal Hydraulic Analysis Code for Reactor Cores,' Volume 1, 2, 3, and 4," NRC Letter to J. A. Blaisdell, UGRA Executive Committee, Attachment: Safety Evaluation Report on EPRI NP-2511-CCM VIPRE-01," May, 1986.

20. Moody, F. S., "Transaction of the ASME, Journal of Heat Transfer," Figure 3, page 134, February 1965.

21. Bosma, J. T. and Grace, M. A. "Power Distribution Control Analysis and Overtemperature N-16 and Overpower N-16 Trip Setpoint Methodology," RXE-90-006-P, TU Electric, February 1991.

22. Giap, H. B. and Sung, Y. X., "TUE-1 Departure from Nucleate Boiling Correlation," RXE-88-102-P, TU Electric, January 1989.

23. Giap, H. B. and Hiltbrand, D. W., "TUE-1 DNB Correlation, Supplement 1," RXE-88-102-P, Supp. 1, TU Electric, December 1990.

24. Tong, L. S., "Prediction of Departure From Nucleate Boiling For An Axially Non-Uniform Heat Flux Distribution," J. Nucl. Energy, 6, 21 (1967).

25. Tong, L. S., "Critical Heat Fluxes in Rod Bundles," Two-Phase Flow and Heat Transfer in Rod Bundles, V. E. Schrock, Ed., American Society of Mechanical Engineers, New York (1969).

26. Thadani, A. S., "Acceptance for Referencing of Licensing Topical Report, WCAP-9226-P/9227-NP, 'Reactor Core Response to Excessive Secondary Steam Releases'," NRC letter to W. J. Johnson, Manager, Nuclear Safety Department, Westinghouse Electric Corporation, January 31, 1989.

27. EPRI NP-2609, Vol. 1-3, "Parametric Study of CHF Data, Compilation of Rod Bundle CHF Data Available at The Columbia University Heat Transfer Research Facility," September 1982.

28. McFadden, J. H., et al., "RETRAN-02, A Program for Transient Thermal Hydraulic Analysis of Complex Fluid Flow Systems, Volume 1: Theory and Numerics (Revision 4)" NP-1850-CCM-A, Revision 4, Electric Power Research Institute, November 1988.

Table 3.3-1

VIPRE-01 Model Summary

- 16 Channels, 20 Rods (12 Subchannels & Four Lumped Channels)
- 38 Axial Nodes
- Reference Radial power Distribution
- Reference Chopped Cosine Axial Power Distribution with Peak/Avg = 1.55
- Percent of Heat Generated in Fuel Rods = 97.4%
- Turbulent Crossflow Mixing, ABETA = 0.038
- No Turbulent Momentum Mixing, FTM = 0.0 (Enthalpy Mixing Only)
- Axial Friction Factor = $0.32*re^{-0.25}$
- Crossflow Resistance Coefficient = 0.5
- Channel Flow Area Dependent Local Loss Coefficients
- 20.55" Grid Spacing (Six (6) Mixing Vane Grids & Two (2) Supporting Grids)
- EPRI Two-Phase Flow Correlations
- Five Percent Flow Reduction in the Hot Assembly
- $F^{E}_{\Delta H}$ Modeled as a Multiplier on Heat Deposited to the Hot Channels
- Direct UPFLOW Solution Scheme
- TUE-1 DNB Correlation

Table 3.3-2

Summary of Input Assumptions for At-Power Steamline Breaks

Parameter	102% Value	70% Value	30% Value
Core Power (1) MW_{th}	3479.22	2387.7	1023.3
RCS Thermal Design Flow Rate, gpm	382,800	382,800	382,800
Pressurizer Pressure, psia	2208	2208	2208
Pressurizer Level, % span	55	44.5	30.5
RCS Average Temperature, °F	594.7	585.0	572.2
Trip Reactivity, pcm	4000	4000	4000
Control Rod Drop Time to DASHPOT	2.67	2.67	2.67
Moderator Density Coefficient, Δk/gm/cc	0.43	0.43	0.43
Doppler Defect, pcm	-1600	-1600	-1600

Table 3.3-3

Reactor Trip Setpoints and Time Delays
for At-Power Steamline Breaks

Reactor Trip Function	Setpoint	Time Delay
Overpower N-16, fraction of RTP	1.18	2.0
Safety Injection Signal from Low Steamline Pressure, psig	380.	2.0

Table 3.3-4

Sequence of Events for Steamline Break at 102% Power and 0.50 ft^2 Break Area per Loop

EVENT	TIME (SEC.)
Steamline Break Initiation	0.0
Low Steamline Pressure Setpoint Reached	2.4
S-signal - Reactor Trip (Rod Motion)	4.4
Turbine Trip	4.7
Minimum DNBR Occurs	5.0

Table 3.3-5

Sequence of Events for Steamline Break at 102% Power and 0.285 ft^2 Break Area per Loop

EVENT	TIME (SEC.)
Steamline Break Initiation	0.0
Overpower N-16 Setpoint Reached	9.5
Reactor Trip (Rod Motion)	11.5
Turbine Trip	11.8
Minimum DNBR Occurs	12.2

Table 3.3-6

Sequence of Events for Steamline Break at 102% Power and 0.0625 ft^2 Break Area per Loop

EVENT	TIME (SEC.)
Steamline Break Initiation	0.0
Equilibrium Condition Reached	~100.

Table 3.3-7

Sequence of Events for Steamline Break at 70% Power and 0.50 ft^2 Break Area per Loop

EVENT	TIME (SEC.)
Steamline Break Initiation	0.0
Low Steamline Pressure Setpoint Reached	2.4
S-signal - Reactor Trip (Rod Motion)	4.4
Turbine Trip	4.7
Minimum DNBR Occurs	5.1

Table 3.3.8

Sequence of Events for Steamline Break at 70% Power and 0.285 ft^2 Break Area per Loop

EVENT	TIME (SEC.)
Steamline Break Initiation	0.0
Overpower N-16 Setpoint Reached	32.0
Reactor Trip (Rod Motion)	34.0
Minimum DNBR Occurs	34.0
Turbine Trip	34.3

Table 3.3-9

Sequence of Events for Steamline Break at 70% Power and 0.0625 ft^2 Break Area per Loop

EVENT	TIME (SEC.)
Steamline Break Initiation	0.0
Equilibrium Condition Reached	~100.

Table 3.3-10

Sequence of Events for Steamline Break at 30% Power and 0.50 ft^2 Break Area per Loop

EVENT	TIME (SEC.)
Steamline Break Initiation	0.0
Low Steamline Pressure Setpoint Reached	2.9
S-signal - Reactor Trip (Rod Motion)	4.9
Turbine Trip	5.2
Minimum DNBR Occurs	5.6

Table 3.3-11

Sequence of Events for Steamline Break at 30% Power and 0.285 ft^2 Break Area per Loop

EVENT	TIME (SEC.)
Steamline Break Initiation	0.0
Equilibrium Condition Reached	~100.

Table 3.4-1

Summary of Modifications to VIPRE-01 Model
for Steamline Breaks at Hot Shutdown

- 31 Channels, 20 Rods (18 Subchannels & 13 Lumped Channels)
- 24 Axial Nodes
- Percent of Heat Generated in Fuel Rods = 97.4%
- Turbulent Crossflow Mixing, ABETA = 0.038
- No Turbulent Momentum Mixing, FTM = 0.0 (Enthalpy Mixing Only)
- Axial Friction Factor = $0.32*re^{-0.25}$
- Crossflow Resistance Coefficient = 0.5
- Channel Flow Area Dependent Local Loss Coefficients
- 20.55" Grid Spacing (Six (6) Mixing Vane Grids & Two (2) Supporting Grids)
- EPRI Two-Phase Flow Correlations
- Five Percent Flow Reduction in the Hot Assembly
- $F^{E}_{\Delta H}$ Modeled as a Multiplier on Heat Deposited to the Hot Channels
- Direct UPFLOW Solution Scheme
- TUE-1 DNB Correlation
- W-3 DNB Correlation

Table 3.4-2

Summary of Initial Conditions for
Steamline Breaks at Hot Shutdown

Parameter	Value
Core Reactivity, pcm	-1600
RCS Thermal Design Flow Rate, gpm	382,800
Pressurizer Pressure, psia	2250
Pressurizer Level, % span	25
RCS Average Temperature, °F	557
Main Feedwater Flow Rate	Nominal Full Power Valve
Auxiliary Feedwater Flow Rate, gpm	1880.
Steam Generator Pressure, psia	1093.

Table 3.4-3

Sequence of Events for Reference Case
Steamline Break at Hot Shutdown

EVENT	TIME (SEC.)
Event Initiation (Break)	0.05
Lo Steamline Pressure Setpoint Reached	0.96
Steamline Isolation Feedwater Isolation	7.96
ECCS Flow to RCS (Unborated)	13.00
Criticality	13.90
Pressurizer Empties	~16.
Borated ECCS Flow Reaches Core	~203.
Peak Power	~204.

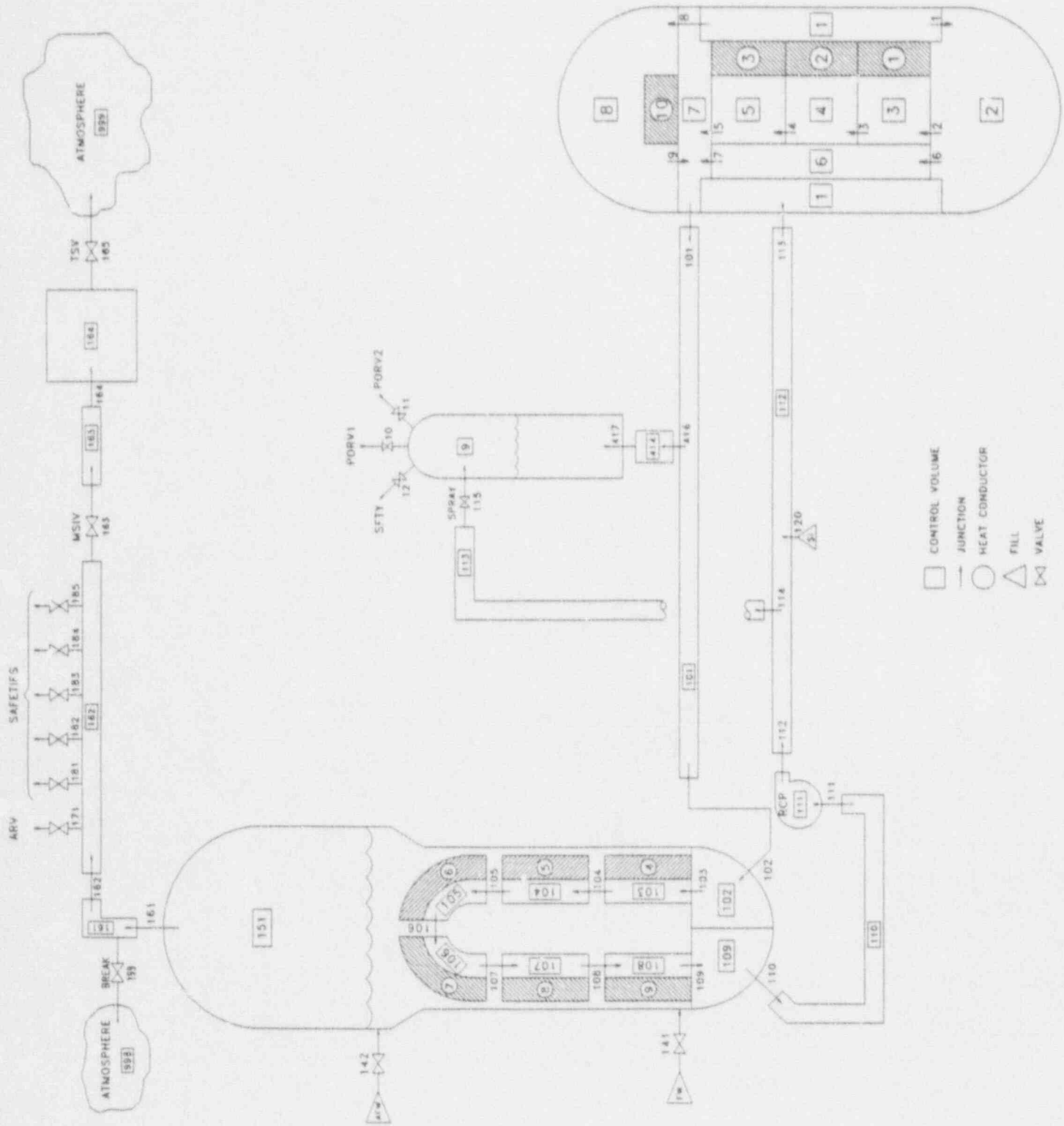

Figure 3.3-1 RETRAN Noding Diagram for At-Power Steamline Break Analysis

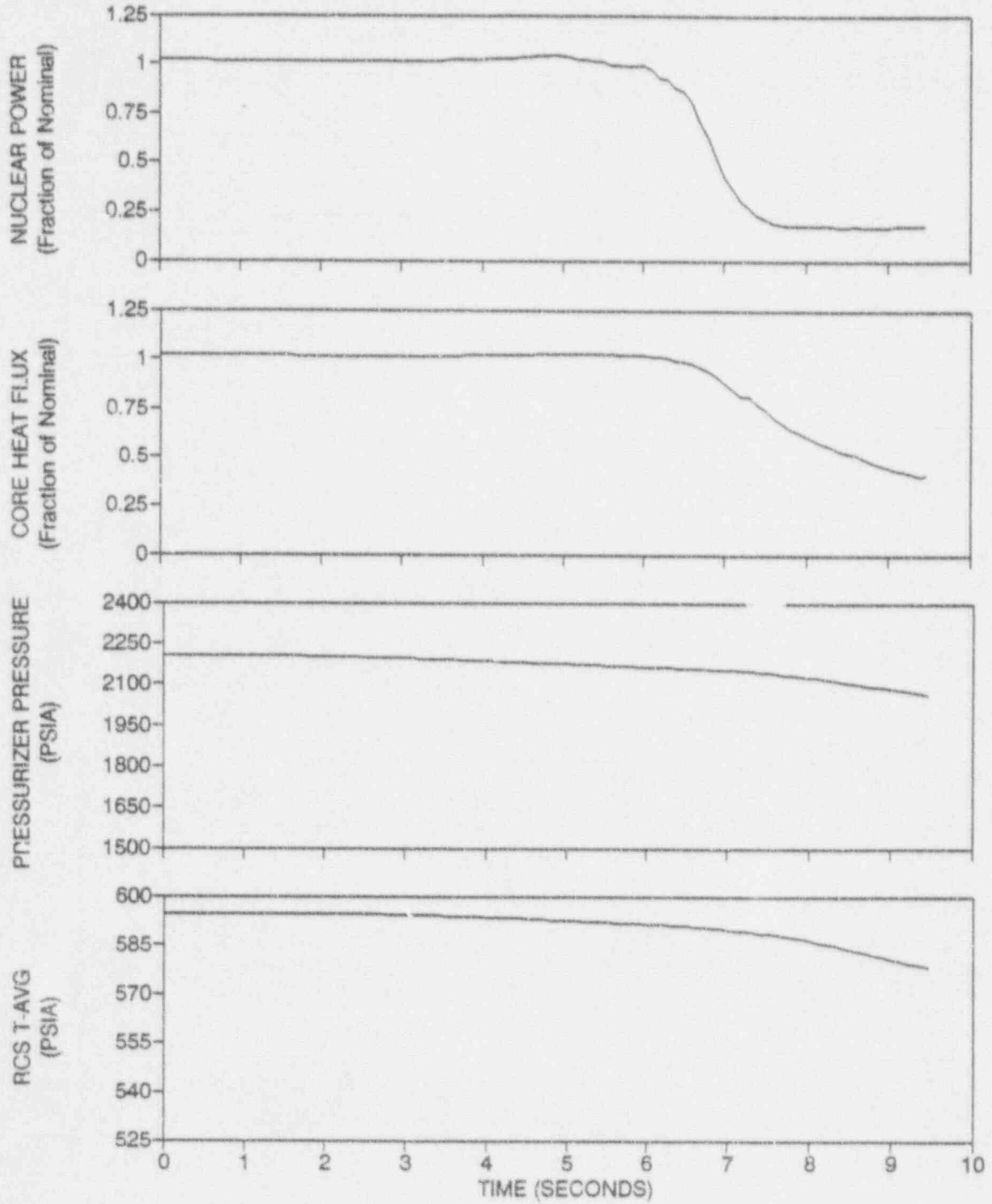

Figure 3.3-2 Nuclear Power, Heat Flux, RCS T-avg, and Pressurizer Pressure for 102% Initial Power, 0.5 Ft^2 Break Area per Loop

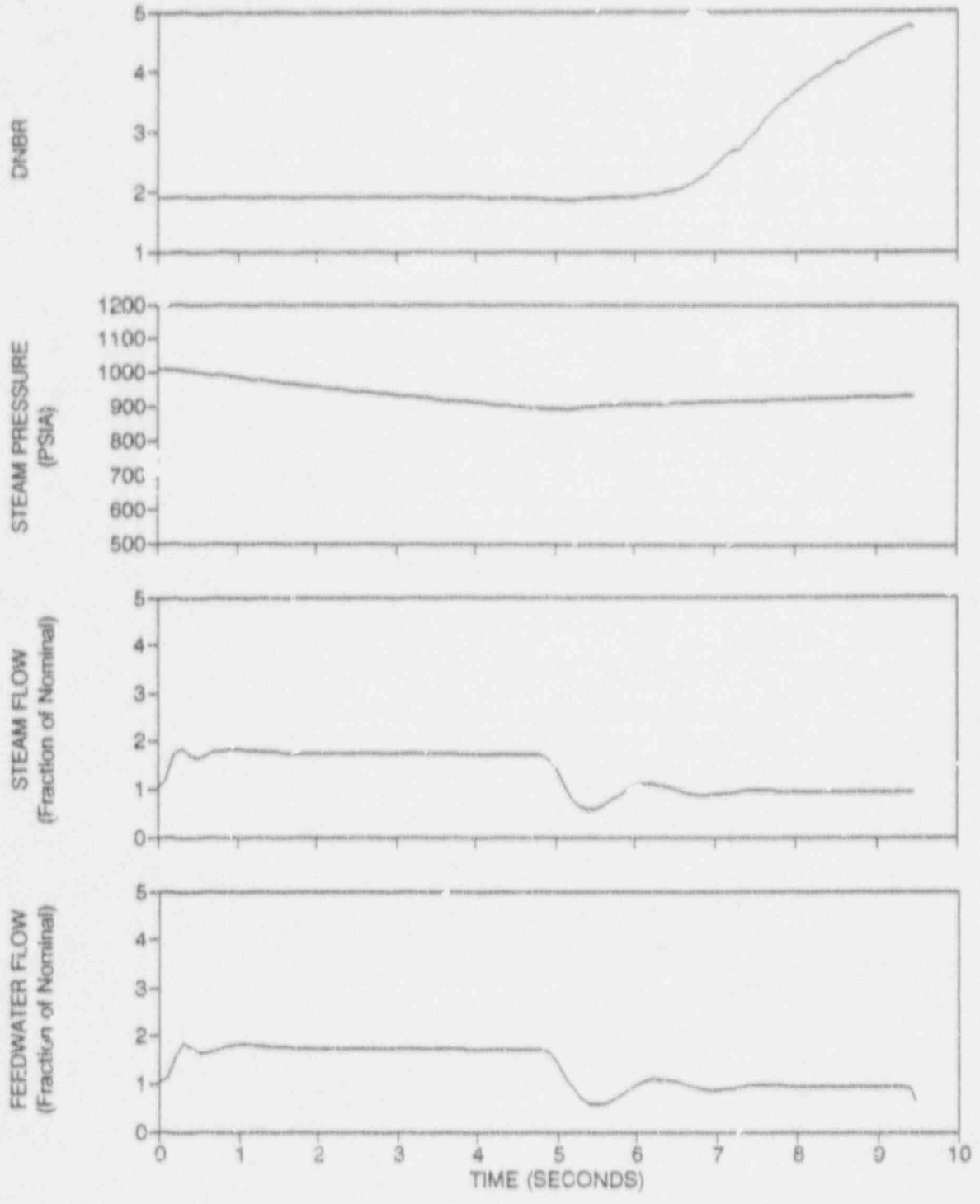

Figure 3.3-3 DNBR, Steam Generator Pressure, Steam Flow, and Feedwater Flow for 102% Initial Power, 0.5 Ft^2 Break Area per Loop

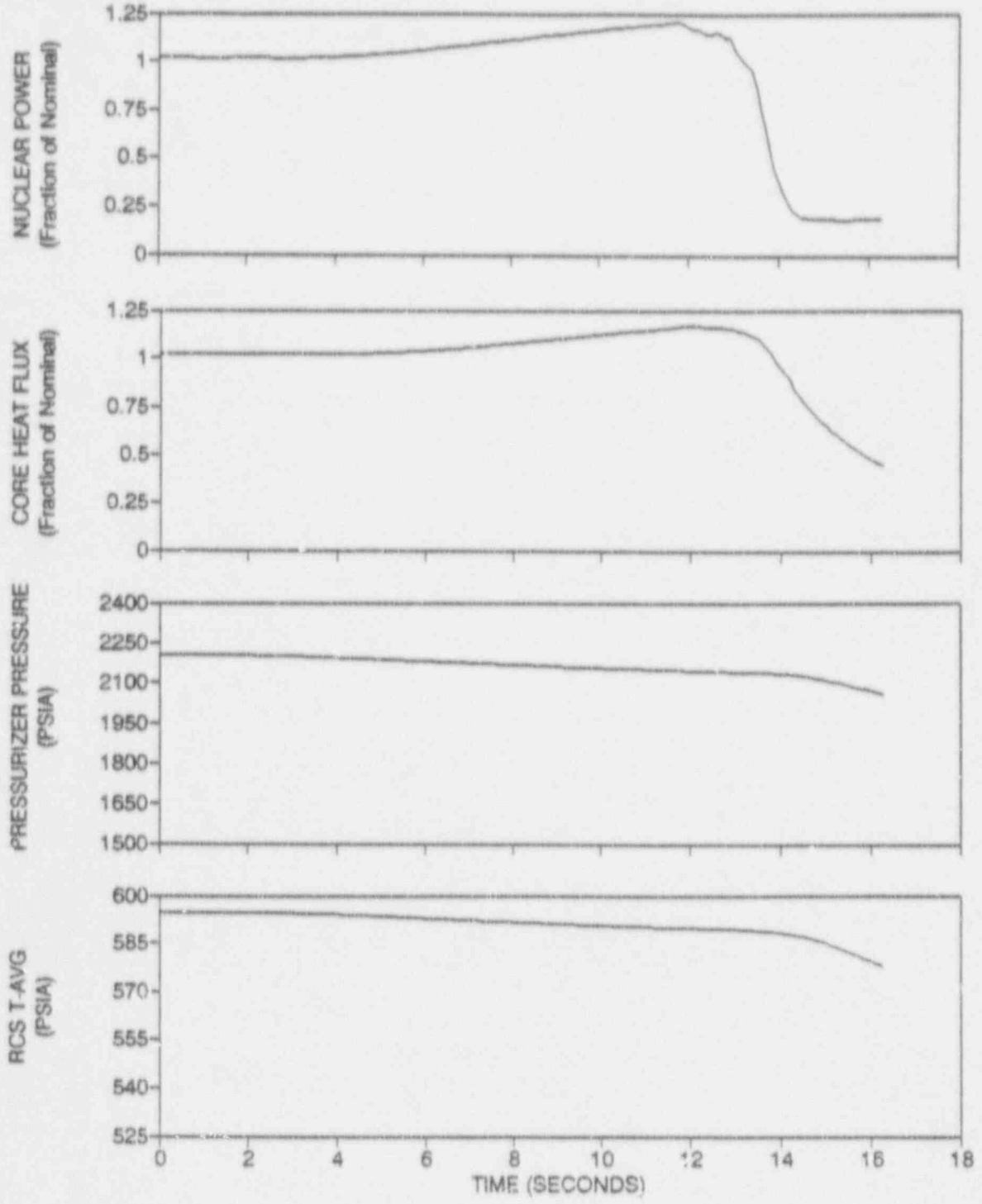

Figure 3.3-4 Nuclear Power, Heat Flux, RCS T-avg, and Pressurizer Pressure for 102% Initial Power, 0.285 Ft^2 Break Area per Loop

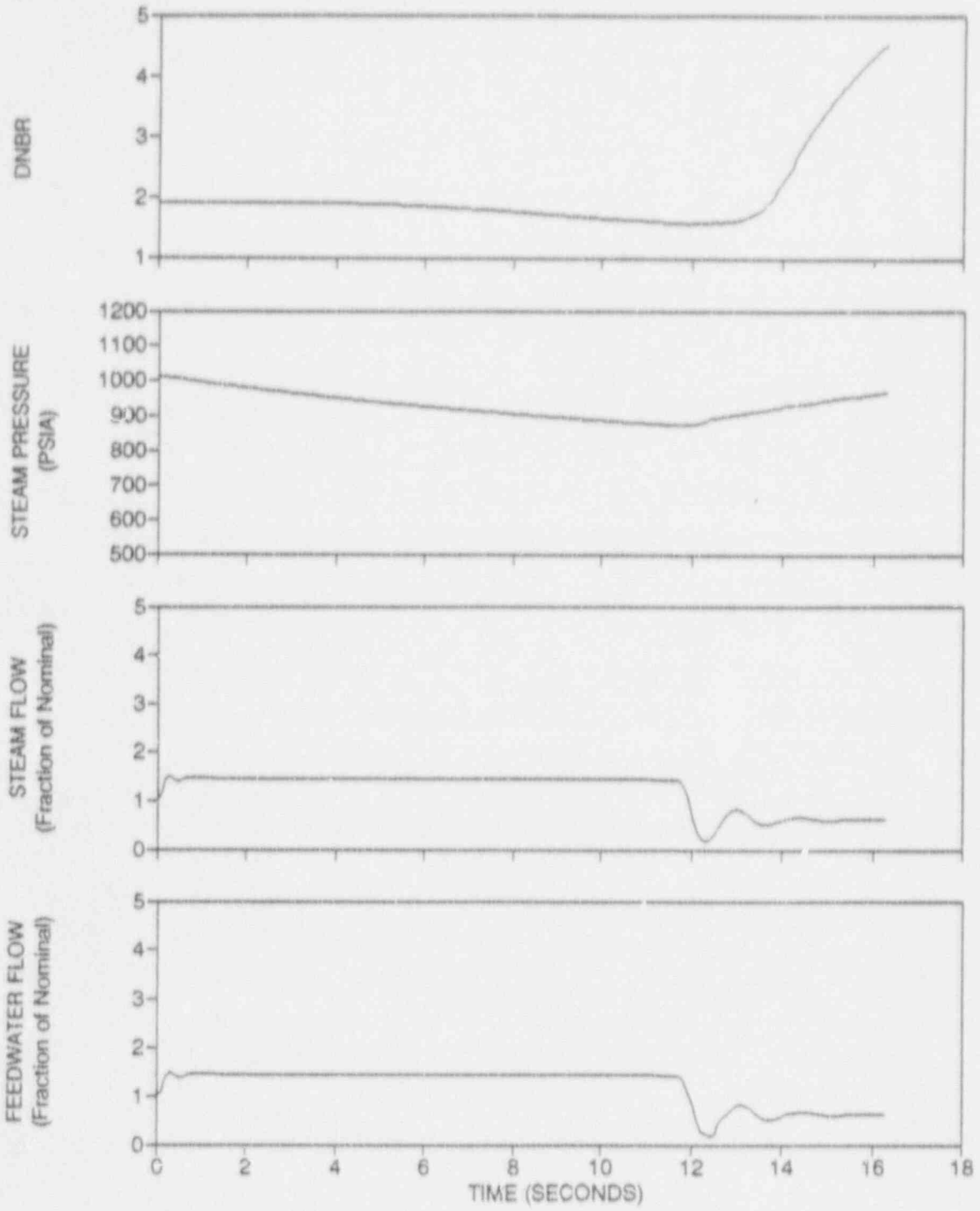

Figure 3.3-5 DNBR, Steam Generator Pressure, Steam Flow, and Feedwater Flow for 102% Initial Power, 0.285 Ft^2 Break Area per Loop

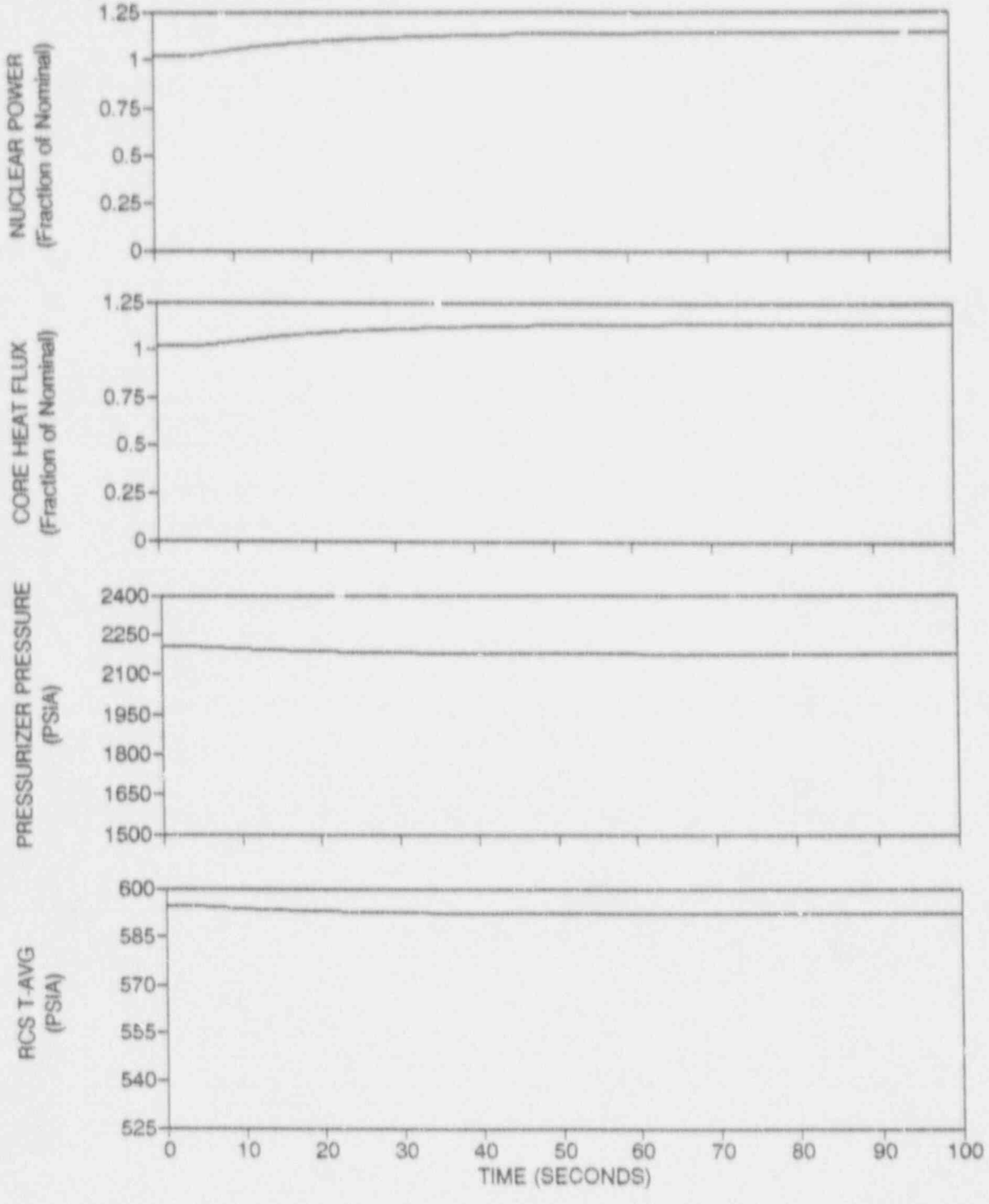

Figure 3.3-6 Nuclear Power, Heat Flux, RCS T-avg, and Pressurizer Pressure for 102% Initial Power, 0.0625 Ft^2 Break Area per Loop

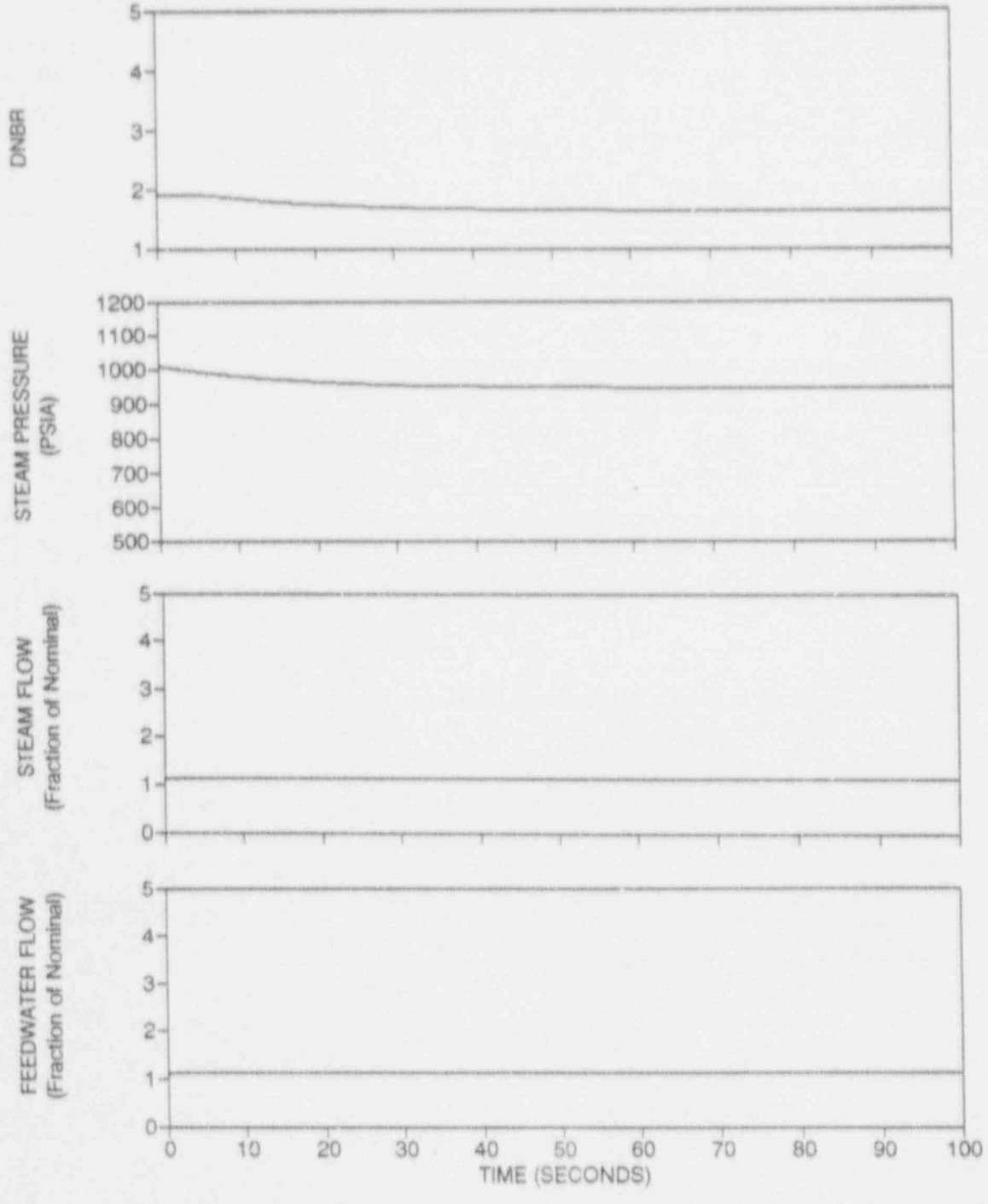

Figure 3.3-7 DNBR, Steam Generator Pressure, Steam Flow, and Feedwater Flow for 102% Initial Power, 0.0625 Ft^2 Break Area per Loop

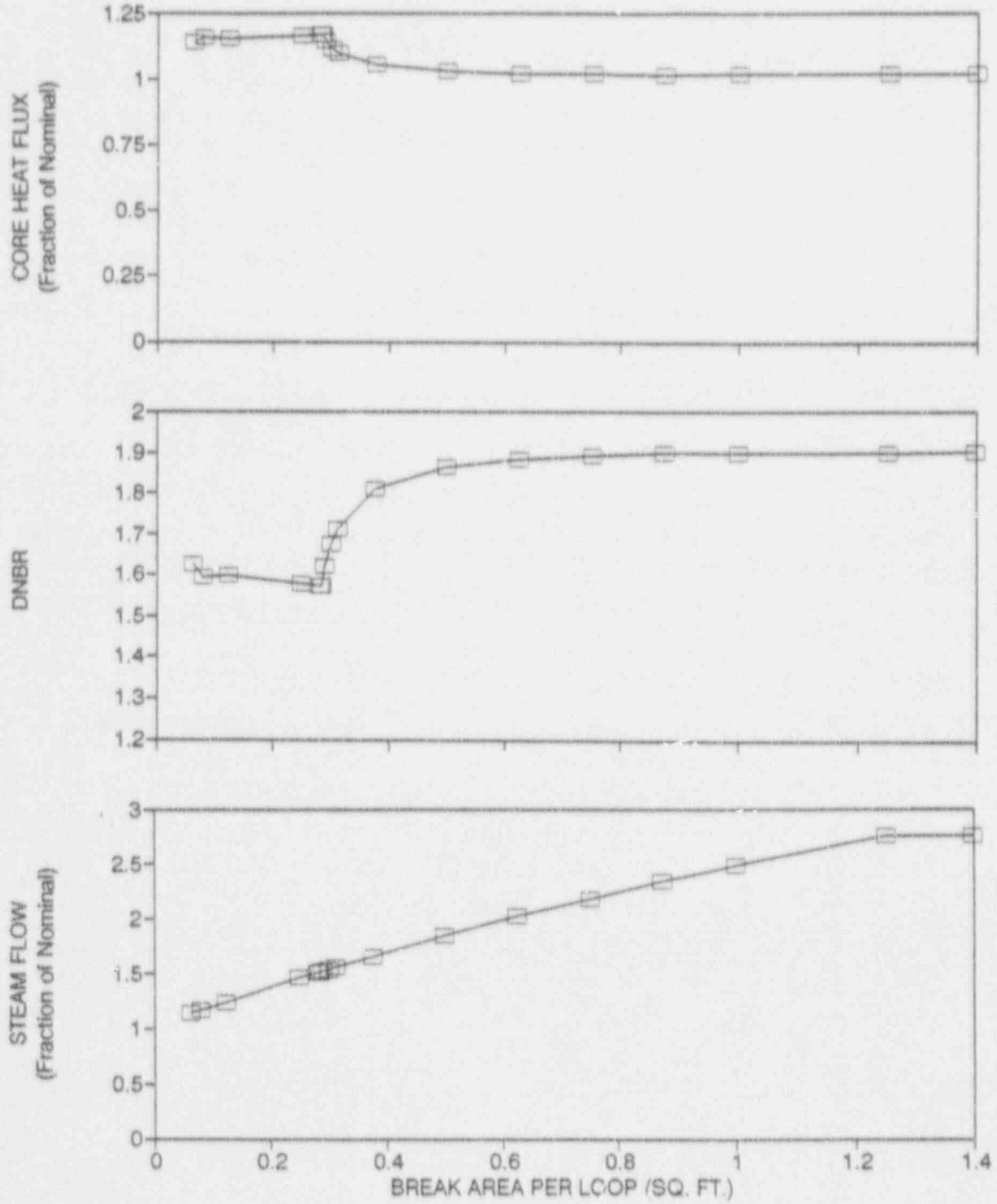

Figure 3.3-8 Maximum Steam Flow, Peak Heat Flux, and Minimum DNBR versus Break Area per Loop for 102% Initial Power

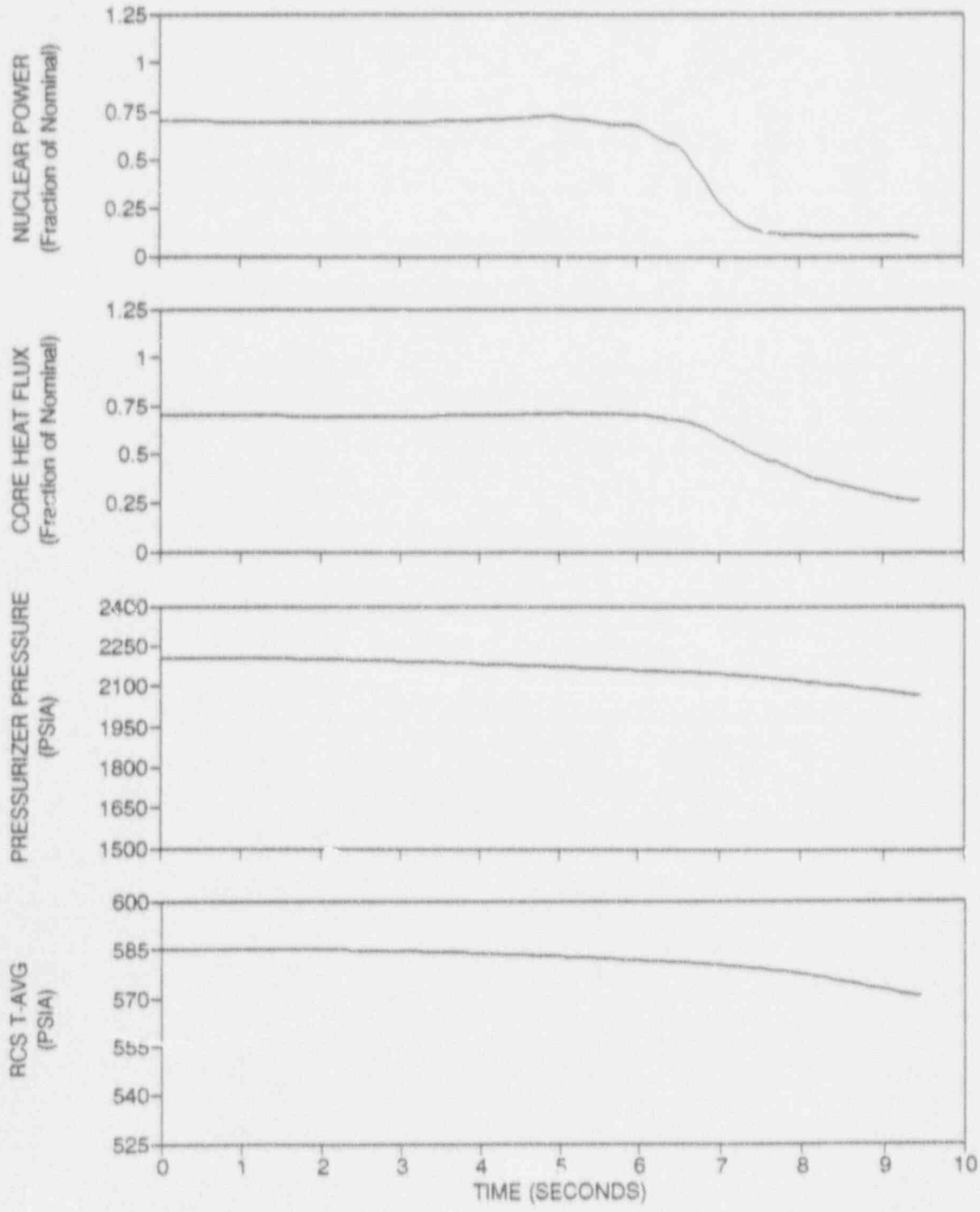

Figure 3.3-9 Nuclear Power, Heat Flux, RCS T-avg, and Pressurizer Pressure for 70% Initial Power, 0.5 Ft^2 Break Area per Loop

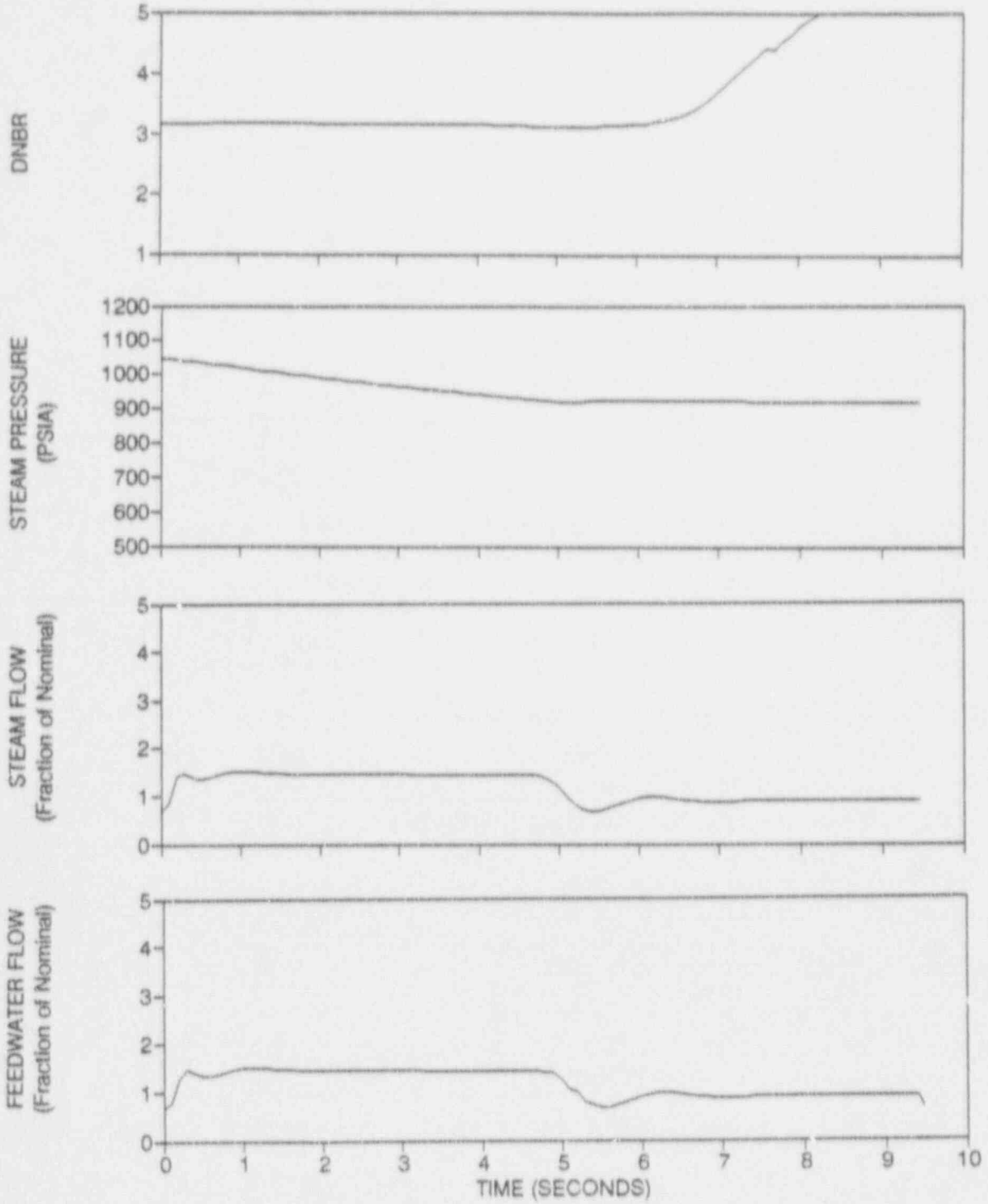

Figure 3.3-10 DNBR, Steam Generator Pressure, Steam Flow, and Feedwater Flow for 70% Initial Power, 0.5 Ft^2 Break Area per Loop

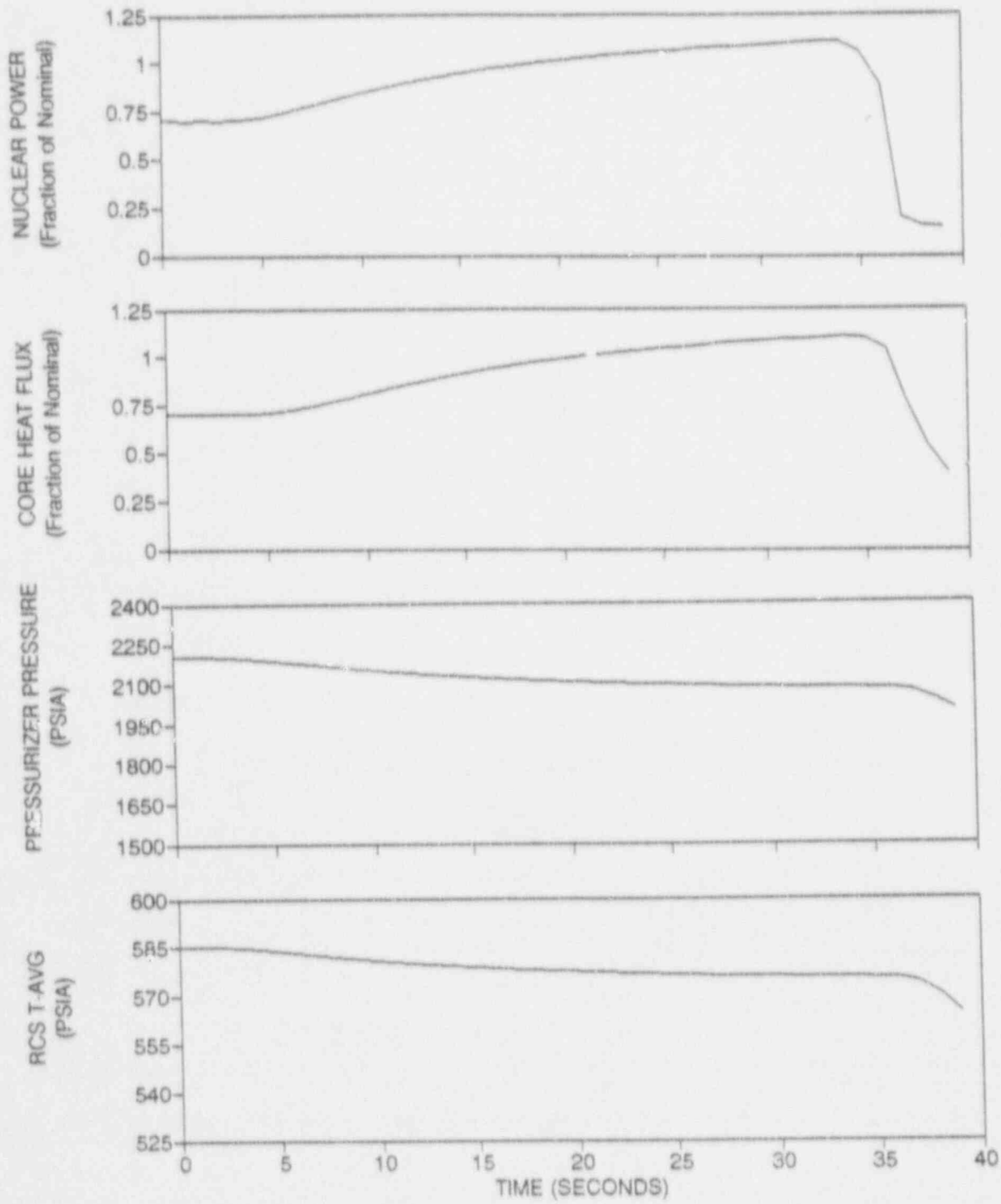

Figure 3.3-11 Nuclear Power, Heat Flux, RCS T-avg, and Pressurizer Pressure for 70% Initial Power, 0.285 Ft^2 Break Area per Loop

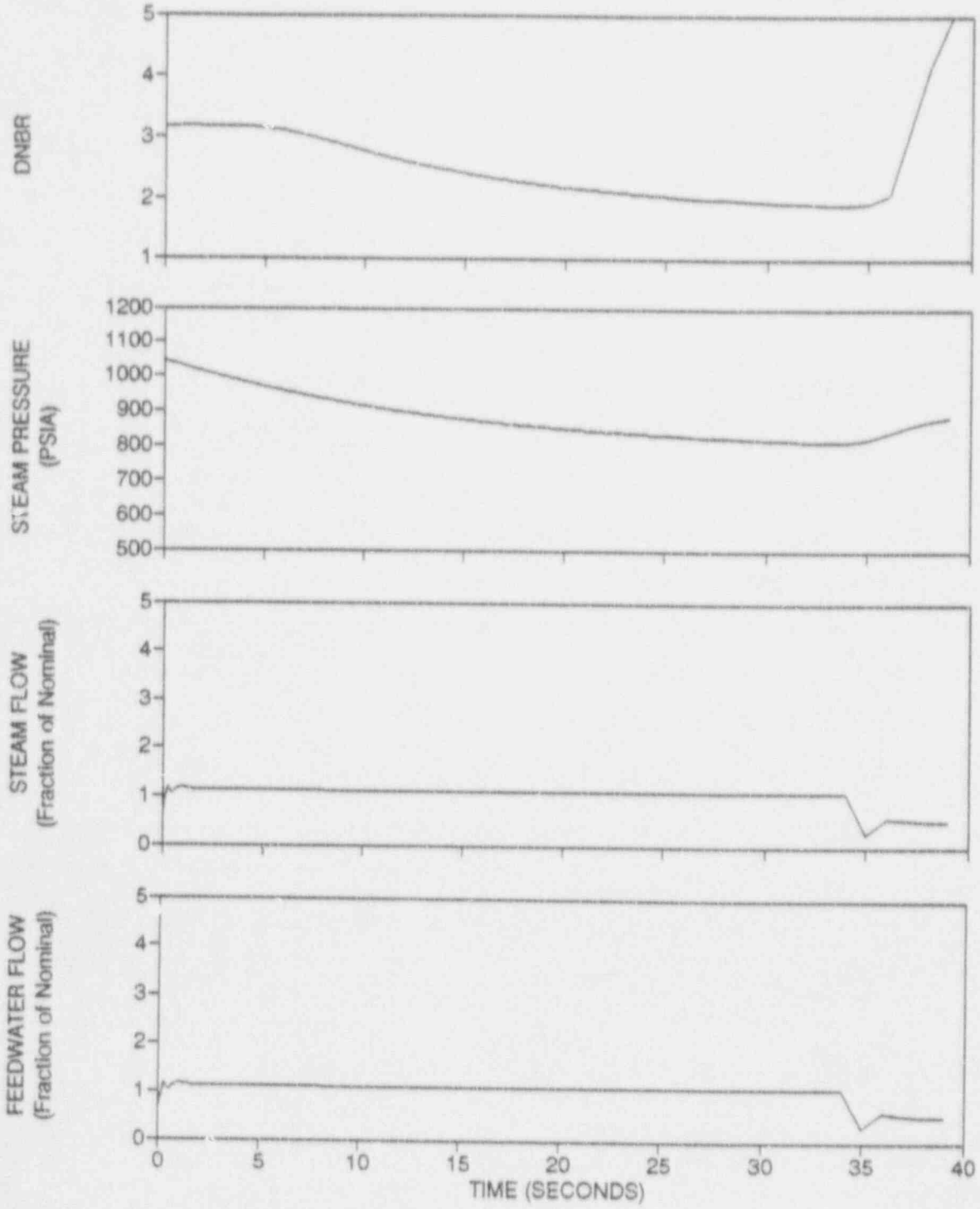

Figure 3.3-12 DNBR, Steam Generator Pressure, Steam Flow, and Feedwater Flow for 70% Initial Power, 0.285 Ft^2 Break Area per Loop

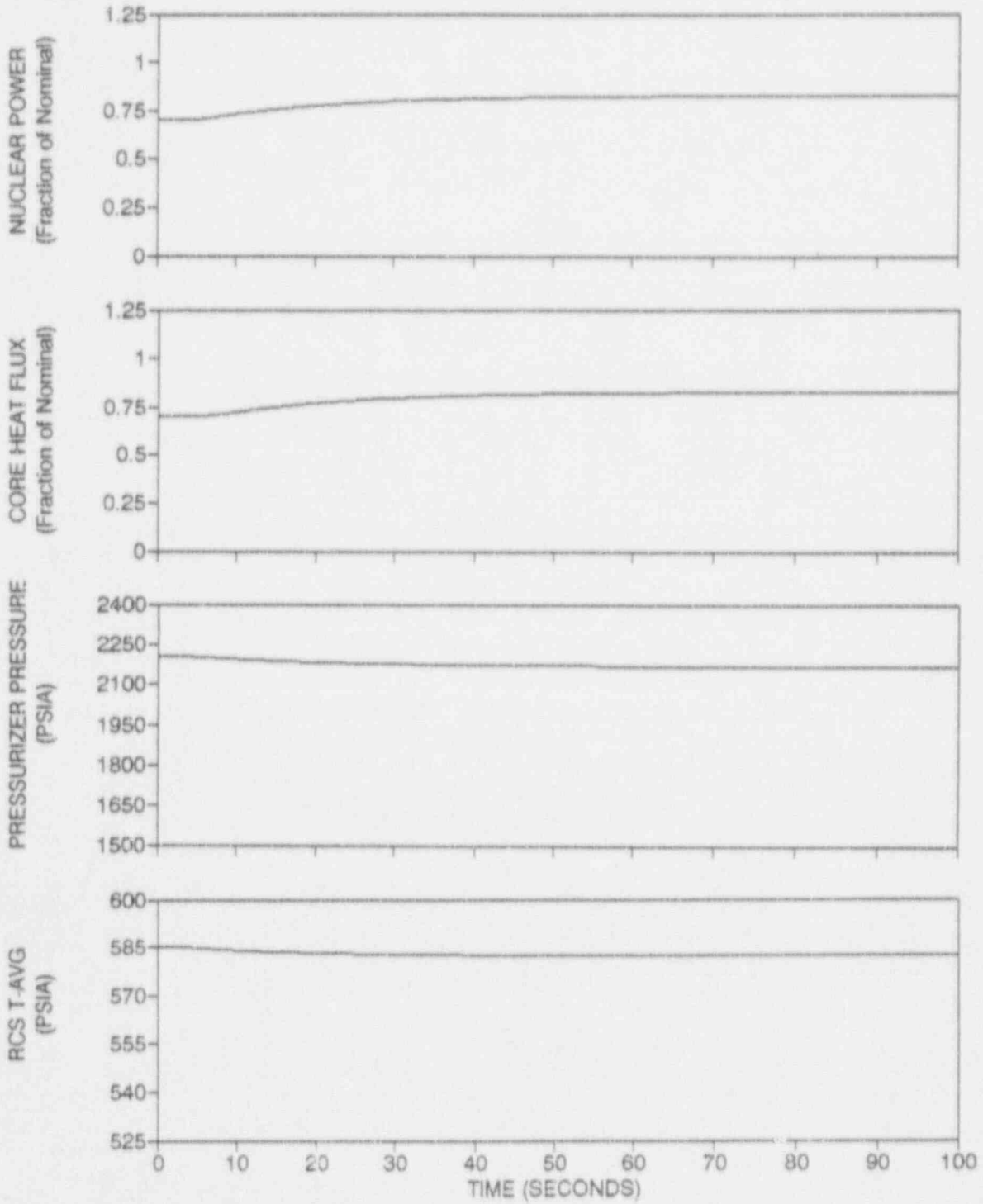

Figure 3.3-13 Nuclear Power, Heat Flux, RCS T-avg, and Pressurizer Pressure for 70% Initial Power, 0.0625 Ft^2 Break Area per Loop

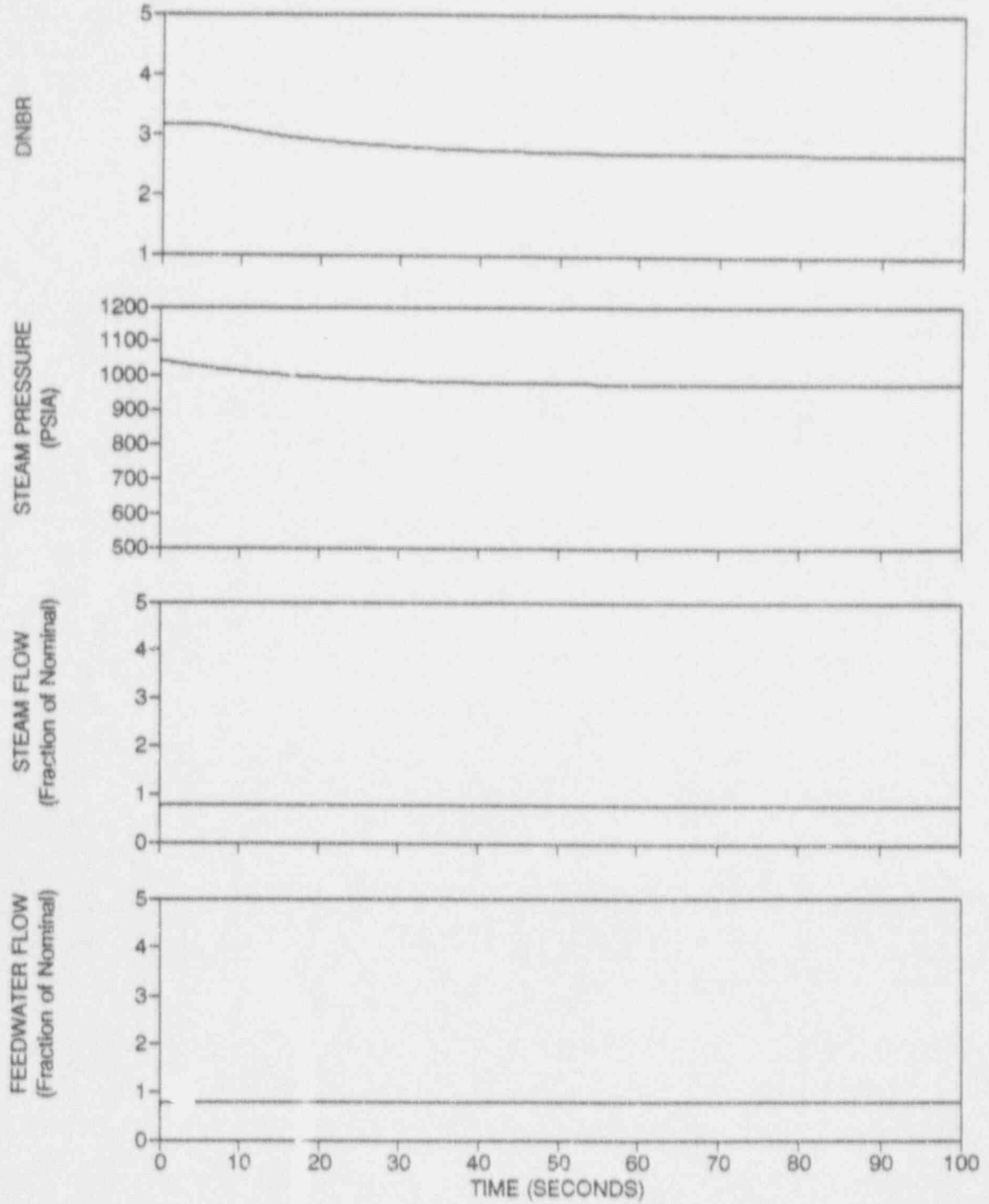

Figure 3.3-14 DNBR, Steam Generator Pressure, Steam Flow, and Feedwater Flow for 70% Initial Power, 0.0625 Ft^2 Break Area per Loop

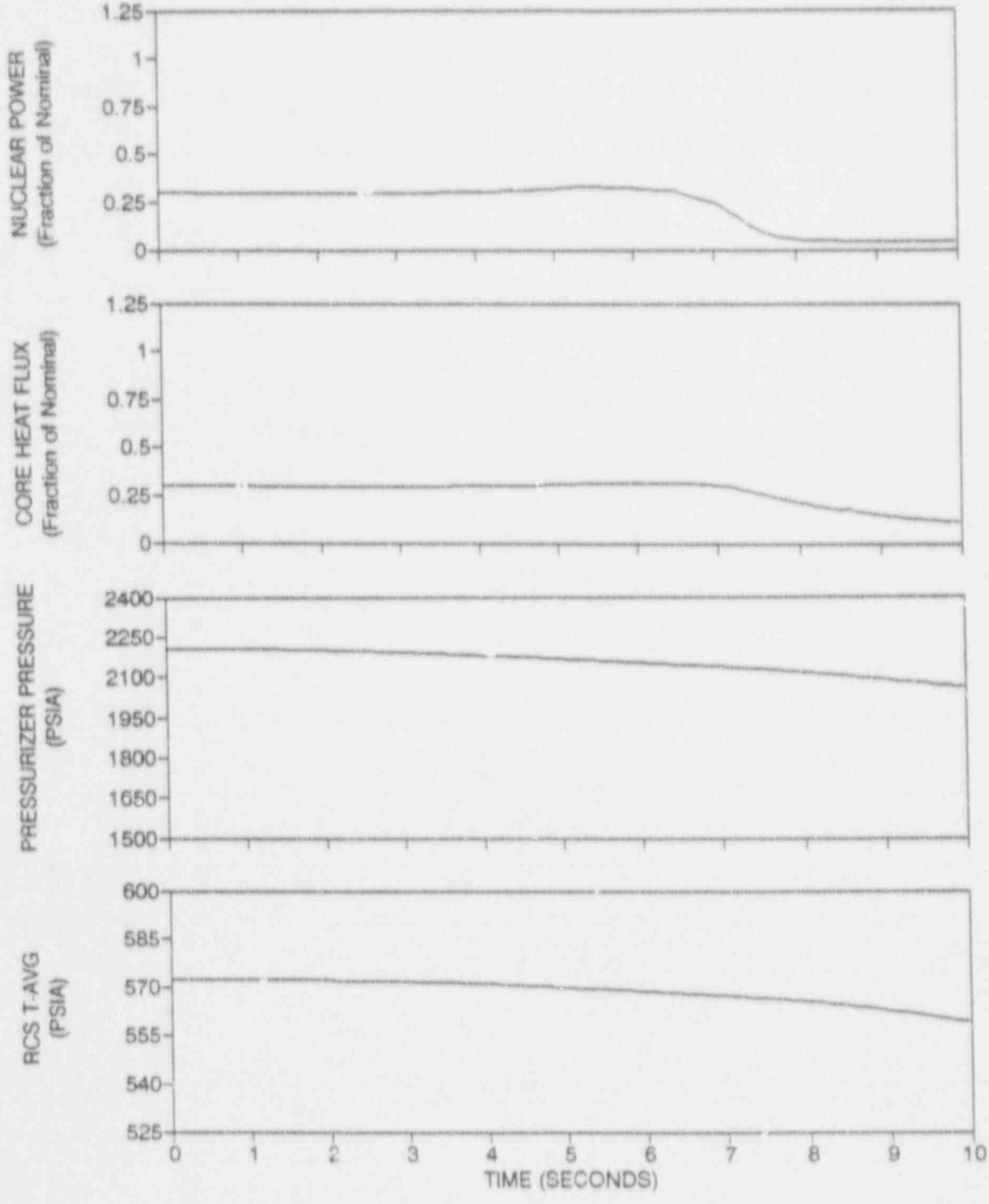

Figure 3.3-15 Nuclear Power, Heat Flux, RCS T-avg, and Pressurizer Pressure for 30% Initial Power, 0.5 Ft^2 Break Area per Loop

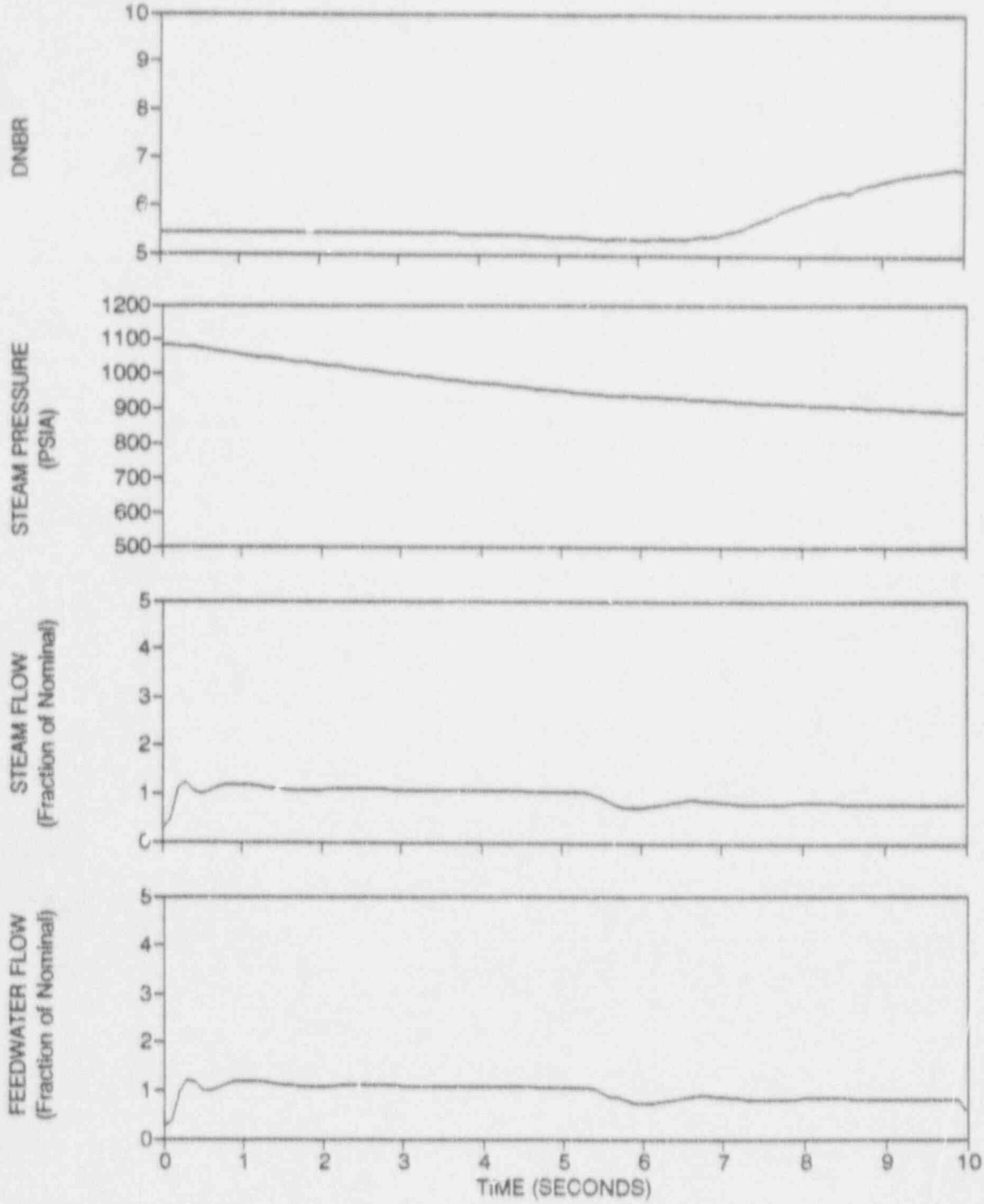

Figure 3.3-16 DNBR, Steam Generator Pressure, Steam Flow, and Feedwater Flow for 30% Initial Power, 0.5 Ft^2 Break Area per Loop

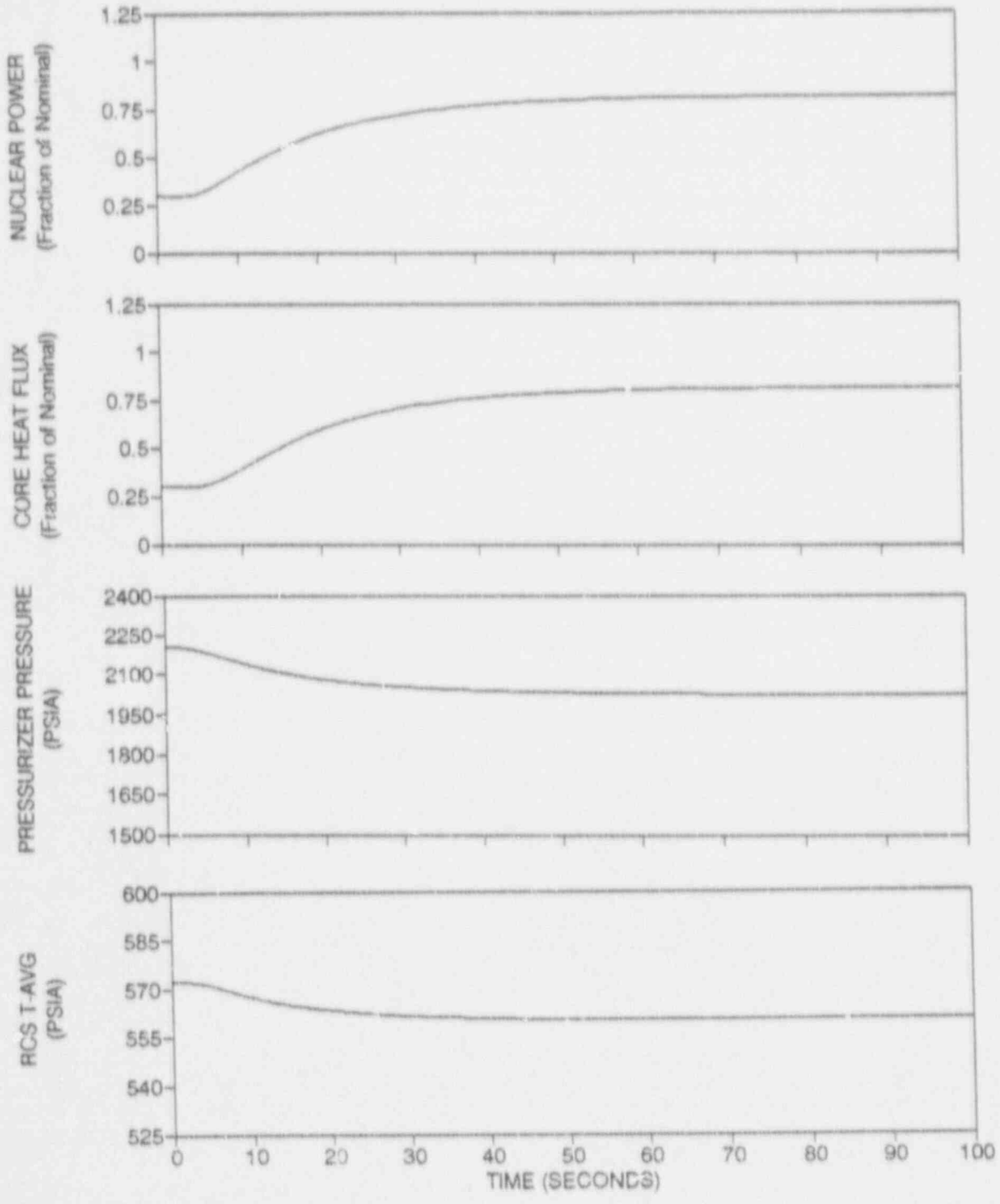

Figure 3.3-17 Nuclear Power, Heat Flux, RCS T-avg, and Pressurizer Pressure for 30% Initial Power, 0.285 Ft^2 Break Area per Loop

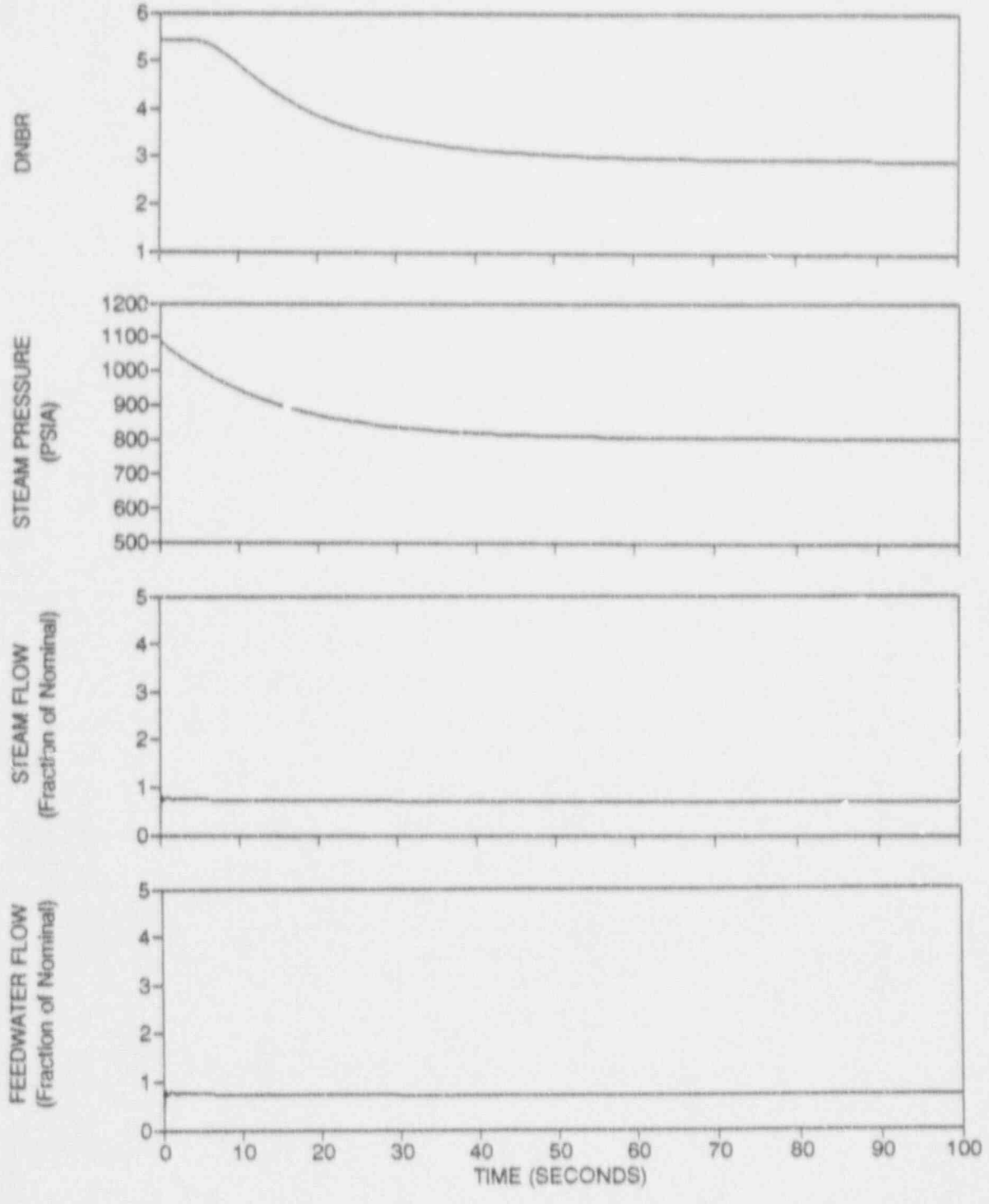

Figure 3.3-18 DNBR, Steam Generator Pressure, Steam Flow, and Feedwater Flow for 30% Initial Power, 0.285 Ft^2 Break Area per Loop

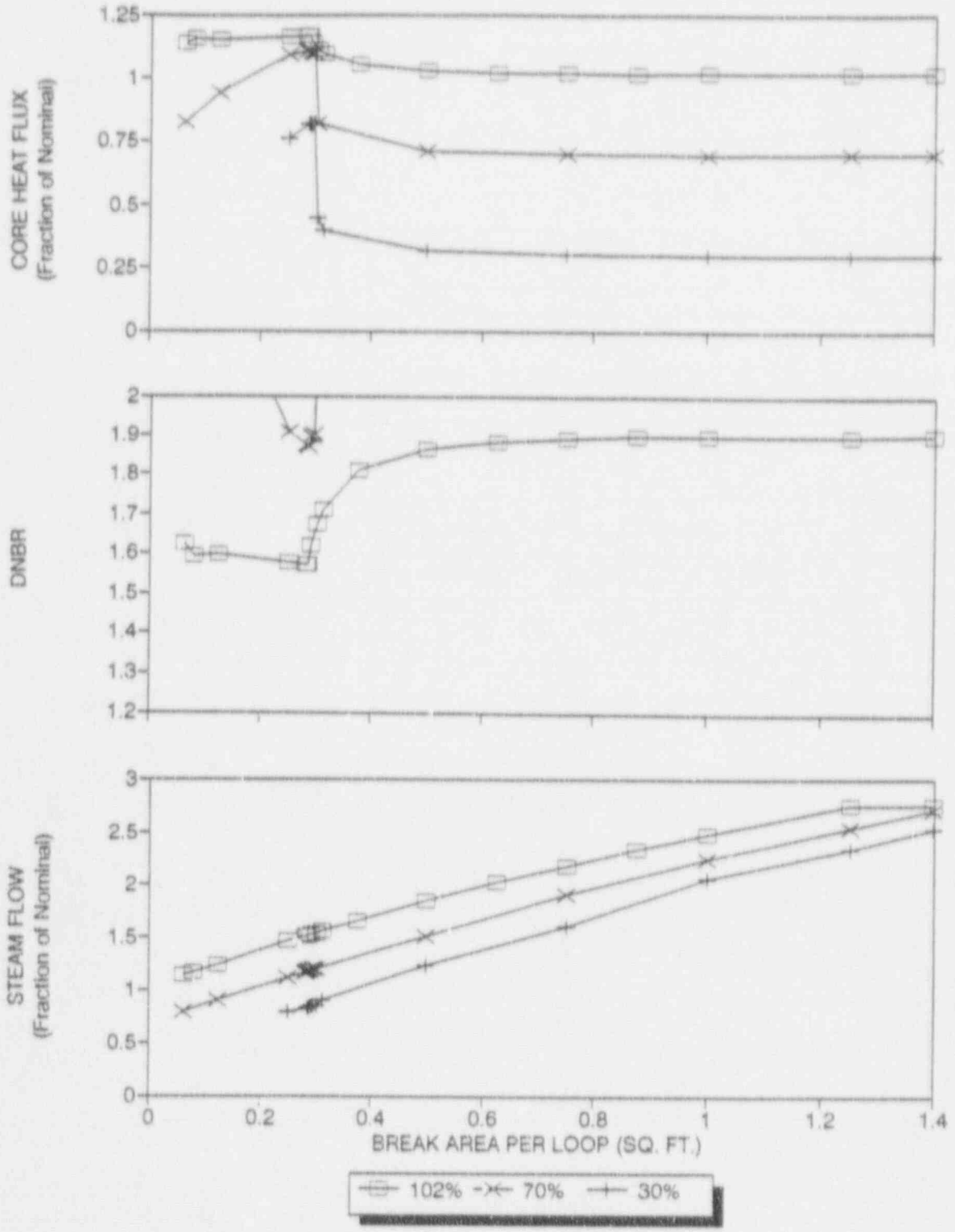

Figure 3.3-19 Maximum Steam Flow, Peak Heat Flux, and Minimum DNBR versus Break Area per Loop for 102%, 70%, and 30% Initial Power

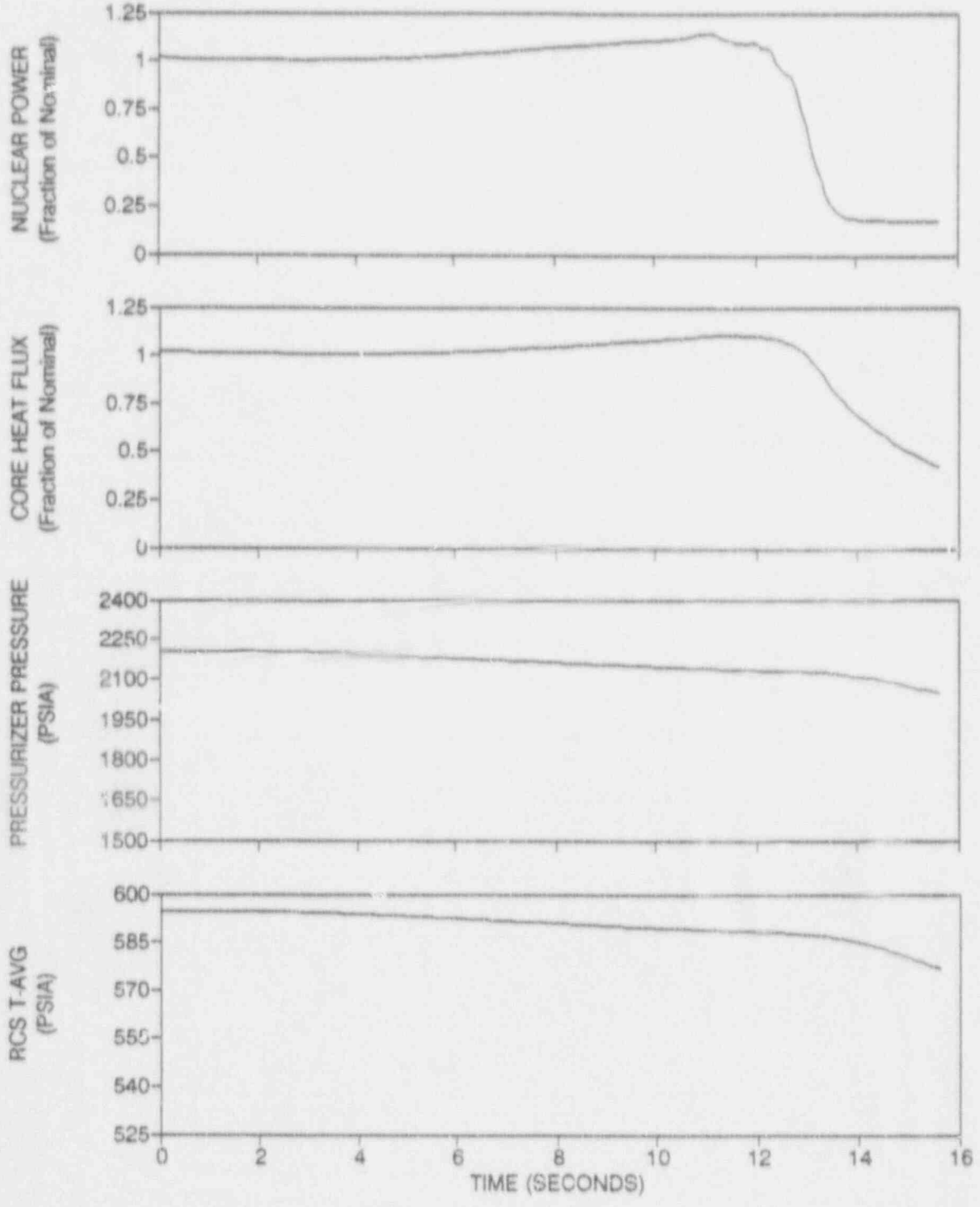

Figure 3.3-20 Nuclear Power, Heat Flux, RCS T-avg, and Pressurizer Pressure for 102% Initial Power, 0.285 Ft^2 Break Area per Loop, and Automatic Rod Control

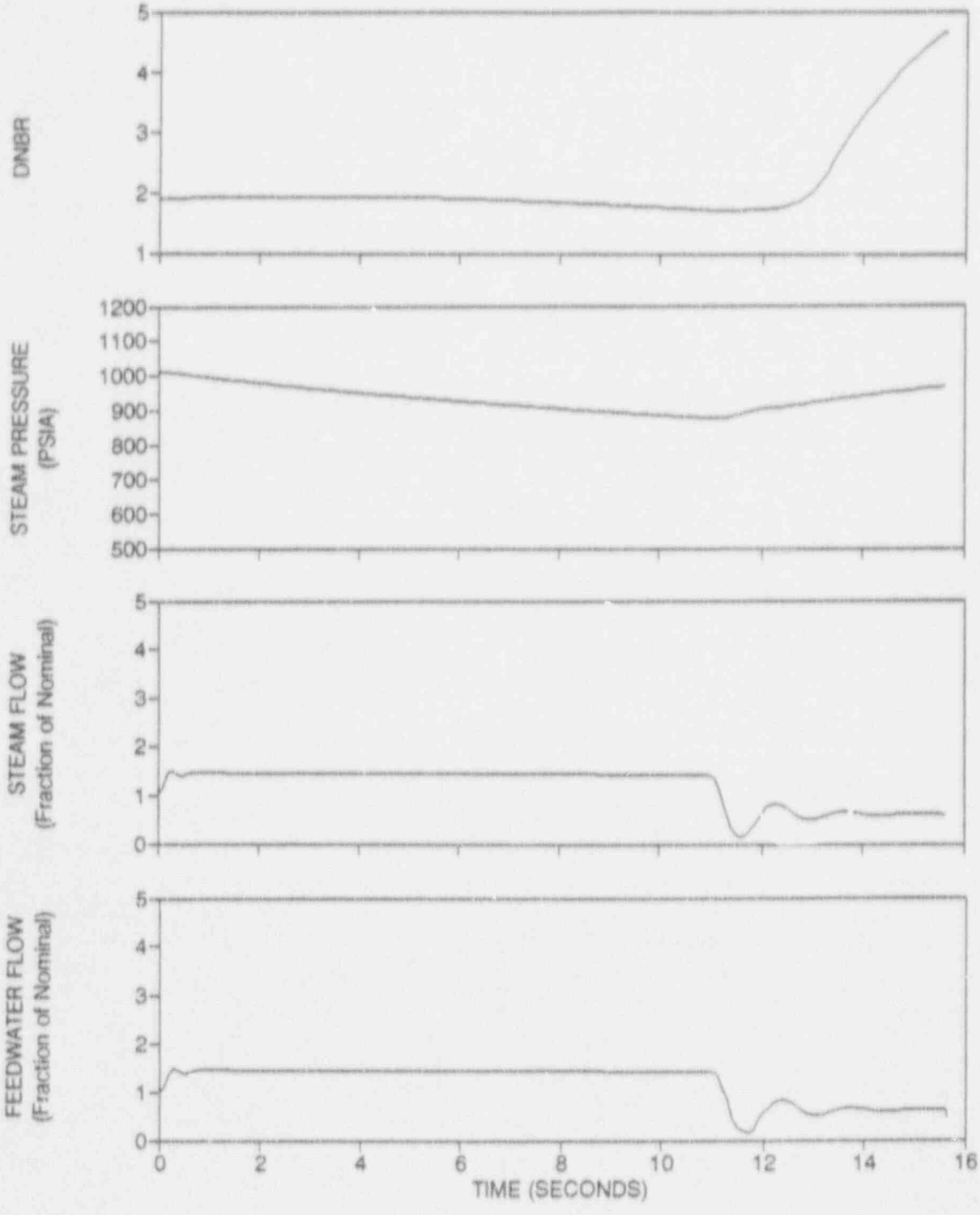

Figure 3.3-21 DNBR, Steam Generator Pressure, Steam Flow, and Feedwater Flow for 102% Initial Power, 0.285 Ft^2 Break Area per Loop, and Automatic Rod Control

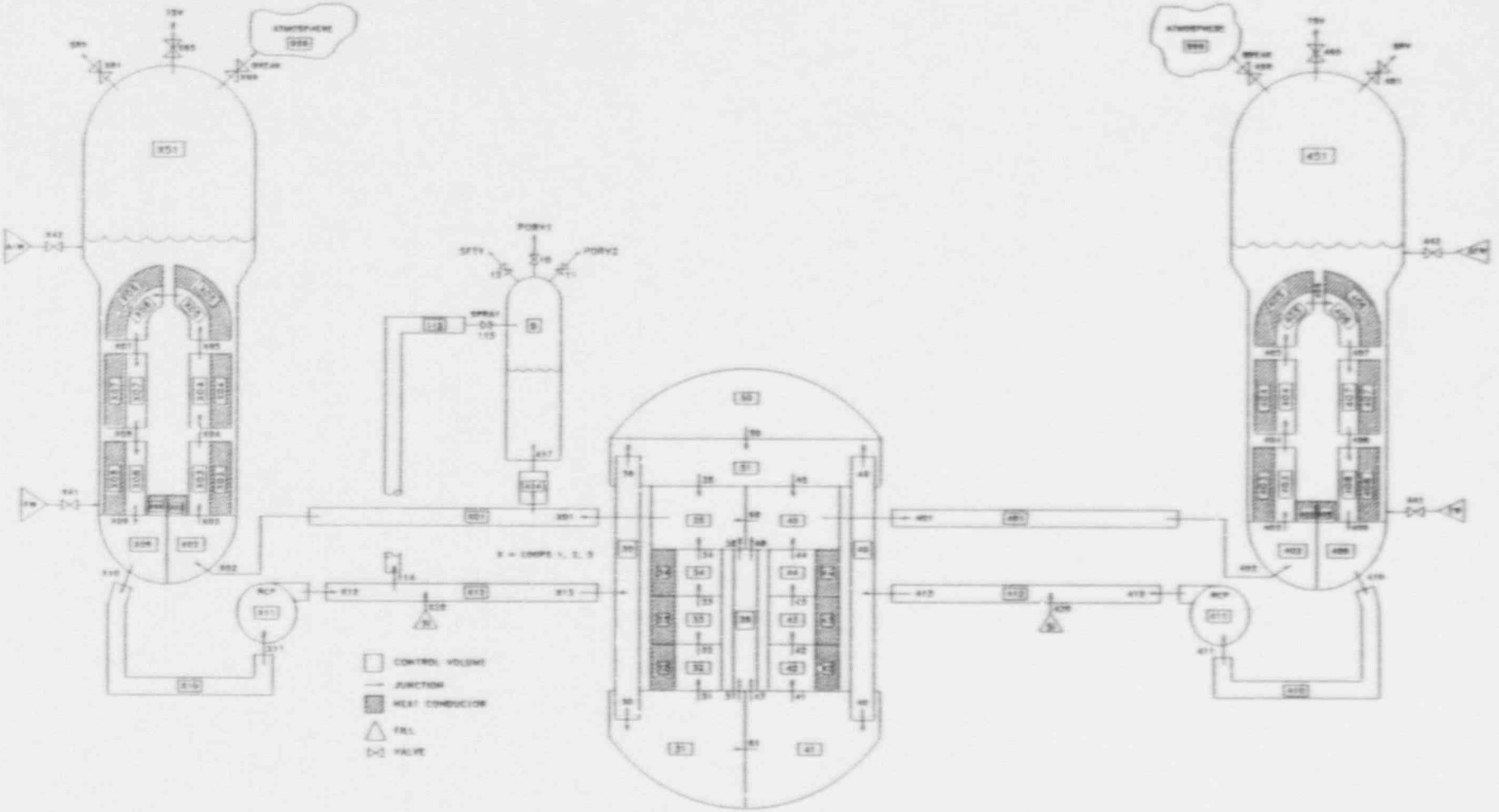

Figure 3.4-2 RETRAN Noding Diagram for Hot Zero Power Steamline Break Analysis

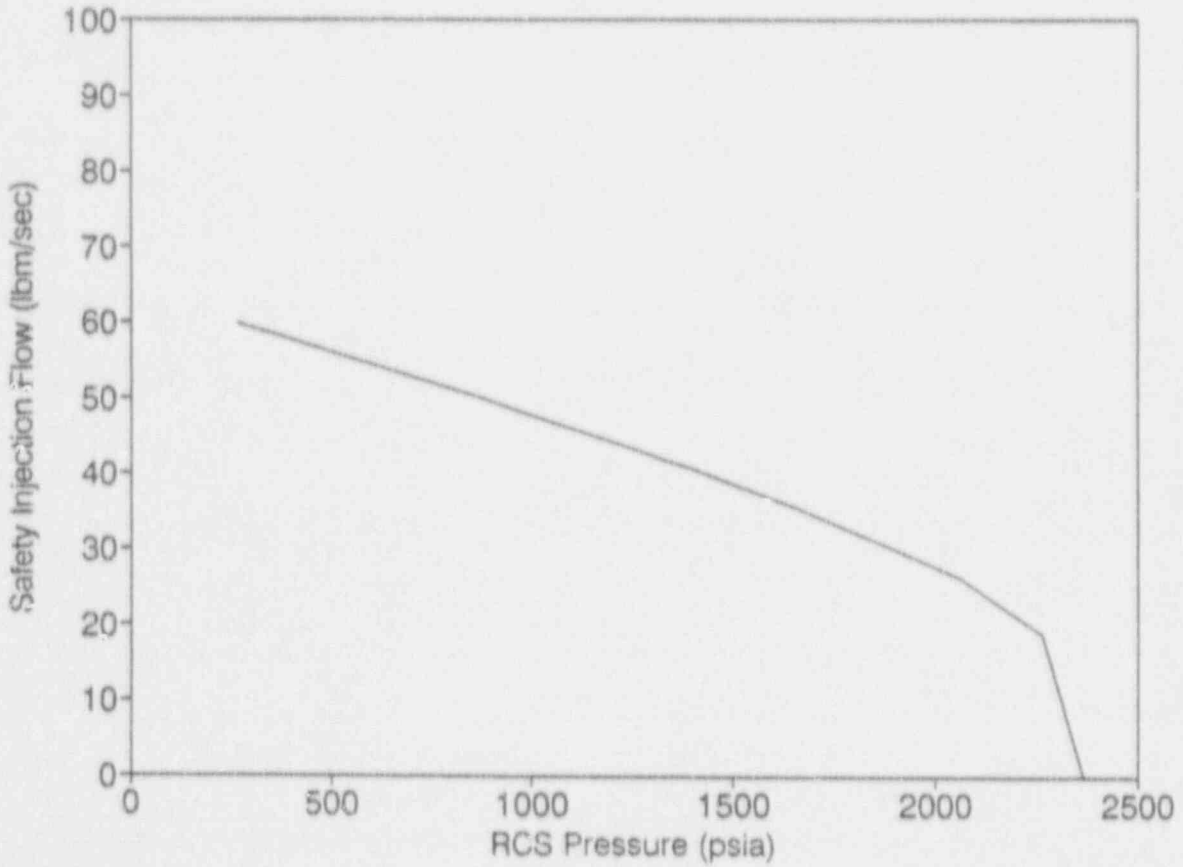

Figure 3.4-2 Safety Injection Flow versus System Pressure

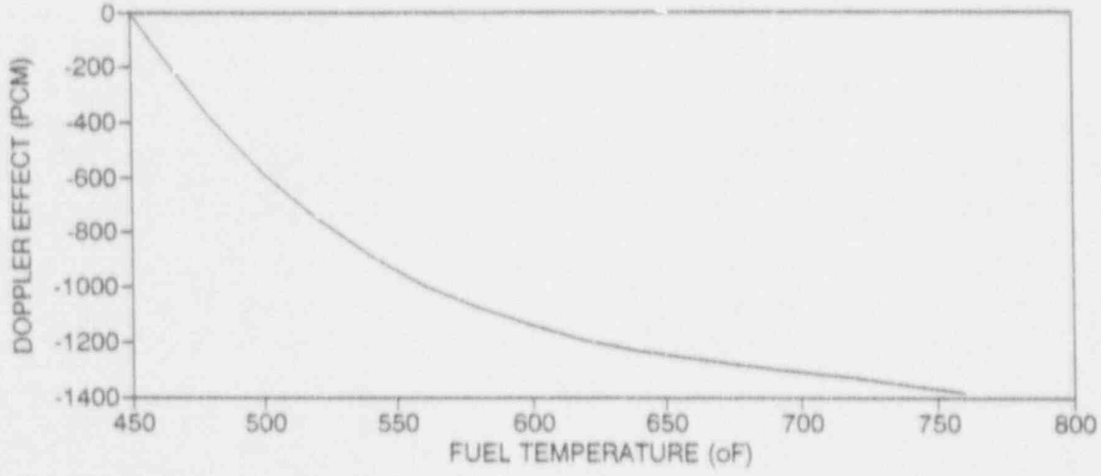

Figure 3.4-3 Typical Doppler Defect for Hot Zero Power, EOL, N-1 Rods Inserted

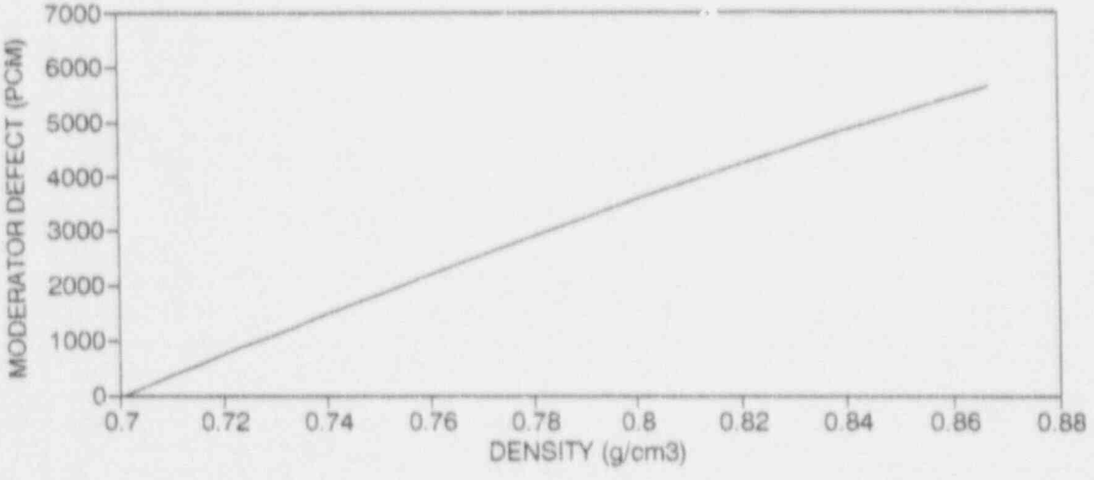

Figure 3.4-4 Typical Moderator Density Defect for Hot Zero Power, EOL, N-1 Rods Inserted

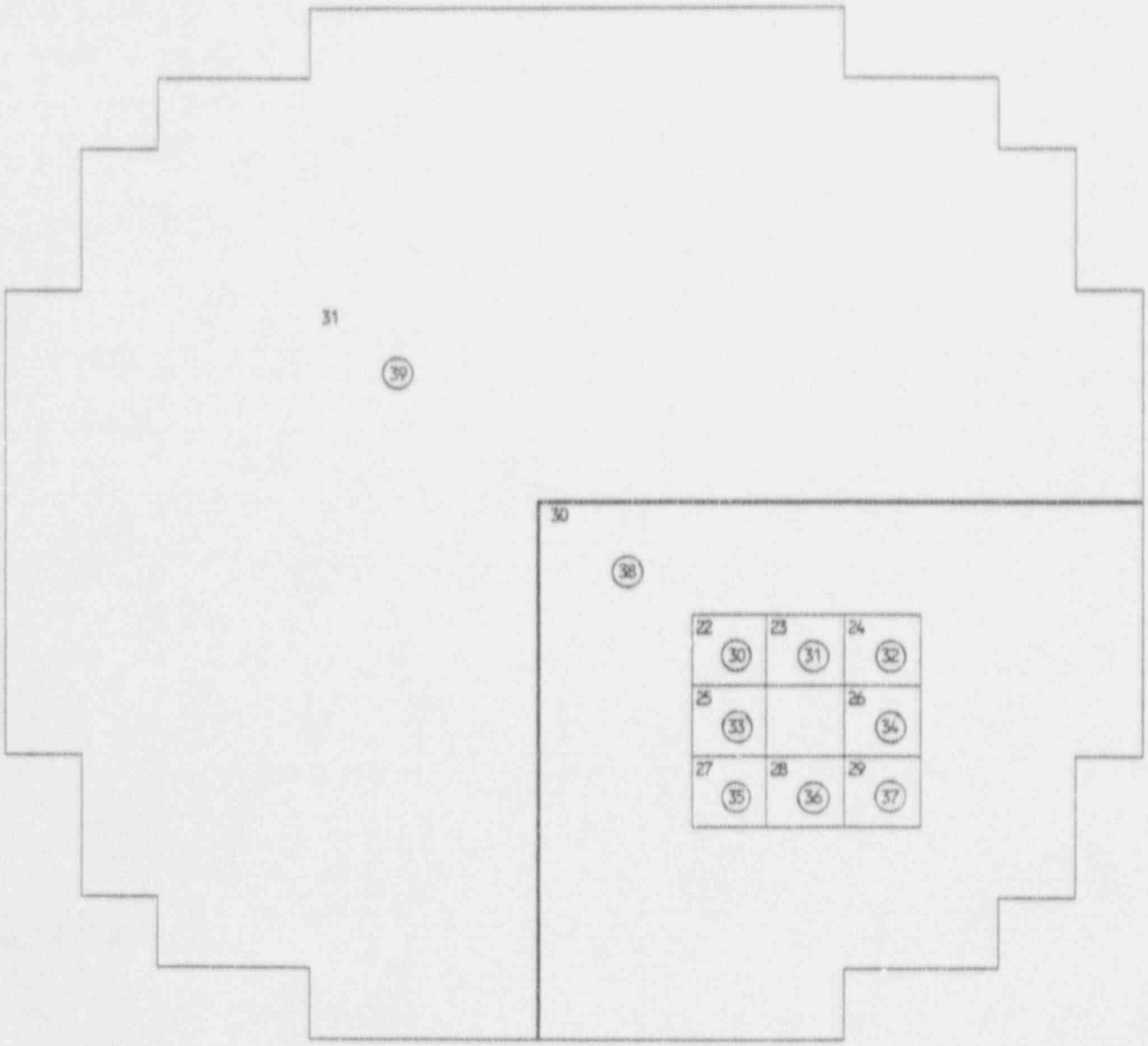

Figure 3.4-5 Full Core VIPRE Model for Hot Zero Power Steamline Break Analysis

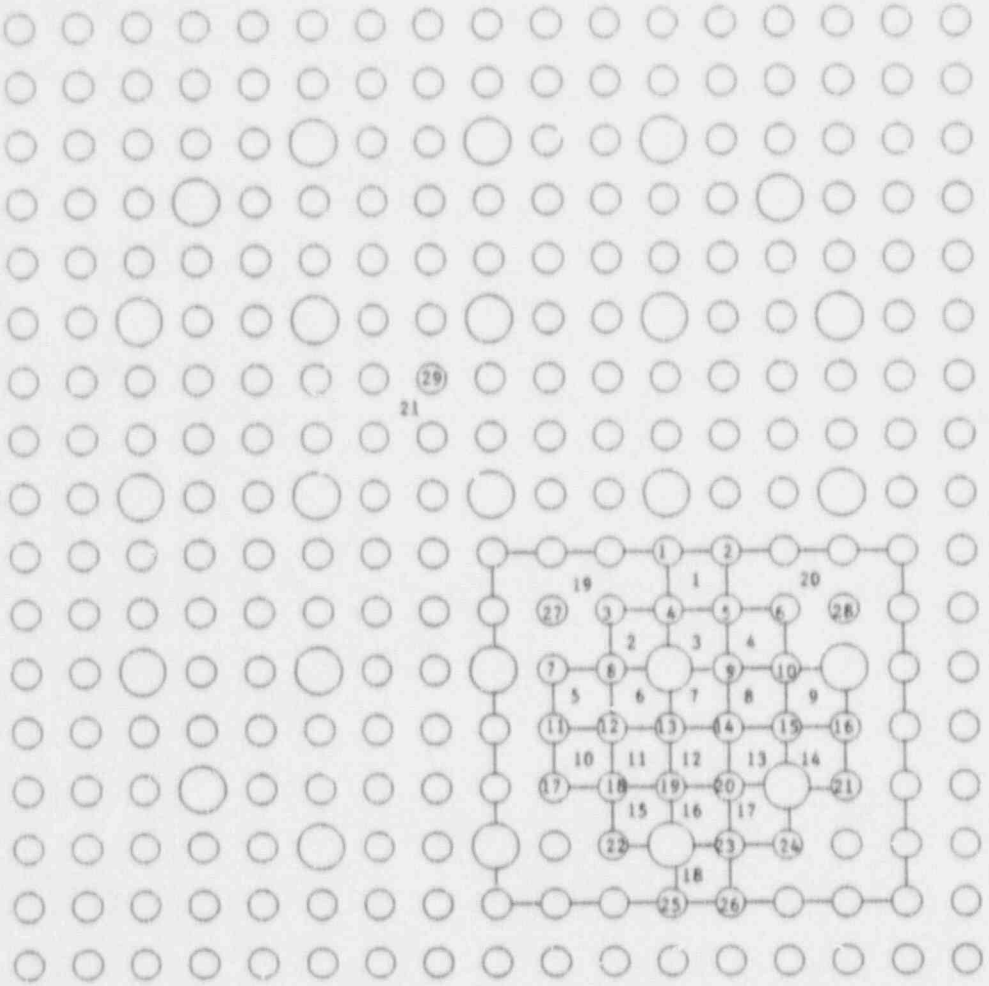

Figure 3.4-6 VIPRE Hot Assembly Model for Hot Zero Power Steamline Break Analysis

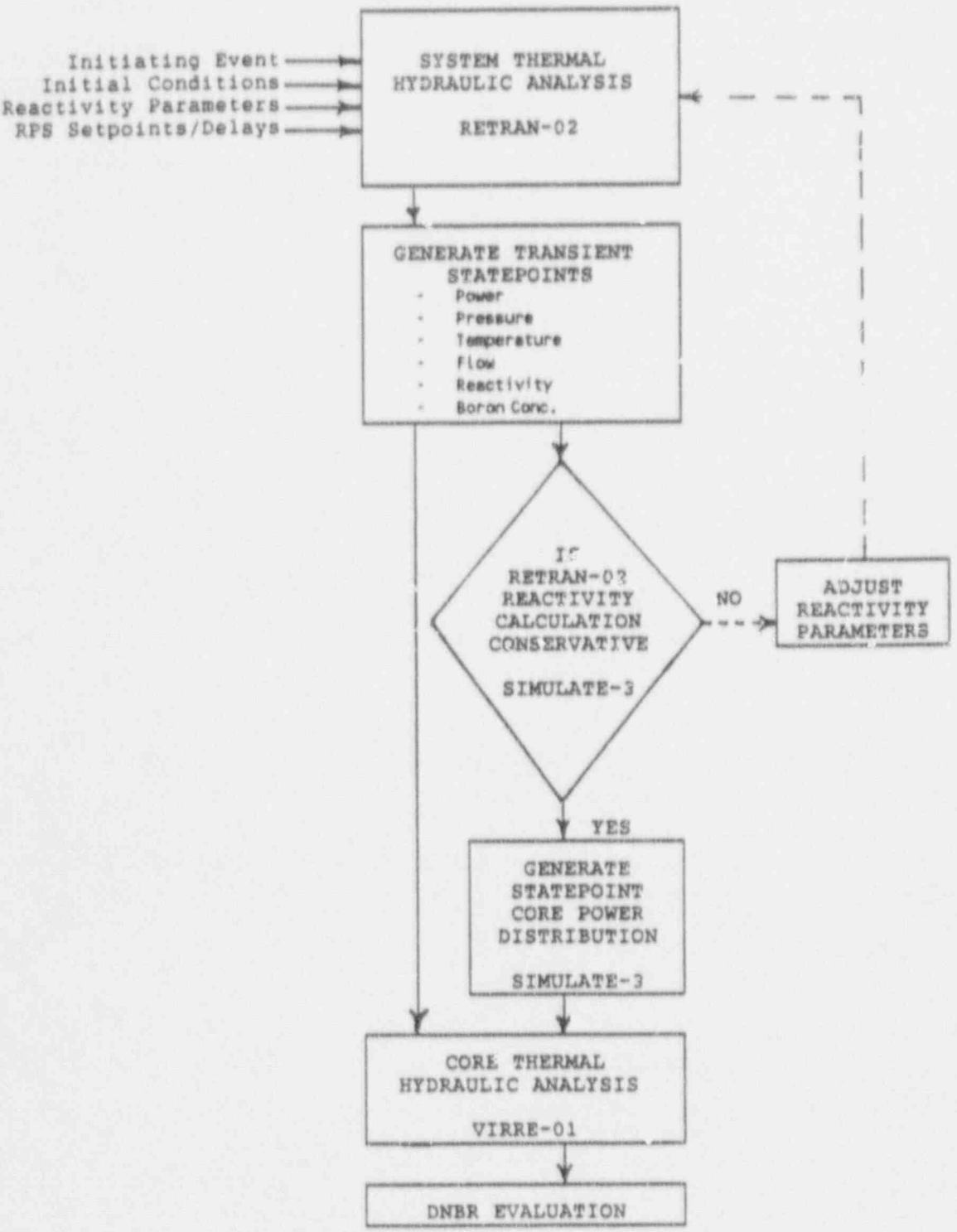

Figure 3.4-7 Calculation Flow Diagram for Hot Zero Power Steamline Break Analysis

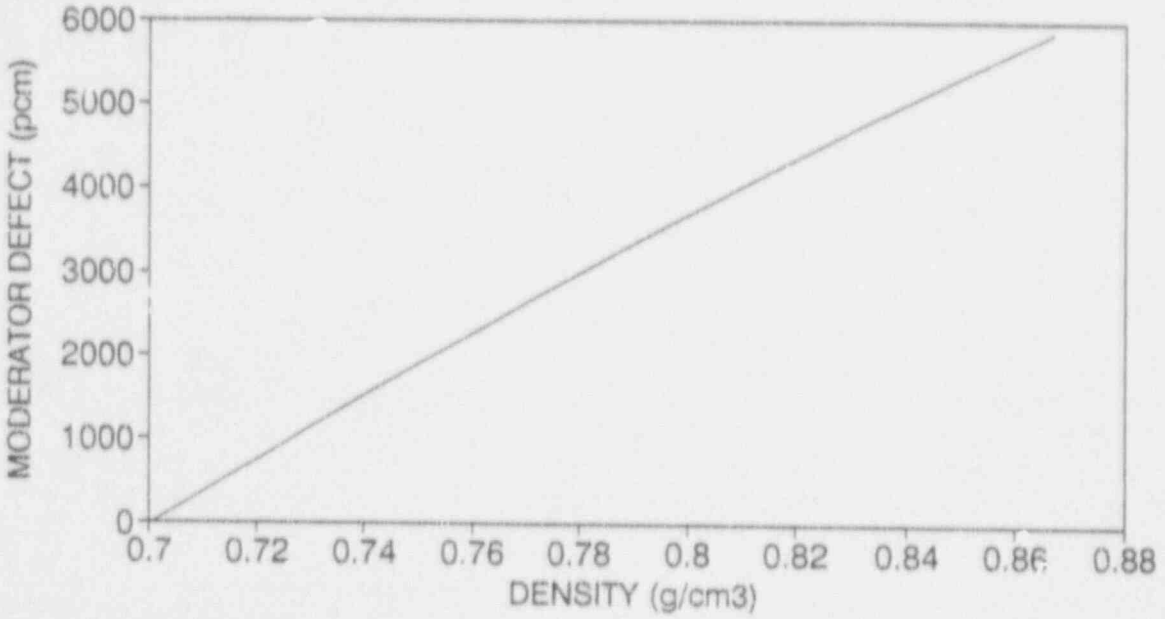

Figure 3.4-8 Moderator Density Defect Used In Reference Case Analysis

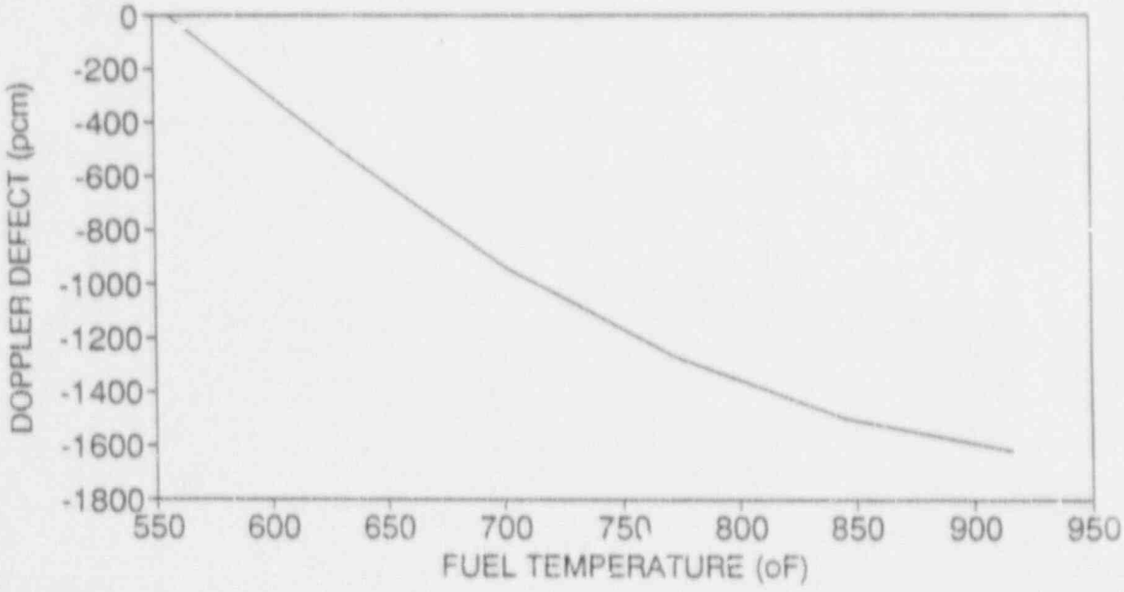

Figure 3.4-9 Doppler Defect Used In Reference Case Analysis

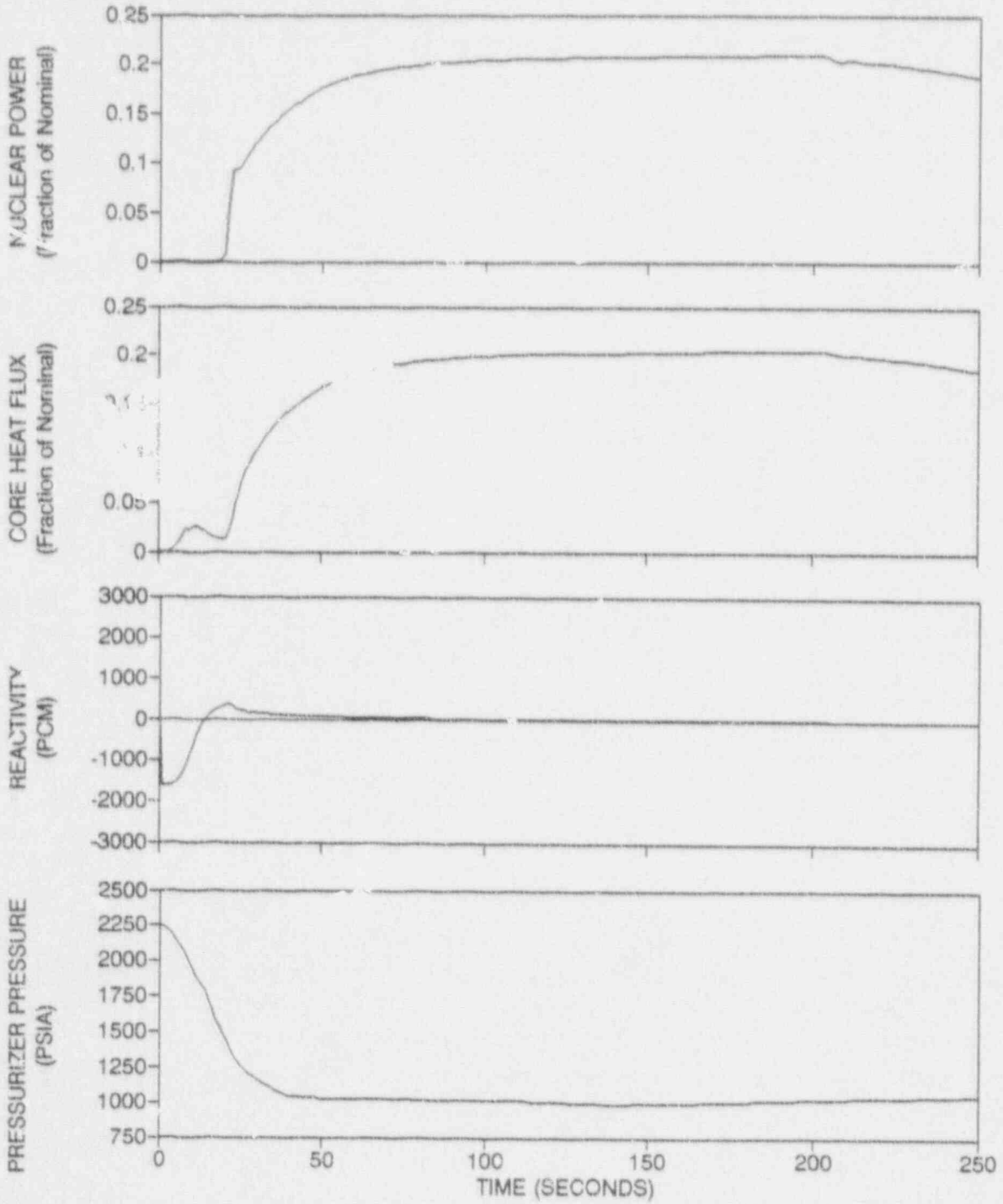

Figure 3.4-10 Nuclear Power, Core Heat Flux, Reactivity, and Pressurizer Pressure Transient for Reference Case from HZP

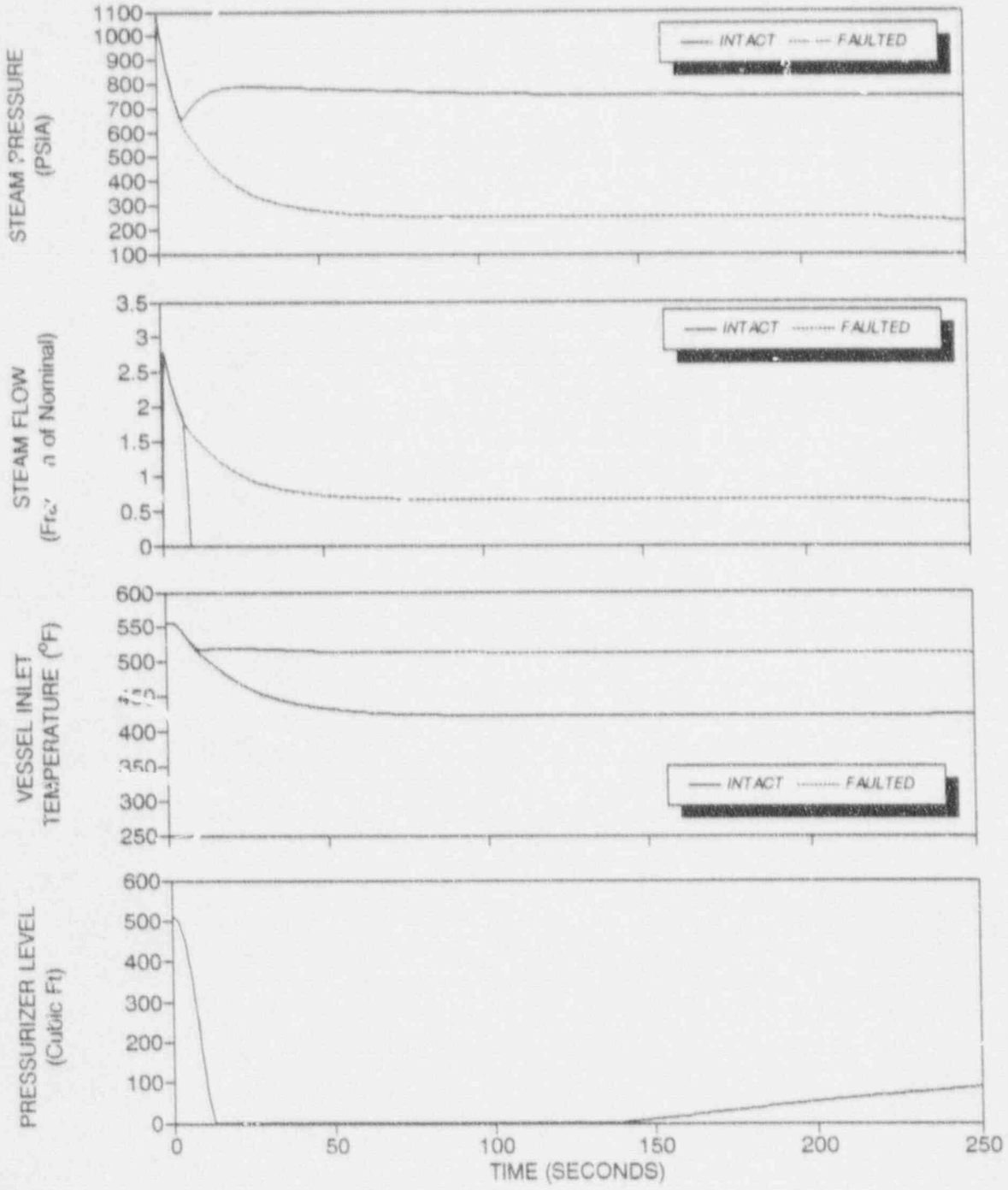

Figure 3.4-11 Pressurizer Level, Steam Generator Pressures, Steam Flows, and Reactor Vessel Inlet Temperatures for Reference Case from HZP

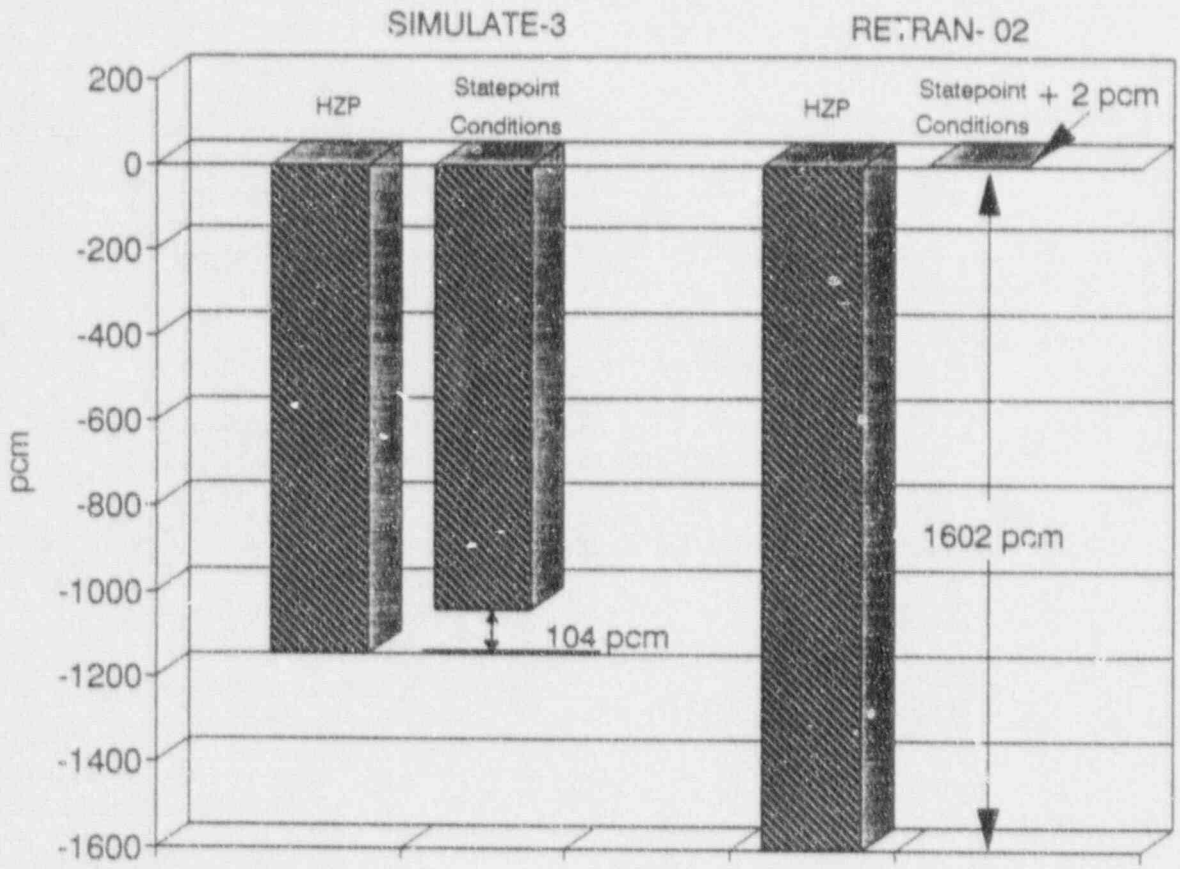

Figure 3.4-12 Reactivity Insertion Comparison Between RETRAN and SIMULATE

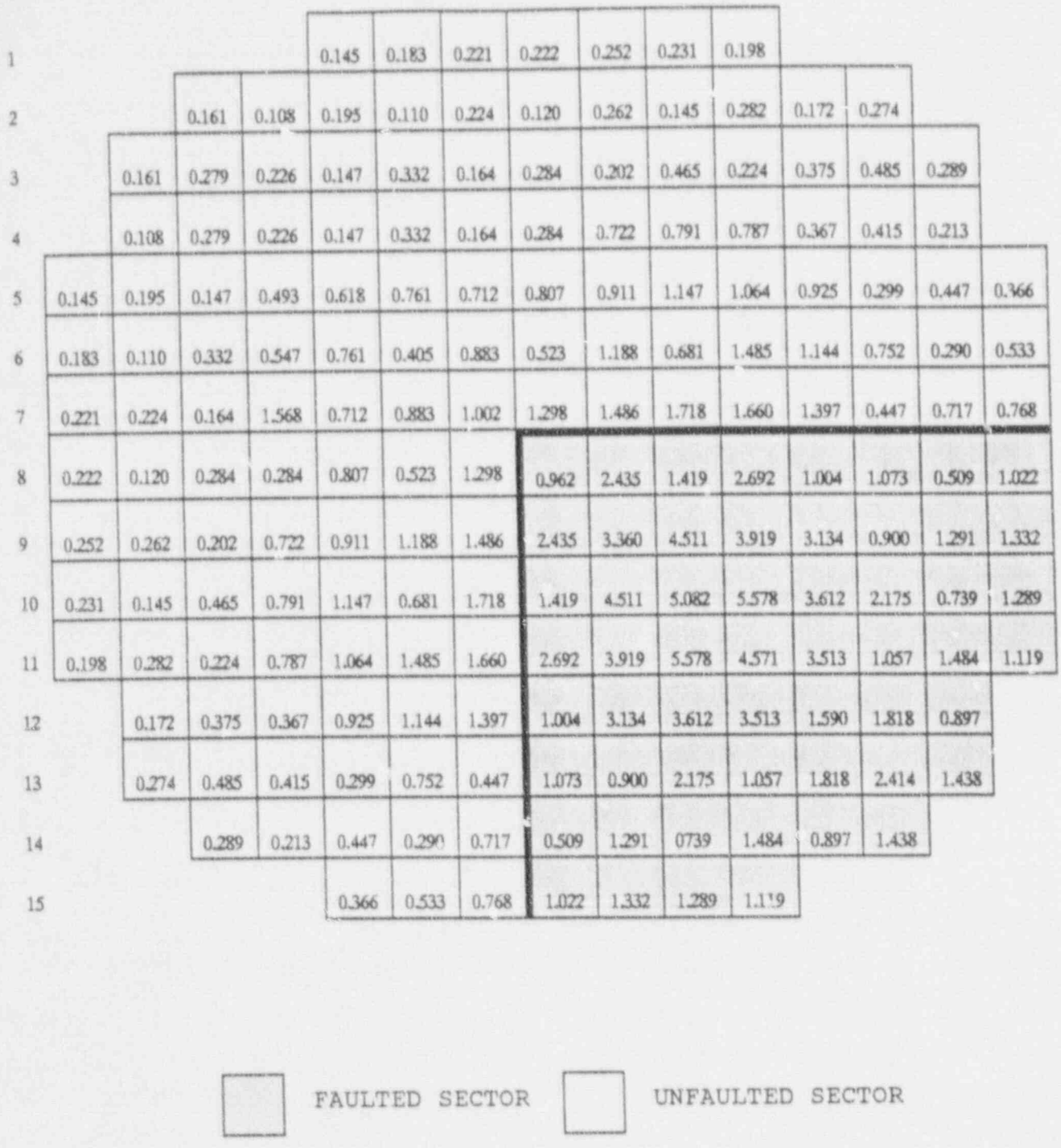

Figure 3.4-13 Core Radial Power Distribution for Reference Case form HZP

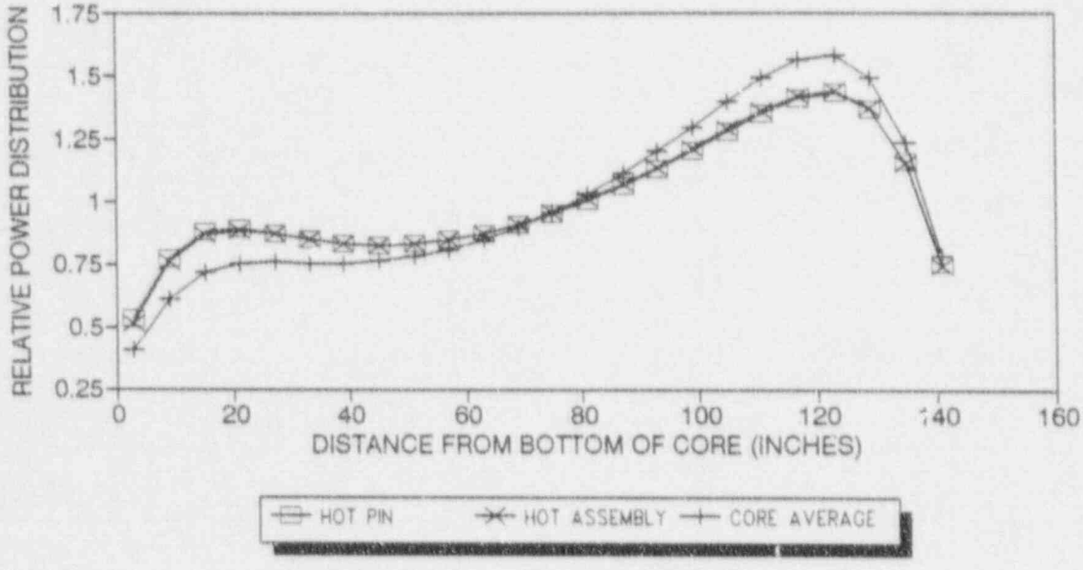

Figure 3.4-14 Core Axial Power Distribution for Reference Case from HZP

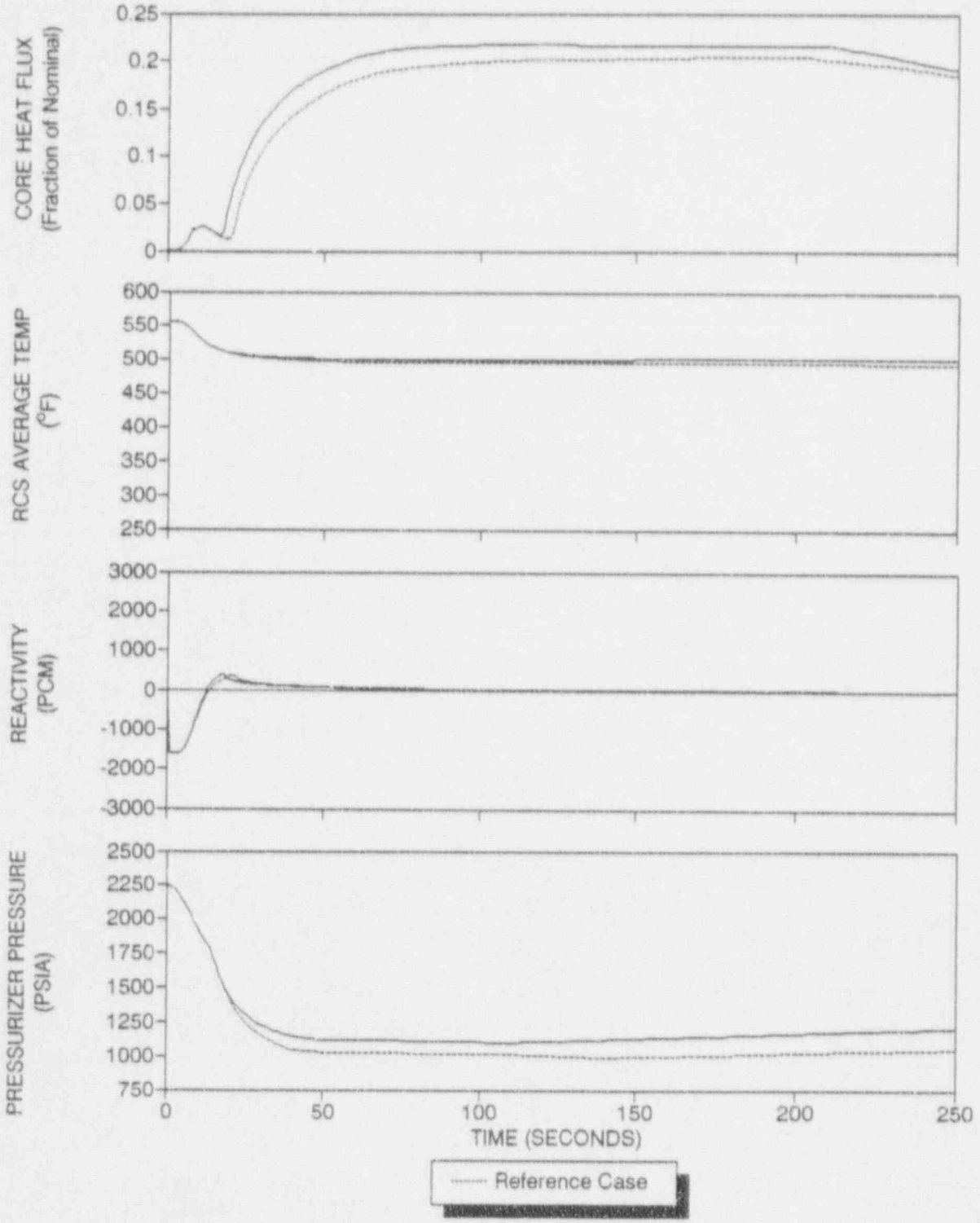

Figure 3.4-15 Transient Results for a +10% Moderator Density Defect

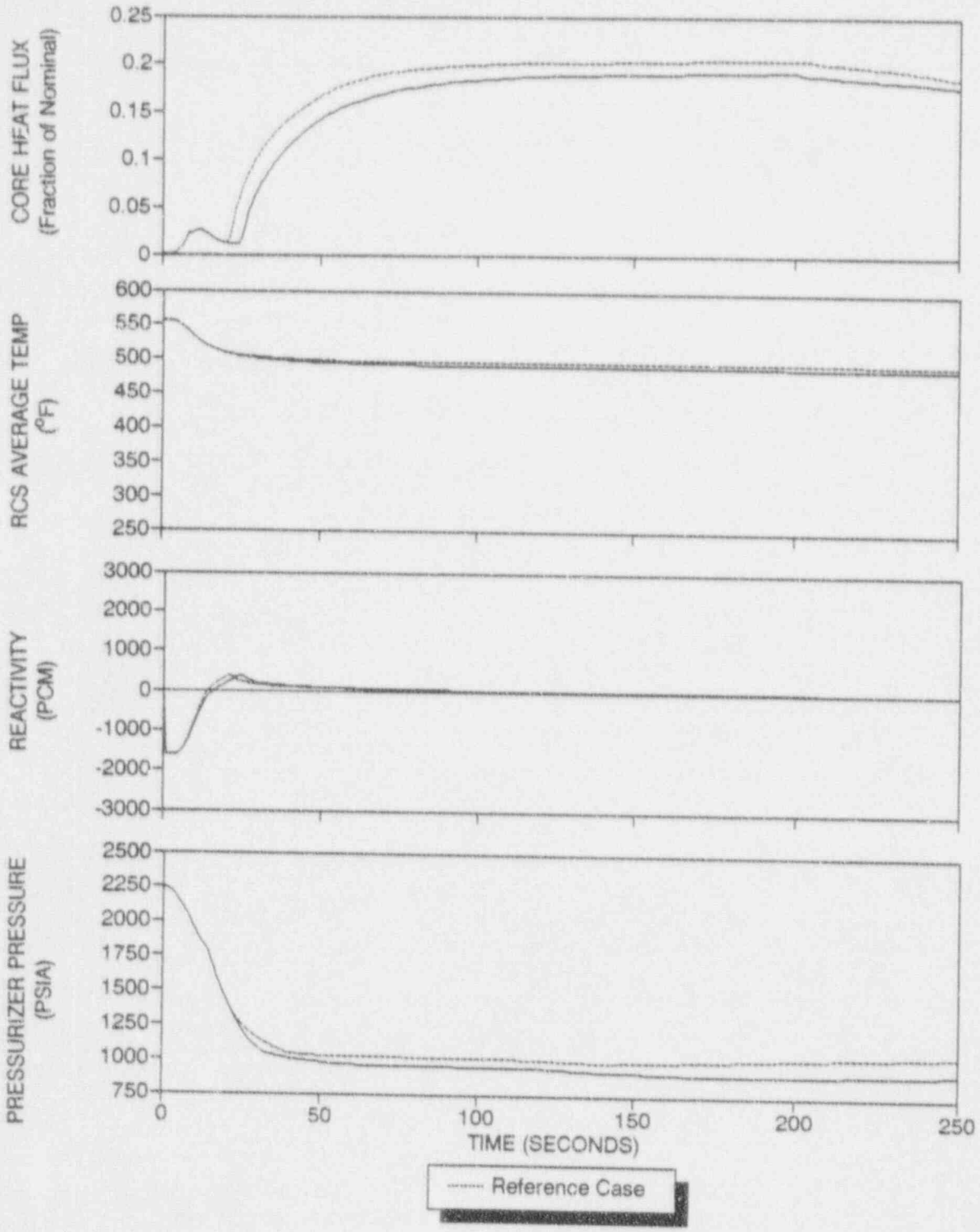

Figure 3.4-16 Transient Results for a -10% Moderator Density Defect

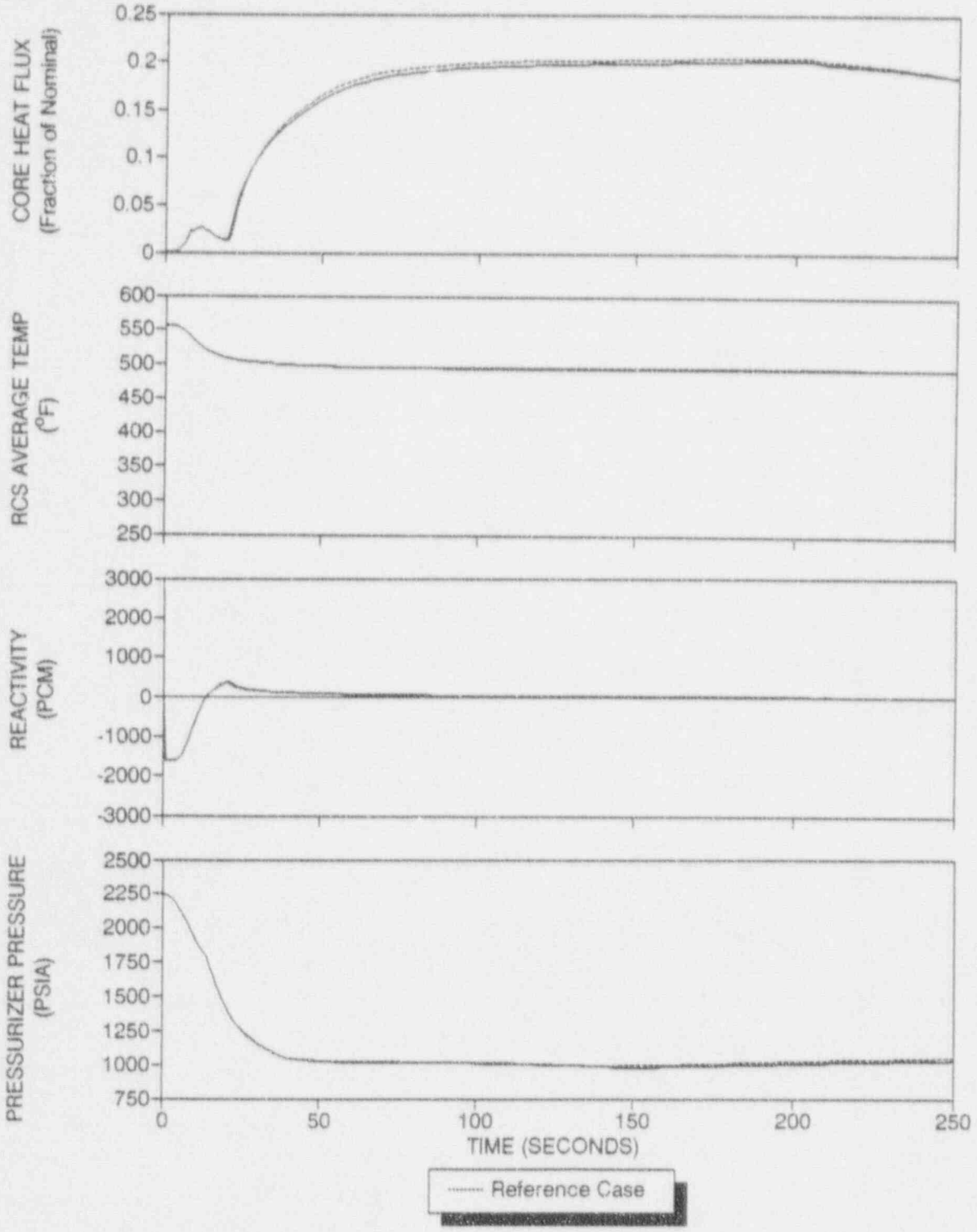

Figure 3.4-17 Transient Results for a +10% Doppler Defect

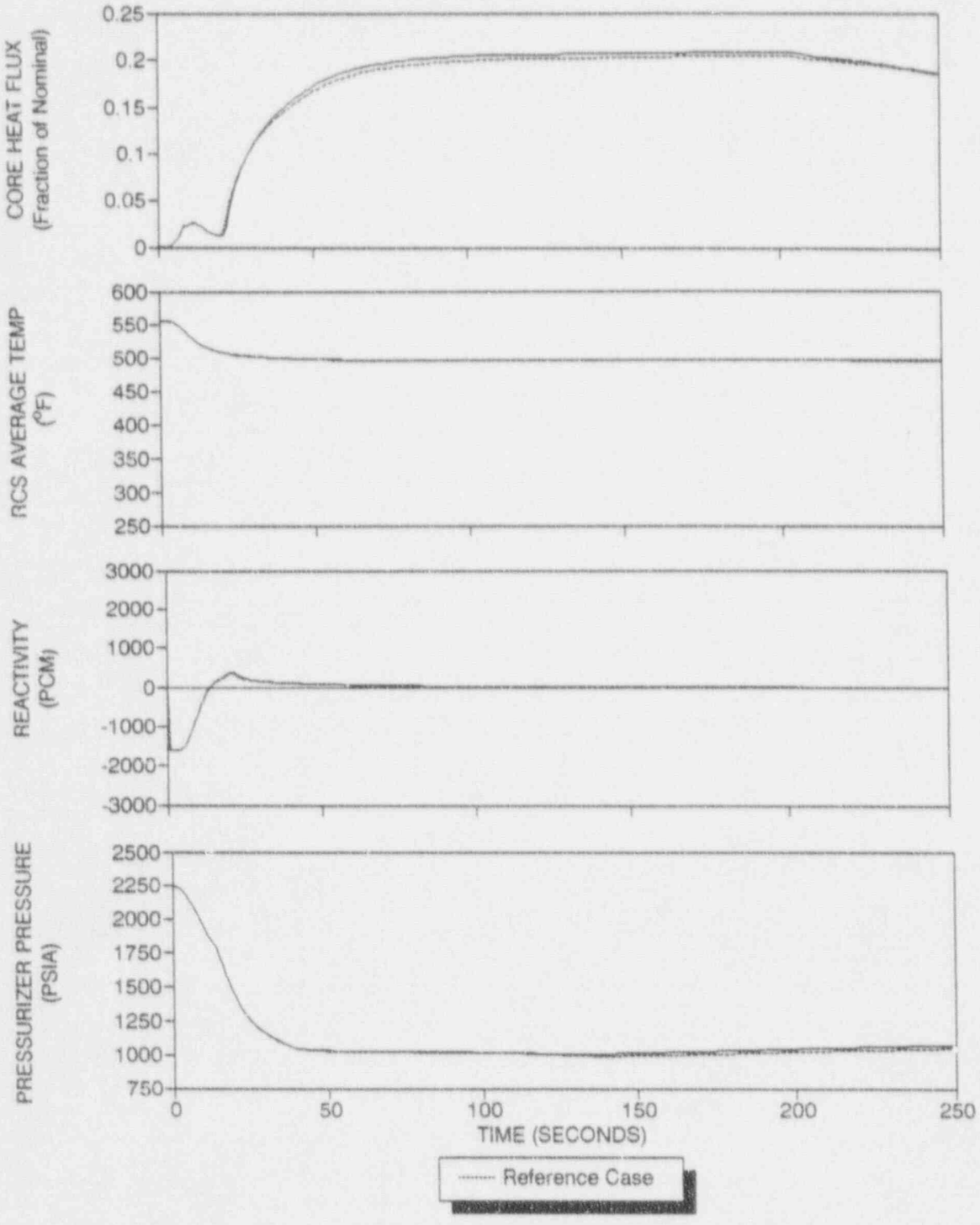

Figure 3.4-18 Transient Results for a -10% Doppler Defect

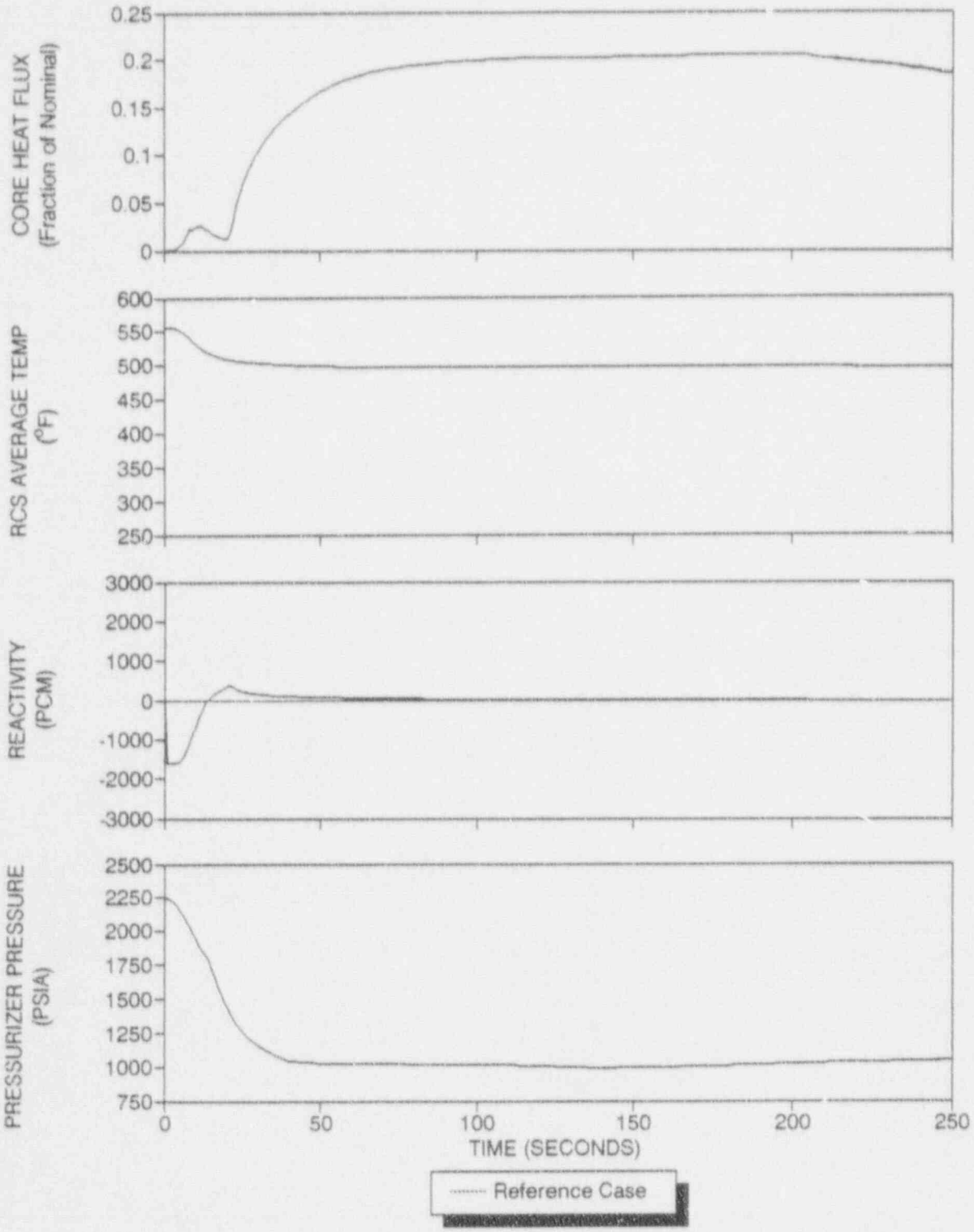

Figure 3.4-19 Transient Results for a +10% Boron Worth

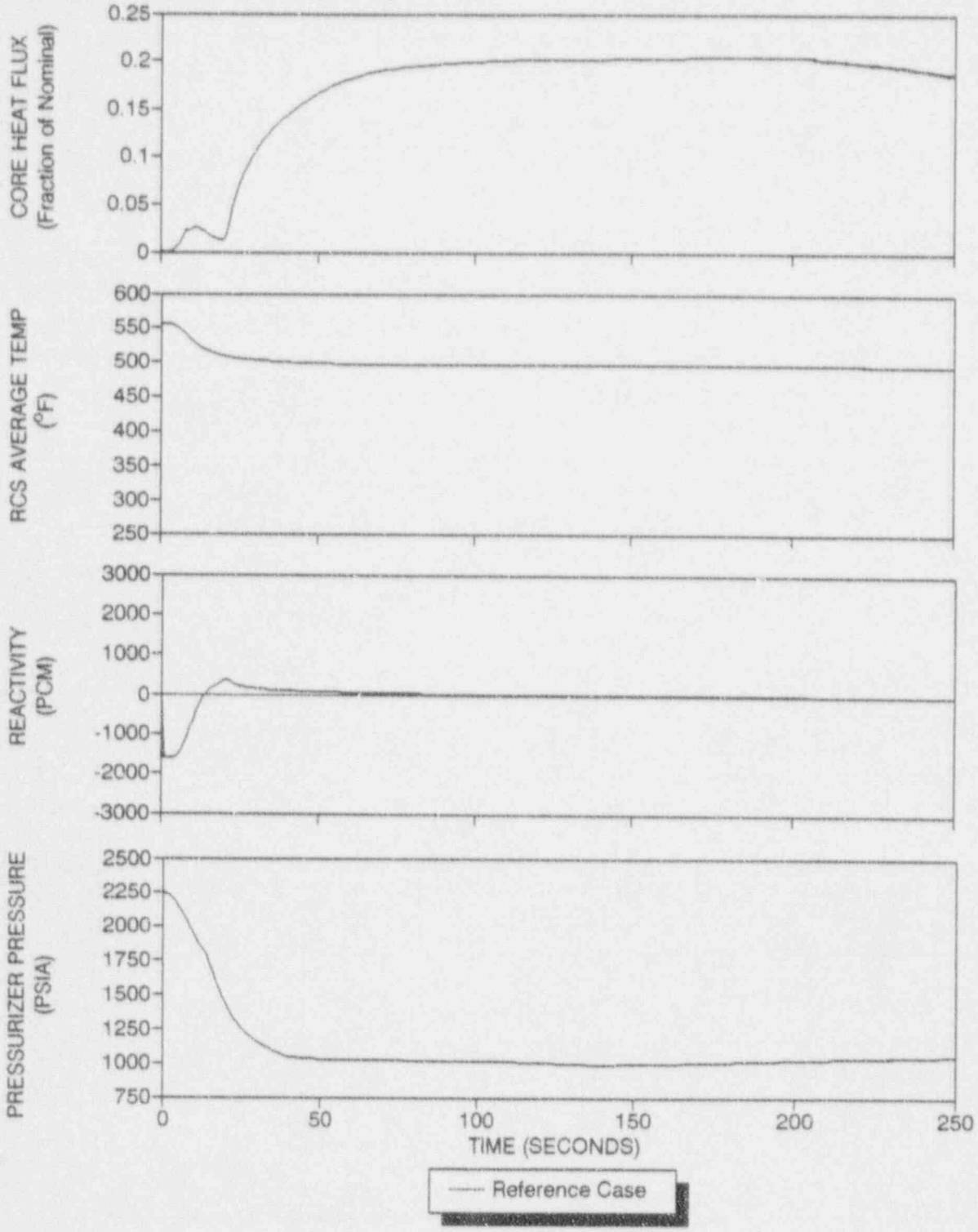

Figure 3.4-20 Transient Results for a -10% Boron Worth

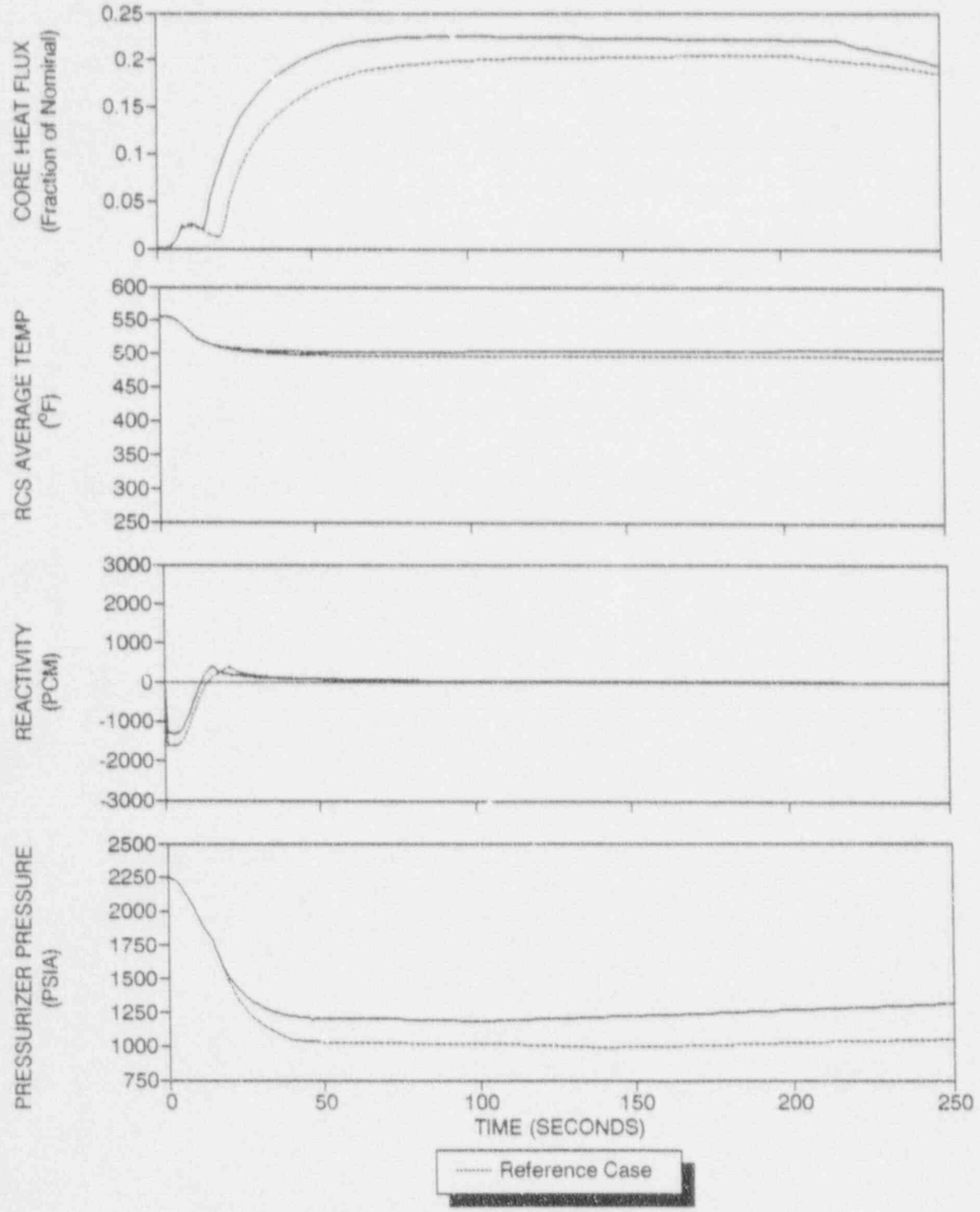

Figure 3.4-21 Transient Results for a 1.3% delta-k/k Shutdown Margin

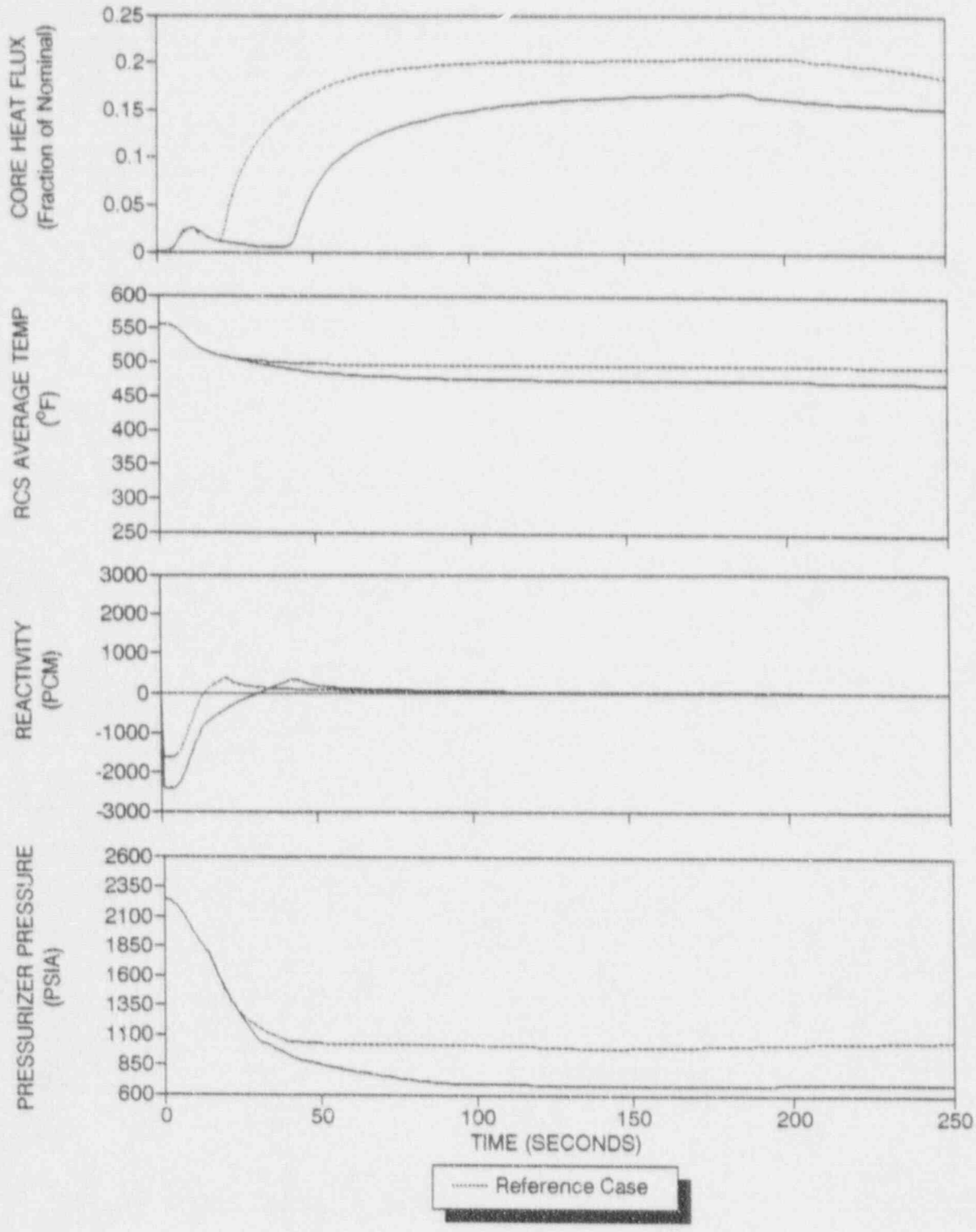

Figure 3.4-22 Transient Results for a 2.4% delta-k/k Shutdown Margin

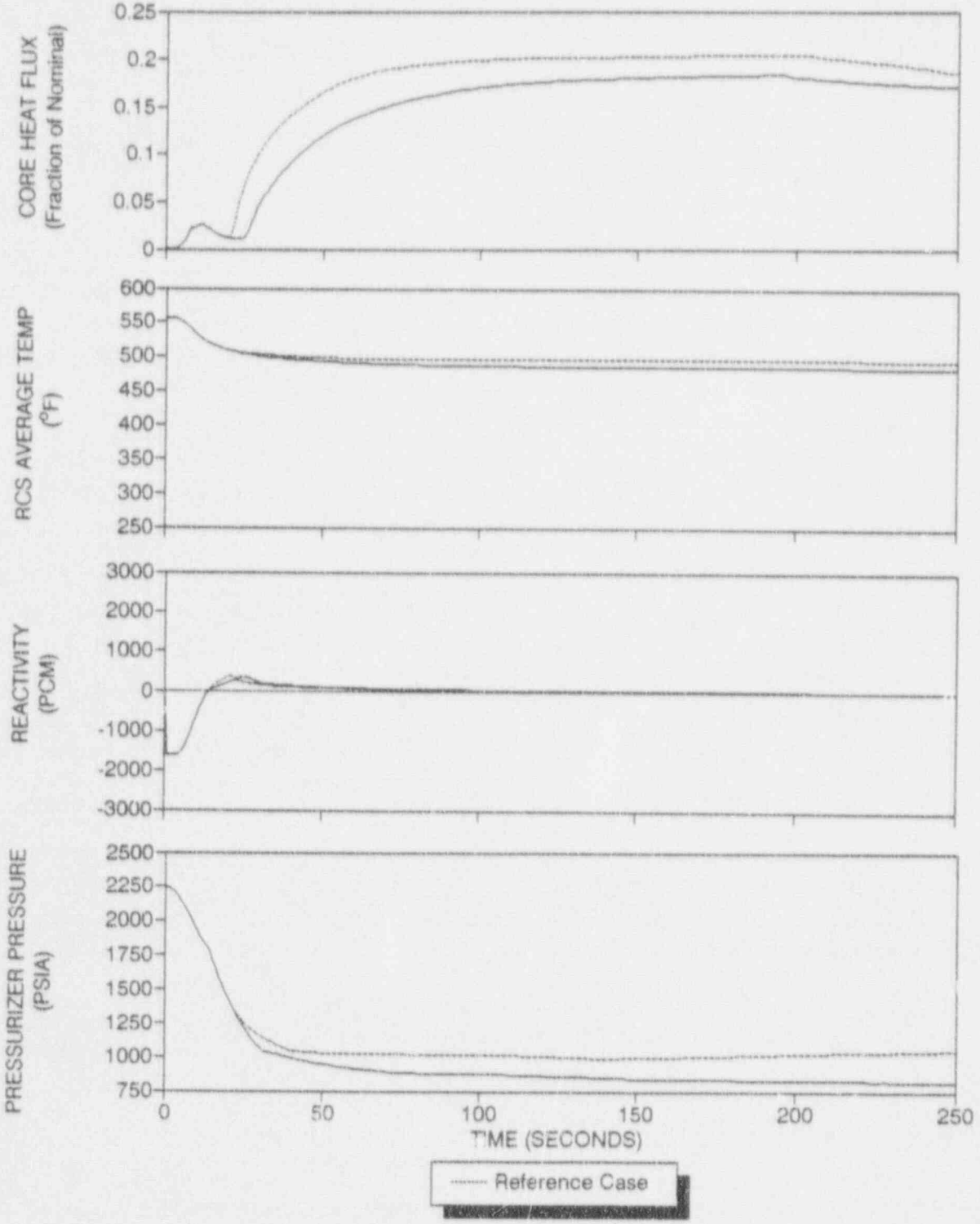

Figure 3.4-23 Transient Results for 25% Reactivity Weighting to the Faulted Sector

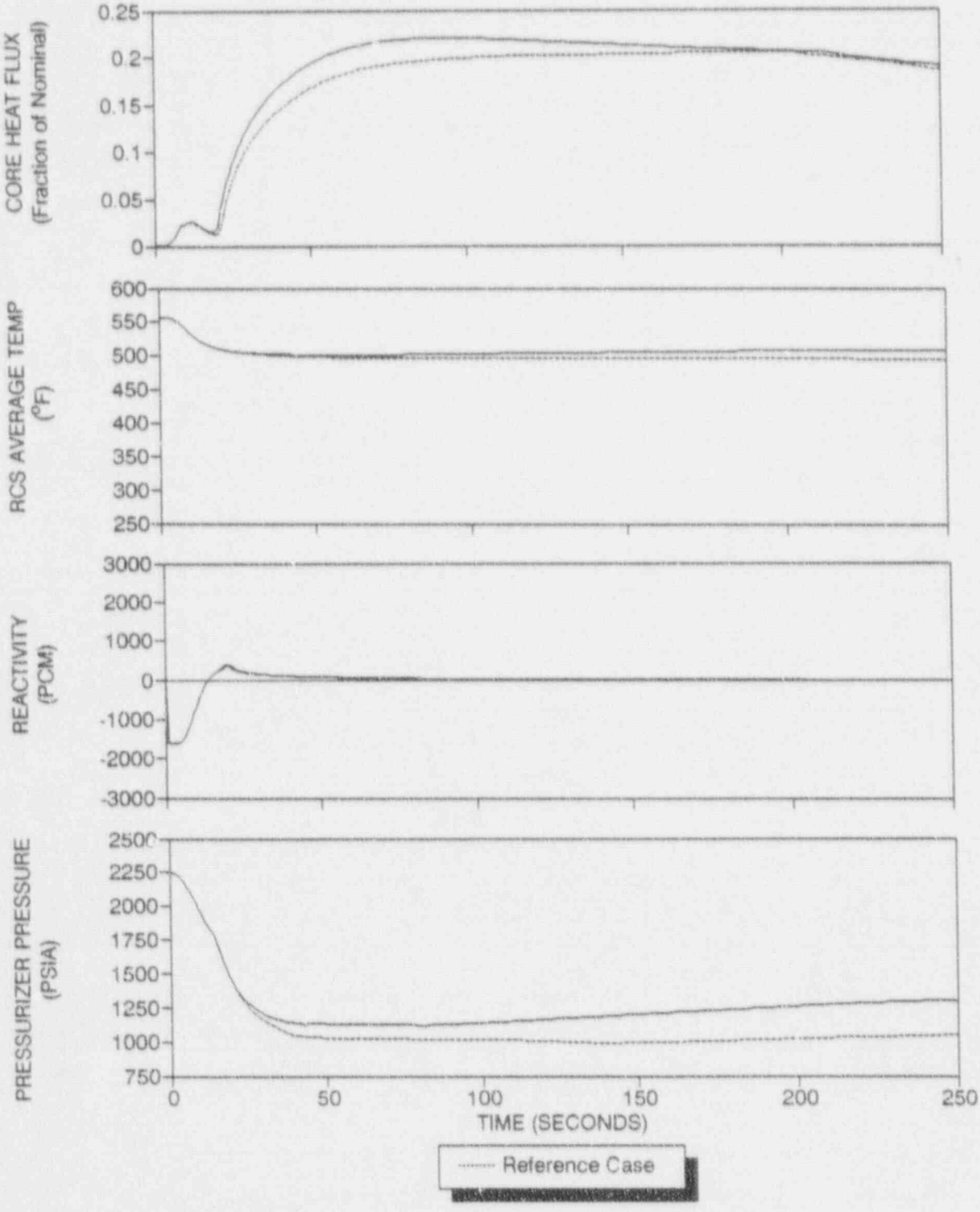

Figure 3.4-24 Transient Results for No Reactor Vessel Inlet Mixing

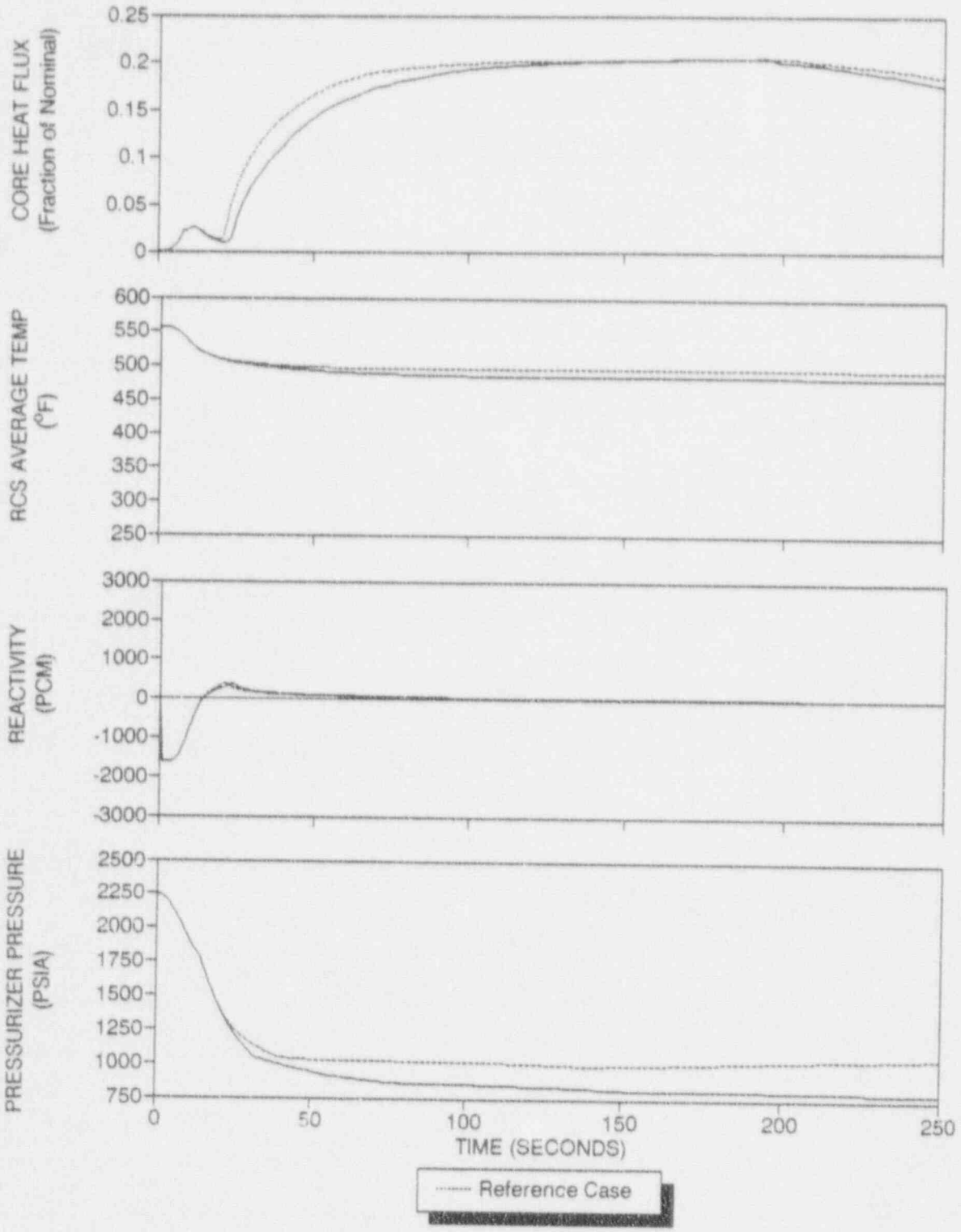

Figure 3.4-25 Transient Results for 50% Reactor Vessel Inlet Mixing

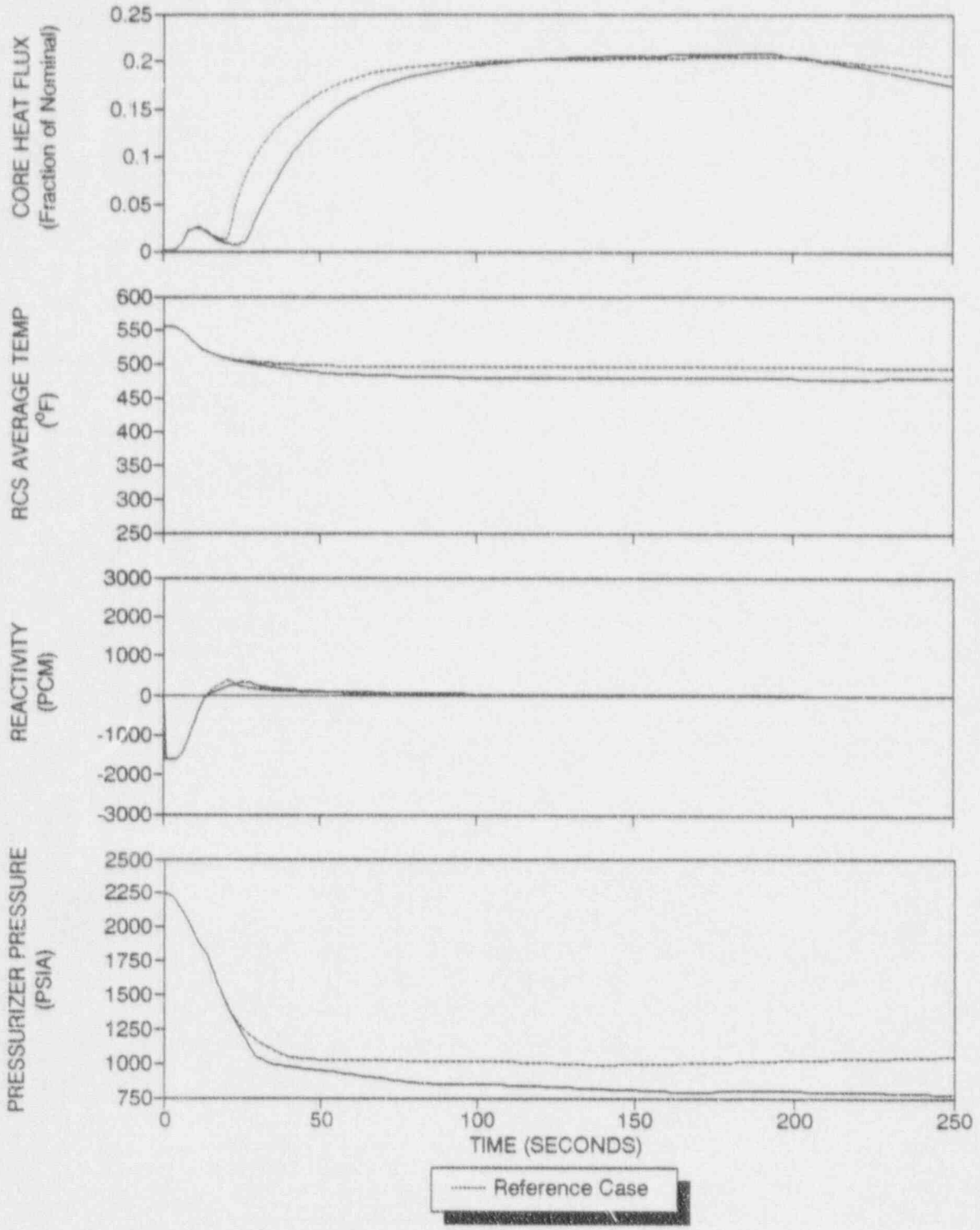

Figure 3.4-26 Transient Results for 100% Reactor Vessel Inlet Mixing

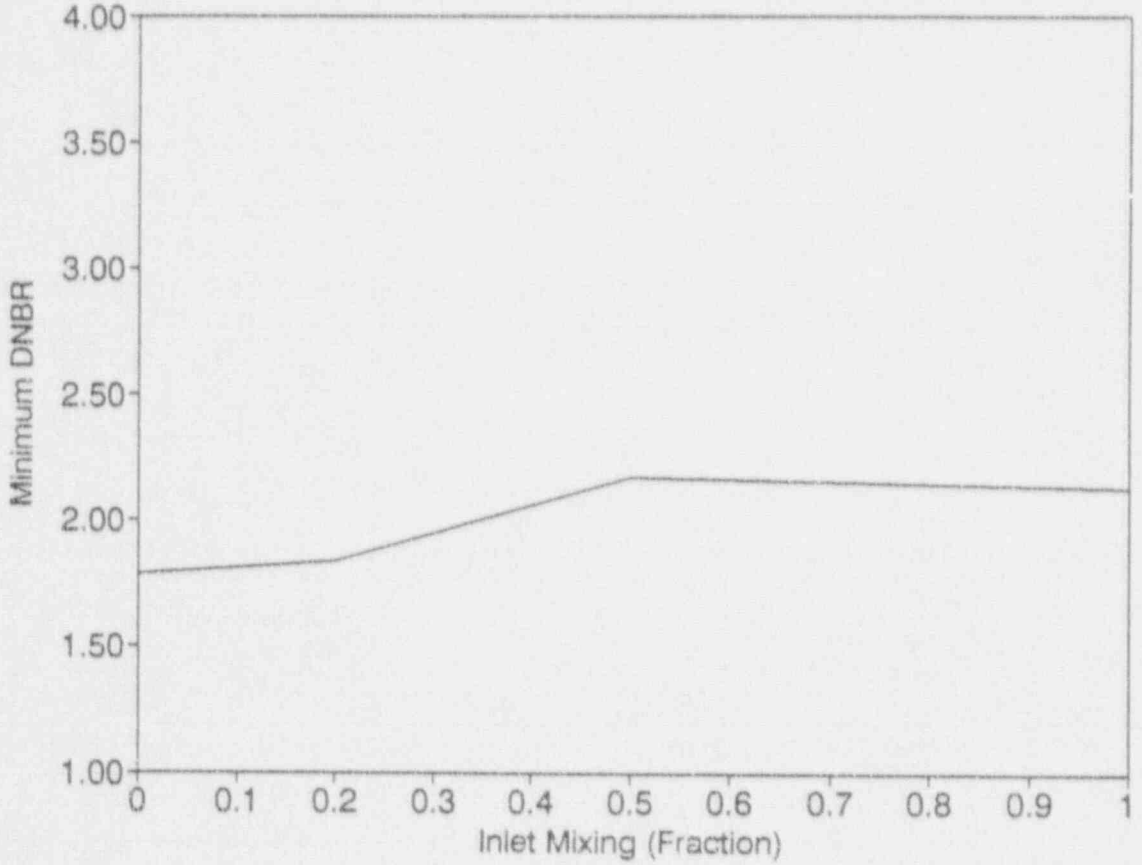

Figure 3.4-27 Minimum DNBR Versus Reactor Vessel Inlet Mixing

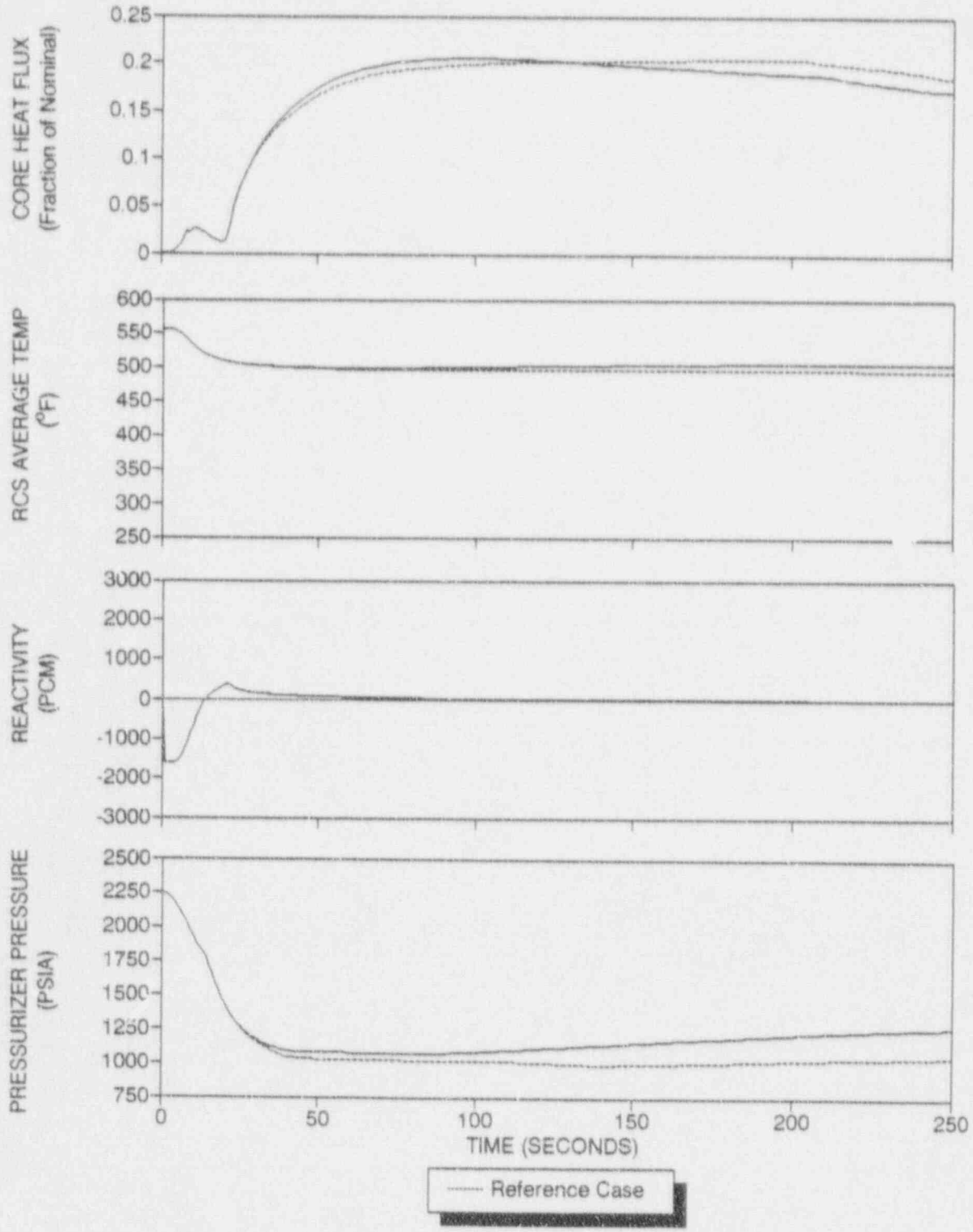

Figure 3.4-28 Transient Results for No Reactor Vessel Outlet Mixing

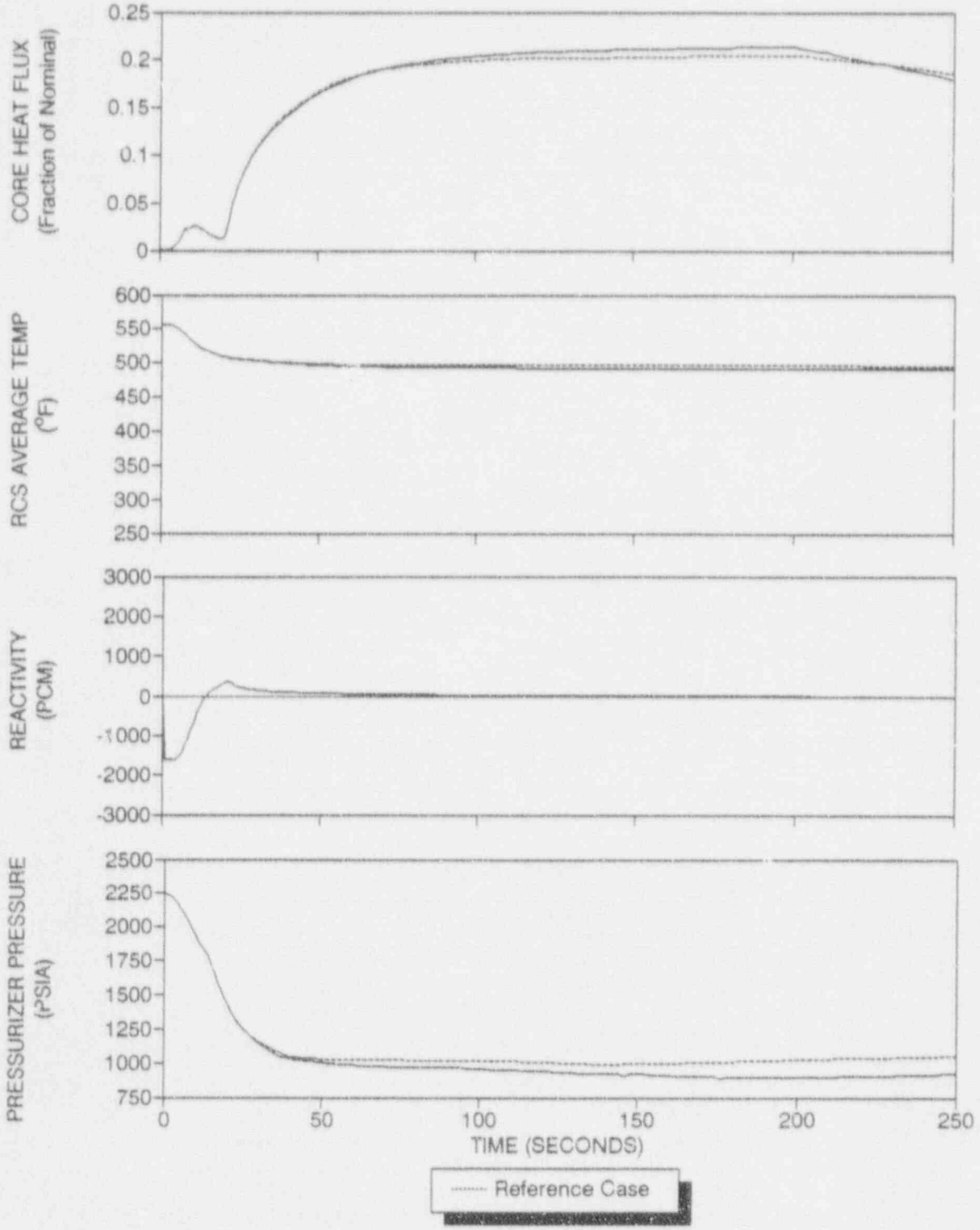

Figure 3.4-29 Transient Results for 50% Reactor Vessel Outlet Mixing

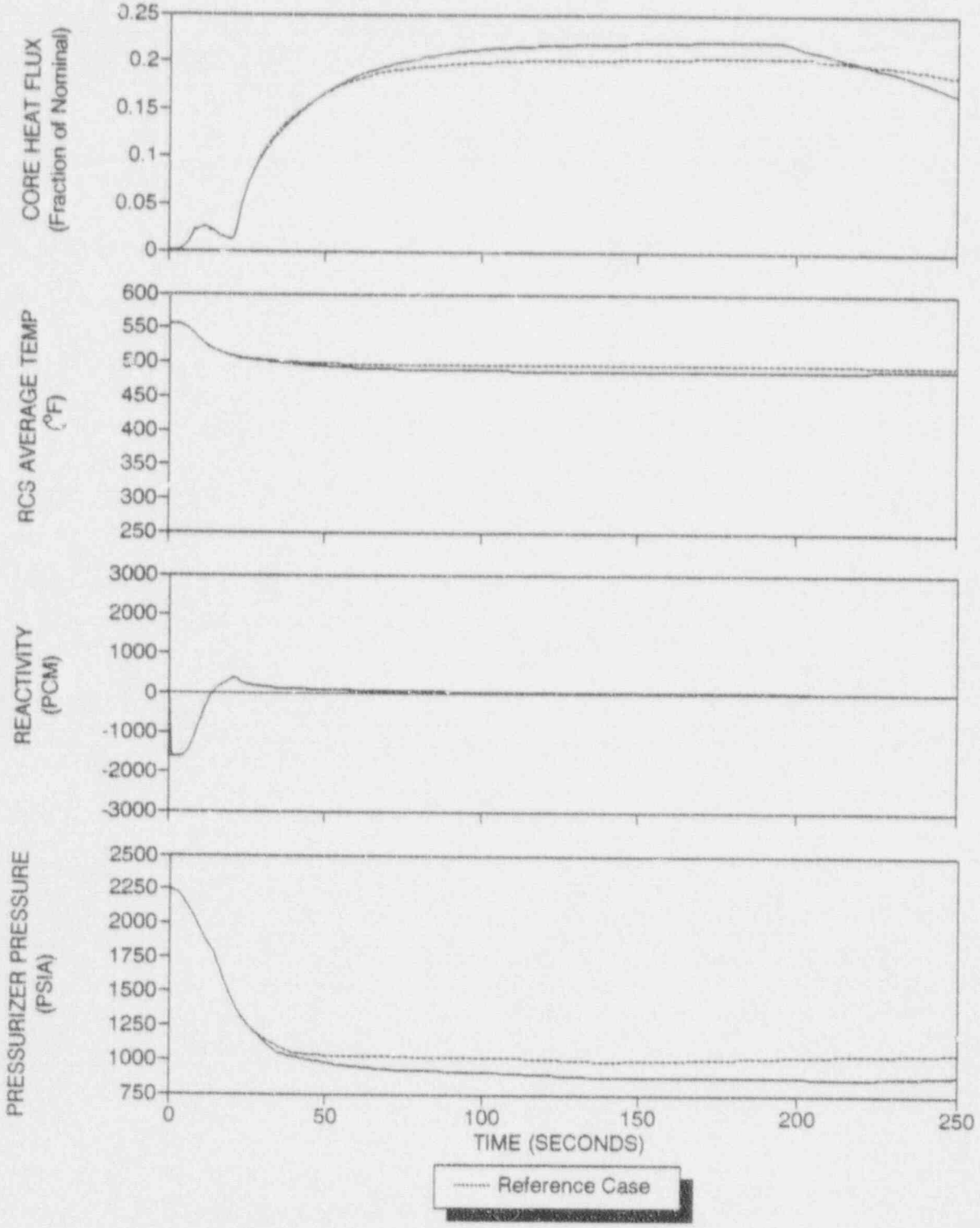

Figure 3.4-30 Transient Results for 100% Reactor Vessel Outlet Mixing

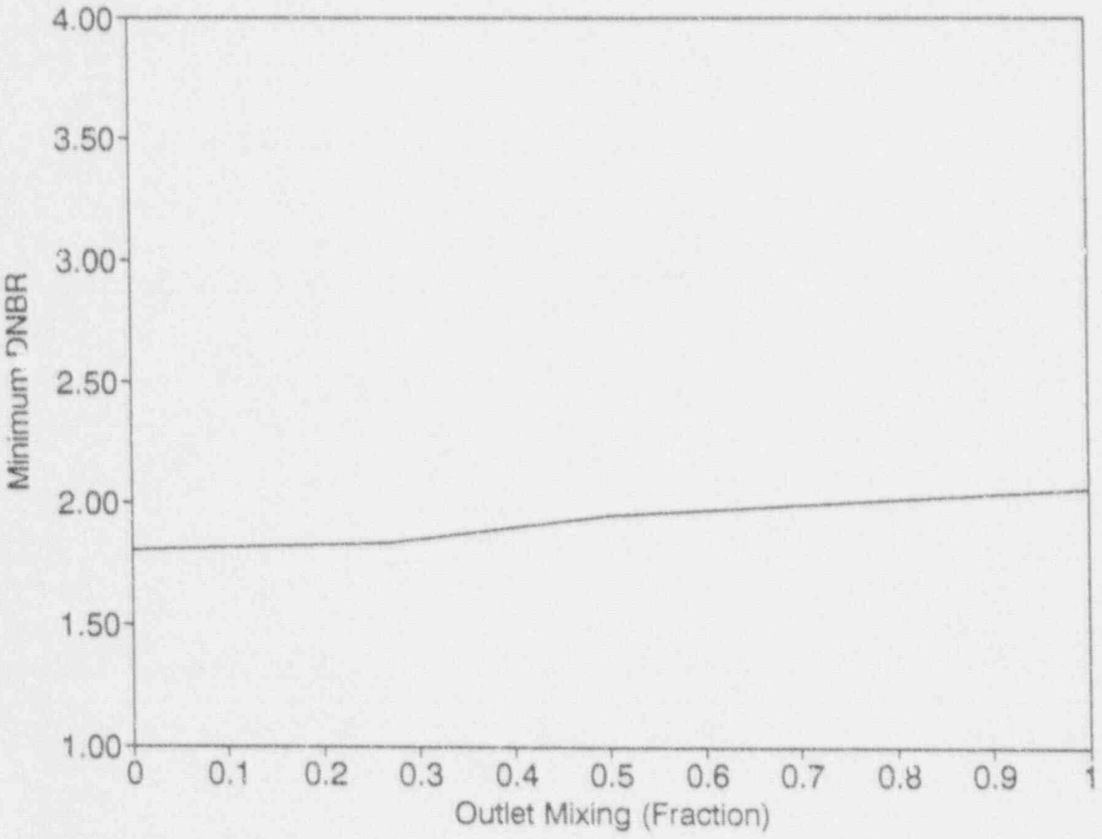

Figure 3.4-31 Minimum DNBR Versus Reactor Vessel Outlet Mixing

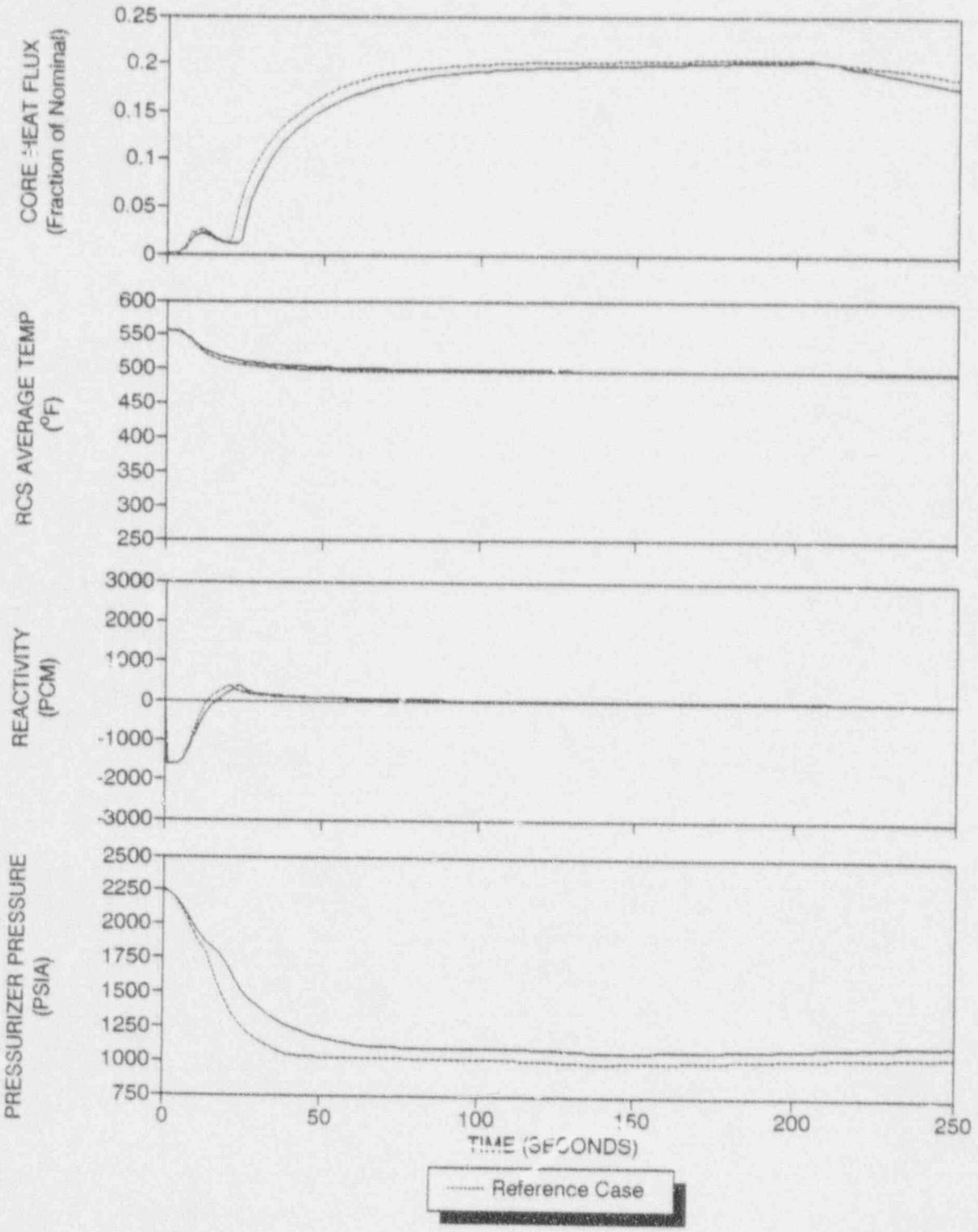

Figure 3.4-32 Transient Results for No Main Feedwater Flow and Reference Auxiliary Feedwater Flow Distribution

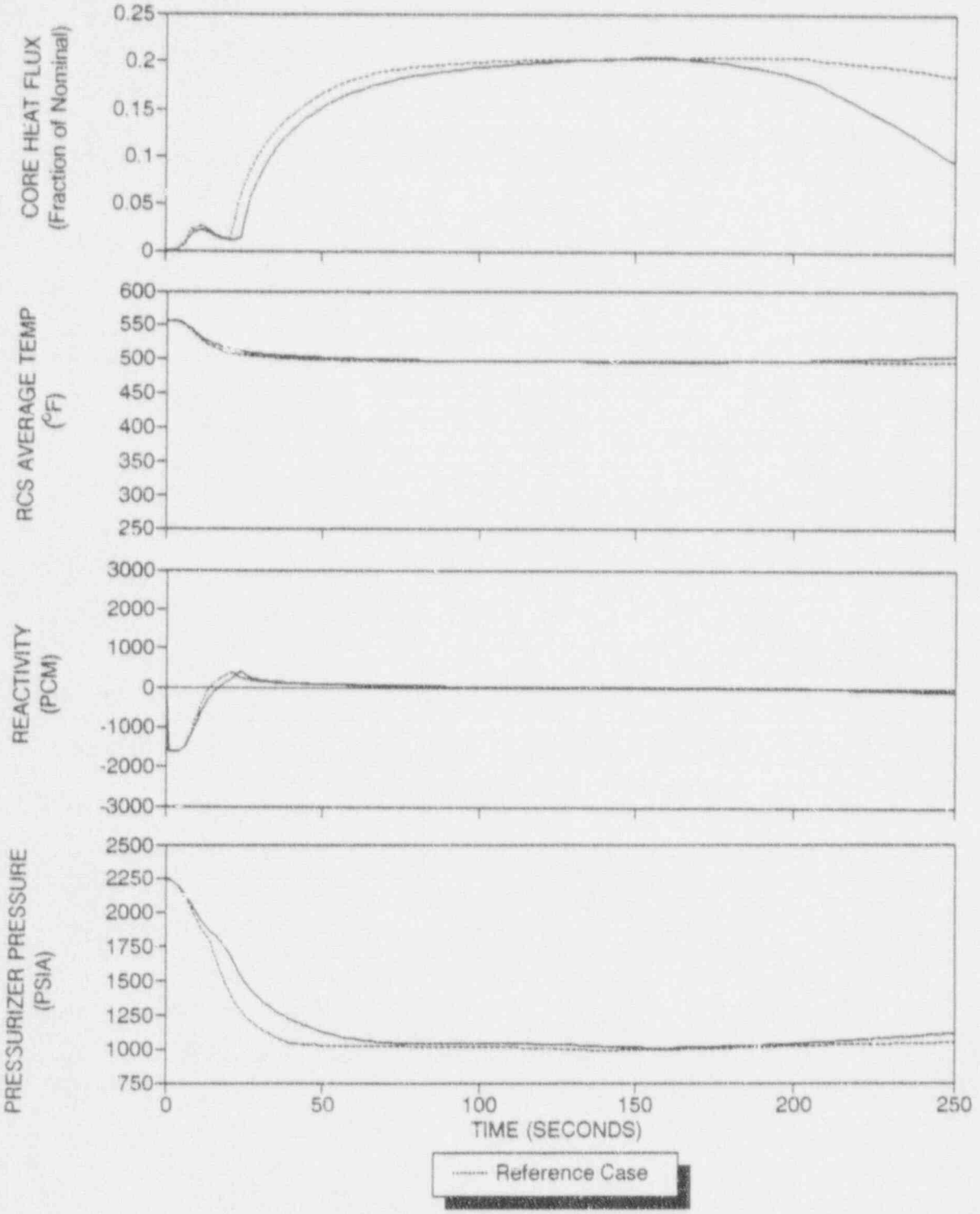

Figure 3.4-33 Transient Results for No Main Feedwater Flow and Equal Auxiliary Feedwater Flow Distribution

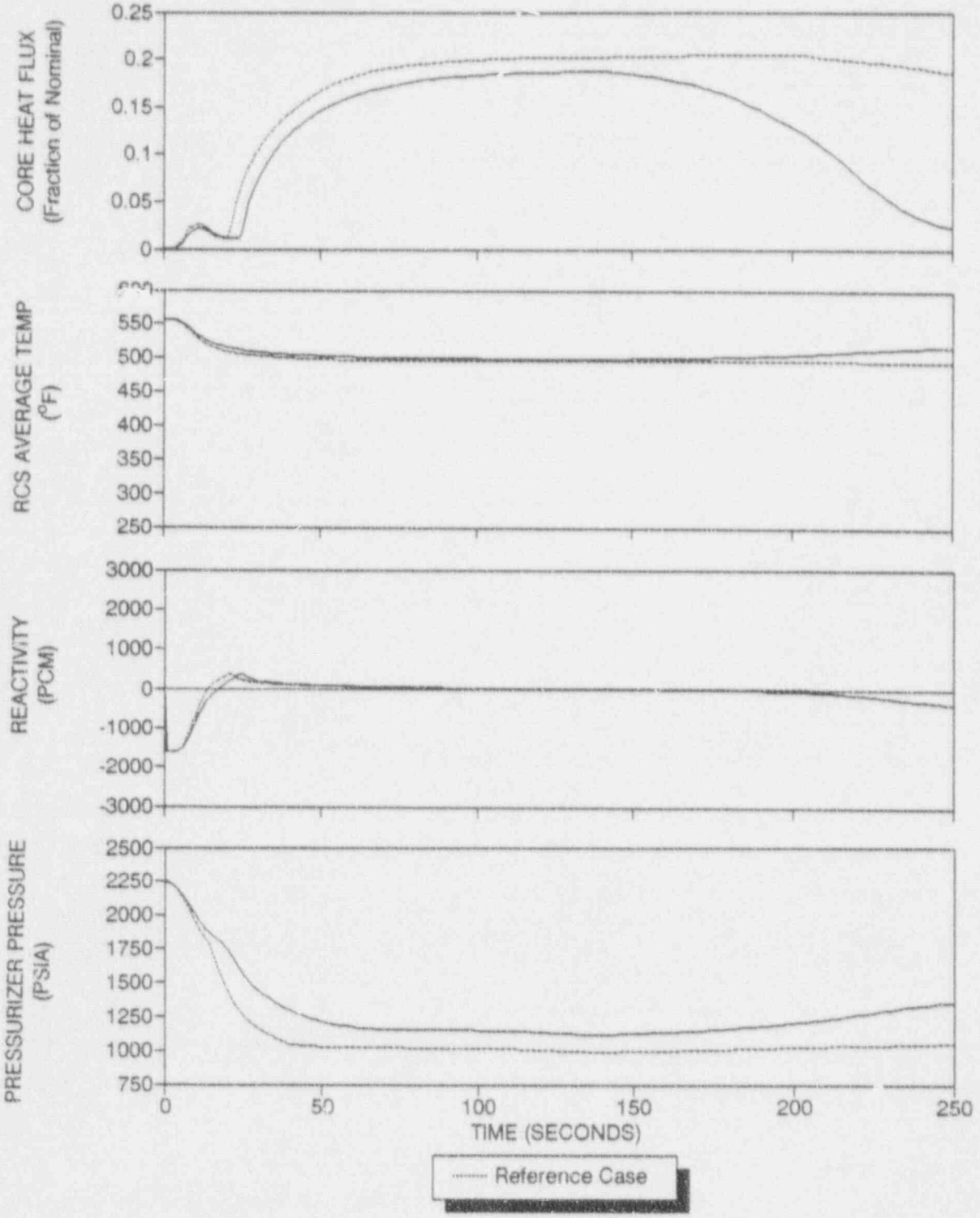

Figure 3.4-34 Transient Results for No Main Feedwater Flow and No Auxiliary Feedwater Flow

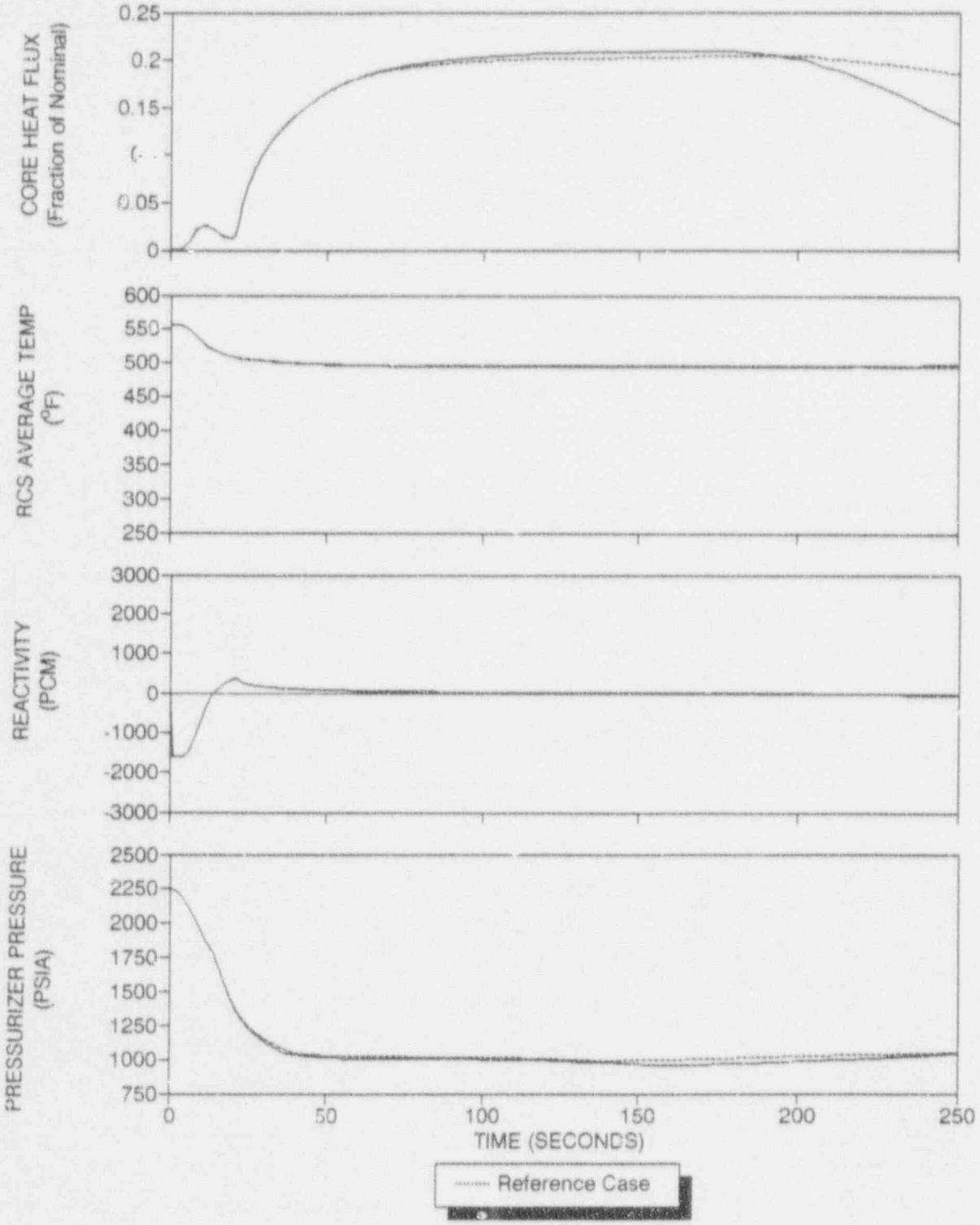

Figure 3.4-35 Transient Results for Reference Main Feedwater and Equal Auxiliary Feedwater Distribution

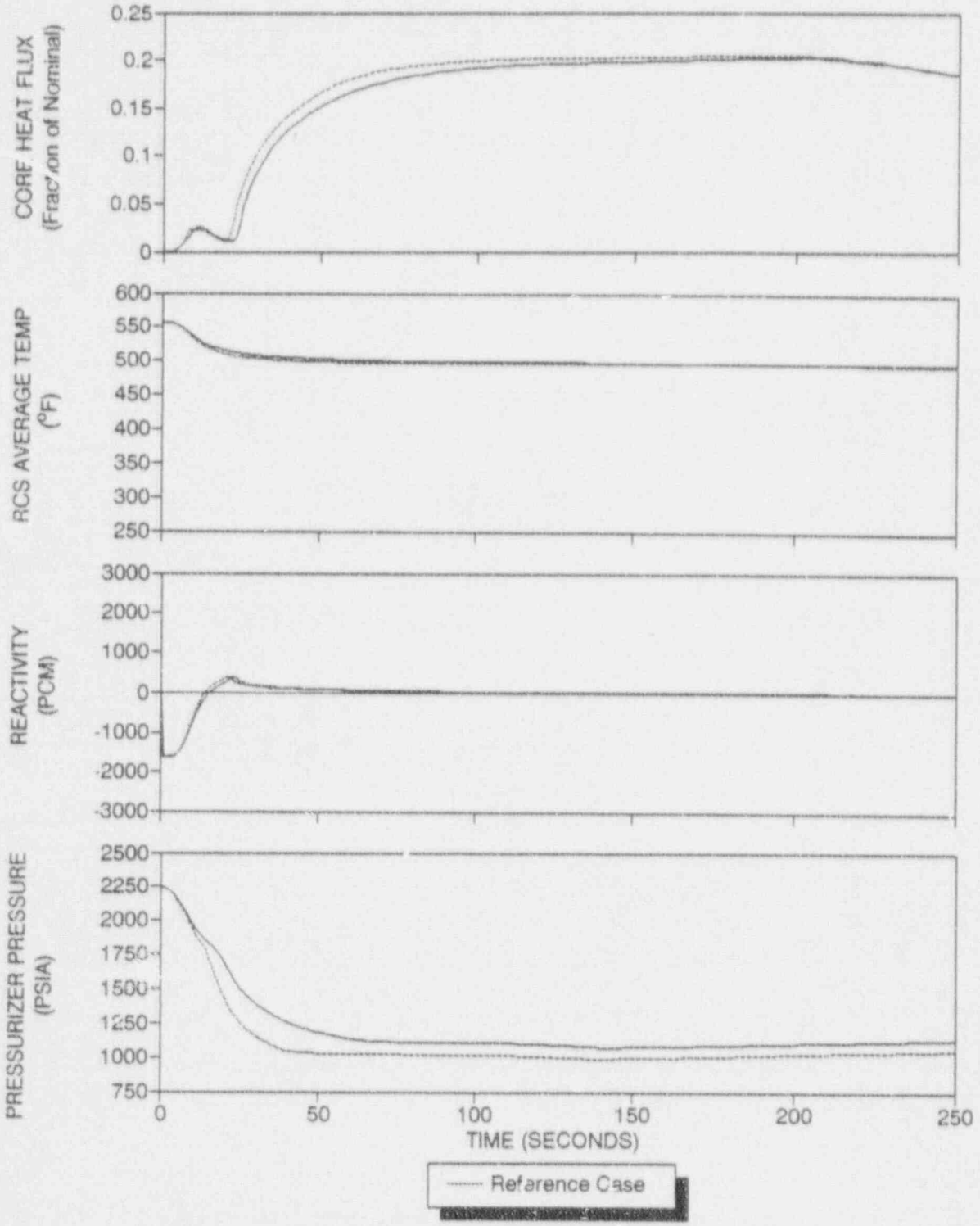

Figure 3.4-36 Transient Results for 100% of Main Feedwater to the Faulted Steam Generator and Reference Auxiliary Feedwater Distribution

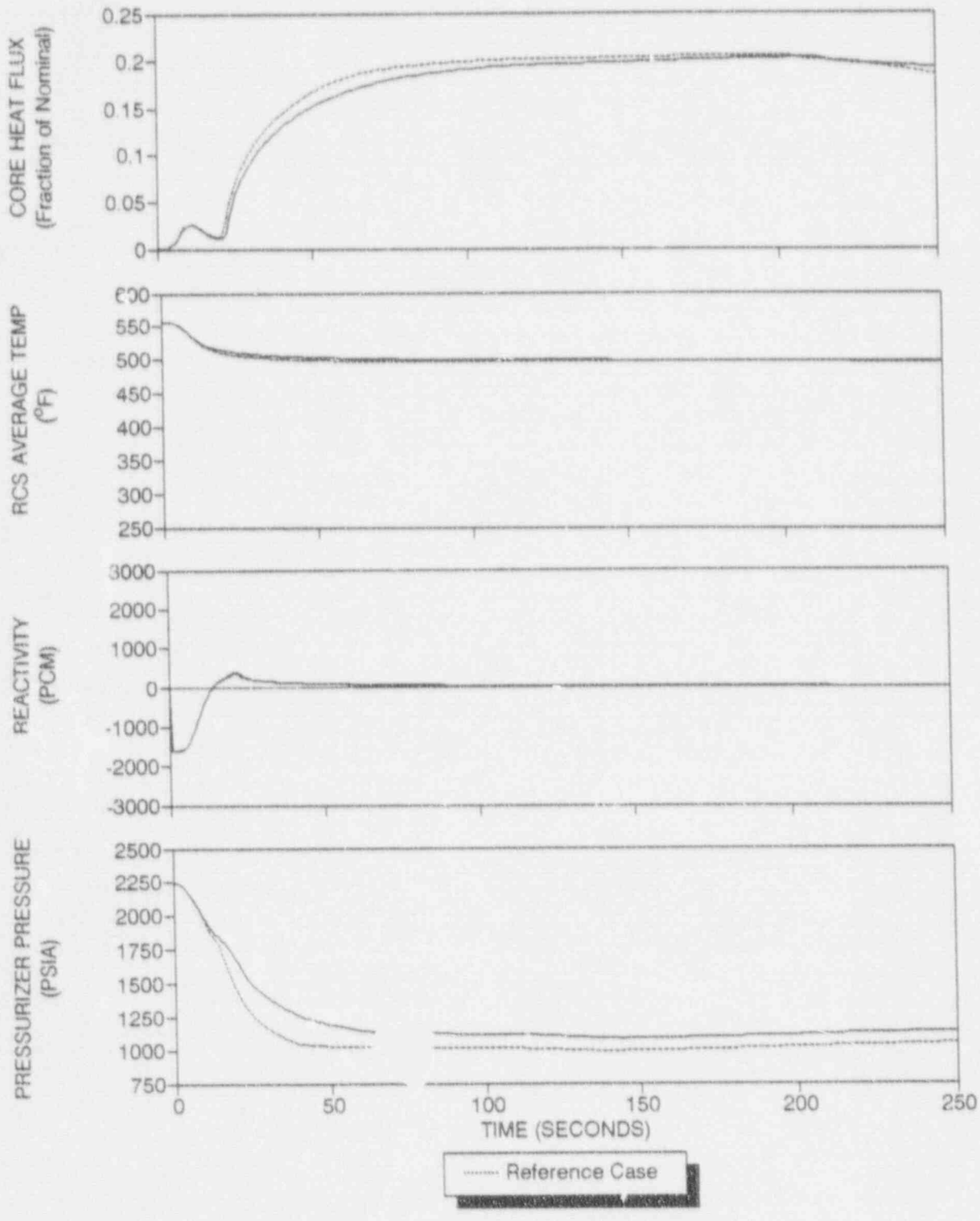

Figure 3.4-37 Transient Results for 220% of Main Feedwater to the Faulted Steam Generator and Reference Auxiliary Feedwater Distribution

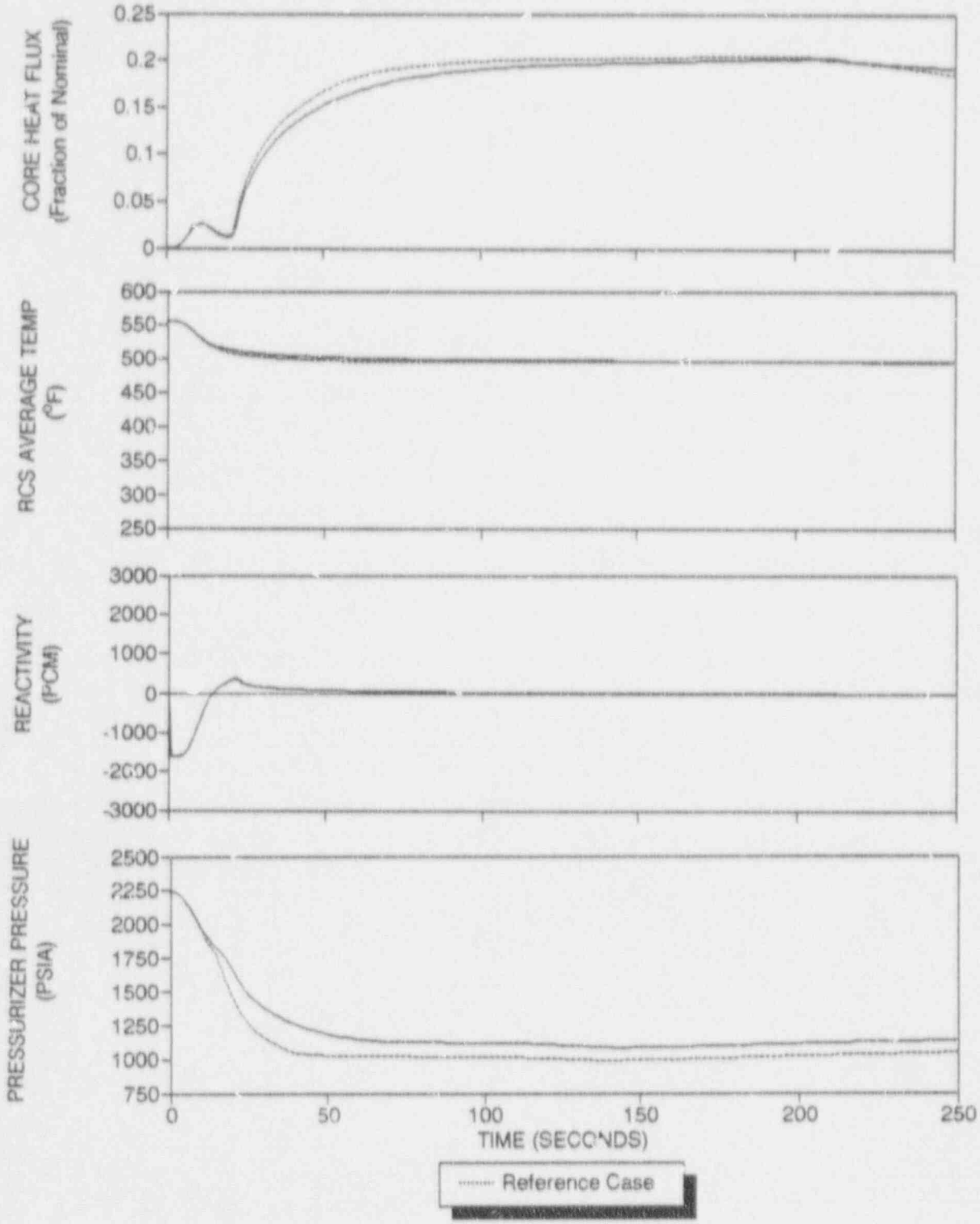

Figure 3.4-38 Transient Results for 250% of Main Feedwater to the Faulted Steam Generator and Reference Auxiliary Feedwater Distribution

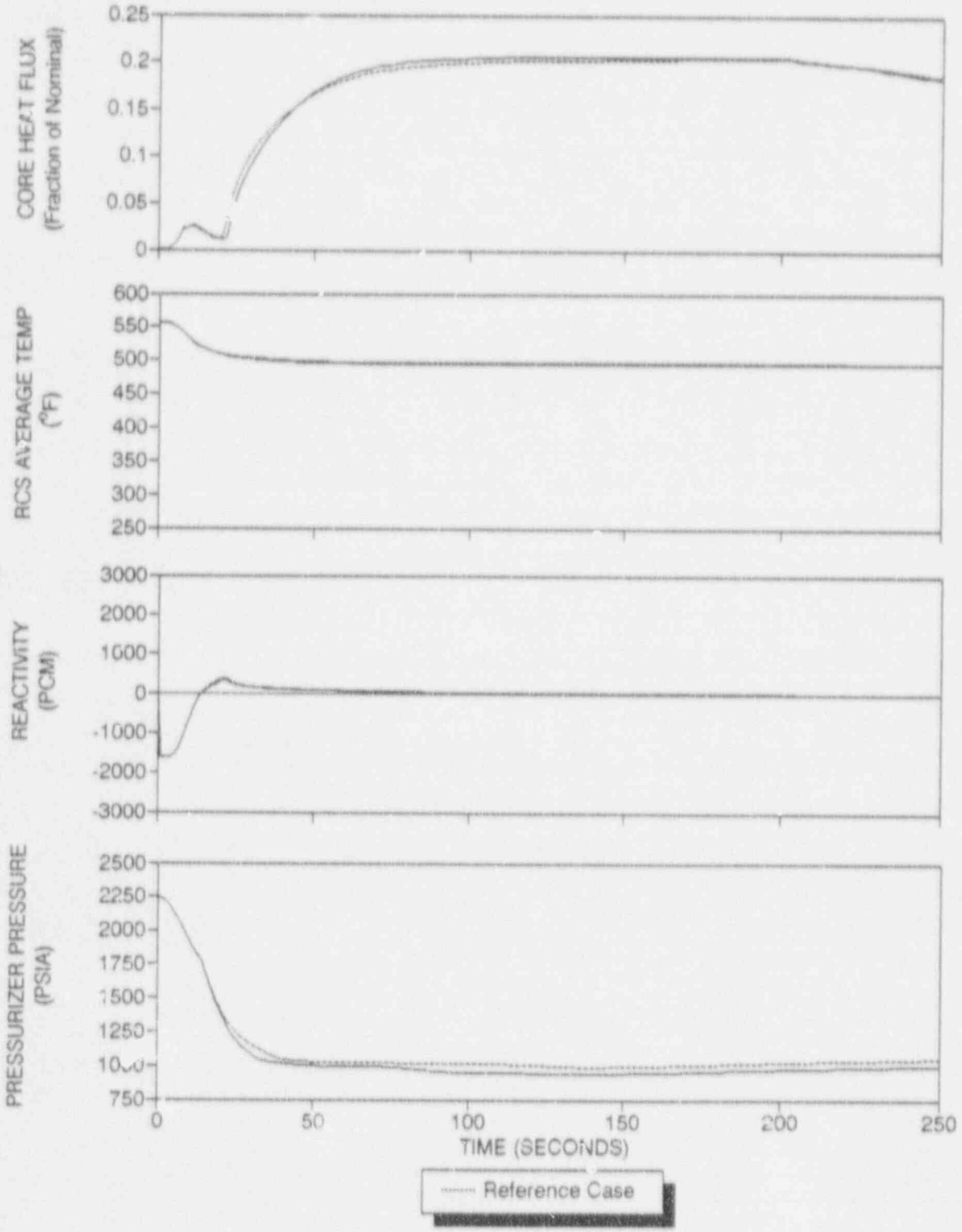

Figure 3.4-39 Transient Results for Pressurizer on the Faulted Loop

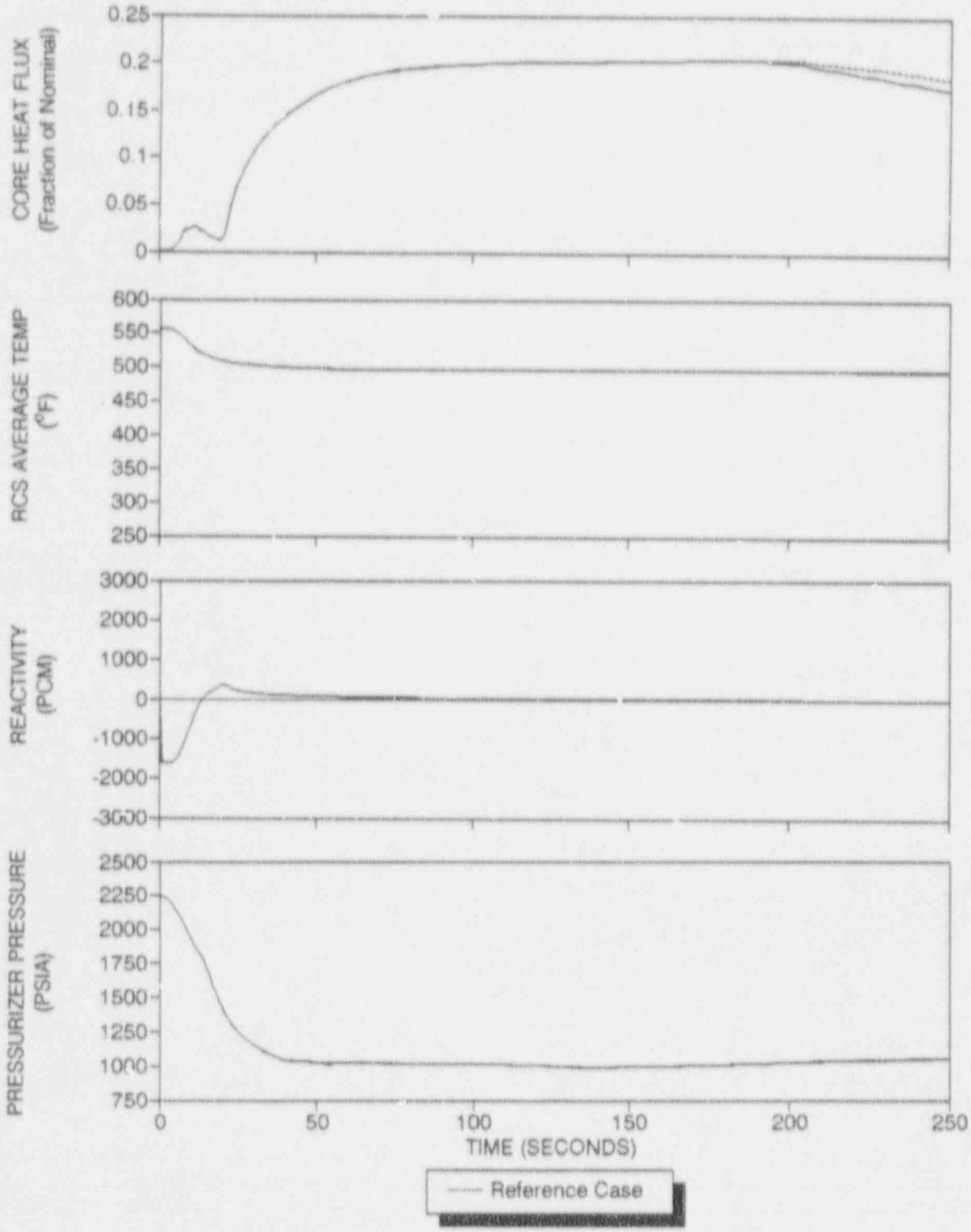

Figure 3.4-40 Transient Results for No Steam Generator Tube Bundle Height Reduction

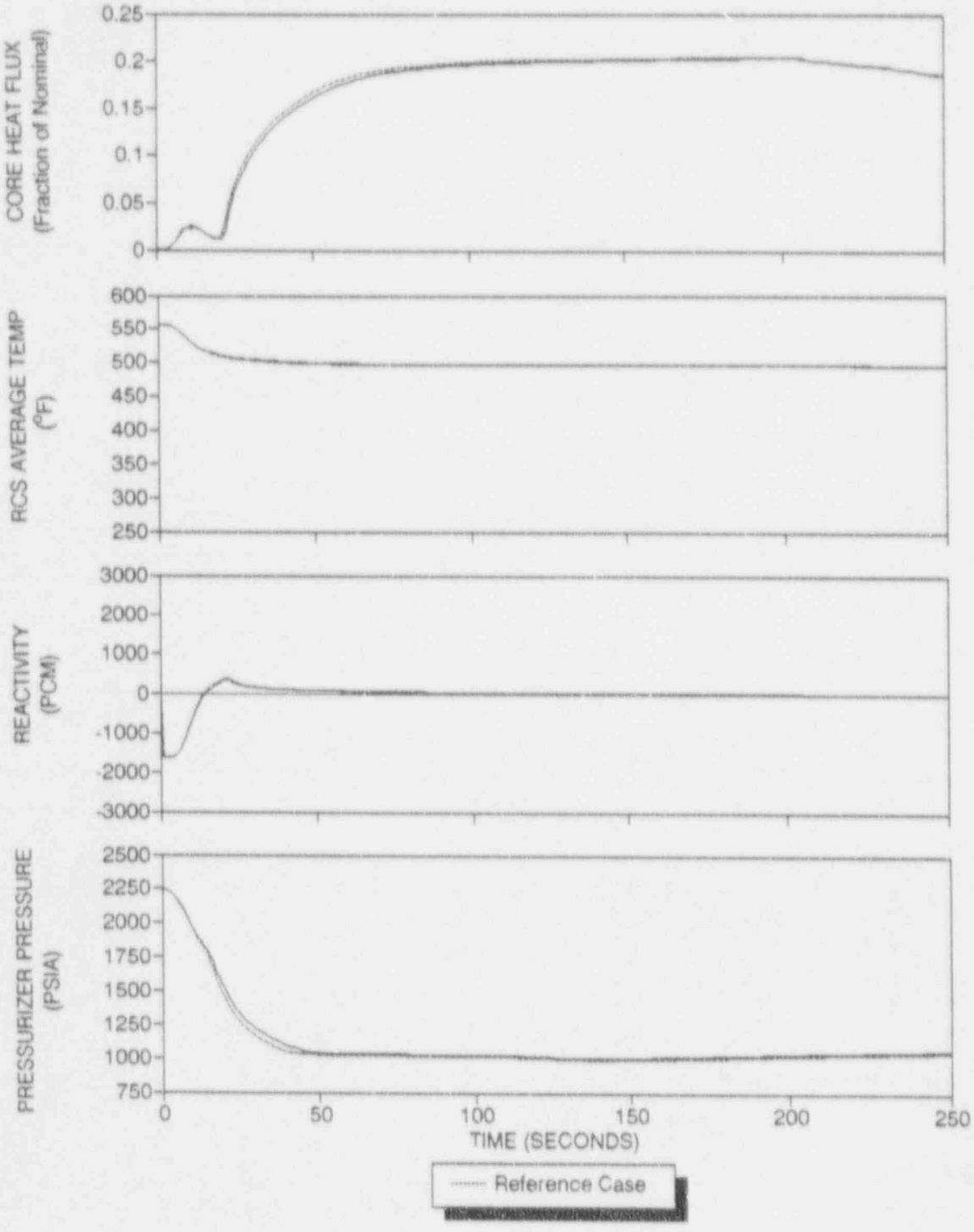

Figure 3.4-41 Transient Results for Isoenthalpic Expansion Choking Model

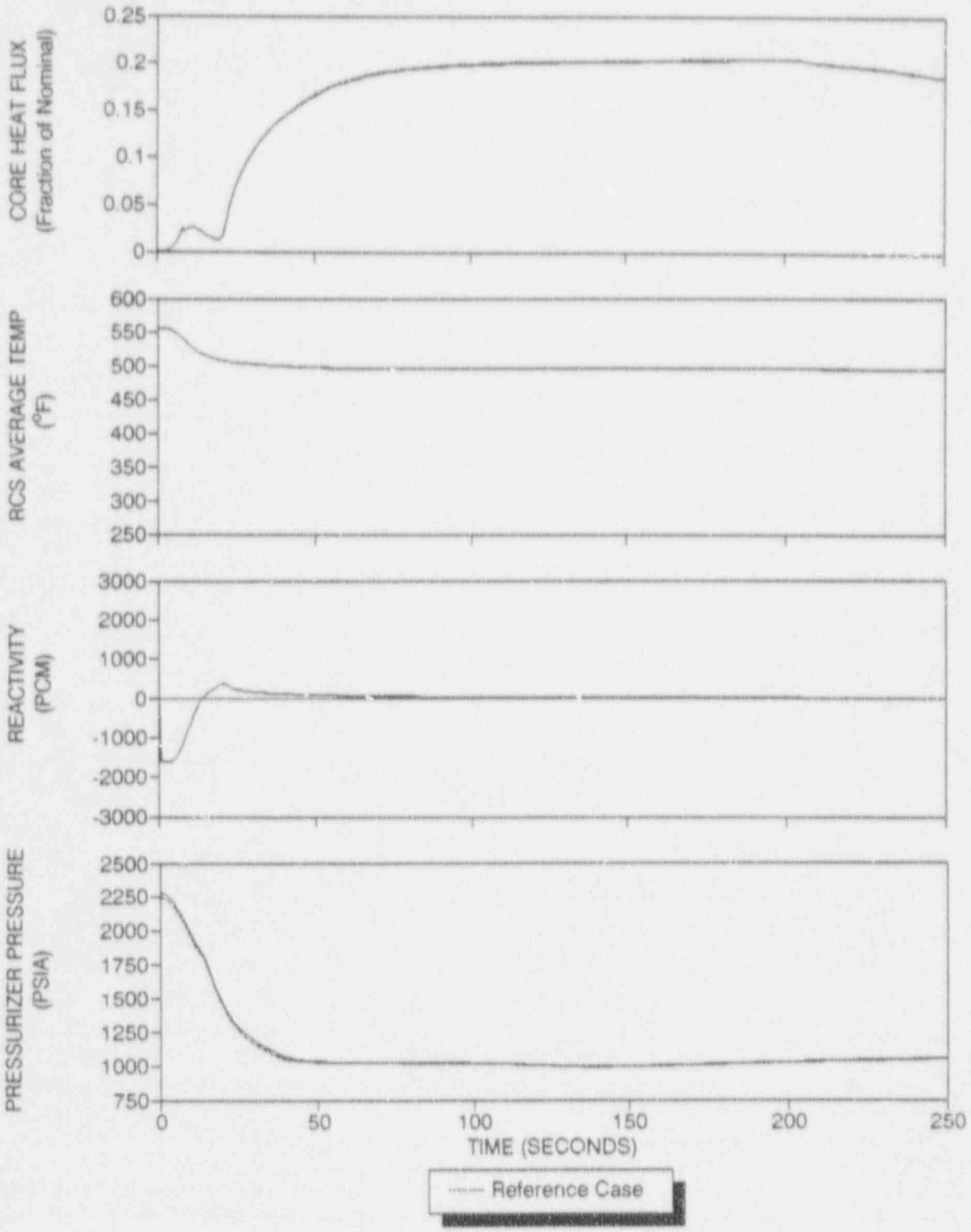

Figure 3.4-42 Transient Results for 2280 psia Initial Pressurizer Pressure

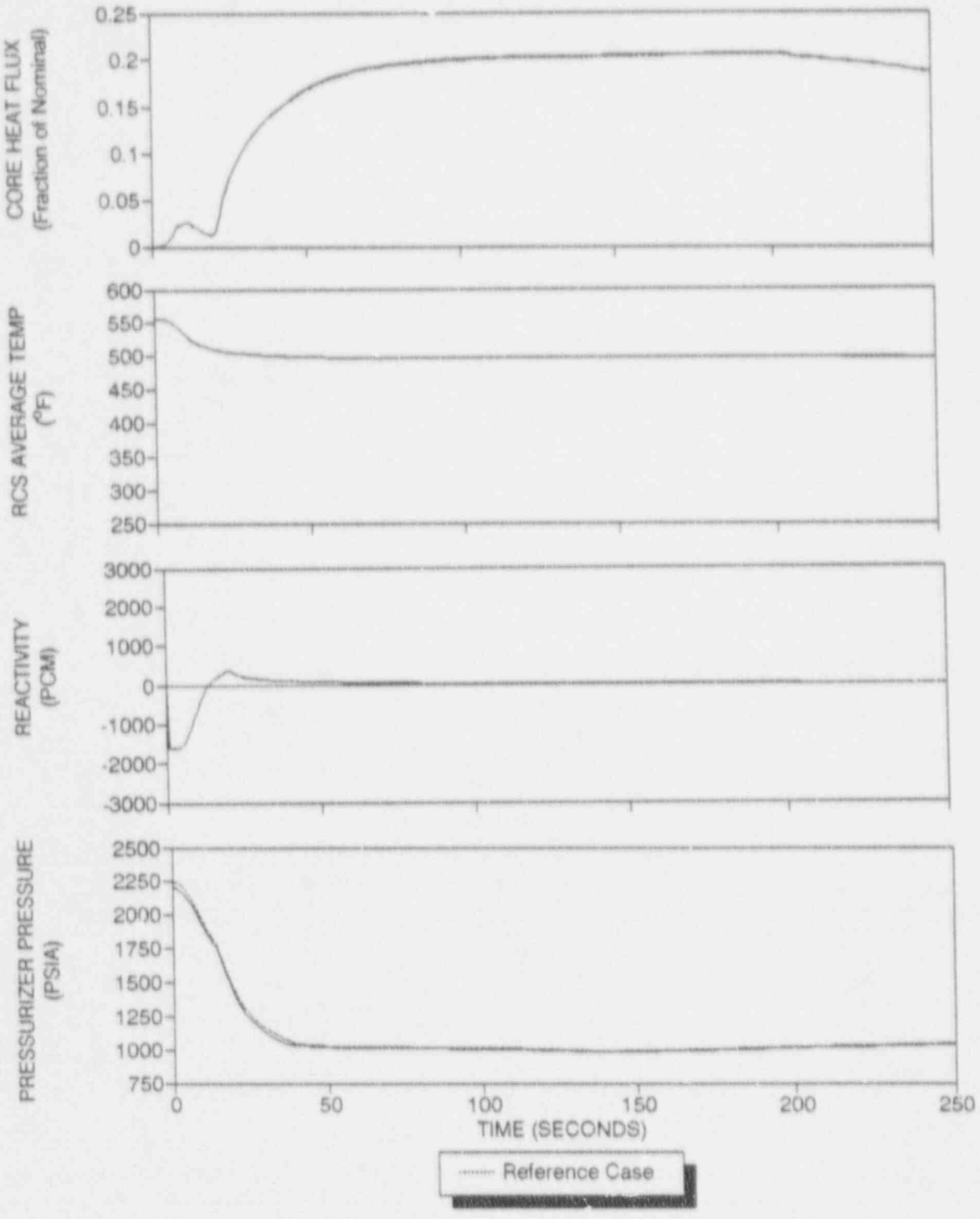

Figure 3.4-43 Transient Results for 2208 psia Initial Pressurizer Pressure

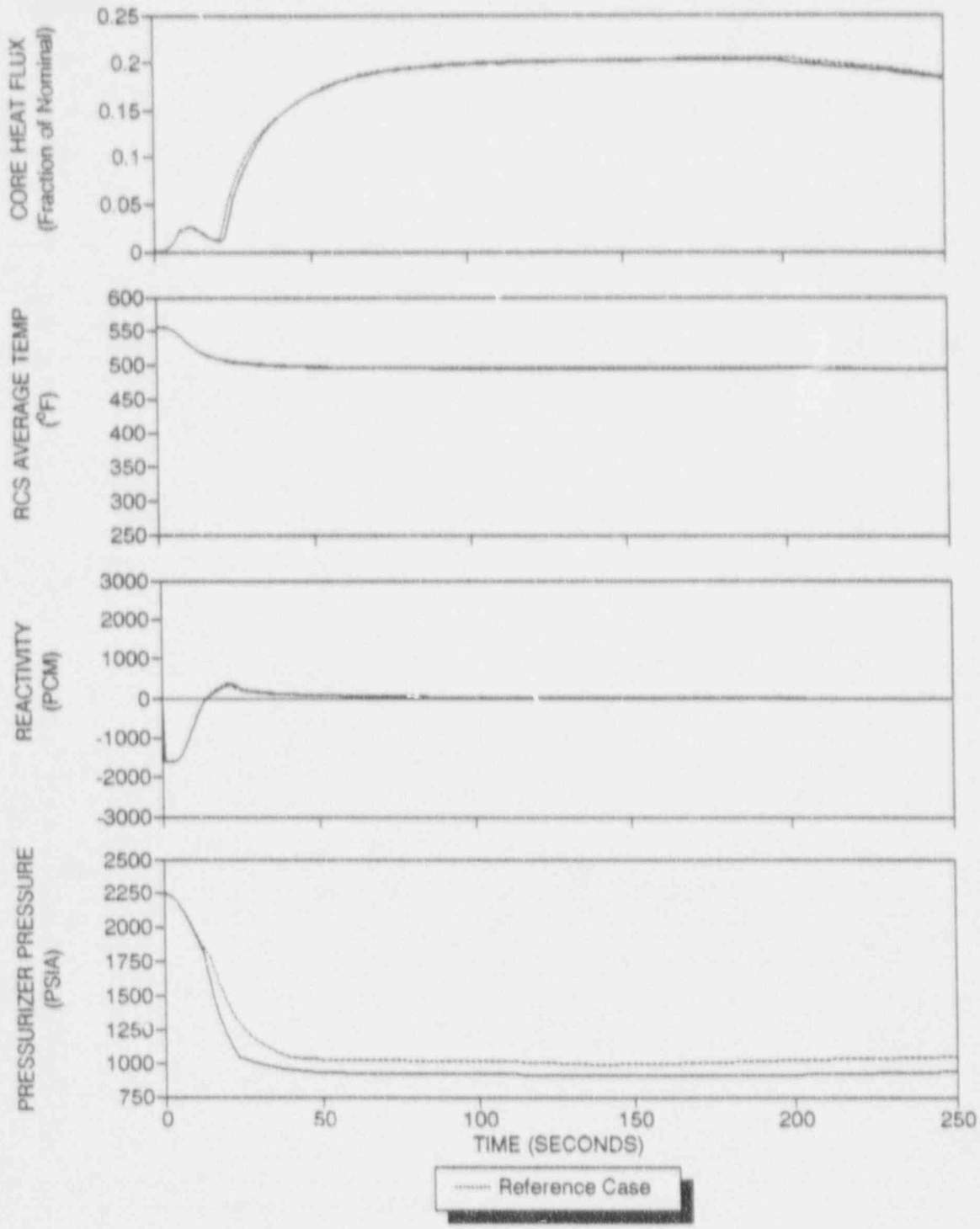

Figure 3.4-44 Transient Results for 20% Initial Pressurizer Level

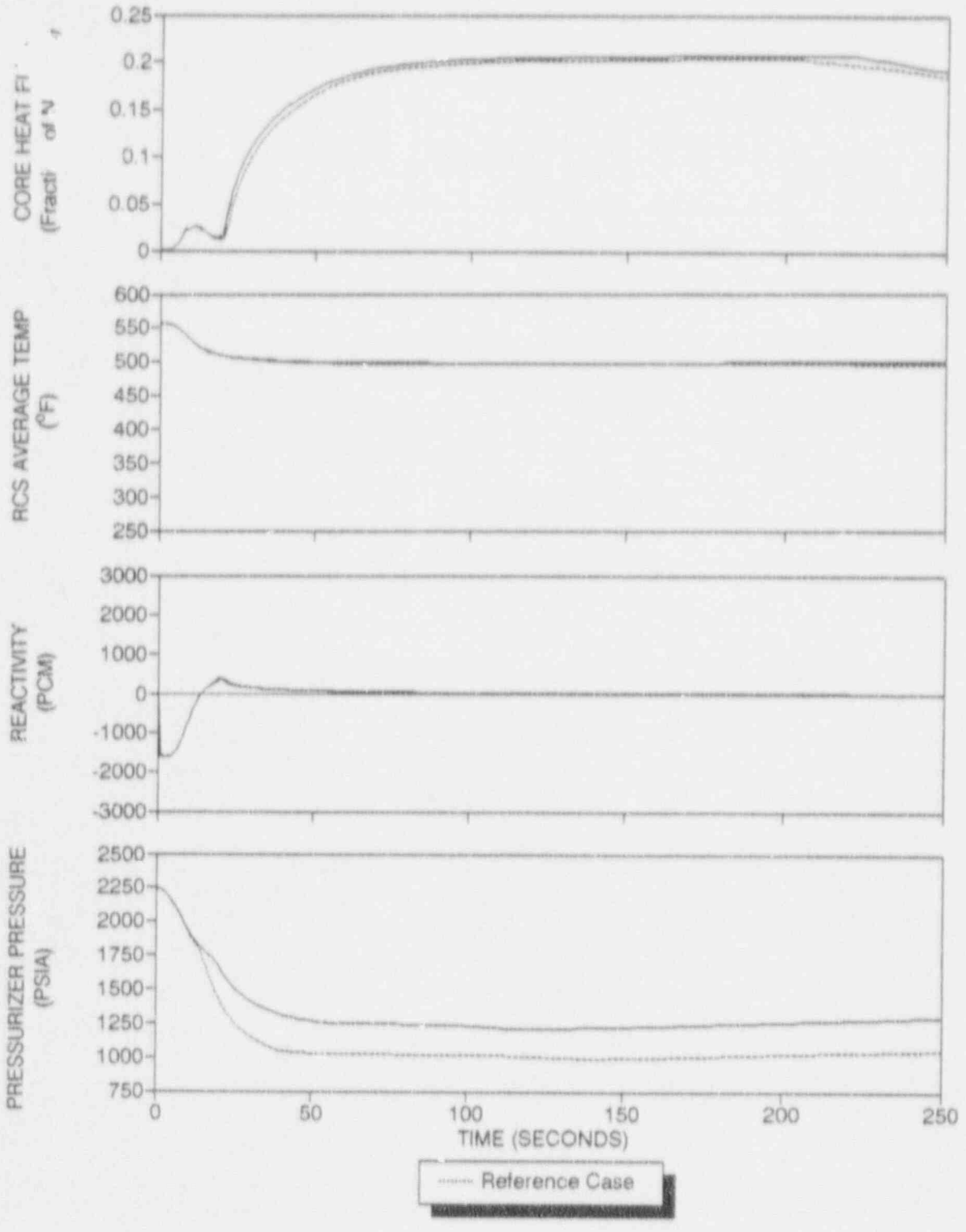

Figure 3.4-45 Transient Results for 30% Initial Pressurizer Level

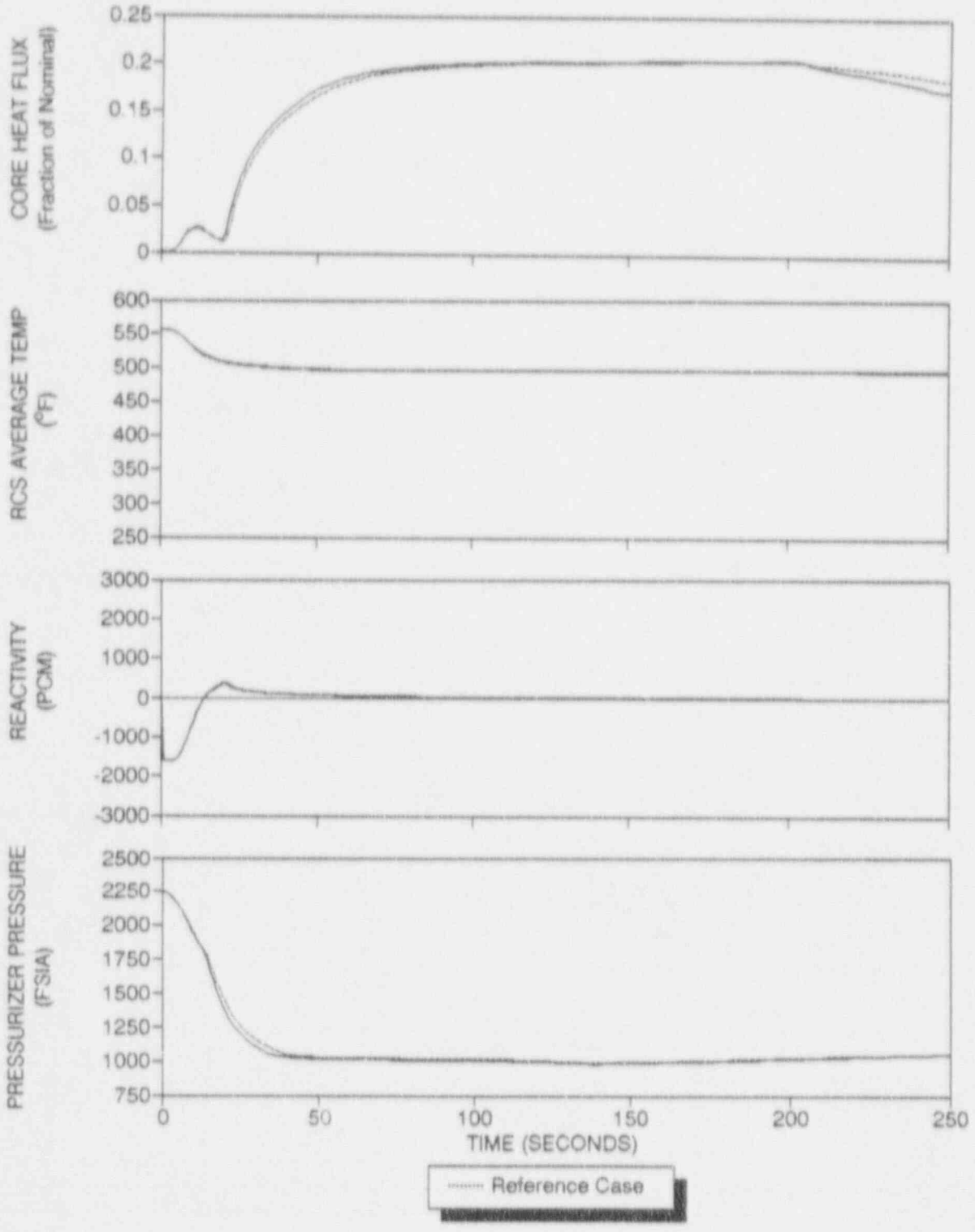

Figure 3.4-46 Transient Results for 100% of Nominal Steam Generator Mass

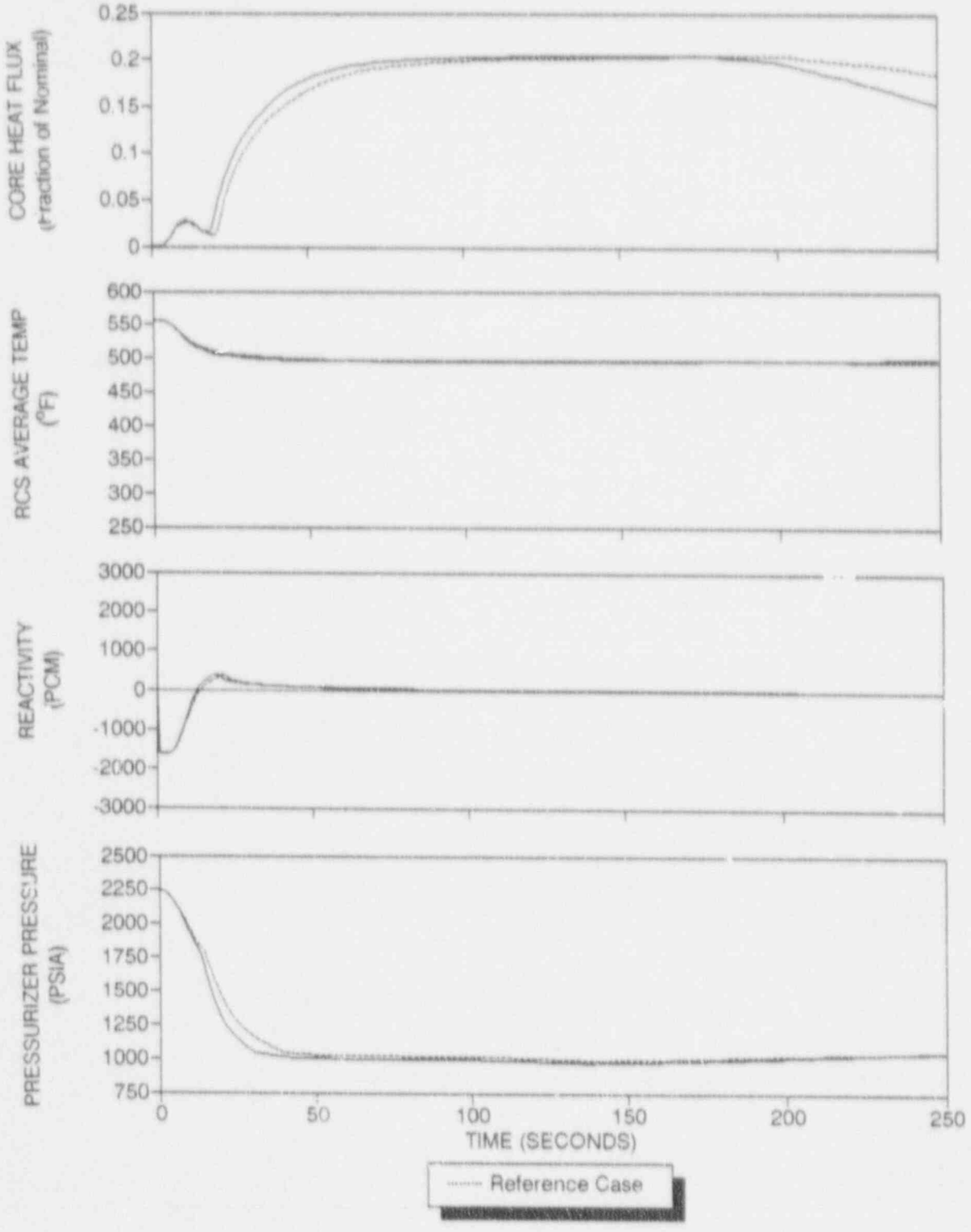

Figure 3.4-47 Transient Results for 90% of Nominal Steam Generator Mass

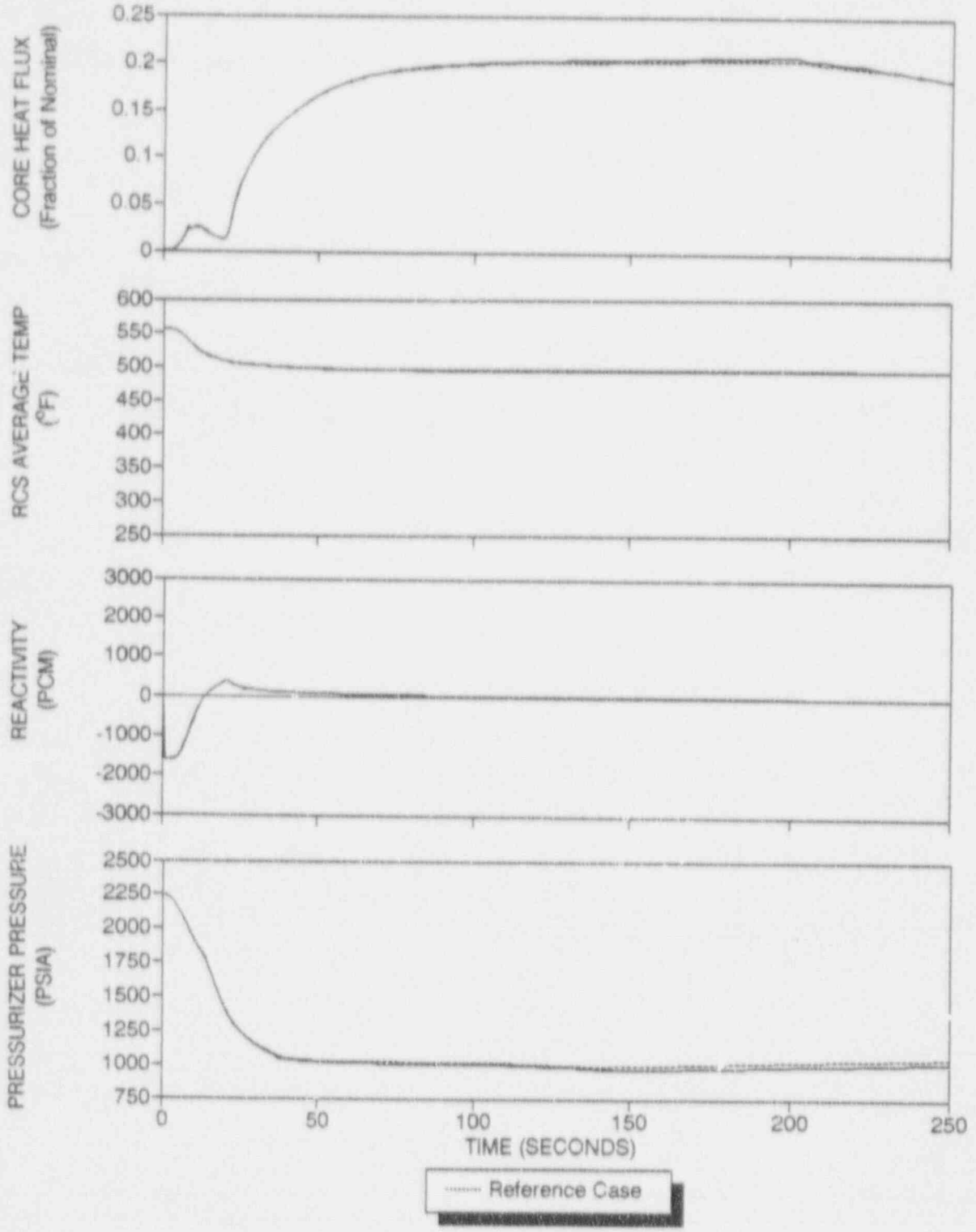

Figure 3.4-48 Transient Results for 10% Higher Reactor Coolant System Flow Rate

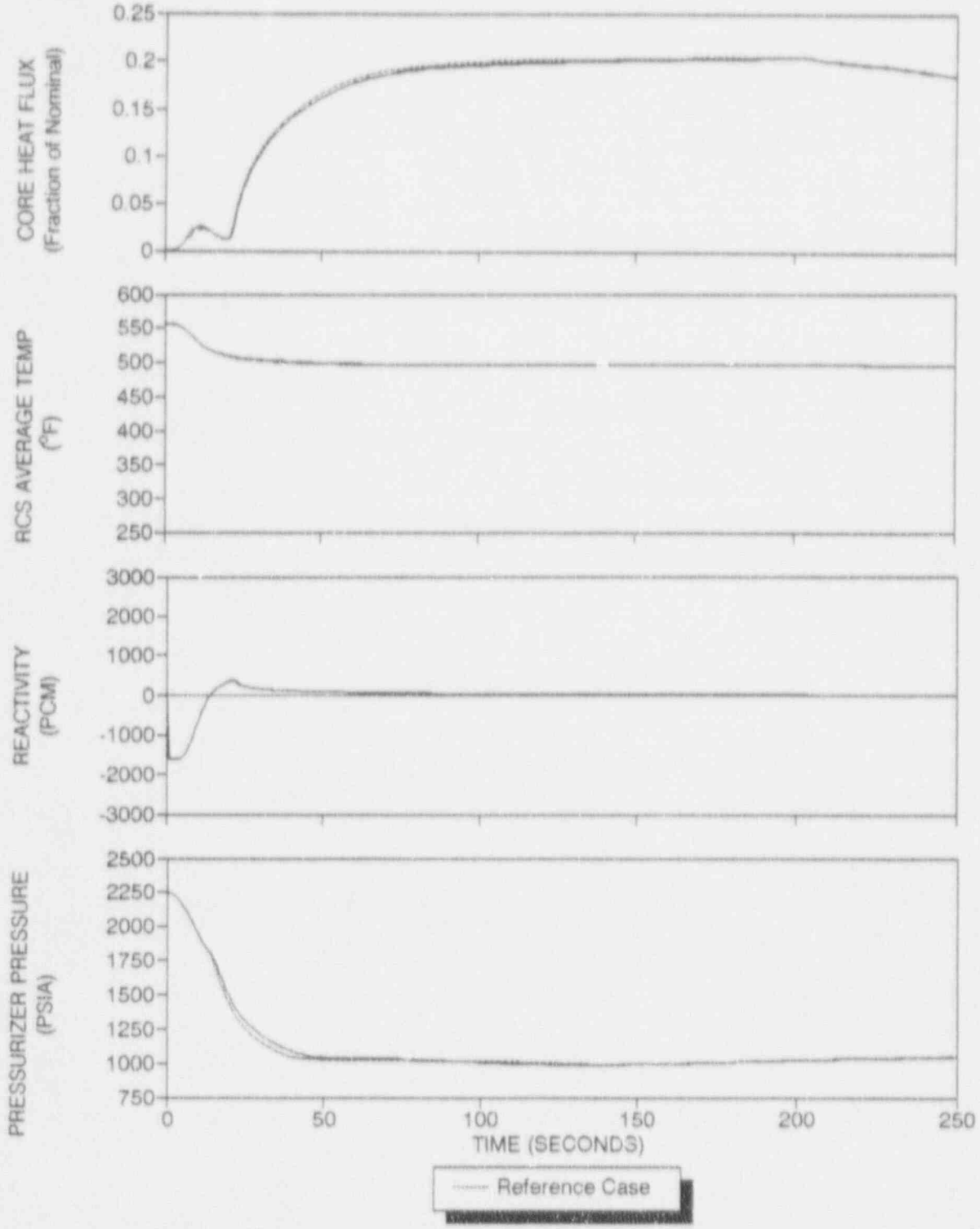

Figure 3.4-49 Transient Results for a 4.0 Ft^2 DER

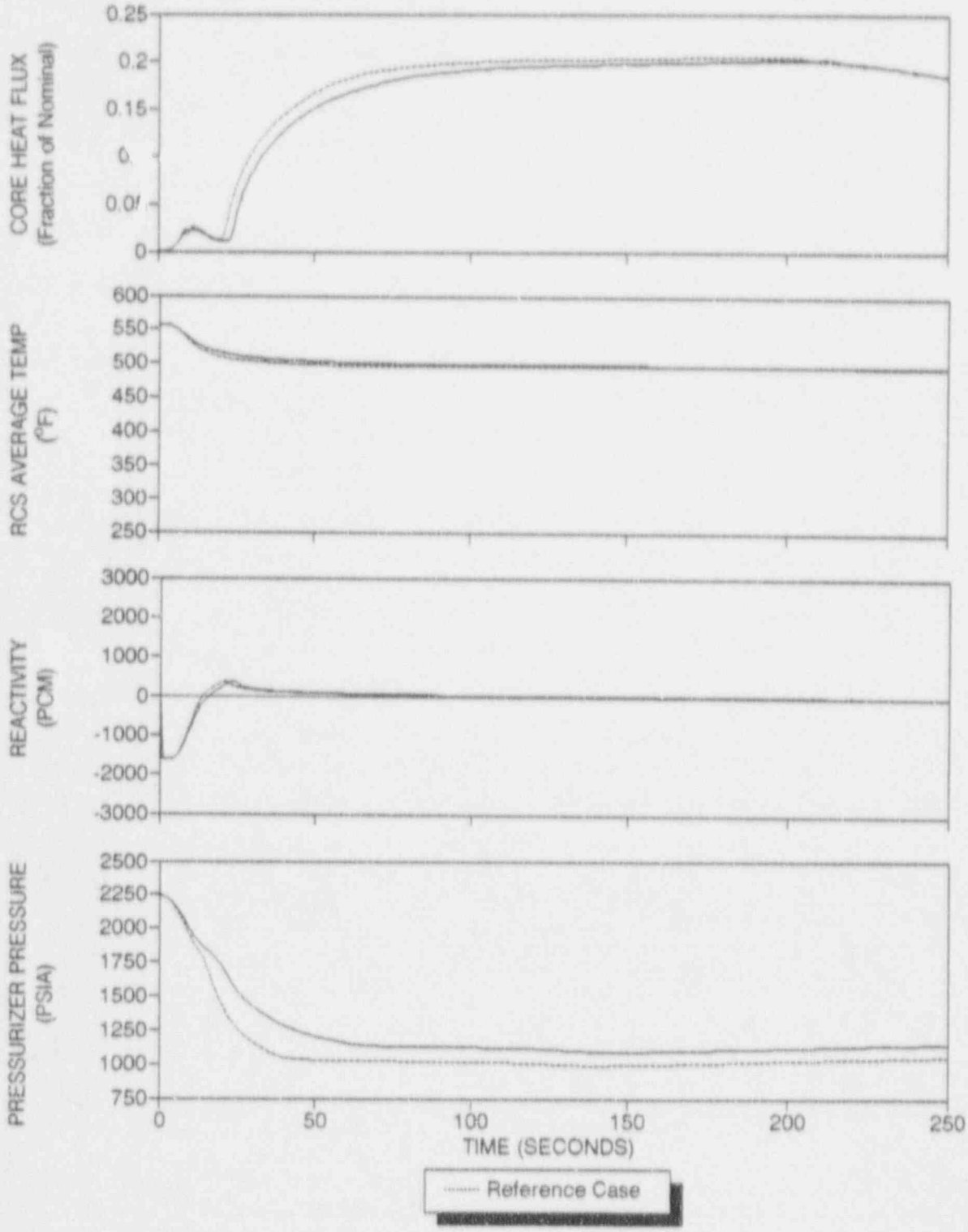

Figure 3.4-50 Transient Results for a 3.0 Ft^2 DER

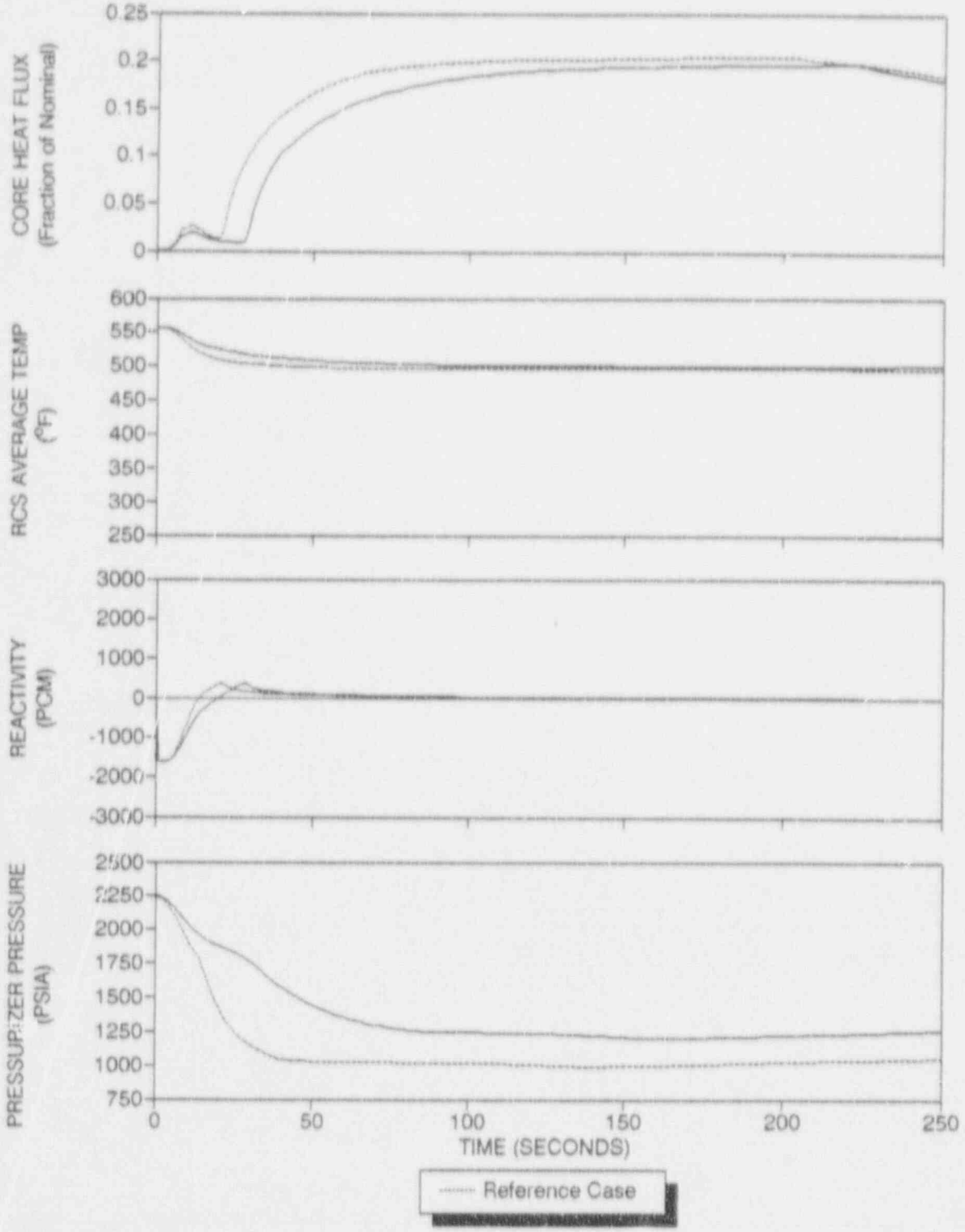

Figure 3.4-51 Transient Results for a 1.4 Ft^2 DER

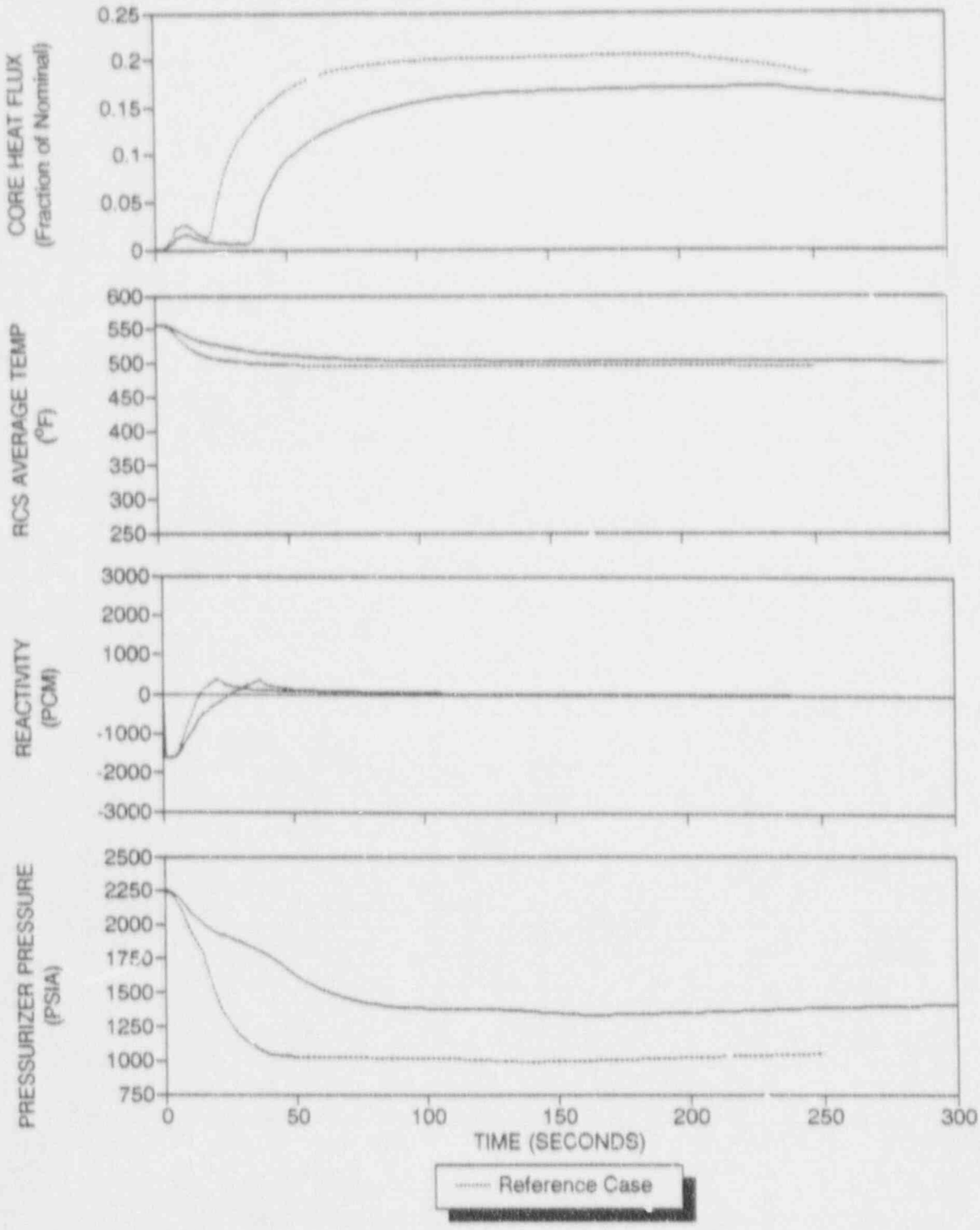

Figure 3.4-52 Transient Results for a 1.0 Ft^2 DER

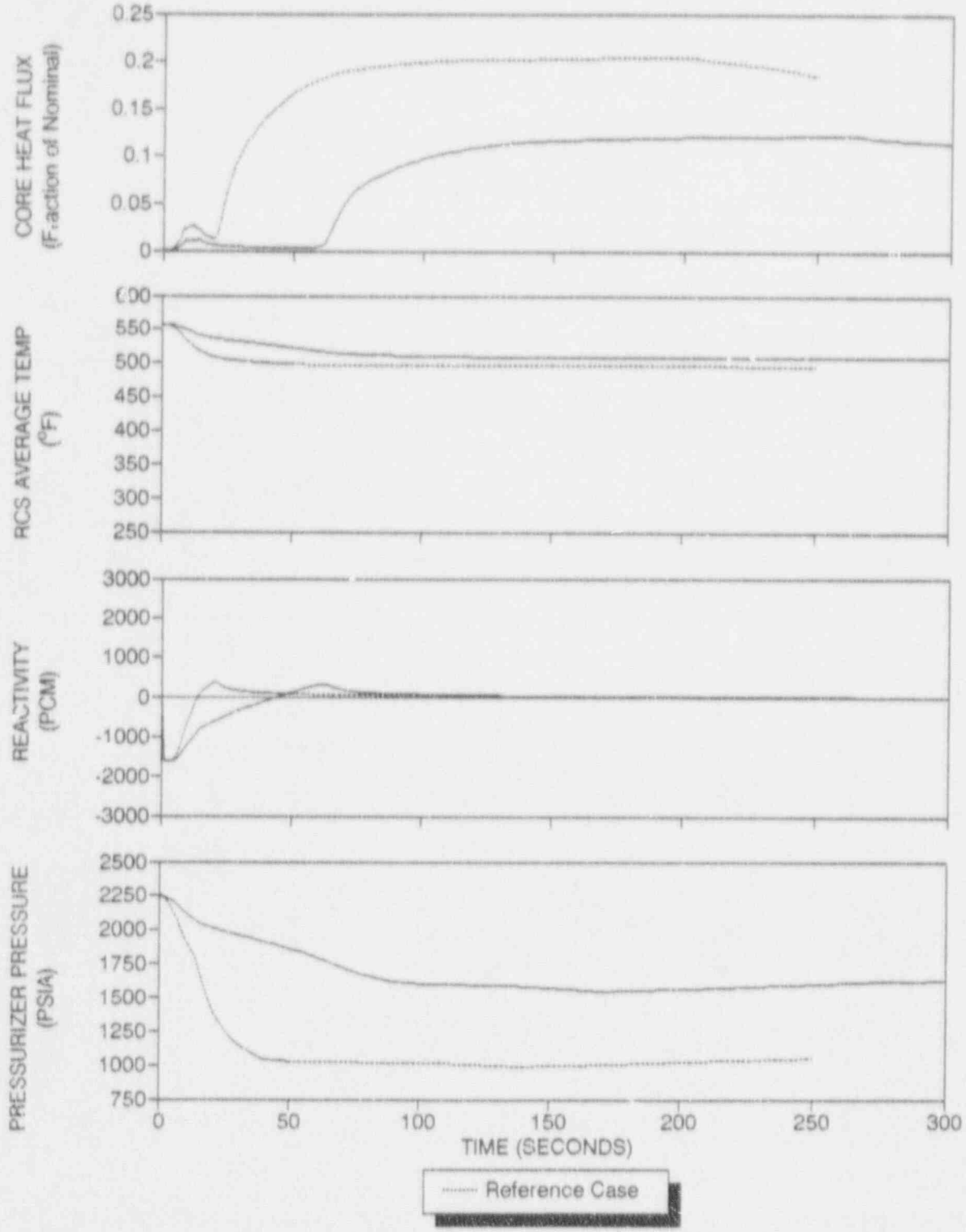

Figure 3.4-53 Transient Results for a 0.5 Ft^2 DER

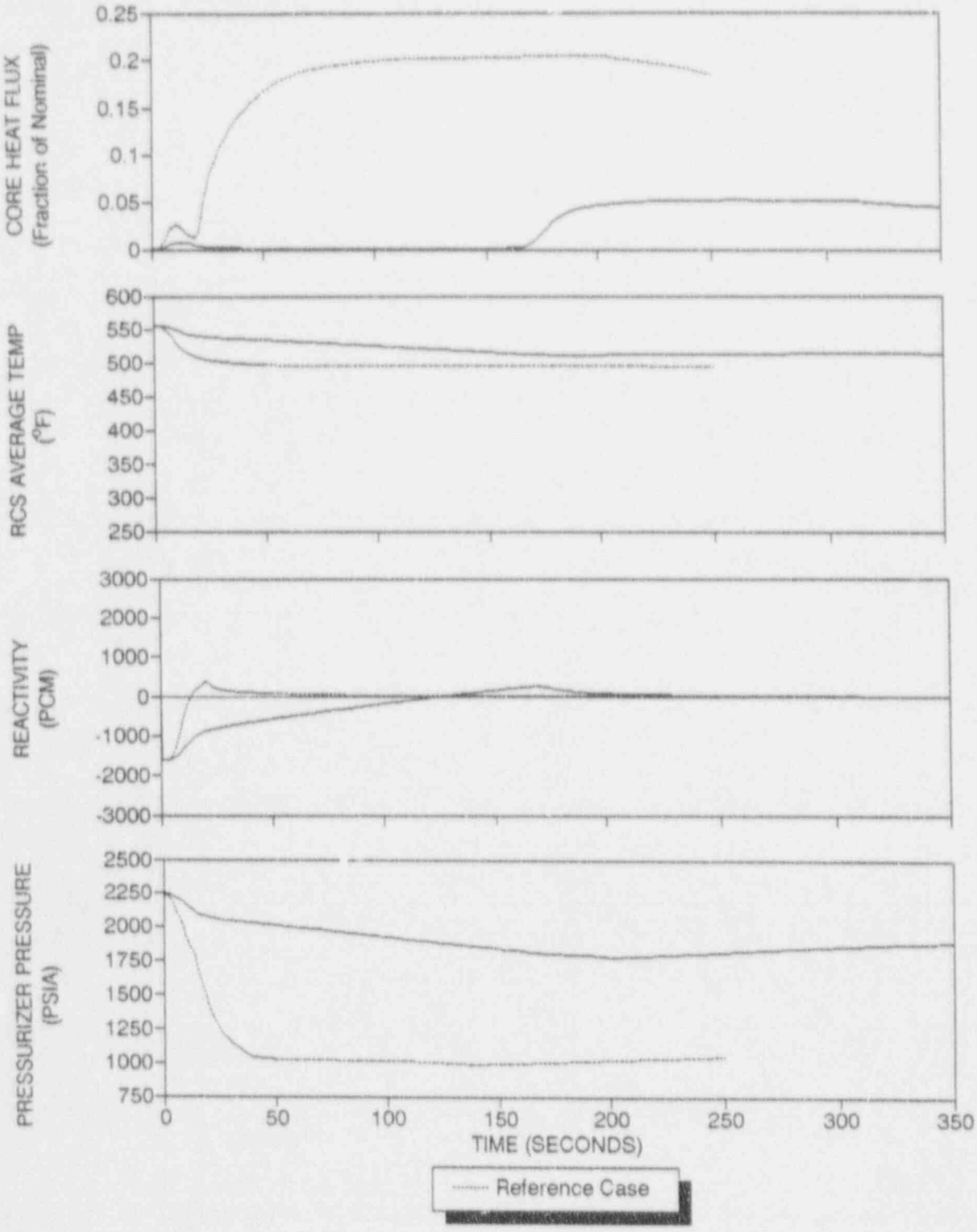

Figure 3.4-54 Transient Results for a 0.1 Ft^2 DER

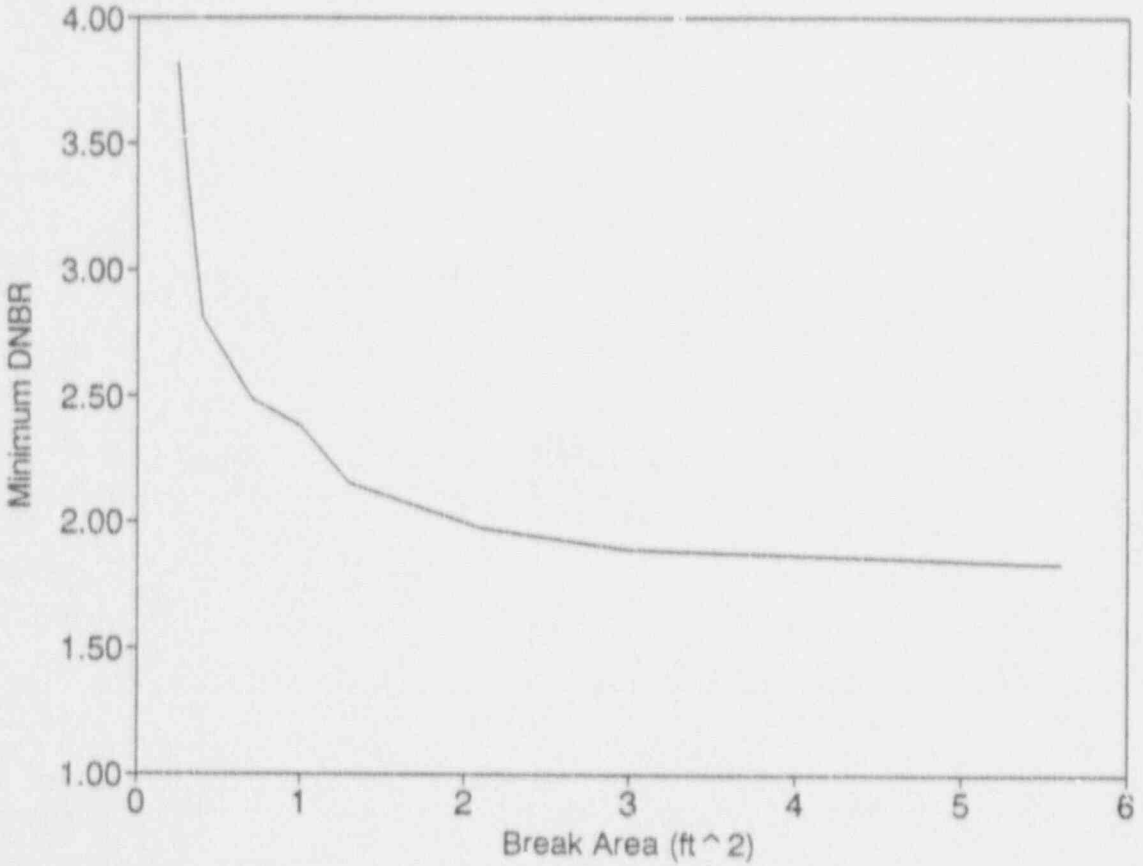

Figure 3.4-55 Minimum DNBR Versus Break Area for DER Cases

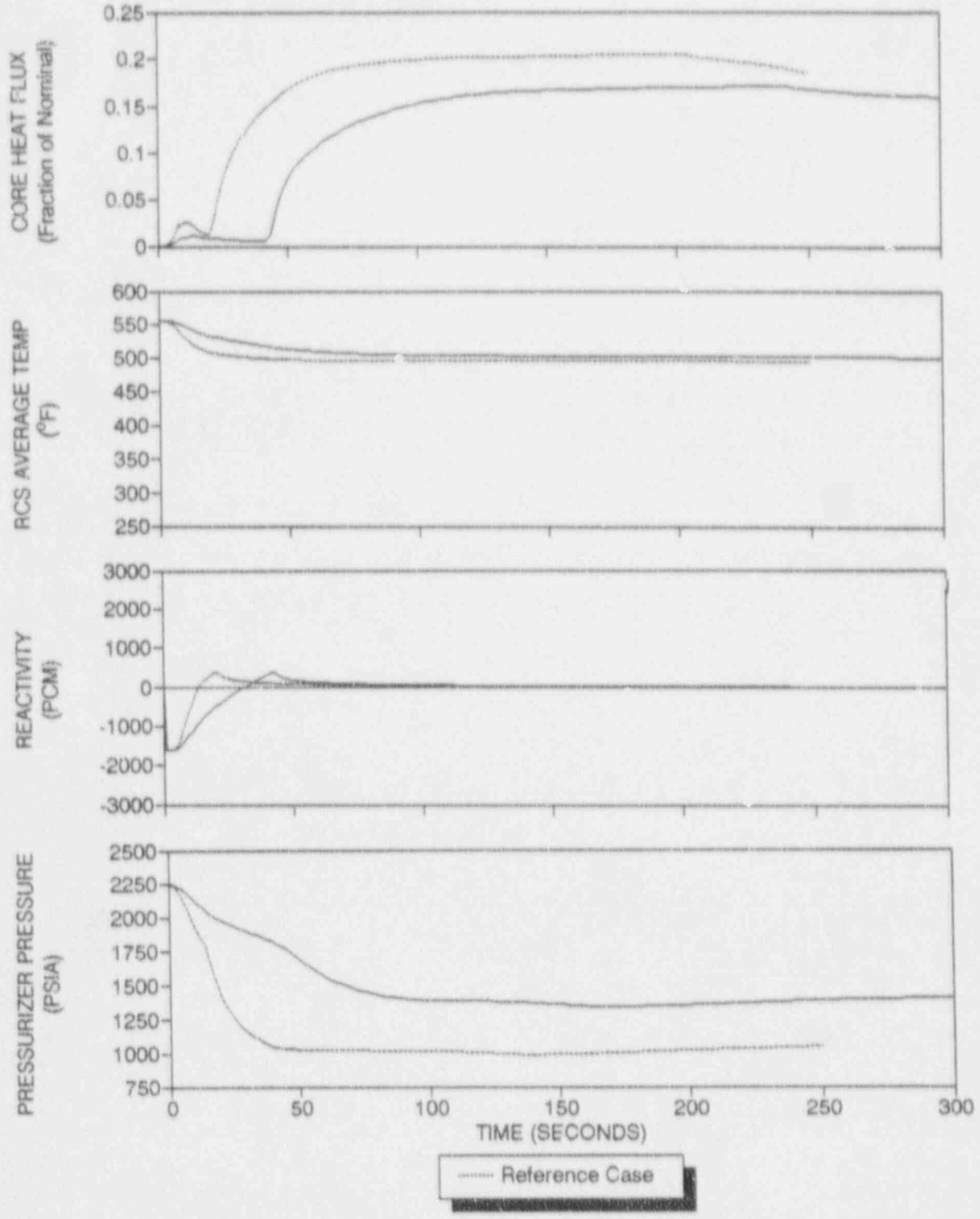

Figure 3.4-56 Transient Results for a 1.2 Ft^2 Split Break

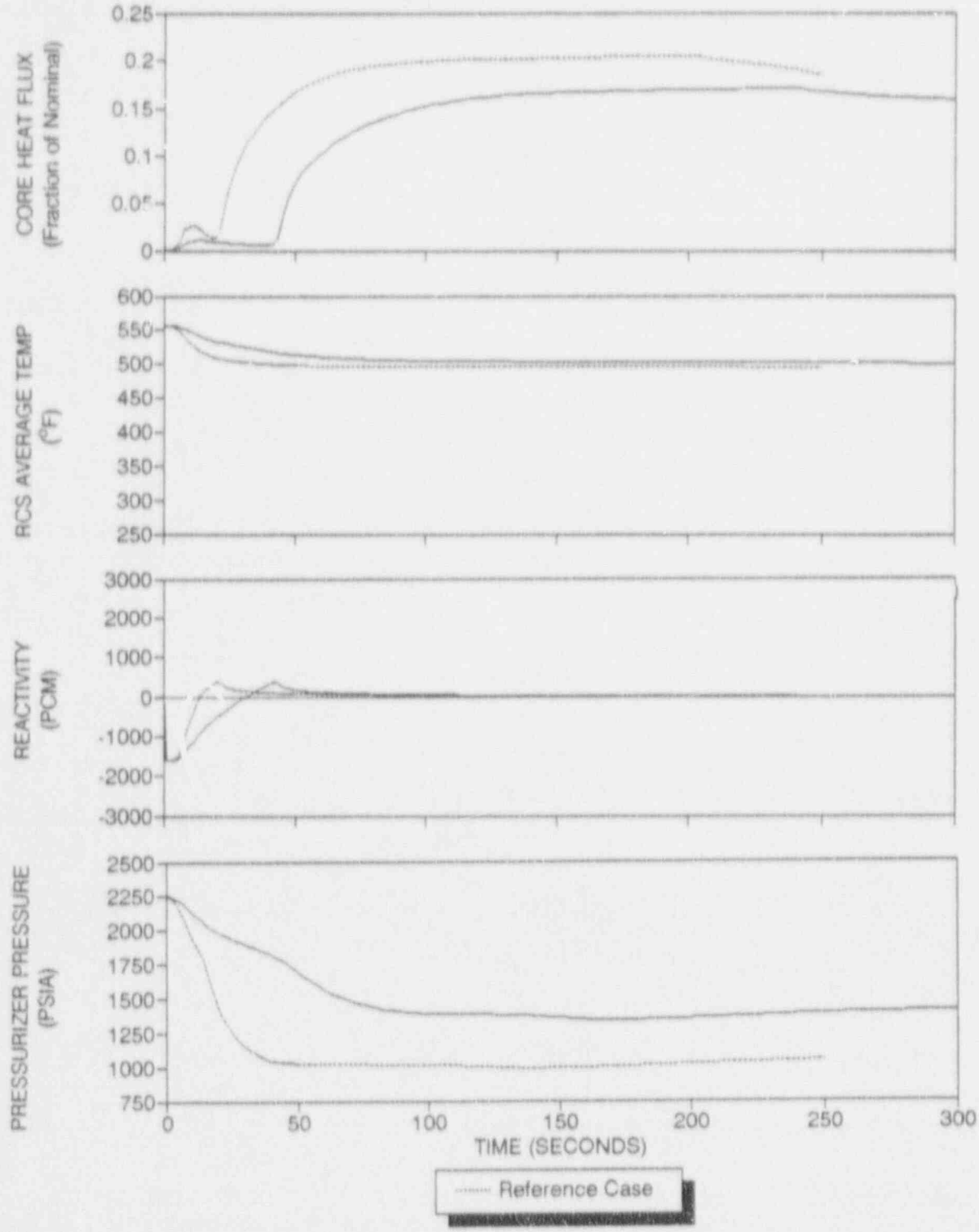

Figure 3.4-57 Transient Results for a 1.0 Ft^2 Split Break

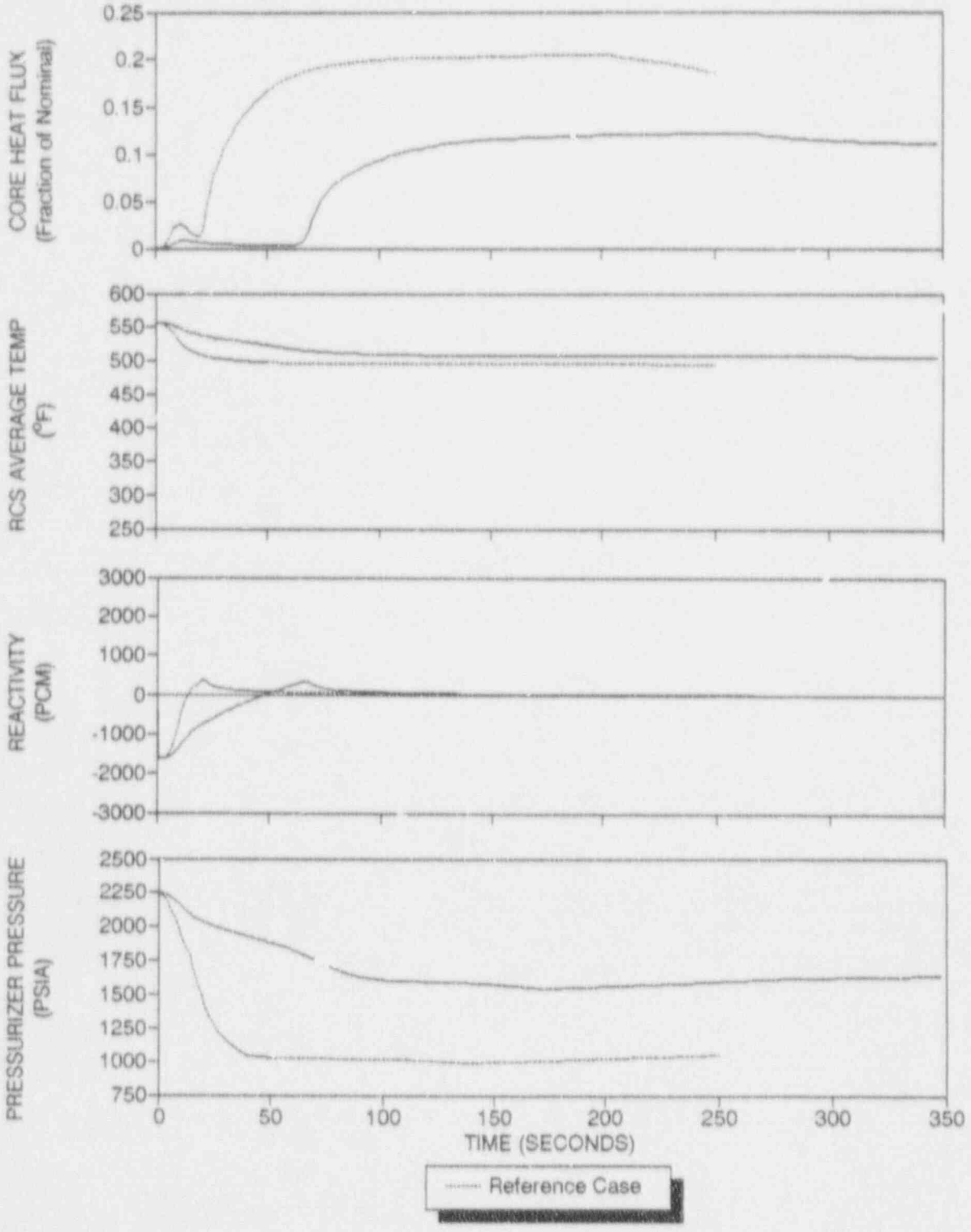

Figure 3.4-58 Transient Results for a 0.5 Ft^2 Split Break

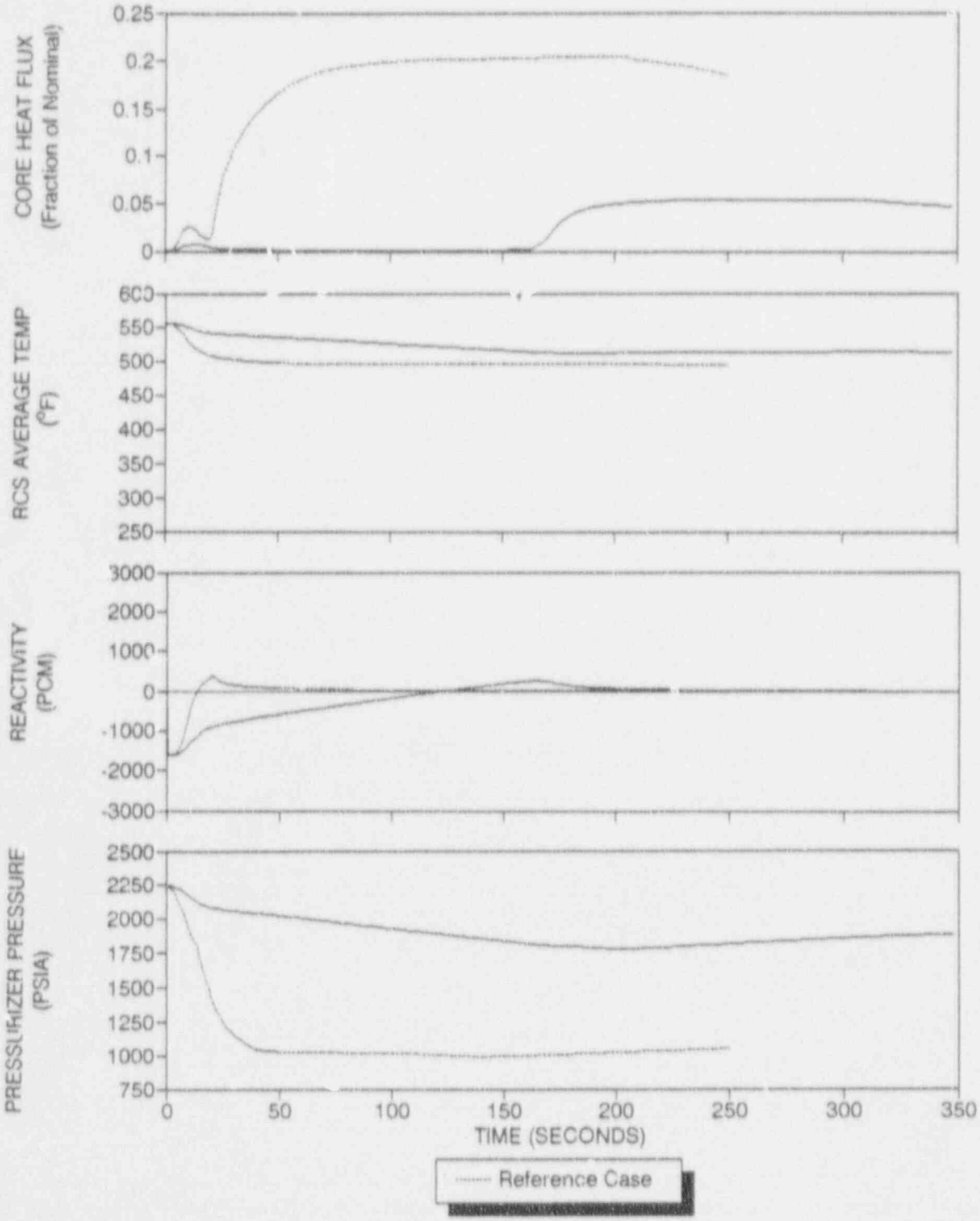

Figure 3.4-59 Transient Results for a 0.111 Ft^2 Split Break

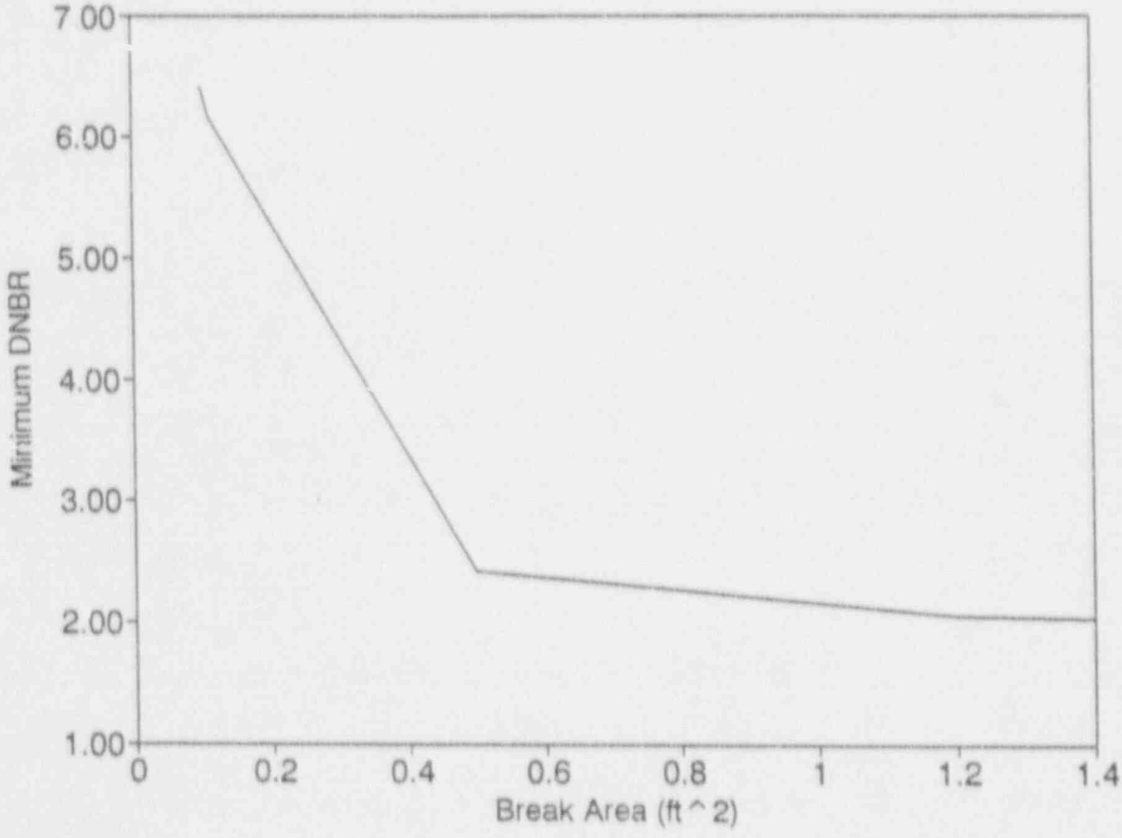

Figure 3.4-60 Minimum DNBR Versus Break Area for Split Break Cases

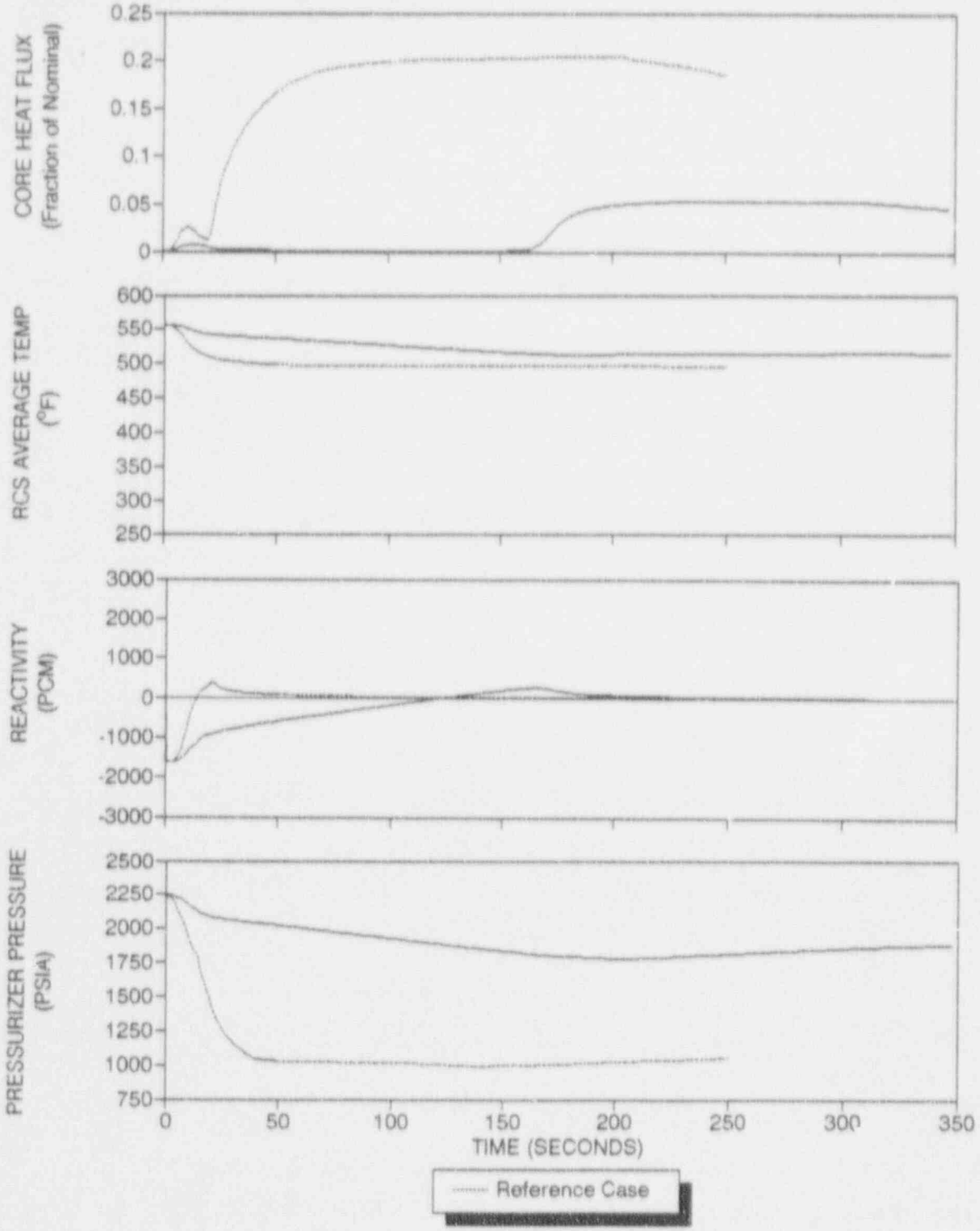

Figure 3.4-61 Transient Results for a Steam Generator Safety Valve Opening

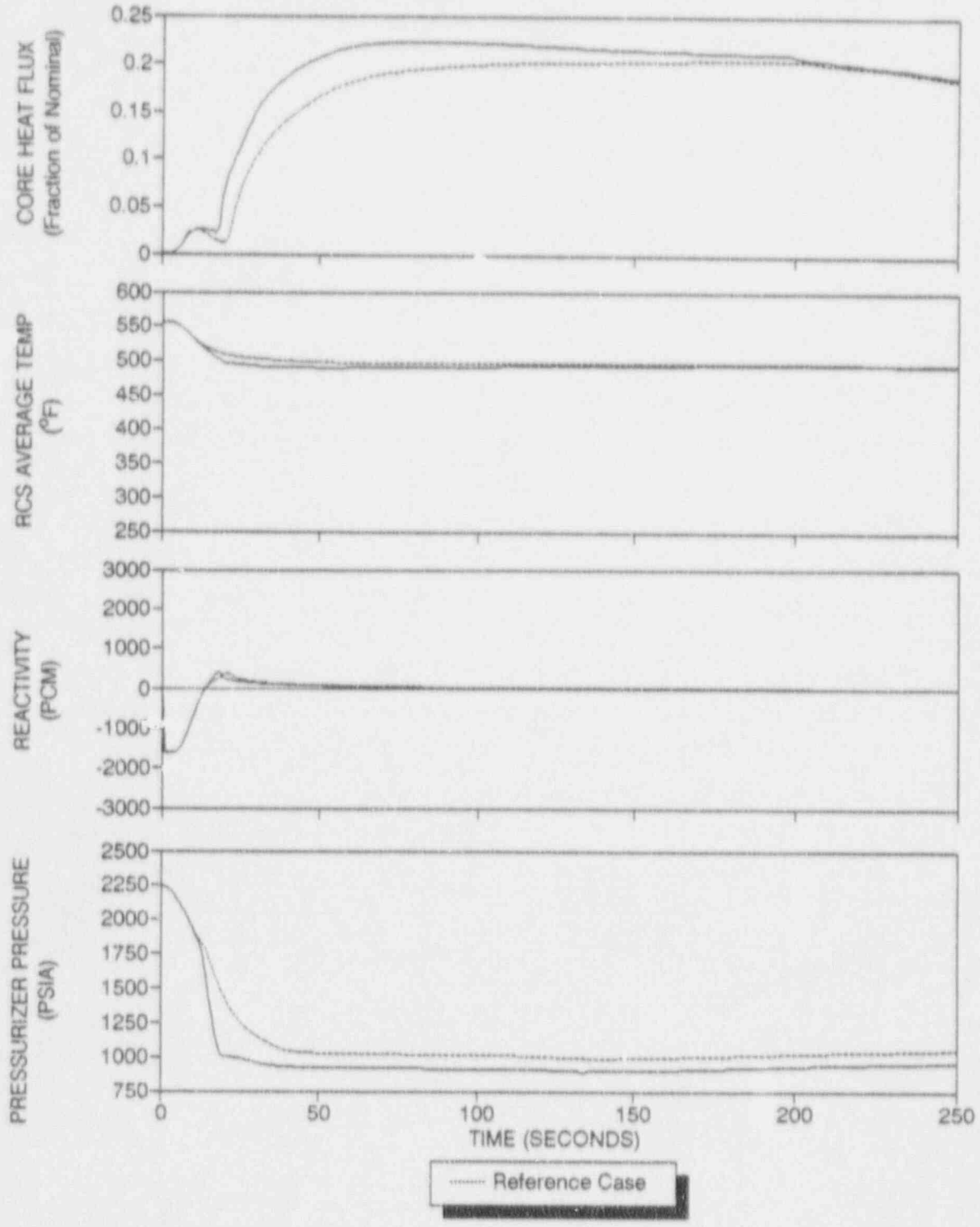

Figure 3.4-62 Transient Results for a Steamline Isolation Response Time of 10.0 Seconds

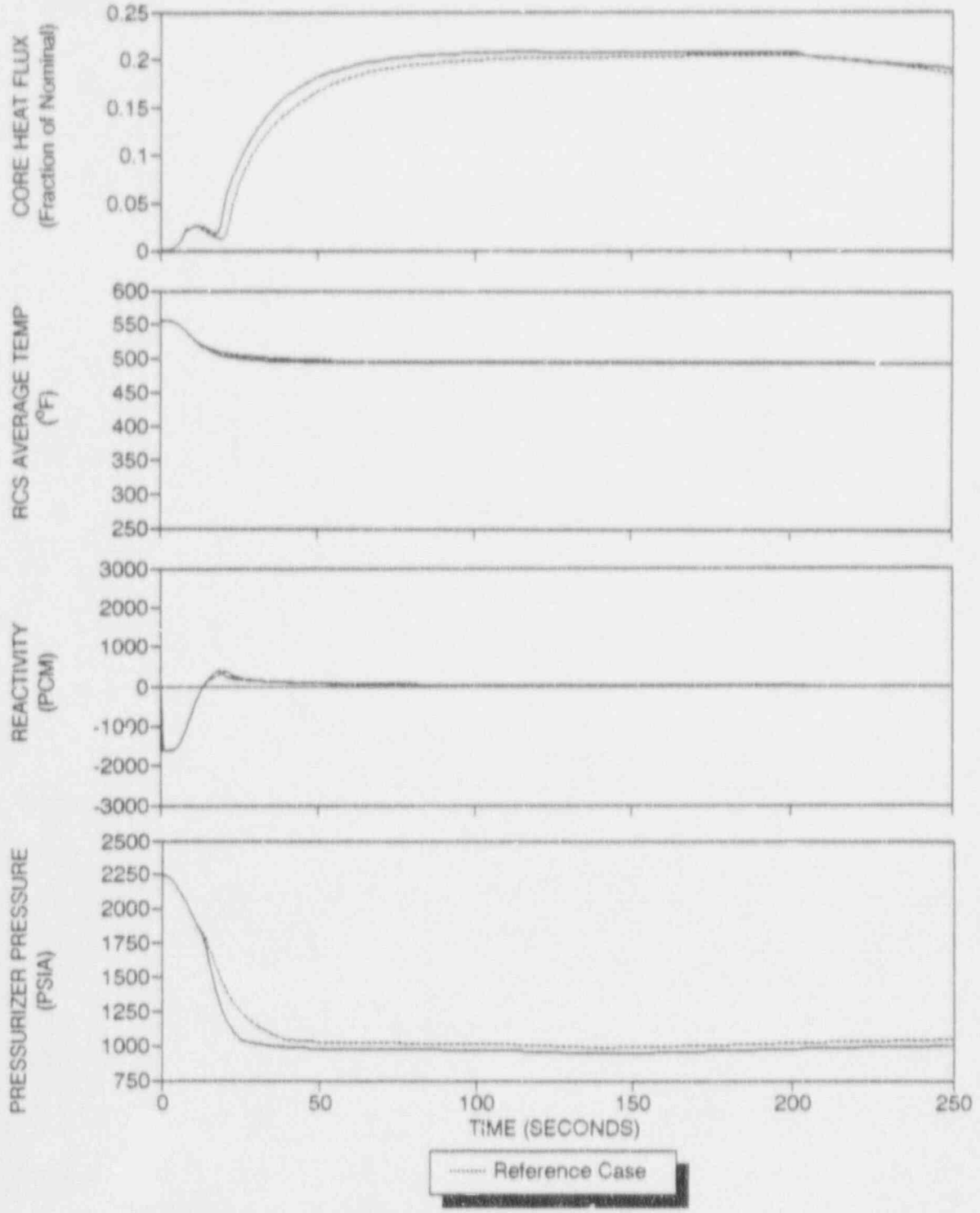

Figure 3.4-63 Transient Results for a Feedwater Line Isolation Response Time of 10.0 Seconds

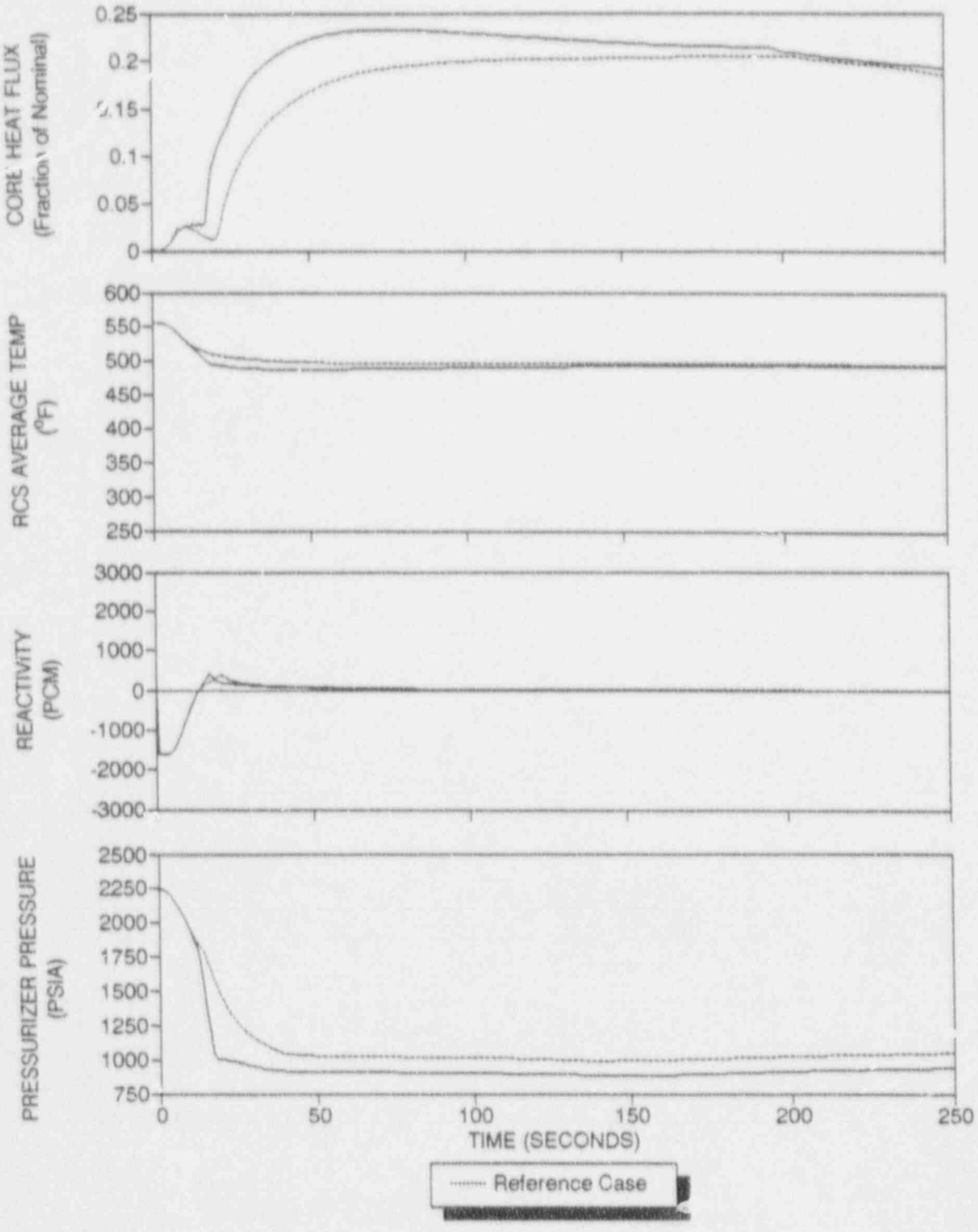

Figure 3.4-64 Transient Results for Both a Steamline and Feedwater Line Isolation Response Time of 10.0 Seconds

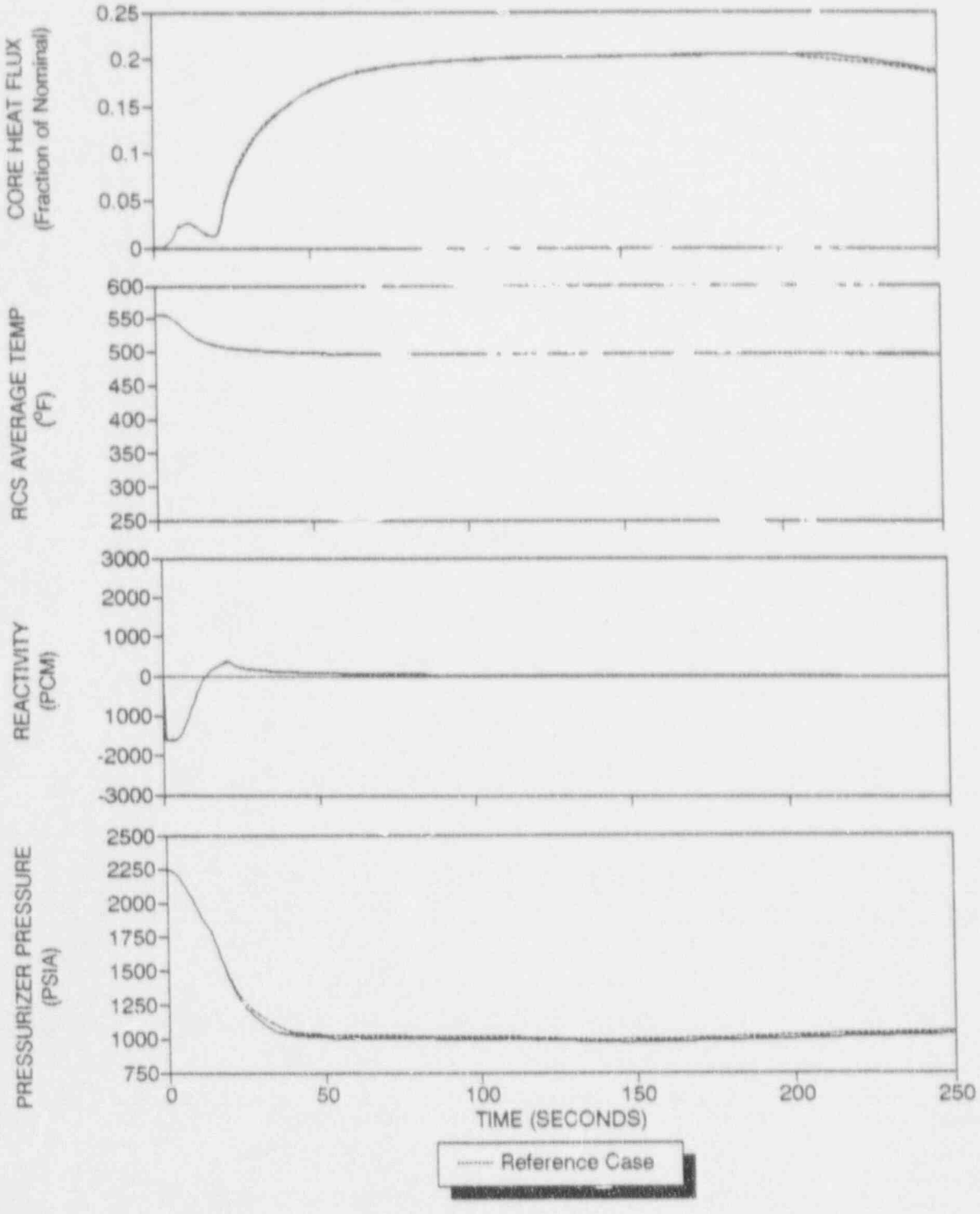

Figure 3.4-65 Transient Results for no Safety Injection on Low Steamline Pressure

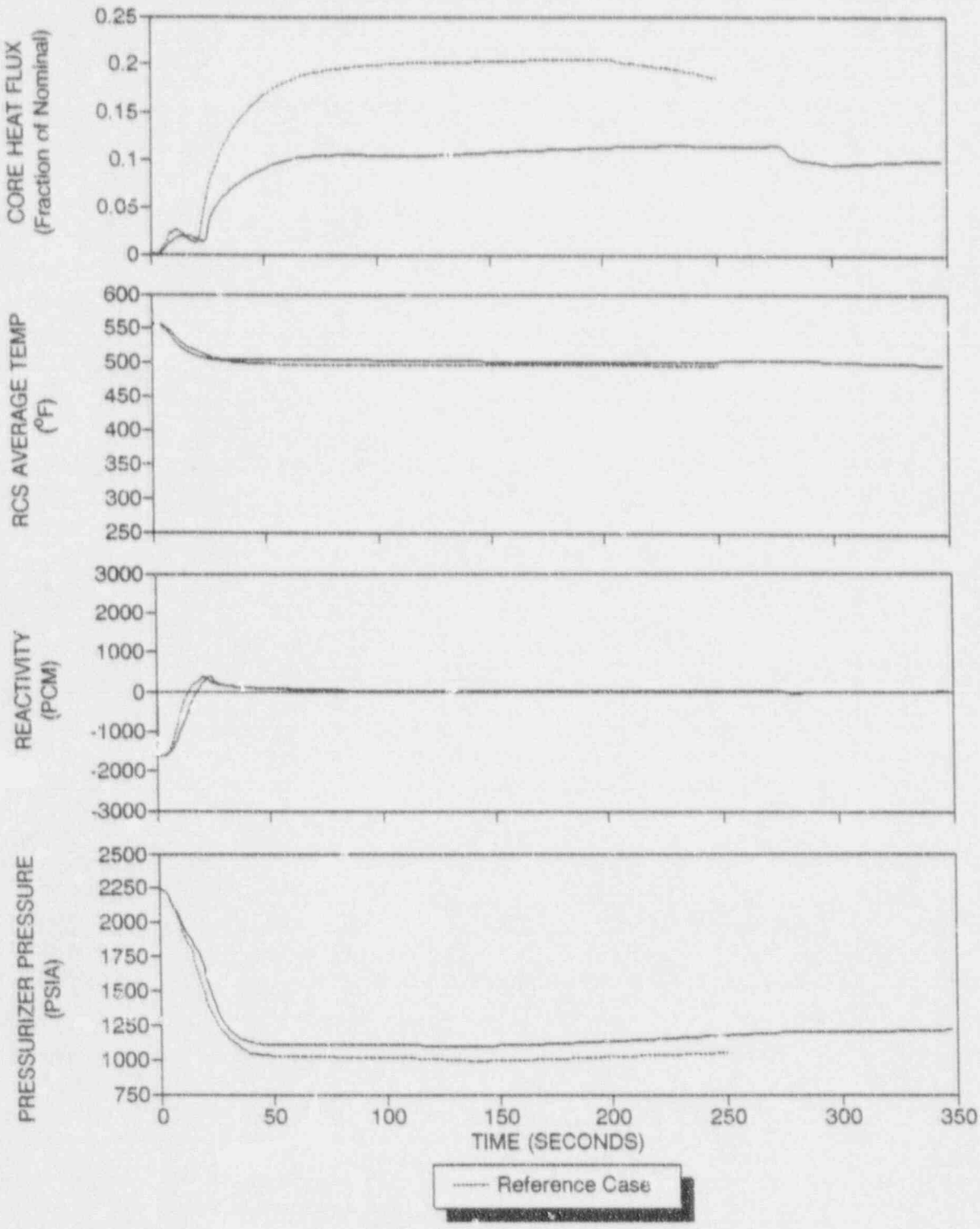

Figure 3.4-66 Transient Results for a Loss of Offsite Power Coincident with Safety Injection Actuation

APPENDIX

FSAR COMPARISON

In this appendix, the Reference Case HZP analysis described in Section 3.4 is compared to the current CPSES-1 FSAR analysis. The results of the comparison are illustrated in Figures A-1 through A-8. As can be seen from the figures, the FSAR analysis results agree very well with the Reference Case. This is expected because the TU Electric methodology is very similar to the FSAR analysis methods and there are no significant differences in the input assumptions used for two analyses.

As shown in Figure A-1, the initial nuclear power increase calculated by RETRAN was steeper than predicted by the FSAR analysis. However, the peak power for the event was nearly the same for both analyses. There are no other notable differences between the two analyses.

FSAR

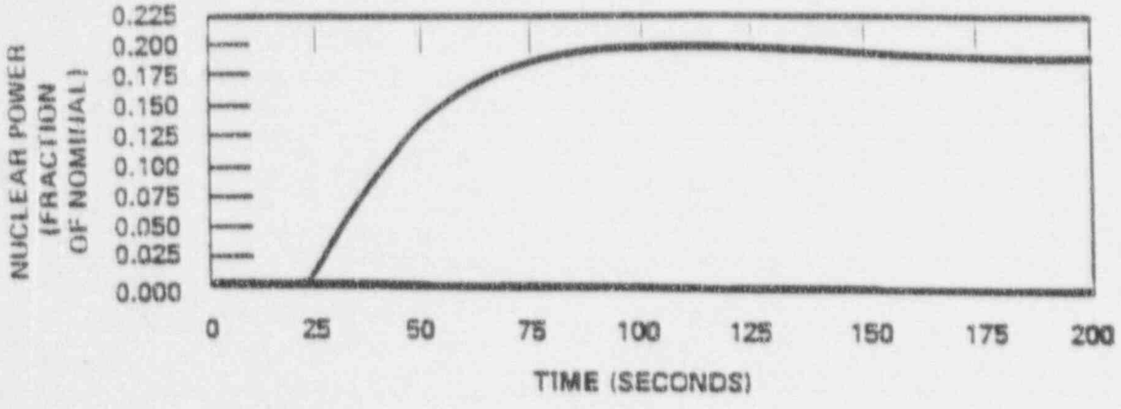

REFERENCE CASE

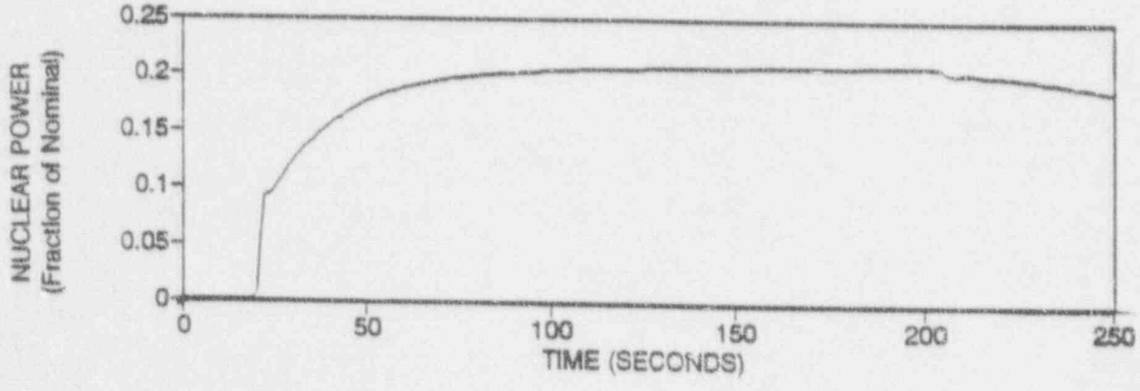

Figure A-1 Reference Case Nuclear Power Response Comparison with FSAR

FSAR

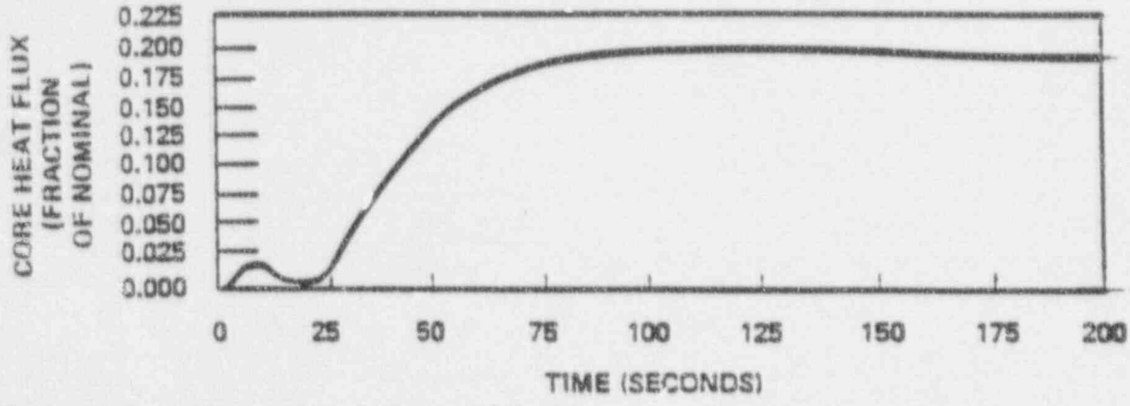

REFERENCE CASE

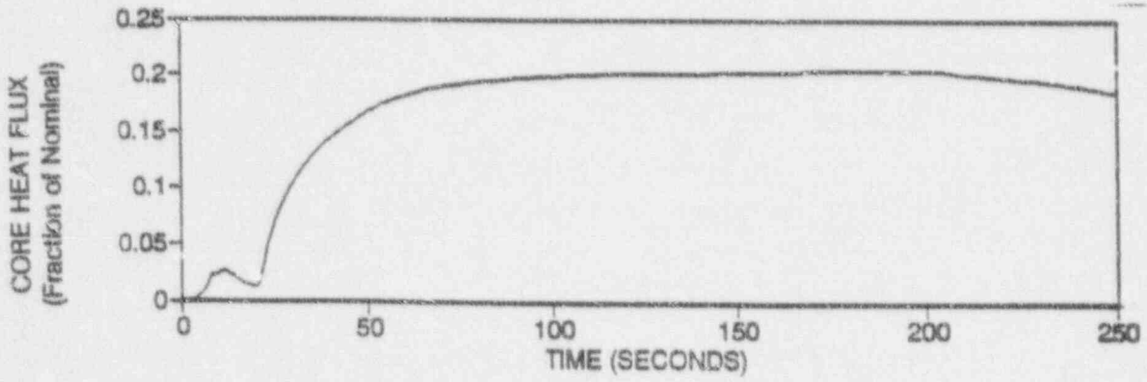

Figure A-2 Reference Case Core Heat Flux Response Comparison with FSAR

FSAR

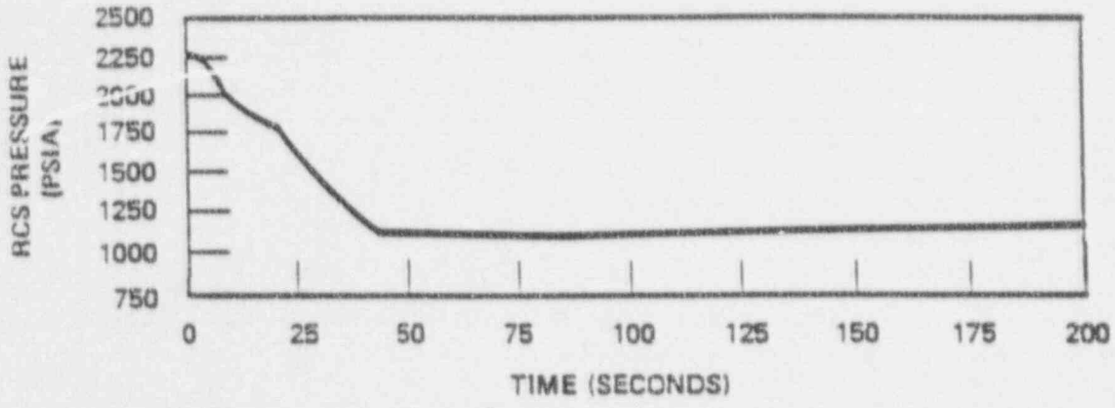

REFERENCE CASE

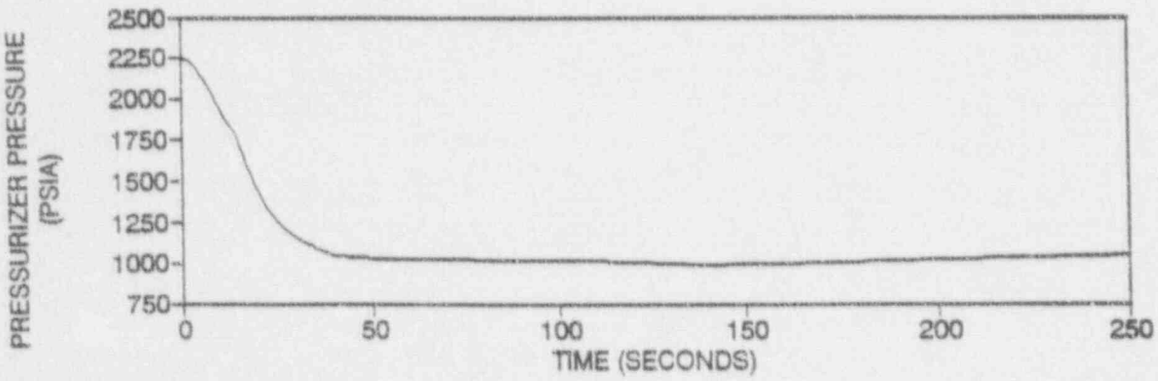

Figure A-3 Reference Case Pressure Response Comparison with FSAR

FSAR

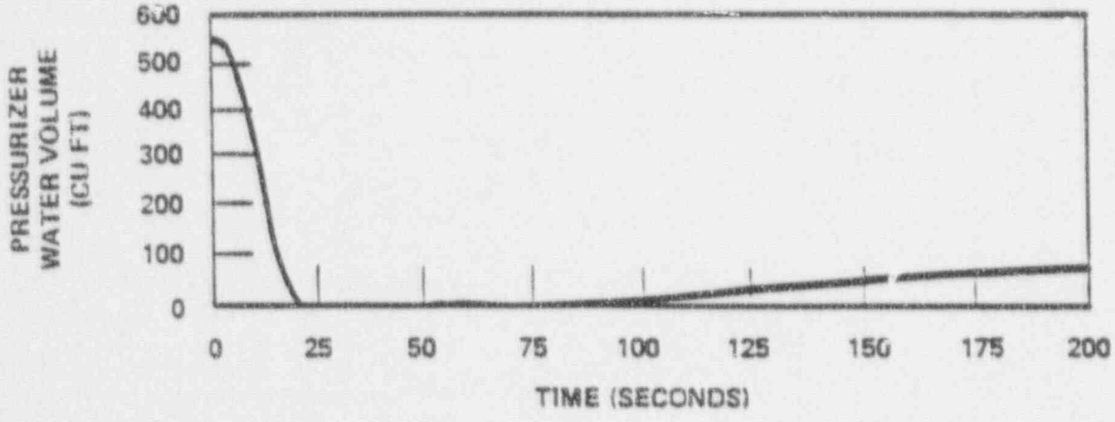

REFERENCE CASE

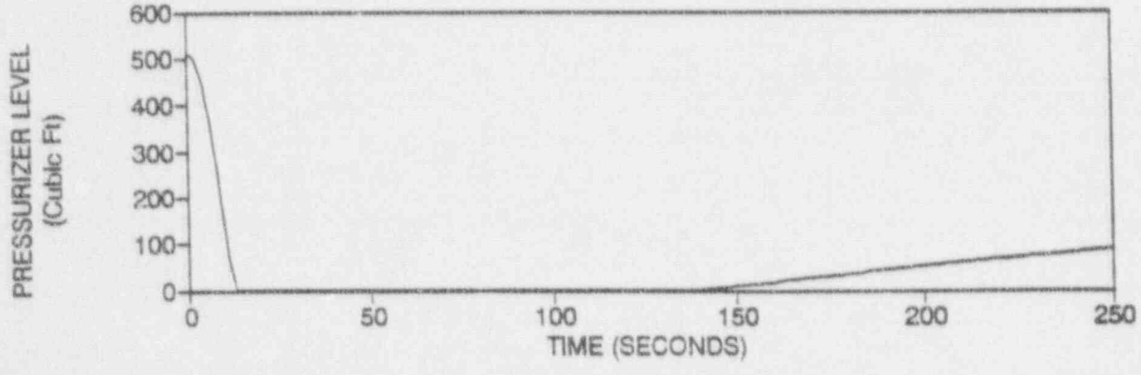

Figure A-4 Reference Case Pressurizer Level Response Comparison with FSAR

FSAR

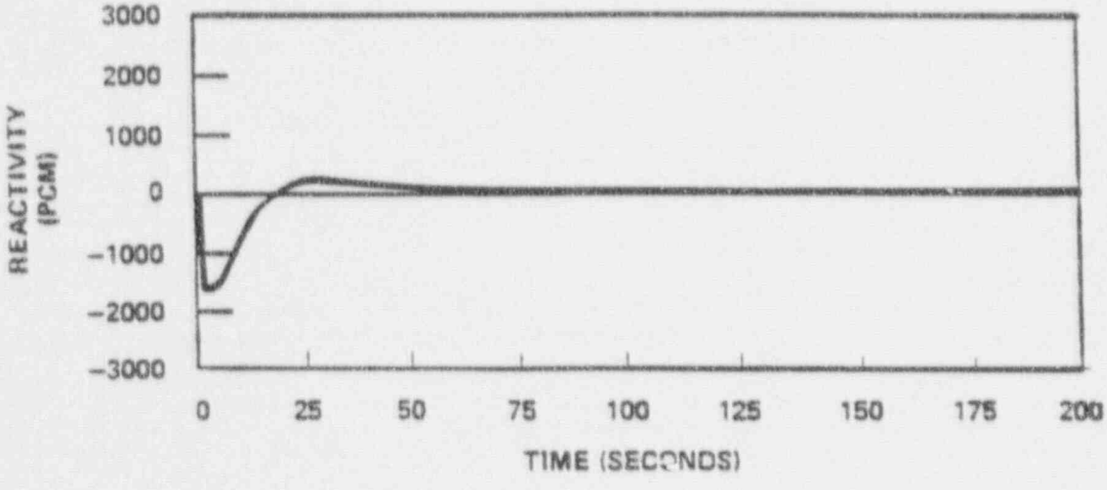

REFERENCE CASE

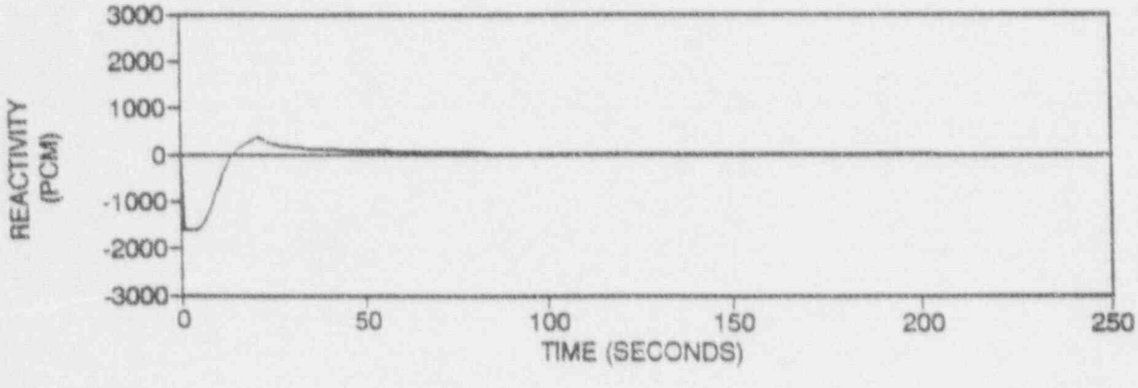

Figure A-5 Reference Case Reactivity Response Comparison with FSAR

FSAR

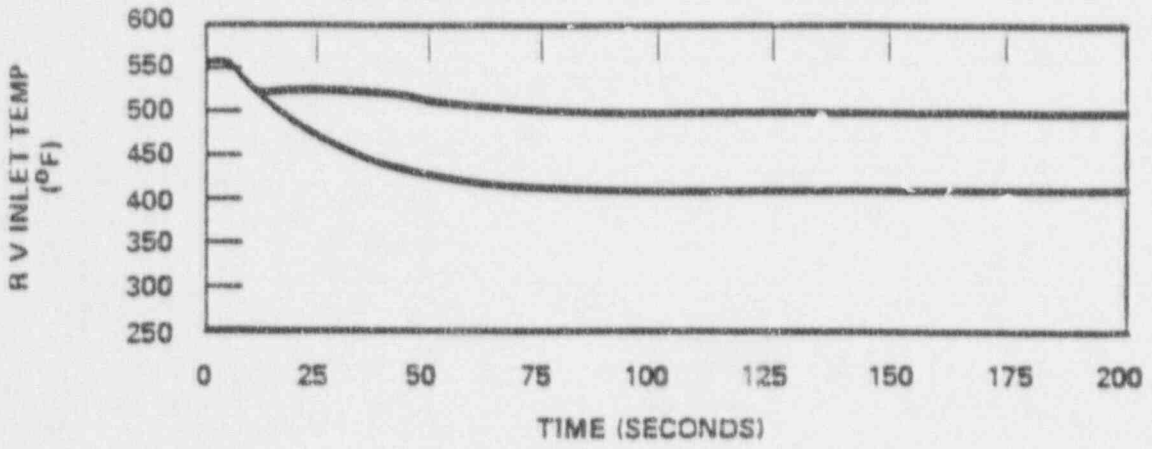

REFERENCE CASE

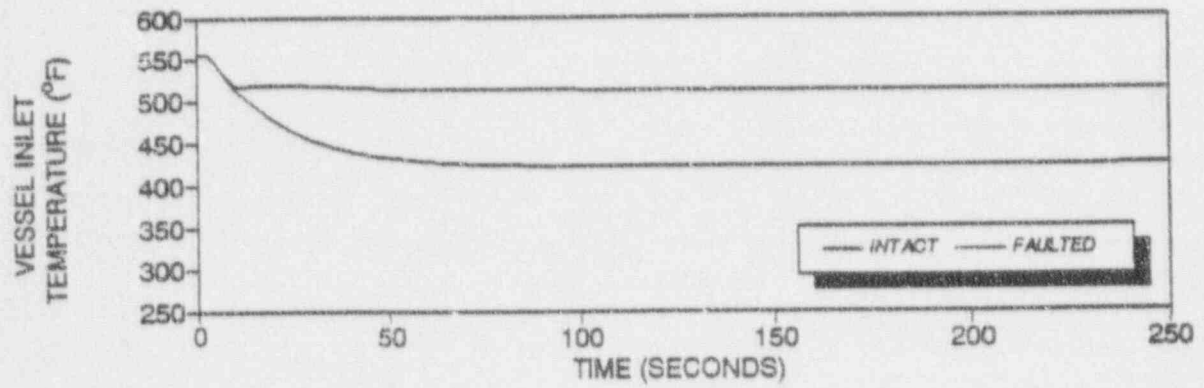

Figure A-6 Reference Case Vessel Inlet Temperature Response Comparison with FSAR

FSAR

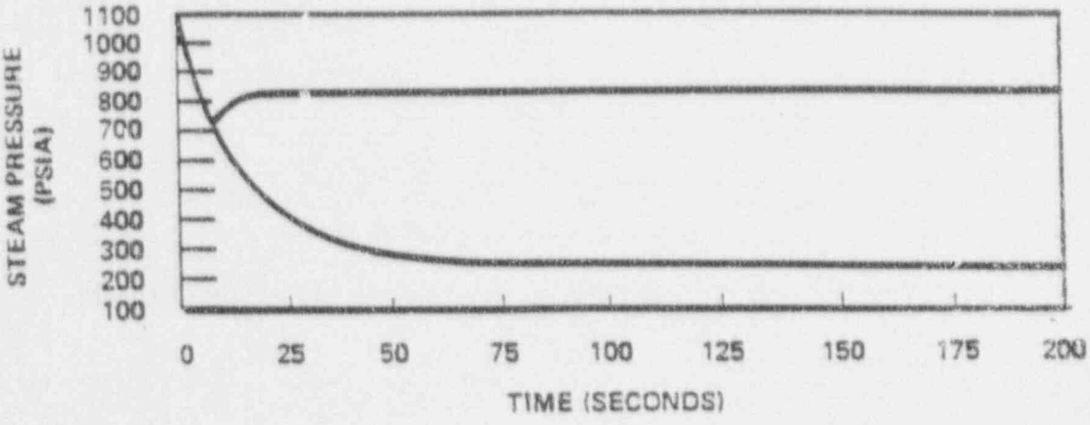

REFERENCE CASE

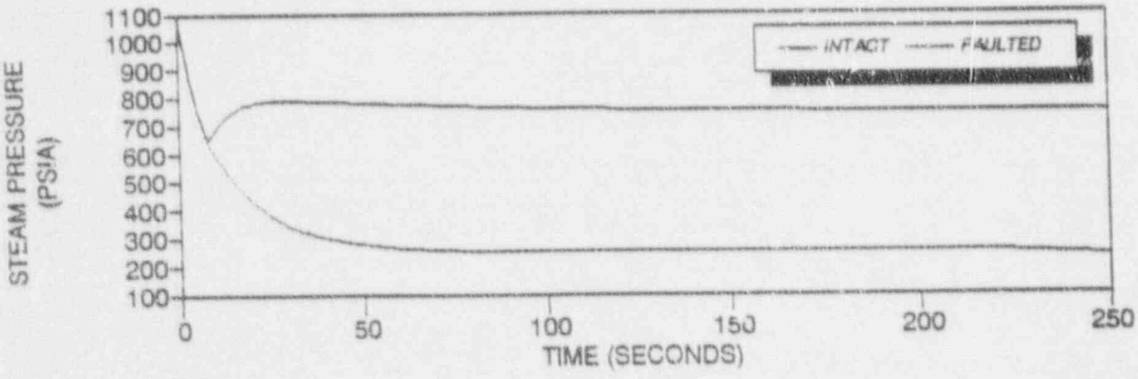

Figure A-7 Reference Case Steam Pressure Response Comparison with FSAR

FSAR

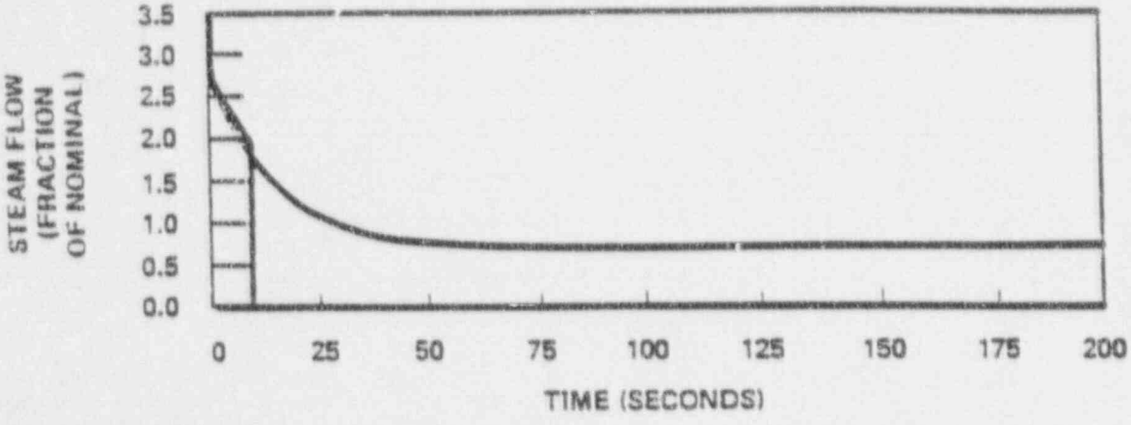

REFERENCE CASE

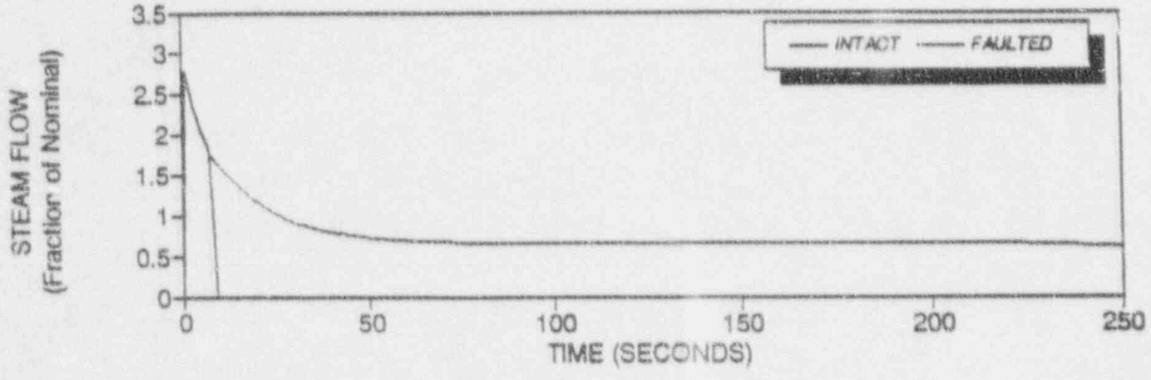

Figure A-8 Reference Case Steam Flow Response Comparison with FSAR